Novel Nicotinic Acetylcholine Receptor Ligands based on Cytisine, Ferruginine, Anatoxin-a and Choline: *In vitro* Evaluation and Structure-Activity Relationships

Dissertation

zur

Erlangung des Doktorgrades (Dr. rer. nat)

der

Mathematisch-Naturwissenschaftlichen Fakultät

der

Rheinischen Friedrich-Wilhelms-Universität Bonn

vorgelegt von

Maria Cristina Tilotta

aus Trapani

Bonn 2004

Angefertigt mit Genehmigung der Mathematisch-Naturwissenschaftlichen Fakultät der Rheinischen Friedrich-Wilhelms-Universität Bonn

1. Referent: PD. Dr. Daniela Gündisch

2. Referent: Prof. Dr. Christa E. Müller

Tag der Promotion: 26.11.04

Die vorliegende Arbeit wurde in der Zeit von Januar 2001 bis November 2004 am Pharmazeutischen Institut der Rheinischen Friedrich-Wilhelms-Universität Bonn unter Leitung von Frau PD Dr. Daniela Gündisch durchgeführt.

Ich danke herzlich Frau PD Dr. Daniela Gündisch für ihre Unterstützung und für die wissenschaftliche Leitung der Arbeit.

Weiterhin möchte ich mich bei Frau Prof. Dr. Christa E. Müller für die freundliche Übernahme des Korreferats bedanken.

To my parents, Enza and Bruno

Ai miei genitori, Enza e Bruno

Table of contents

I. Introduction

I/1. Nicotinic Acetylcholine Receptors (nAChRs)

I/1.1. Historical perspective of the receptor

Almost 100 years ago, John Langley of Cambridge University developed the idea of the "receptive substance" or "receptor" by using nicotine as an experimental tool [1]. He suggested “pharmacological substances could possess the structure necessary for the combination with appropriate molecules on cells” [2]. Between 1905 and 1907, Langley carried out a series of experiments on the somatic neuromuscular junction and postulated the existence of transmitter receptors [3]. Later, Dale and his colleagues identified acetylcholine (ACh) **1** as the transmitter that acts on the receptors discovered by Langley (neuromuscular junction) as well as on receptors in the heart. In 1914, Dale distinguished the action of muscarine **2** and (S)(-)-nicotine **3** that historically resulted in the recognition of two pharmacologically distinct families of receptors for ACh **1** [4].

I/1.2. The endogenous neurotransmitter acetylcholine

Acetylcholine (ACh) **1** (Fig. I/1.1) is an endogenous neurotransmitter synthesized at the axon terminal from choline **4** and acetyl-CoA by action of the synthesizing enzyme, choline acetyl transferase (Fig. I/1.1) and is stored in vesicles in the presynaptic neuron. Depolarisation of the nerve terminal and the influx of calcium ion produce the release of ACh **1** from storage vesicles in the synaptic cleft. The neurotransmitter combines with receptors present on the postsynaptic neuron causing conformational change that allows the passage of cations. Afterwards, ACh **1** is broken down by hydrolysis into acetate and choline **4** in the reaction catalysed by the metabolising enzyme acetylcholinesterase [5].

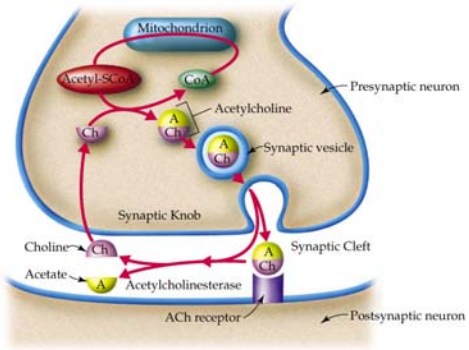

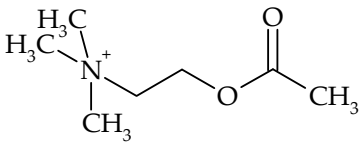

ACh 1

Figure I/1.1: On the left: structure of acetylcholine (ACh) **1.** On the right: acetylcholine release and re-uptake in synaptic junction. ACh **1** is stored in vesicles in the presynaptic neuron until released. The enzyme acetylcholine esterase inactivates acetylcholine after combining with its receptor [5].

Acetylcholine **1** exerts its effect both in the central and peripheral nervous systems through two distinct classes of cholinergic receptors: the muscarinic and nicotinic acetylcholine receptors (mAChRs and nAChRs), respectively named on the basis of their natural agonists, the plant alkaloids muscarine **2** and (-)-nicotine **3** [6].

I/1.2.1. Muscarinic receptors

The muscarinic receptors are members of the membrane bound G-protein coupled receptor family (GPCRs), which mediate their responses by activating a cascade of intracellular pathways. Muscarinic receptors are characterized by a single polypeptide chain of 400-500 residues, likely to correspond to transmembrane α-helices (7-transmembrane (7-TM) spanning receptors) (Fig. I/1.2). Acetylcholine **1** binds a site surrounded by the transmembrane regions of the receptor protein [7]. The carboxy-terminal is on the intracellular side of the membrane and is involved in coupling to G-proteins. G-proteins are compounds of three subunits of different size, weight and function (α, β and γ) [7]. The α subunit activates the appropriate second messenger system (e.g. activation of phospholipase C (inositol phosphate pathway), producing the mobilization of intracellular Ca^{2+}, for M_1 or M_3 and M_5 receptors; inhibition of adenylyl cyclase for M_2 or M_4, reducing the cytoplasmatic concentration of cAMP) [8]. The β and γ subunit can exert independent actions [8].

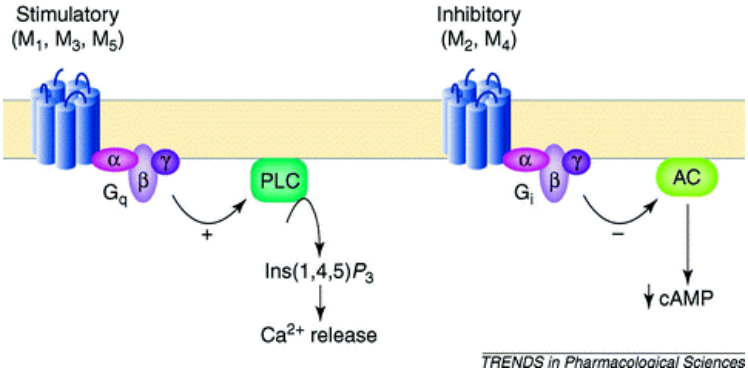

Figure I/1.2: There are five subtypes of muscarinic acetylcholine receptors that mediate the effects of acetylcholine. M_1, M_3 and M_5 receptors have a stimulatory function. They promote the release of the intracellular Ca^{2+}. M_2 and M_4 receptors have an inhibitory function and negatively modulate adenylyl cyclase (AC). This process reduces the cytoplasmatic concentrations of cAMP [9].

Muscarine **2** *4-Hydroxy-5-methyl-tetrahydro-furan-2-ylmethyl-)trimethyl-ammonium* is the prototypical muscarinic agonist and derives from the poisonous fly agaric mushroom *Amanita muscaria* (Fig. I/1.3) [7]. Similar to acetylcholine **1**, muscarine **2** contains a quaternary nitrogen that is important for action at the anionic site of the receptor (an aspartate residue in transmembrane domain III) [8] (Fig. I/1.3).

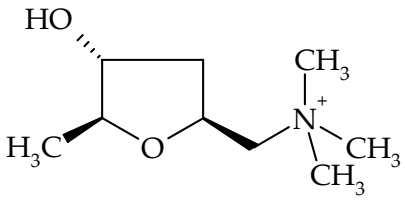

2

Figure I/1.3: Structure of muscarine **2**, the alkaloids from the poisonous mushroom *amanita muscaria* [10].

Muscarine simulates the interaction of ACh **1** with the acetylcholine receptors, thus mediating (interaction with G protein) its metabotropic effect. Several subtypes of muscarinic receptors have been identified: the **M_1** subtype has been found in various secretory glands and within the CNS (cortex and hippocampus). The **M_2** receptors predominate in the heart, particularly in the myocardium and can also be found in

smooth muscle. The **M_3** and **M_4** subtypes are located in smooth muscle and secretory glands. The last subtype known so far is the **M_5** subtype whose mRNA is found in the substantia nigra [8]. The activation of muscarinic receptors produces parasympathetic responses, including increased sweating, secretion of glands in the digestive system, decreased heart rate, constricted pupils, and contraction of the smooth muscle of the respiratory, digestive and urinary systems [9].

I/1.2.2. Nicotinic acetylcholine receptors (nAChRs)

The nAChRs are members of the ligand-gated ion channels (LGIC) family [11](Fig. I/1.4). The LGIC family includes different subfamilies that can be classified into three different groups. The "cis loop" receptor family includes the nAChR, the γ-aminobutyric acid receptor ($GABA_A$, $GABA_C$), glycine receptor (glyR) and serotonine (5-hydroxytryptamine, $5\text{-}HT_3$) receptor [11-14]. They are characterized by a pentameric structure and by the presence of a disulfide bridge between two cysteine residues in the extracellular domain of each subunit [15]. The second group comprises the ionotropic glutamate receptors that have a tetrameric structure and mediate excitatory response [16]. The last group is the ATP-gated purinoreceptor family (PX2R) that seems to be constituted by three homomeric subunits and contains only two transmembrane domains in each subunit [17]. All nAChR known so far are selective with regard to cations whereas other members of the LGIC family are anionic-permeable channels (e.g. chloride permeable glutamate receptors (GluRCl), glyR, etc.) [11]. NAChRs are responsible for mediating cholinergic neurotransmission at the neuromuscular junction of striated muscles, in the autonomous peripheral ganglia and at several sites in the central nervous system [6,15]. The receptor of this family controls the fast synaptic events in the nervous system by increasing transient permeability to particular ions [12]. In nAChRs, binding of two ACh molecules causes a rapid (ms) opening of the sodium channel. The opening of the channel results in a flux of ions that diffuse in the direction of their gradient (Na^+ in and K^+ out-currents) thereby causing depolarisation and an excitatory postsynaptic potential (EPSP) [18,19] (Fig. I/1.4).

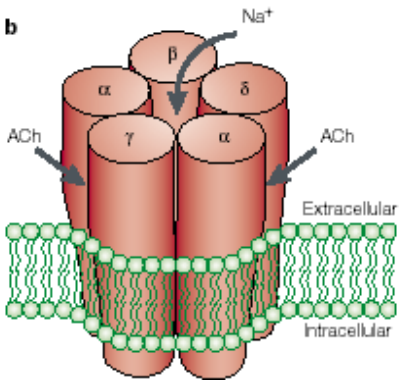

Figure I/1.4: The nicotinic acetylcholine receptor is composed of five subunits that are arranged to form a pore. The *α* subunit carries the binding site for ACh. The binding of two ACh molecules causes a rapid (ms) opening of the sodium channel. Na^+ flows down its concentration gradient into the cell causing depolarisation and an excitatory postsynaptic potential (EPSP) [15].

(S)(-)-Nicotine **3** (-)-*1-methyl-2-(3-pyridyl)-pyrrolidine* is the prototypical agonist of the nicotinic acetylcholine receptors [20]. The structure of (S)(-)-nicotine **3** consists of a pyridine and a pyrrolidine ring (Fig. I/1.5).

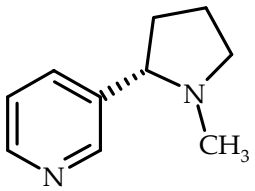

3

Figure I/1.5: *Nicotinana tabacum*, the tobacco plant. The structure of (S)(-)-nicotine **3** the most known alkaloid present in the tobacco leaves [21].

(S)(-)-Nicotine **3** acts on the neuromuscular junction, in the autonomic peripheral ganglia, in adrenal medullar cells and at several sites in the central nervous system (CNS) (see chapter I/2 for pharmacological actions of nicotine). (S)(-)-Nicotine **3** is an alkaloid that is found in the leaves of *Nicotiana tabacum* (Fig. I/1.5), the tobacco plant. Christopher Columbus, who brought it back from the Bahamas in 1492, introduced it to Europe. He wrote in his log that he had "met men and women who carried fire in their hands, and who smoked to keep off the tiredness". In 1828, Posselt and

Reimann at the University of Heidelberg were the first to extract nicotine from tobacco [22]. The name "nicotine" originates from Jean Nicot, a French ambassador to Portugal who introduced the Queen Consort and Regent of France, Catherine de Medici, to tobacco.

I/1.3. The architecture of the nAChR

The ACh receptor–channel complex has a molecular weight of approximately. 300 kDa. The channel is approximately 12 nm long in total and protrudes from the external surface of the membrane by about 6.5 nm and reaches 2 nm into the cytoplasm [23,24] **(**Fig. I/1.6). NAChRs are composed of five membrane spanning subunits forming a barrel-like structure around the central ion channel (Fig. I/ 1.6b) [25]. This pore has a diameter of ~ 25 Å at the synaptic entrance and becomes narrower at the transmembrane level [26](Fig. I/1.6c). Each subunit consists of a number of distinct functional domains [26]:

1) **The long N-terminal extracellular domain** (constinsting of about 210 amino acids) that carries the ACh binding sites and a conserved disulphide bridge between two cysteine residues separated by 15 amino acids [26-28].
2) **Four highly hydrophobic segments named M1, M2, M3 and M4** [29] form the transmembrane domains [30]. The second membrane spanning segment, M2, shapes the lumen of the pore in the ion channel and determines ion´s conductance and selectivity [11, 23, 28, 31, 32].
3) A short extracellular **C-terminal domain** [11, 23, 28, 31, 32].

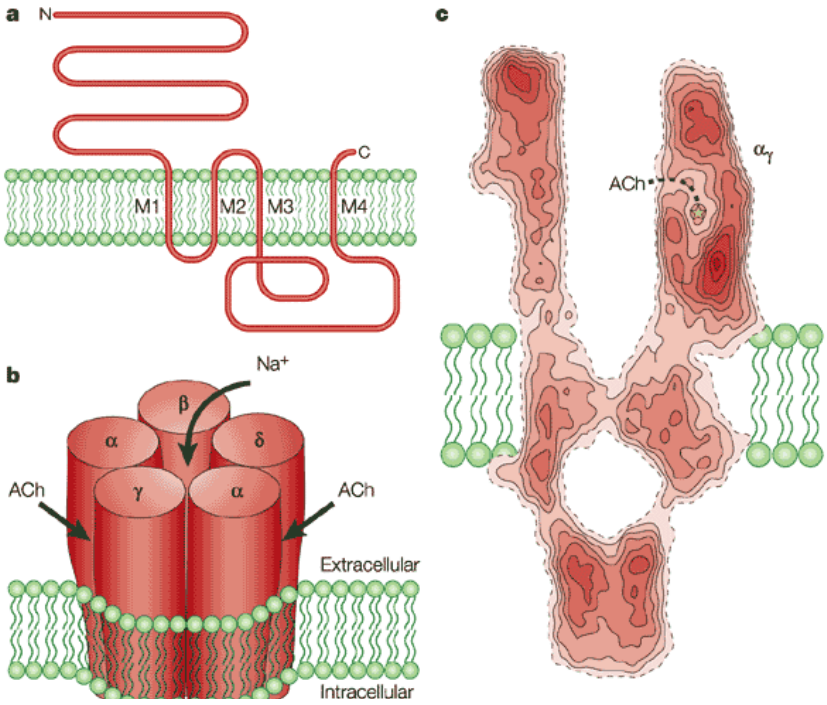

Figure I/1.6: Structure of the nicotinic acetylcholine receptor (nAChR). a: The functional domain of the receptor through the membrane: the amino terminal hydrophilic portion, the transmembrane domain and the small hydrophilic C-terminal domain. b: Schematic representation of the subunits in the muscle-type receptor, the location of the two acetylcholine (ACh) binding sites (between an α and γ-subunit, and an α and δ-subunit), and the central ion conducting channel. c: A cross-section through the 4.6-Å structure of the receptor determined by electron microscopy of tubular crystals of *Torpedo californica* membrane embedded in ice [15].

NAChRs are commonly divided into three subfamilies [20, 33]:

- **Heteromeric muscle type receptors** that are selectively labelled and blocked by the antagonist α-bungarotoxin (α-Bgt) **5** as present in snake venom of *Bungarus multicinctus* [34].
- **Heteromeric neuronal nicotinic receptors** composed of a combination of α and β subunits that are α-bungarotoxin-insensitive or resistant [20, 33].
- **Homomeric neuronal nAChRs** composed of an association of α7, α8 or α9-subunits which binds α-bungarotoxin (α-Bgt) **5** [20].

I/1.3.1. Composition of nAChRs in the neuromuscular junction (NMJ)

The major structural information of LGIC has been obtained from studies conducted on the muscle-type AChRs [35]. In the 1970s, the large amount of nAChRs protein available in the electric organs of *Torpedo californica* (Eel, Electrophorus) and the high degree of homology with the embryonic vertebrate muscle type receptor allowed the elucidation of the structure and function of nAChRs [30, 36]. Muscle nAChRs are located on the postsynaptic membrane of the neuromuscular endplate [37] and are built up of $\alpha 1$, $\beta 1$, γ and δ subunits in the fixed stoichiometry 2:1:1:1. (Fig. I/1.6b) [20, 38]. The order of assembly of the subunits that form the pentameric muscle receptor is highly constrained in a clockwise sequence of $\alpha 1\gamma\alpha 1\beta 1\delta$ (Fig. I/1.6b). In adult muscle the γ subunit is replaced by an ε to give $\alpha 1\varepsilon\alpha 1\beta 1\delta$ [39].

I/1.3.2. Composition of nAChRs in the brain

Neuronal nAChR are pentameric receptors that differ from the muscle type as they have no δ, ε, or γ subunits. So far, 12 neuronal nAChRs subunits have been identified, of these nine are α ($\alpha 2$ to $\alpha 10$) and three β ($\beta 2$ to $\beta 4$) [40,41]. Neuronal nAChRs will have distinct pharmacological and physiological properties resulting from the combination of different subunits [42 43]. *Heteromeric* nAChRs are composed of α and β subunits that combine an $\alpha_x\beta_y$ stoichiometry to form functional channels. The $\alpha 2$, $\alpha 3$, $\alpha 4$, $\alpha 5$ and $\alpha 6$ subunits can assemble with $\beta 2$, $\beta 3$ or $\beta 4$ [20, 38, 42] with the exception of $\alpha 5$ and $\beta 3$ which do not form functional receptors when expressed alone or with a single β subunit [40, 44, 45]. The $\alpha 10$ subunit is only incorporated into a functional nAChR when co-expressed with $\alpha 9$ [41]. *Homomeric receptor*s are formed by $\alpha 7$, $\alpha 8$ and $\alpha 9$ subunits. These receptors share many different physiological features. Each of them is able to form functional homomers, bind α-bungarotoxin (α-Bgt) **5**, and exhibit high calcium permeability and fast desensitisation [46, 47, 48].

I/1.4. Ligand binding sites

I/1.4.1. ACh binding sites

The structure of the ACh binding sites has been investigated by a number of different methods, including photoaffinity labelling and site-directed mutagenesis [32]. It was found that a specific agonist-binding site is located on both α subunits [52] in a pocket approximately 30-35 Å above the membrane surface [32]. Studies of the muscle-type receptor suggest that the receptor contains two different **ligand-binding sites** with different affinities for ACh. One binding site is located at the interface of the α and the δ subunit and a second binding site is at the interface of the α and the γ subunit (analogous to α/β subunit interface in neuronal nAChRs) (Fig. I/1.7a) [24, 26]. Six loops of amino acids, termed A-F, have been identified to participate in the formation of the ACh binding site. The *principal component* of the binding site comprises three loops A-B-C, located on the α-subunit. They are involved in the binding of ACh [53]. The *complementary component* of the binding pocket, made up of loops D-E-F, is located on the neighbouring subunit residues (α in homomeric, β in heteromeric) (Fig. I/1.7b) [26]. The α subunit is defined by the presence of a cysteine pair (e.g. α1 Cys192-Cys193 in loop C) [24, 32]. The loop B contains aromatic side chains (amino acid Trp 143, homologues to Trp 149 in torpedo), which are presumed to exert cation-π interaction with the quaternary ammonium group of ACh [54]. At least two binding sites have to be occupied for a maximal activation of nAChR. The disulphide bridge between Cys192-Cys193 in loop C is essential for the stability of the open channel conformation [32].

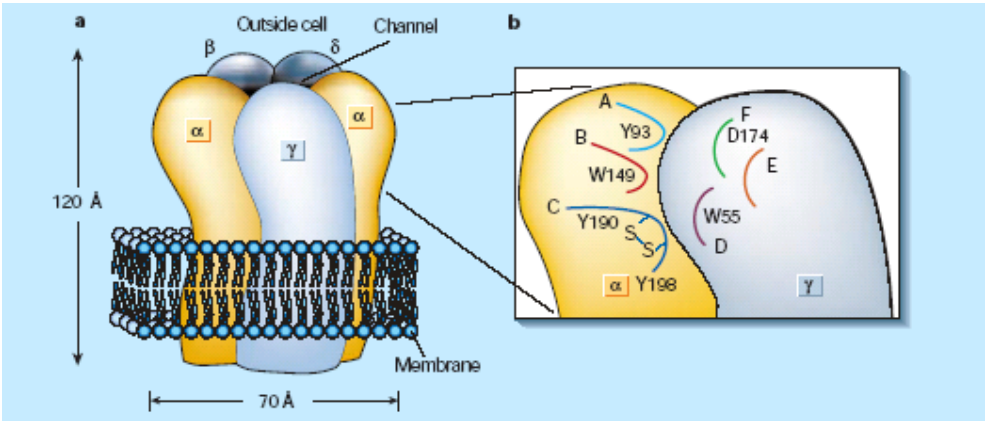

Figure I/1.7: a: The subunit composition of the muscle type nicotinic acetylcholine receptors ($\alpha 1, \beta 1, \gamma$ and δ subunits in the fixed stoichiometry 2:1:1:1.). **b:** The *principal component* for the binding site, located on an α-subunit and formed by the three loops A-B-C. The c*omplementary component* of the binding pocket made up of loops D-E-F and located on a neighbouring subunit [55].

Our understanding of the ligand binding sites has been greatly improved by the discovery of a soluble protein in a snail (*Lymnaea stagnalis*) from European fresh waters that binds nicotinic ligands and α-bungarotoxin (α-Bgt) **5** [56]. This acetylcholine-binding protein (AChBP) is produced and stored in glial cells and released into cholinergic synaptic clefts where it modulates synaptic transmission [56]. Recently, Brejc reported the crystal structure of acetylcholine-binding protein (AChBP) at 2.7 Å resolutions [57]. The X-ray crystallographic analysis of AChBP reveals an oligomer of five identical subunits (composed of 210 amino acid chains), arranged in an anticlockwise manner along an axis (Fig. I/1.8). AChBP amino acids domain resemble for ~ 24% the extracellular parts of the α subunit ($\alpha 7$). However, unlike nAChR, AChBP lacks the transmembranic and intracellular domains [56, 57].

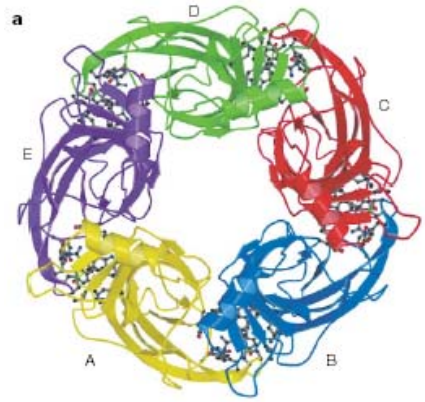

Figure I/1.8: The acetylcholine-binding protein (AChBP) viewed down the fivefold axis. Different colours are used to indicate the five subunits, and they are categorized as A, B, C, D or E.

I/1.4.1. Allosteric binding sites

The function of neuronal nAChRs is subject to modulation by a variety of compounds that interact at other receptors or other sites of the receptor protein. They belong to different classes of drugs, have different structures and can have activatory or inhibitory effects (Tab. I/1.1).

Table I/1.1: Allosteric activators and allosteric inhibitors of AChRs

Allosteric activators	Allosteric inhibitors
Physostigmine, Galantamine, Tacrine Ivermectine Benzoquinonium Codeine 5-HT	Ethanol [a] Phencyclidine, Chlorpromazine [a] Progesterone, Corticosterone, Dexamethasone [b] Nimodipine, Nifedipine [c]
	a: binds to the negative allosteric site b: binds to the steroid site c: binds to the dihydropyridine site

***Non-competitive allosteric activator site*:** The allosteric *activator* combines with a site located on the α subunit of the receptor protein which is distinct from the classical binding site for ACh **1** [58, 59]. The acetylcholinesterase inhibitors, including galantamine **6**, tacrine **7** and physostigmine **8** have been shown to act as allosterically potentiating ligands (APLs) (Fig. I/1.9). They increase the probability and the frequency of channel opening and thus potentiate the channel activity of nicotinic receptors in response to ACh **1** [60-62].

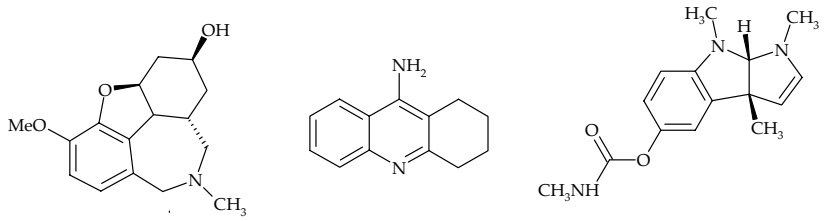

galantamine **6** tacrine **7** physostigmine **8**

Figure I/1.9: Structure of galantamine **6,** tacrine **7** and physostigmine **8**

Other allosteric potentiators are for example the opiate codeine, the anthelminthic drug ivermectin **9** and the neurotransmitter serotonin (5-HT, µM range). Ivermectine **9** potentiates ACh evoked currents at chick and human α7* nAChRs in Xenopous oocytes [63] (Fig. I/1.10).

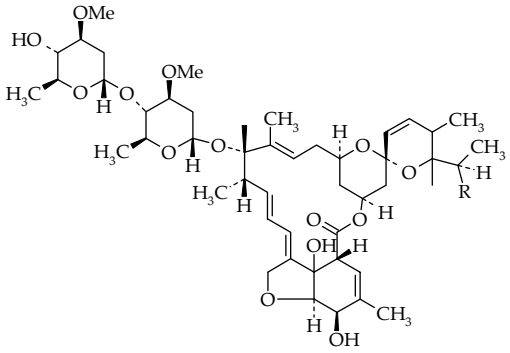

(85 %) 22,23-Dihydroavermectin B1a : R = C_2H_5

(15%) 22,23-Dihydroavermectin B1b : R = CH_3

Figure I/1.10: Structure of ivermectine **9**

Non-competitive negative allosteric site ligands: *Negative allosteric* ligands include ethanol, phencyclidine, chlorpromazine, local anaesthetics and barbiturates for instance (Tab. I/1.1). They inhibit ion channel function without interacting with the ACh binding site by acting on two distinct sites. The first site binds ligands in the nanomolar range (high affinity site). It is thought to be located within the ion channel and produces rapid reversible channel blockade by steric hindrance [25, 64]. The second site binds ligands with low affinity (µM range) and is probably located at the interface between the lipid membrane and the receptor protein.

Dihydropyridine site: Some Ca^{2+} channel antagonists such as nifedipine and nimodipine have been found able to block agonist induced activation of nicotinic

receptors. The mechanism of action is unknown, but it is assumed that they bind to a site that exists within the ion channel [65].

***Steroid binding site*:** The binding site for steroids is located in the extracellular hydrophilic domain that is distinct from the ACh **1** binding site. Progesterone, corticosterone and dexamethasone have been classified **as negative** allosteric effectors due to their ability to desensitise nAChRs [25, 66] (Tab. I/1.1).

I/1.5. Transition and functional states of the nAChR

The nAChR is a prototype of allosteric membrane protein [11]. The term allosteric, from the Greek meaning "other site", refers to the characteristic to possess multiple ligand binding sites. It also refers to other properties associated with classical allosteric proteins, such as multiple possible conformations and stabilization of specific protein conformation by ligands [19,67]. The binding of a ligand to a specific allosteric site leads to a reversible alteration of the protein conformation that modifies the properties of the biologically active site. In 1965, Monod et al. proposed the first allosteric enzyme models [68]. They hypothesized that 1) regulatory proteins are oligomers 2) the allosteric oligomers can spontaneously exist in a minimum of two freely interconvertible states (open↔closed) and 3) ligand binding stabilizes the state for which it has a higher affinity. Further investigation led to the hypothesis that the nAChR pass through a cycle involving three types of functional states: an active state **(A),** a desensitised state **(D)** and a resting state **(R)** [11,19] (Fig. I/1.11). The active state **(A),** when the channel is open (on a microsecond to millisecond scale), allows the passage of monovalent and divalent cations in favour of the electrochemical gradient. This state has a low affinity for ACh (1-10 μM) [12]. The continued presence of any agonists leads to receptor desensitisation **(D)** and ion channel closure **(R).** In the desensitised condition, the receptor is refractory to activation (on a millisecond-minute timescale) although it displays a higher affinity for agonist binding (ACh 10 nM-1μM) [12,] After a prolonged exposition to an agonist, the receptor in the desensitised channel state **(D)** (closed) may change to an inactivated state (I), from which the rate of recovery is very slow (Fig. I/1.11) [12].

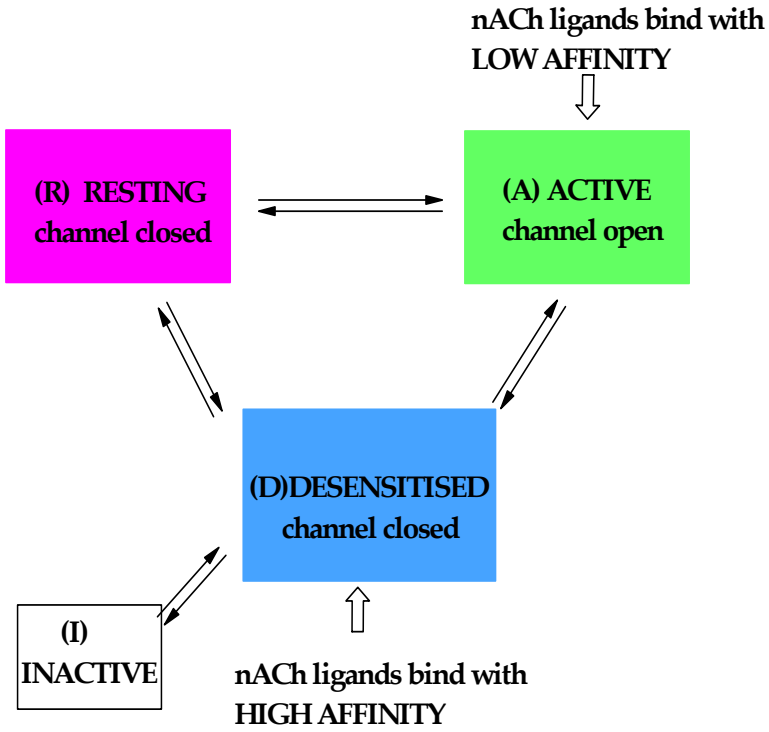

Figure I/1.11: Transition and functional states of nicotinic receptors

I/1.5.1. Up-regulation

It is known that continued exposure to agonists causes receptor down-regulation, while over-exposure to antagonists induces receptor up-regulation [25]. However, nicotinic receptors go against this convention: a prolonged exposure to an agonist produces an up-regulation, with an increase in the density of nicotine binding sites in the brain tissue [25,69]. Two models have been proposed to explain the mechanism of functional up-regulation of $\alpha 4\beta 2^*$ receptors (Fig. I/1.12) [70].

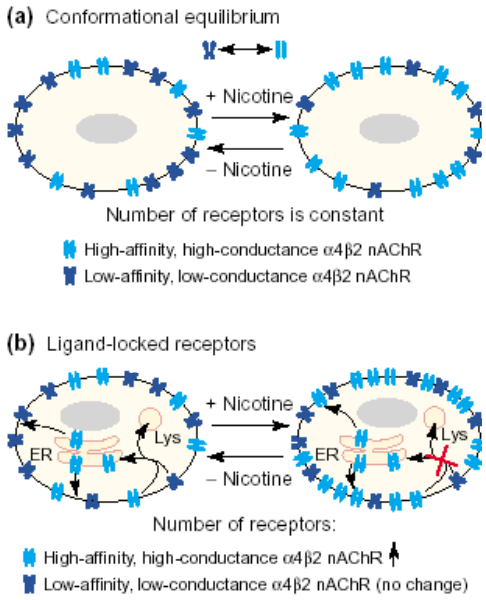

Figure I/1.12: Possible mechanisms for the functional up-regulation of α4ß2-subtype nicotinic acetylcholine receptors (nAChRs). a: The conformational equilibrium hypothesis. b: The ligand-locked receptor hypothesis[70] .

In the first model (Fig. I/1.12a), **the conformational equilibrium hypothesis** proposes that α4β2 receptors exist in two interconvertible states, one with high affinity for nicotine and the other with low affinity for nicotine, and that chronic exposure to nicotine (or an another nAChR ligand) stabilizes a larger fraction of receptors in the high affinity, large conductance state. In the second model (Fig. I/1.12b), **the ligand-locked receptor hypothesis** presumes that α4β2 receptors may be rapidly recycled on the cell membrane. Chronic exposure to nicotine slows down receptor endocytosis and increases the membrane density by inserting additional, pre-synthesized receptors (high affinity receptor) from a sub-membranous pool. NAChRs subtypes have different levels of sensitivity to up-regulation by nicotine exposure. For instance, α4β2 and α7 nAChRs are more sensitive to up-regulation than other subtypes [25]. The α4β2 are readily up-regulated following chronic exposure to nicotine and return slowly to control levels [71,72]. Instead, α3-containing nAChRs are usually less readily up-regulated, but appear to recover more rapidly from whatever up-regulation does occur [73].

I/1.6. NAChRs in the central nervous system

I/1.6.1.Distribution of nAChRs in the brain

The topographical distribution of nAChRs in the brain has been studied through various methods: immunohistological and immunoprecipitation experiments, radioligand binding and autoradiographic techniques. The subunit composition of functional receptors in different brain areas is an ongoing question. Zoli and others mapped the distribution of (-)-[^{3}H]ACh, (-)-[^{3}H]nicotine, (-)-[^{3}H]cytisine, (±)-[^{3}H]epibatidine and [^{125}I]α-Bgt binding site in β2 knock-out (KO) mice and wild mice [74]. Through autoradiographic and patch clamp studies they identified four types of nAChRs (Table I/1.2) [74].

Table I/1.2: Classification of nAChRs in the mouse brain [74].

Receptor type	Subunit composition	Predominant localization in CNS	Pharmacology
I	α7	cortex, limbic area, hippocampal formation, hypothalamus and other telencephalic areas	α-Bgt and MLA sensitive very fast desensitising
II	α4β2 (α5?)	CNS	nicotine > cytisine
	(α2?)β2	interpeduncular nucleus	
	(α3?)β2	hippocampus	
	(α6β3?)β2	catecholaminergic nuclei	
III	α3β4 (α5?)	medial habenula, interpeduncular nucleus, dorsal medulla	MLA-insensitive (concentration dependent) nicotine = cytisine
IV	(α4β4?)	lateral habenula	MLA insensitive nicotine = cytisine
	(α2β4?)	dorsal interpeduncular nucleus	

Type I - receptors: they are α-Bgt and MLA sensitive. Their distribution does not change in β2 -/- KO mice, whereas they disappear in α7* mutant mice. The **α7* nAChRs** are present in high density in the hippocampal formation, hypothalamus

and other telencephalic areas [75,76]. This subunit distribution correlates well with the high level of [^{125}I]α-Bgt binding in these regions (K_D = 1 nM for [^{125}I]α-Bgt) [75].

Type II- receptors: They contain the **β2 subunit** and represent the vast majority of nAChRs in the mouse brain. (-)-[^{3}H]nicotine-binding sites disappear in β2 -/- KO mice. The composition of the major expressed subunits is α4β2*nAChRs which are all localized ubiquitously in the CNS. They are present in high density in the cerebral cortex (layers III and IV), thalamus, ventral tegmental area (VTA), the media habenula and substantia nigra. [77] (Tab. I/1.2). Other subunits, namely α2, α3 and α5, are likely to co-assemble with β2 [78] and β4 [79]. The α3β2* nAChR is reported to be expressed mostly in the CNS, in the habenula system and in dopaminergic regions [80]. In situ hybridisation studies of the α6 mRNA in the adult rat central nervous system show that the distribution is especially high in several catecholaminergic nuclei, the locus coeruleus, the ventral tegmental area and the substantia nigra [81,82]. The β3 subunit is predominantly present in the midbrain [79,83]. It has to be co-expressed with other subunits, such as α3, α4, α6 or β2/β4 to form functional receptors.

Type III- receptors: They do not contain the β2 subunit; but they bind (±)-epibatidine **13** with high affinity in equilibrium binding experiments. The type III corresponds to the distribution of **α3β4* nAChRs**. This subtype is predominant in ganglions, in MHb, in the habenulo-peduncular system, in the locus coeruleus, area postrema, cerebellum and the pineal gland [79, 80, 83]. The α5 subunit can participate in α3β4* receptors with $\alpha_x\alpha_y\beta$ combinations [44, 84].

Type IV-receptors: These receptors do not contain β2 subunit. They bind (±)-[^{3}H]epibatidine and (-)-[^{3}H]cytisine with high affinity, but the binding of other nicotinic agonists is limited or absent. They display a faster desensitisation rate suggesting a composition of **α2 and α4 with β4** [46, 74].

I/1.6.2. Distribution and function of nAChRs in the autonomous nervous system (ANS)

The CNS integrates the sensory inputs and sends neuronal commands back to the organ through the ANS. Autonomic ganglia are the peripheral sites for the control of organs and tissues by the nervous system. Nicotinic acetylcholine receptors are involved in the neuronal information process because they are mediators of fast synaptic transmission in ganglia [85]. Ganglionic nAChRs possess different functional and pharmacological characteristics due to the expression of various nAChRs subunits. Despite their various functions, they share some common features, including relatively slow gating, moderate Ca^{2+} permeability and significant rectification of the postsynaptic responses [86]. Autonomic ganglia present high levels of mRNA coding for α3 and β4 nAChRs subunits, but they also contain transcripts for α4, α5, α7 and β2 nAChRs subunits [87-89]. *In vivo* and *in vitro* studies indicate that the principal receptors involved in neurotransmission in the intracardiac ganglia contain at least two different subtypes on nAChRs: one consist of α3β4 subunits and one of α7 subunits [89,90]. For instance, it was found that α3 subunits in the rat are mostly combined with β4 and it seems that this subunit combination contributes to the positive chronotropic effects of nicotine, resulting in an increase in the heart rate [91]. The *α*7 subunit is expressed in both para- and sympathetic neurons innervating the heart, whereby they contribute to the negative chronotropic effects, resulting in decrease in the heart rate [91]. It has been suggested that *α*7 in the rat intrinsic cardiac neurons interact with other nAChRs subunit to form heteromeric nAChRs [91]. NAChRs in ANS are also involved in the control of other organ systems, such as the gut and bladder systems [92]. Very little information is available about the subunit composition of nAChRs in these organs. The presence of β2 and β4 subunits was revealed from the disruption of gut mobility in mutant mice lacking these two subunit nAChRs [89]. Recent studies also reported the presence of *α*3 in the human gut [93]. Furthermore, nAChR containing the *α*3β4 subtype are able to mediate ganglionic

transmission in the bladder [92]. In fact, nicotine failed to induce the contraction of the bladder smooth muscle in α3, β2 and β4 null-mutant mice [93].

I/1.7. Distribution and function of nAChRs in non-neuronal cells

There is growing evidence that activation of nAChRs via acetylcholine **1** can modulate some cellular functions outside the synaptic transmission in the central and peripheral nervous system. This is supported by the fact that non-neuronal cells, such as skin keratinocytes [94], bronchial epithelial [95], aortic endothelial cells and immune tissue, express functional nAChRs of various subtypes (Tab. I/1.3) [96, 97]. Skok et al. identified α4 and α7-containing nAChRs in B-lymphocyte cell lines by using a various α-subunit specific antibody [97]. The localization of nAChRs in lymphocytes is of special interest because it would demonstrate the participation of α7* nAChRs in the promotion of tumor cell proliferation as well as in antibody production [97]. In situ hybridisation studies revealed that the α9 and α10 subunits are distributed in the lymphoid system (tonsil, thymus and spleen) [41,98]. The α9 subunit is expressed in sensory organs and in particular in outer hair cells where it modulates the encoding of auditory stimuli [49] (Table I/1.3).

Table I/1.3: Distribution of nAChRs in non-neuronal cells

Cell type	Subunit	Reference
Lymphocytes	α7, α4, α9 and α10	97
Vascular endothelial cells (human)	α3, α5, α7, β4, β2	99
Bronchial epithelium (human, rat)	α3, α5, α7, β4, β	95
Keratocytes	α5, α3,	94

I/1.8. Knock-out (KO) mice

The creation of knock-out mice, missing one or more genes for the nAChRs subunits, or mice which express mutant genes [100] paves the way for the investigation of the relationship between subunit diversity and *in vivo* receptor function in the brain and in the autonomous nervous system (ANS) [101-104]. KO mice have been created lacking the **α3** [88], **α4** [102,103] **α5** [85], **α6** [104], **α7*** [105], **α9** [106], **β2** [74, 89] or **β4** [89] subunit. The antinociceptive

effects of nicotine are reduced in both α4 and β2 null mutant mice [102]. Mice lacking the **β2** have a superficial normal phenotype, but show abnormal passive avoidance and increased neurodegeneration [101, 107, 108]. The lack of the nAChR **β4** subunit alters the behavioural responses to certain anxiety-provoking experimental paradigms [109]. Mice lacking **β2** and **β4** have some autonomic nervous system defects, such as enlarged bladder and dilated ocular pupils [89]. The deletion of **β3** subunit increases locomotors activity, a behaviour that is related to alterations in nicotine-induced dopamine release in the striatum [110]. Mice lacking the α6 subunit did not display any obvious neuro-anatomical or behavioural abnormalities [104]. Neither the **α5** nor **α4** subunits are obligatory for normal development and survival [85]. The **α5** null mice grow to adulthood with no visible phenotypic abnormalities and show normal behaviour in basic conditions [85]. The function of the ***α*3** subunit, which is expressed ubiquitously in autonomic ganglia and in some parts of the brain, is poorly understood in the living system. KO mice lacking the ***α*3** subunit usually die in the first week after birth due to multiorgan autonomic dysfunction [88]. The phenotype in ***α*3** (-/-) mice may be similar to the rare human genetic disorder of megacystis-microcolon-intestinal-hypo-peristalsis syndrome [111]. Moreover, the ***α*3**-KO-mice exhibit extreme bladder enlargement, dribbling urination, bladder infection, urinary stones, and widely dilated ocular pupils that do not contract in response to light. These conditions can be attributed to a failure of ***α*3** in the autonomic ganglia [88]. KO mice lacking the ***α*9** subunit showed abnormal development of synaptic connections in the cochlear outer hair cells [106].

I/1.9. Pathophysiology

Interest in the field of neuronal nicotinic receptors has recently been stimulated by the discovery of the association between the decrease of nicotinic receptors in binding sites or mutation and between human neurobiological and psychiatric conditions, such as attention-deficit disorders, Parkinson′s disease, Alzheimer′s disease, schizophrenia, Tourette's syndrome, epilepsy, anxiety, depression, tobacco dependence or analgesia [112, 113] (Tab. I/1.4).

Table I/1.4: Classification and brain location of subunits linked to pathological conditions

Subunit involved	Brain location	Physiological functions and Pathological links
α4, α5, α7, α3, α4, β2	Temporal and frontal cortex Hippocampus	Possible role in AD [114, 115]
α4 mutation (replacing a serine at position 247 of the M2 channel with a phenylalanine)	All layers of the frontal cortex	Human autosomal dominant nocturnal frontal lobe epilepsy [116]
α7 (dinucleotide polymorphism at chromosome 15, which is the locus for the α7 nAChR)	CA 3 regions of hippocampus Auditory cortex Visual cortex	Schizophrenia [117]
α4	Nucleus raphé magnus	Pain [118]
β2	Mesolymbic regions	Nicotine addiction[108]

NAChRs, which were expressed in non-neuronal cells, have been found to be responsible for the development of other illnesses, such as cell lung carcinoma, respiratory disease, asthma, chronic bronchitis, tumours, skin aging, arteriosclerosis, megacystis-microcolon-intestinal hypoperistalsis syndrome and Chron's disease. Advances in the understanding of the structure, function and the distribution of nAChRs in the CNS and non-neuronal cells are required to understand the role that these receptors may play in the human physiology [119].

I/1.9.1. Tobacco Dependence

Tobacco dependence is the most common substance abuse disorder and preventable cause of death in the United States [120]. Over three million smoking related deaths are reported annually worldwide [120]. Smoking contributes to coronary heart disease, stroke, vascular disease, chronic lung disease and lung cancer. Although the dangers of smoking are well known, people continue to smoke and tobacco use is increasing in many developing countries [121]. Even though tobacco smoke contains more than 4,000 chemical compounds, the alkaloid nicotine is recognized as the primary psychoactive ingredient in tobacco. It is considered to be responsible for the withdrawal syndrome, tolerance and dependence effects of smoking in both animals and humans [122, 123]. Nicotine **3** and other addictive drugs, such as cocaine, heroin and marijuana generate feelings of pleasure in combination with an increased level of the neurotransmitter dopamine in the nucleus accumbens (nACC) and ventral tegmental area (VTA) in the mesolymbic region which control the mesolymbic reward-pathways in humans and other species [124, 125]. A particular subunit, the β2, has been pinpointed as a critical component in nicotine addiction. Mice that lack this subunit fail to self-administer nicotine, implying that without the β2 subunit mice do not experience the positive reinforcing properties of nicotine [108].

I/1.9.2. Alzheimer's Disease (AD)

AD is a progressive neurodegenerative disorder affecting almost one in 10 individuals over the age of 65. It is correlated to deterioration of higher cognitive function and memory related dysfunctions. Clinical manifestation of AD is first observed as short-term memory, progressing to language problems, social withdrawal, and deterioration of executive function [119]. The histological hallmark of AD is the deposition of β-amyloid plaques in the limbic, cerebral cortices (mainly extra-cellular deposit) [126, 127] and the formation of neurofibrillary tangles in neurons (intra-cellularly) [128]. The major constituents of the amyloid plaques are β-amyloid peptides, derived from the proteolytic cleavage of the amyloid precursor protein (APP) that is present in almost all tissues and whose physiological functions are still

unknown [126, 127]. The most consistent and severe neurochemical abnormality associated with AD is the loss of cholinergic innervations of the cerebral cortex and hippocampus [115] ("cholinergic hypothesis") [129]. Loss of high affinity binding sites, measured in post-mortem tissue, is a consistent marker of AD [130]. Evidence indicates that α4β2 nAChRs constitute the major subtype of nAChRs lost in AD, associated with a dramatic reduction in the cortex of α4 (but not α3 or α7) nAChRs subunits [80,114,130]. These data are also supported by the observation that α4 and β2 subunit mRNA levels decrease in the frontal cortex of human brain with age [62]. Many therapeutic agents for AD are under development. The design of clinical trials has been hampered by the difficulty of identifying patients at an early stage of the disease. Even today, the only FDA approved drugs for symptomatic treatment of AD are inhibitors of acetylcholinesterase (e.g. tacrine **7** (Cognex®), donepezil (Aricept®), rivastigmine (Exelon®) and galantamine **6** (Reminyl®)) [131]. These agents do not stop the progression of the disease but rather prevent the breakdown of ACh that is released from cholinergic neurons and thereby increase the concentration of the transmitter that is able to interact with the receptors. Other strategies have been investigated to enhance the cholinergic function, such as the use of precursors, e.g. choline **4,** as well as the use of other nicotinic and muscarinic agonists. However, up to now, none of these strategies have been proven to be effective, due to poor bioavailability, limited efficacy and various side effects. In 1999, Potter et al. examined the effects of the novel selective cholinergic channel activator (ChCA) ABT-418 **10** on cognitive functioning in Alzheimer's disease [132]. Improvements were seen in non-verbal learning tasks such as spatial learning, memory and repeated acquisition [133]. These findings suggest that selective ChCAs have a potential as therapeutic agents in neurodegenerative disorders. Nevertheless, further study into AD and/or Parkinson's disease is warranted.

I/1.9.3. Parkinson's disease

Parkinson's disease is a progressive neurodegenerative disease, involving the dopaminergic neurons of the substantia nigra. [114]. It is characterized by motor

dysfunction resulting in muscular rigidity, tremor and difficulty in initiating and sustaining movement. In addition to the movement disorder, PD patients often show cognitive impairment or dementia due to the loss of cholinergic transmission [134]. Receptor binding studies with (-)-[^{3}H]nicotine demonstrated a decrease of up to 50% ligand binding site in the frontal and temporal cortex and hippocampus. These regions are associated with memory and teaching [80]. Nicotine administration may be neuroprotective in animal models of nigrostriatal degeneration. In fact, smokers were observed to have a lower incidence of PD than the rest of the population, with half the risk of developing PD [135]. Prolonged nicotine administration prevents neuronal dopaminergic degeneration and increases synaptic dopamine levels in the substantia nigra and striatum [133]. These positive effects are probably due to an inhibition of dopamine breakdown by MAO-B [136]. With regard to the nAChRs subtype involved, recent evidence suggests the participation of the synaptic α4-containing receptors [137]. In fact, the nicotine analogue, SIB-1508Y **11**, selective for the α4β2 nAChRs demonstrated to be active in experimental models of PD [138]. The neuroprotective effects of nicotine also involve the activation of α7 receptors [134, 139]. Stimulation of this nAChRs subtype determines a Ca^{2+} influx that triggers a wide range of processes, including an increase of neurotrophic factors in the brain [139].

I/1.9.4. Dementia with Lewy Bodies

Dementia with Lewy Bodies is reported (after Alzheimer's) to be the second most common degenerative disease associated with ageing [140]. It is characterized by a loss of nicotinic receptors from dopaminergic neurons, and a higher reduction of nicotine binding in the parietal cortex and in the reticular nucleus [140].

I/1.9.5. Tourette's syndrome

Gilles de la Tourette's syndrome (TS) is a neuropsychiatry disorder of unknown aetiology and is probably transmitted in an autosomal dominant manner. It is generally diagnosed before the age of 18 and involves severe learning difficulties, persistent motor and verbal tics; as well as anxieties, phobias or obsessive-

compulsive disorders [25,39,141]. The pathogenesis is not yet known. The disease is believed to be associated with abnormal dopamine-transmission in the basal ganglia via a receptor hypersensibilitation. A number of studies support the thesis that oral or transdermal administration of nicotine may enhance cognition, thus ameliorating the symptoms of TS in therapy with neuroleptics such as haloperidol [142-144]. The underlying mechanistic principle for using nicotine with beneficial effects in TS is still unclear. It may possibly involve modulation of dopamine release or is related to a desensitization and eventually permanent inactivation of nAChRs (in particular α4β2 and α7 nAChRs) [25, 145]. Studies with antagonists such as mecamylamine **12** or agonists with desensiting properties are therefore of great interest [143].

I/1.9.6. Schizophrenia

Schizophrenia is a common and complex disorder with diverse symptoms including auditory hallucinations, delusion and flat affect [146]. Neuronal nicotinic receptors have been implicated in the occurrence of schizophrenia on the basis of several reasons. The first is due to the high incidence of tobacco smoking in patients effected by this disease, which was 90% compared to 30% of the control group [147, 148]. Secondly, [^{125}I]-α-Bgt binding sites in the hippocampus have been reduced in post-mortem tissue [117, 149]. Finally, the linkage between auditory P50 deficits and the region of chromosome 15 coding the α7 nAChR subunit has to be taken into account [146]. In fact, P50 auditory evoked potential gating deficit is a neuronal defect, considered to be characteristic of schizophrenia. The inheritance has been linked to a dinucleotide polymorphism at chromosome 15 q13-14 that is also the locus for the α7 subunit gene [149].

I/1.9.7. Epilepsy

Epilepsy affects around 1% of the general population [39]. Autosomal dominant nocturnal frontal lobe epilepsy (ADNFLE) is the human idiopathic epilepsy that was first linked to specific gene defects. It has been associated with mutations in the gene coding for either the α4 or β2 subunit of the nAChRs [150]. The gene coding for the α4 subunit is located on chromosome 20(20q.13.33) and the gene coding for β2 subunit is

on chromosome 1q.23.1. To date, five different mutations that lead to ADNFLE have been identified in different families [116, 151, 152]. It is genetically transmitted in an autosomal dominant mode [153]; this indicates that sufferers are heterozygous for this locus and carry one normal and one mutated allele. ADNFLE is characterized by a seizure that originates from the frontal lobe during sleep. In more than half of the patients, the seizures start in the first or second decade of the expected lifetime [151, 154]. One minor locus has been identified for this disorder, but additional loci are still to be discovered [152].

I/1.9.8. Depression

A considerable body of evidence shows a positive correlation between nicotine dependence and major depression [132, 155]. Bupropion, originally marketed as an atypical antidepressant, was the first non-nicotine drug that demonstrates efficacy in the treatment of tobacco dependence (Wellbutrin®; GlaxoSmithKline) [156]. Individuals with major depression may use nicotine **3** as a form of self-medication, since nAChR activation enhances the release of some neurotransmitters (norepinephrine (NE), dopamine (DA), serotonine (5-HT) that are reduced in depression [119]. Various antidepressants act through modulation of the biogenic amine neurotransmitter pathway, e.g. MAO-inhibitor drugs. MAO A and B are enzymes with different substrate and inhibitor specifities, responsible for breaking down the biogenic amine neurotransmitters norepinephrine, serotonine, and dopamine. Recently, it has been shown that smokers have reduced levels of MAO, both in peripheral organs as well as in the brain [136].

I/1.9.9. Pain

In the U.S.A., more than 100 million people will suffer from moderate to severe pain within any year [118]. There are several therapeutic approaches towards pain relief, and the most powerful agents so far are those that bind to opioid receptors and inhibitors of cyclooxygenase (NSAIDs). Both general classes of agents have undesirable side effects. This has prompted a search for mechanistically different analgesic agents.

Activation of the cholinergic pathway through smoking and nicotine has been shown to reduce pain in humans. The analgesic effect of nicotine **3** was first reported in the early 1930s. However, interest in nAChRs agonists as potential analgesics emerged after the discovery of the frog alkaloid, (±)-epibatidine **13** by Daly et al. The antinociceptive effect of (±)-epibatidine **13** is 200 times stronger than morphine by acting on nAChRs rather than on opioid receptors [157]. Although analgesic properties of (±)-epibatidine **13** and other nAChRs agonists have been known for many years, high toxicity has reduced the therapeutic potential of these drugs. The receptor, which seems to be involved with antinociception, is composed of α4β2 [118]. Selective compounds have been designed that show a separation of antinociception from toxic effects, which seems to be correlated with selectivity for the brain nACh receptors over the ganglionic and neuromuscular subtypes [158]. One such example is ABT-594 **14**, highly selective for α4β2* nAChRs. It has more than 5 fold greater separation between antinociceptive and lethal doses than epibatidine [118, 159]. Due to its improved safety profile, ABT-594 **14** is currently in Phase II clinical trials as analgesic. The role of nAChRs in analgesia is further supported by the discovery that nicotinic antinociception is reduced in α4 and β2 knockout mice. Marubio et al. identified the particular subunit involved in analgesic processes by generating mice with a deficiency of the α4 subunit and studying these together with previously generated mutant mice lacking the β2 nAChRs subunit [102]. However, there is evidence that other subtypes may also be involved [102].

I/1.9.10. Inflammation

The immune system is responsible for the involuntary setting in motion of inflammatory responses [160]. Excessive inflammation and the tumour-necrosis factor (TNF) synthesis cause morbidity and mortality in the form of several human diseases, including endotoxaemia, sepsis, rheumatoid arthritis and inflammatory bowel disease [160,161]. Through a "cholinergic anti-inflammatory pathway", acetylcholine can inhibit the release of macrophage TNF in the nervous system significantly and rapidly. The α7* nAChRs is the nAChR subtype considered to be

involved to attenuate systemic inflammatory responses inhibiting excessive inflammation and tumour-necrosis factor (TNF) release [162,163].

I/1.9.11. Ulcerative colitis

Several epidemiological studies report that smoking has predictable effects on inflammatory bowel disease (IBD) [164, 165]. It is beneficial in ulcerative colitis (UC) but deleterious in Chron's disease (CD) [164, 166]. The positive effects of smoking have been attributed to nicotine, but the mechanisms that underlie the adverse effect are still under investigation [167]. As nicotine delays the developing of ulcerative colitis and improves the clinical pattern, transdermal nicotine could be used therapeutically as a drug for this disease [161]. In contrast, smoking and passive smoking increase the risk of developing CD. These effects could be due to the different influences of nicotine on the autonomic nervous system [167].

I/2. Modulators on nAChRs

I/2.1. Nicotine and its pharmacological action in the ANS and CNS

(S)(-)-Nicotine **3** is the natural ligand that gives the name to the receptor. (S)(-)-Nicotine stimulates nicotinic receptors found on muscle cells, within autonomic ganglia and within the central nervous system [168].

I/2.2.1. Nicotine as ganglionic stimulating drug

In the peripheral nervous system and within autonomic ganglia, the pharmacological actions of (-)-nicotine **3** are complex. In fact, (-)-nicotine **3** acts on both sympathetic and parasympathetic ganglia and its stimulation is frequently followed by depolarisation blockade. The effects of (-)-nicotine **3** include:

- Stimulation of the release of epinephrine from the adrenal medulla.
- Excitation of the cardiorespiratory reflexes by a direct effect on the chemoreceptors of the carotid and aortic bodies.
- Excitation of cardiovascular responses secondary to evoked blood pressure changes mediated by baroreceptors.
- Stimulation and blocking of CNS cholinergic pathways in the medulla influencing heart rate.

Activation of autonomic ganglia in the CNS causes tremors, which leads to convulsions as the dose is increased. Another nicotine effect in the central nervous system (CNS) is the stimulation of the area postrema i.e. the chemoreceptor trigger zone that induces vomiting [169].

Nicotinic receptors in ganglia can be blocked by ganglionic blockers, such as hexamethonium **15,** trimethapan **16** and mecamylamine **12** (Fig. I/2.1). These structures possess different mechanism of action. Hexamethonium **15** and related agents interfere with the ACh receptor directly, blocking the ion channel. Trimetaphan **16** and mecamylamine **12** are competitive antagonists. They block ganglionic transmission in ANS by competition with ACh **1.** Trimethaphan **16** has

two direct effects: vasodilatation and histamine release, therefore it has been used to induce controlled hypotension (Fig. I/2.1).

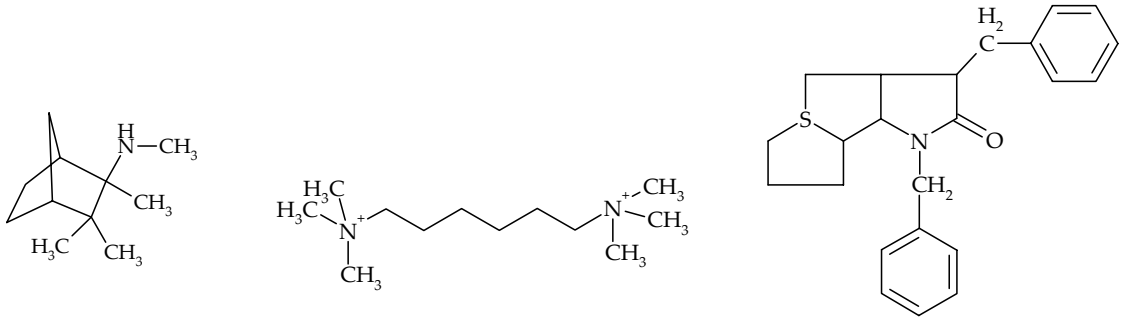

12 **15** **16**

Figure I/2.1: Structures of the ganglionic blockers: mecamylamine **12**, hexamethonium **15** and trimethapan **16**

I/2.1.2. Nicotine as CNS stimulating drug

(-)-Nicotine **3** acts on nAChRs widely distributed in the brain. Low doses of (-)-nicotine **3** (6-8 mg) facilitate relaxation and cause mild euphoria. (-)-Nicotine **3** also causes acetylcholine and norepinephrine levels to raise facilitating performance and memory ability, so improving attention as well as problem-solving skills. Its increasing dopamine level causes pleasure enhancement. The release of endorphins reduces anxiety and tension, whilst weights gain decrease by appetite reduction.

I/2.1.3. Potential therapeutic effects of nicotine

In the past, nicotinic acetylcholine receptor ligands were used only as ganglioplegic, for the management of hypertension, or as neuromuscular blockers. Only the peripheral effect of nicotine stimulation was taken under consideration [170]. The potential therapeutic actions of nicotine and its use as a drug are, like some other natural compounds, limited by some detrimental effect (neuromuscular paralysis, respiratory distress, hypertension, hypothermia, emesis and dependence). The collateral effect is due to the lack of nicotine's ability in discriminating between activation of receptors in the ANS (sympathetic and parasympathetic ganglia) and neuromuscular junction. In recent years, interest in the field of neuronal nicotinic receptors has grown. The pharmacological effect elicited by (-)-nicotine **3** in the

central nervous system have been taken into consideration in view of the involvement of nicotine in many neurodegenerative diseases. Synthetic and semi-synthetic new compounds, based mostly on the structure of natural products of plants and animals, have been synthesized and investigated in order to improve potency and selectivity and to reduce the toxicity.

I/2.2. Modulators on nAChRs (small ligand based)

Choline (Ch)

Choline **4** is the precursor and metabolite of acetylcholine **1** (Fig. I/2.2). It is a full agonist for α7* nAChRs (EC_{50} = 1.6 mM) even if it presents very low affinities for α4β2* (K_i = 112 μM) and α7* nAChRs (K_i = 2.2 mM) in binding assays [171]. Although its concentration in the brain is not exactly known, it is accepted that at concentrations above 200 μM, choline **4** activates α7* receptors [171]. There are some speculations that choline **4** rather than acetylcholine **1** was the natural transmitter for α7*, and that the evolution to ACh **1** was in part caused by the need to have a "two step transmitter", i.e. a rapidly acting, rapidly inactivable one (ACh) **1** and a more slowly removed one (choline) **4** [172].

Acetylcholine (ACh)

The neurotransmitter acetylcholine (ACh) **1** is the endogenous agonist for nAChRs and mAChRs (Fig. I/2.2). Acetylcholine **1** binds with high affinity at α4β2* (K_i = 10 nM) [173], α3β4* (Ki = 560 nM) [174] and muscle type (Ki = 15 nM, *Torpedo californica*, [^{3}H]ACh) [175], but with lower affinity to α7* (K_i = 4,000 nM). Its utility as nicotinic ligand is limited by its lack of selectivity for nAChRs versus muscarinic and its susceptibility to hydrolysis.

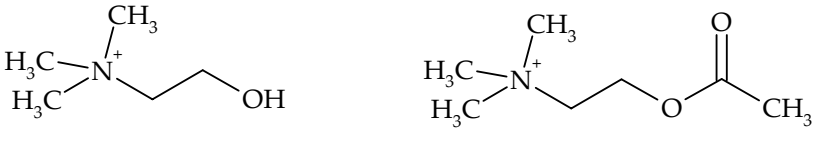

4 **1**

Figure I/2.2: Structures of the endogenous ligands choline (Ch) **4** and acetylcholine (ACh) **1**

Structural analogues of Acetylcholine

Modification of the ammonium group e.g. replacement of one N-methyl by an ethyl group permits retention of cholinergic activity, while a replacement by a longer substituent, such as a n-propyl or n-butyl group causes almost a complete loss of cholinergic activity. [176]. The presence of a methyl in α-position (Fig. I/2.2) enhances the nicotinic activity versus the muscarinic.

CCh, MCC, DMCC

Stabilization of the ester group of ACh as a carbamate group gives the hydrolysis resistant analogue carbamylcholine **17** (carbachol, CCh). CCh has been widely used as a mAChR agonist although it possesses a moderate affinity to neuronal α4β2* nAChRs (Ki = 750 nM) [177]. Introduction of one or two methyl groups at the carbamate nitrogen of CCh **17** gives N-methylcarbamoylcholine (MCC) **18** and N,N-dimethylcarbamoylcholine (DMCC) **19** respectively (Fig. I/2.3), which display nanomolar binding affinities to nAChRs and a high degree of selectivity for nicotinic versus muscarinic ACh receptors (neuronal / muscarinic ratio is 7 for MCC **18** and 60 for DMCC) **19** [177].

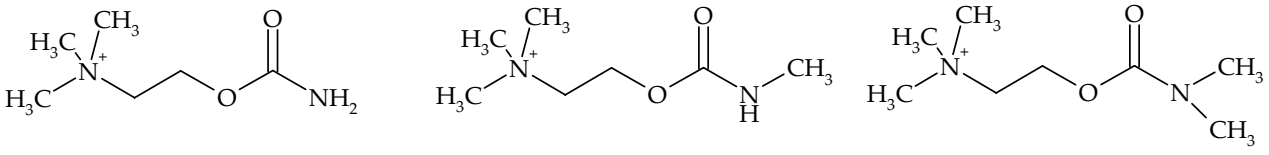

Carbachol CCh **17** MCC **18** DMCC **19**

Figure I/2.3: Analogues of acetylcholine: CCh **17,** MCC **18** and DMCC **19.**

(S)(-)-AR-R17779 **20** *Spiro[1-azabicyclo[2.2.2]octane-3,5´-oxazolidin-2´-one]* is a conformationally restricted analogue of acetylcholine (Fig. I/2.4). It is a full agonist for the α7* nicotinic receptor (efficacy = 96% compared to ACh). [178] and twice as potent as (-)-nicotine **3** in activating ion current at α7 receptor expressed in *Xenopus* oocytes. Its (S) enantiomer possesses selectivity for the α7* receptor versus the α4β2*

nicotinic receptor (Ki = 92 nM for α7* and Ki = 16,000 nM for α4β2*) [178]. Introduction of a methyl group to the amide nitrogen reduces the affinity for α7* (Ki = 220 nM) increasing that for α4β2* (Ki = 200 nM) [178].

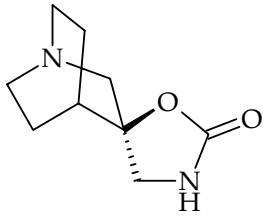

Figure I/2.4: (-) AR-R17779 **20**

(-)-Nicotine

(-)-Nicotine **3** *(S)-3-(1-methyl-2-pyrrolidin-yl)-pyridin* binds with high affinity to α4β2* nAChRs using (±)-[^{3}H]epibatidine (K_i = 0.838 nM) in competition experiment [179]. However, a lower affinity was shown towards the α7* nAChR (K_i = 127 nM) when tested in competition assays with [^{125}I]α-Bgt and a micromolar affinity (K_i = 1 μM) was shown using [^{125}I]α-Bgt and *Torpedo californica* [180]. (-)-Nicotine **3** is widely used in behavioural studies because it can readily cross the blood brain barrier and its pharmacokinetics is well documented. But its utility as a tracer for *in vivo* imaging (PET and SPECT) of nAChRs in the human brain was hindered due to its rapid clearance and relatively low affinity [181,182]. (-)[^{3}H]Nicotine is also used in radioligand binding assays to label primarily the *α*4β2* [74] but it has some negative aspects, due to its instability, high non-specific binding and light sensitivity [183].

Structural analogues of nicotine

Since the discovery of the potentially therapeutic use of (-)-nicotine **3** and nicotinic derivatives for treatments of a variety of cognitive disorders, different scientists have focused their attention on developing novel analogues of this alkaloid **3**. Synthetic modifications at different positions of the skeletal structure of **3** have been carried out in order to improve the potency, selectivity, and stability as well as to reduce its toxicity (Fig. I/2.5) [184]. The question was to find out the structural features required for the high affinity binding of nicotine related compounds. Four principal parts of the (-)-nicotine **3** structure were investigated:

a: pyridine ring

b: substituent at pyrrolidine nitrogen

c: chiral centre

d: pyrrolidine ring

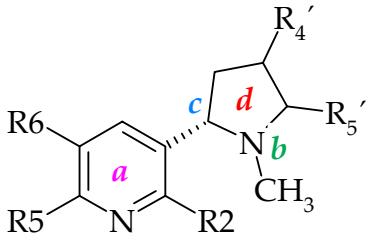

Figure I/2.5: Structure of (S)(-)-nicotine **3** and its possible sites of substitution.

Only small substituents in position 5 and 6 at the pyridine ring are tolerated and can even slightly improve the affinity in comparison to (-)-nicotine **3** [185] (Fig. I/2.5 part a). Bromine and methoxy substitution at position C-5 of the pyridine moiety [186] despite their high affinity (K_i = 6.9 and 14.3 nM, (-)-[^{3}H]nicotine, rat brain) do not show antinociceptive, hypolocomotor or hypothermic effects in mice. Introduction of a halogen at position C-6 markedly enhances α4β2* affinity, (6-Br > 6-Cl > 6-F) (K_i = 0.45, 0.63, and 1.3 nM)[187]. Small aliphatic and alkyl moieties are accepted at this position, whereas a decrease in affinity is observed upon the introduction of a polar group, such as a hydroxyl moiety at position C-6 (K_i = 1062 nM) [187, 188]. As far as substitutions at the pyrrolidine nitrogen are concerned, it has been demonstrated that both (R) and (S)-nornicotine **21** bind to the agonist site in the brain with 10- to 20-fold lower affinity than (-)-nicotine **3** (Fig. I/2.5 part b). N-alkyl substitutions on the cationic side are detrimental for the affinity to α4β2* [184], confirming that an N-methyl substituent might be optimal for the binding of (-)-nicotine **3** to the receptor. Since (-)-nicotine **3** possesses a chiral atom, the ability of the two enantiomers to interact with the receptor has been investigated. It has been found that (S)-nicotine is 10-100 fold more potent than the (R)-enantiomer [13] (Fig. I/2.5 part c). With regard to the pyrrolidine ring, its aromatisation or opening has been proved to be detrimental to the affinity [189, 190]. Damaj and co-workers found that an intact pyrrolidine ring would seem to be indispensable for nicotinic activity [184]. Introduction of a large substituent at the R4′ and R5′ positions in the pyrrolidine ring is detrimental to the binding affinity (Fig. I/2.5 part d) [191]. In the last years, some interesting analogues of (-)-nicotine **3** have been synthesized and tested.

SIB-1508Y **11** *3-ethynyl-5-(1-methyl-pyrrolidin-2-yl)-pyridine* (Altinicline) [185, 192] is a 5-substituted nicotine derivative characterized by a 5-ethinyl group (Fig. I/2.6). It possesses high affinity (K_i = 3 nM) for (-)-[^{3}H]nicotine binding sites in the rat brain. Given the ability to stimulate release of dopamine from rat striatum, it is under clinical evaluation for the treatment of Parkinson's disease [193, 194].

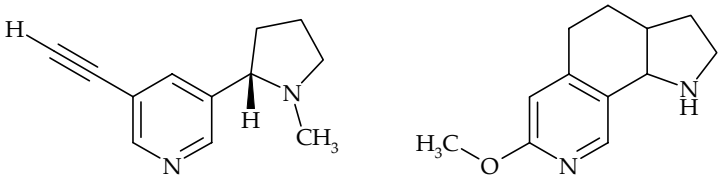

SIB-1508Y **11** SIB-1663 **22**

Figure I/2.6: Structures of SIB-1508Y **11** and SIB-1663 **22**

SIB-1663 **22** *7-methoxy-2,3,3a,4,5,9b-hexahydro-1-H-pyrrolo[3,2-h]isoquinoline* is a novel conformational restricted analogue of nicotine, (IC_{50} =1.9 μM) ((-)-[^{3}H]nicotine in rat brain) [195] (Fig. 2.6). Mecamylamine **12,** DH*β*E **36,** atropine or naloxone do not block the analgesic activity of this constrained derivative. Therefore its pain-relieving function might be due to interactions with a different binding site which is not labelled by (-)-[^{3}H]nicotine [184].

SIB-1553A **23** *4-[2-((S)1-methyl-pyrrolidin-2-yl)ethylsulfanyl]phenol* is a derivative of (-)-nicotine **3**. A thio-ethyl connector was introduced to separate the pyrrolidine ring from a phenol ring (Fig. I/2.7). SIB-1553A **23** represents a pharmacological tool to explore the function of specific nAChR subtypes, given the fact that it is presently one of the few β4 subunit-selective ligands described in literature [196].

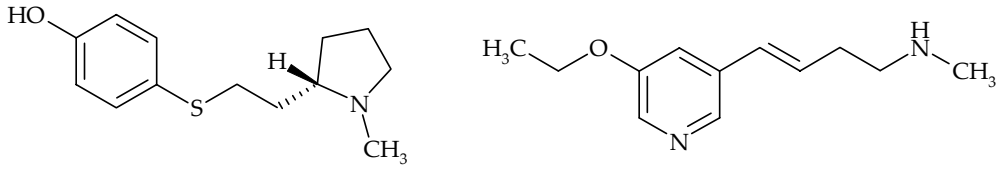

SIB-1553A **23** TC-2559 **24**

Figure I/2. 7: Structures of SIB-1553A **23** and TC-2559 **24**

TC-2559 **24** *4-(5-ethoxy-pyridin-3-yl]-but-3-enyl]methyl-amine* is a metanicotine analogue described by the Targacept company (Fig. I/2.7). This compound is

reported to be markedly selective for neuronal nAChRs (K_i = 5 nM α4β2*, (-)-[^{3}H]nicotine, rat brain thalamic tissue) compared to ganglionic and peripheral nAChRs (selectivity ratio for central nervous system (CNS) to peripheral nervous system (PNS) > 4,000) [197].

ABT-418 **10** *3-methyl-5- ((S)-1-methyl-pyrrolidin-2-yl)-isoxazole* is an isoxazole isostere of nicotine (Fig. I/2.8) [198].

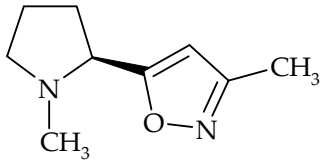

ABT-418
10

Figure I/2.8: Structure of ABT-418 **10**

ABT-418 **10** possesses improved functional selectivity for α4β2* (K_i = 4.2 nM) [199] over synaptic ganglionic-like nAChRs [13, 200]. ABT-418 **10** is effective in compensating cognitive deficits associated with lesions in the forebrain cholinergic system and in exerting anxiolytic activities with reduced side effects [201]. Other substitutions than the methyl group of the heteroaromatic ring have shown that the ABT-418 **10** almost loses affinity towards α4β2* nAChRs subtypes. Exchanging the isoxazole with an isothiazole moiety leads to compounds with lower affinity for α4β2* (12-54 fold lower) [185].

Pyridyl Ethers

Introducing a methyl ether moiety between the pyridyl and the pyrrolidinyl moiety of nicotine leads to pyridyl ether derivatives showing subnanomolar affinities for central neuronal nicotinic receptors (Fig. I/2.9) [202].

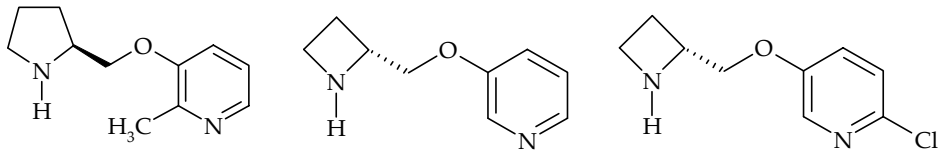

ABT-089 **25** A-85380 **26** ABT-594 **14**

Figure I/2.9: Structures of the pyridyl ether derivatives, ABT-089 **25,** A-85380 **26** and ABT-594 **14**

Among these, ABT-089 **25** *2-methyl-3-(S)-1-pyrrolidin-2-ylmethoxy)-pyridine* is a cholinergic channel modulator (Fig. 2.9). In radioligand binding studies, ABT-089 **25** was shown to display selectivity towards the α4β2* nAChRs (K_i = 16.7 nM) relative to the α7* (K_i = 10000 nM) and $(\alpha 1)_2\beta 1\gamma\delta$ nAChRs subtype (K_i = > 1000 nM) [203]. It possesses a high oral bio-availability, excellent safety and behavioural efficacy [204]. On the basis of its neuroprotective properties against an excitotoxic insult (glutamate and β-amyloid) and its cognitive enhancing activity in rodents and primates, it was selected for advanced preclinical evaluation.

A-85380 **26** *3-((R)-1-azetidin-2-ylmethoxy)-pyridine* (Fig. I/2.9) has been identified as a high-affinity nAChR ligand [202]. In radioligand binding studies it has been shown to be a potent and selective ligand for the human α4β2* nAChR subtype (K_i = 0.05 nM) relative to the human α7* (K_i = 148 nM) and the muscle $(\alpha 1)_2\beta 1\gamma\delta$ subtype expressed in Torpedo electroplax (K_i = 314 nM)[205]. Functionally, A-85380 **26** is a potent activator of cation efflux on the human α4β2* (EC_{50} = 0.7 μM) and ganglionic (EC_{50} = 0.8 μM) subtypes, effects that are attenuated by pre-treatment with mecamylamine (10 μM). In all cases, A-85380 **26** is more potent than (-)-nicotine but less potent than (±)-epibatidine [202].

ABT-594 **14** *5-((R)-1-azetidin-2-ylmethoxy)-2-chloro-pyridine* is a chloro analogue of A-85380 [158] (Fig. I/2.9) and a potent inhibitor of the binding of (-)-[^{3}H]cytisine to α4β2* neuronal nAChRs (K_i = 37 pM, rat brain) [206]. At the $(\alpha 1)_2\beta 1\gamma\delta$ neuromuscular nAChR, ABT-594 **(14)** has a Ki value of 10,000 nM (labelled by [^{125}I]α-Btx), resulting in a greater than 180,000-fold selectivity for the neuronal α4β2* over muscle type nAChR. It has been developed as a promising nonopioid analgesic having affinity for α4β2* nAChRs comparable to that of epibatidine, but lacking its toxicity [159]. Like the parent compounds nicotine and epibatidine, ABT-594 **14** establishes increased response latencies in the hot-plate test in rats (0.05 and 0.1 mg/kg s.c.) but causes hypothermia and dose-dependent increase in blood pressure [206]. Both the antinociceptive and toxic effects (hypothermia and hypertension) were abolished by pre-treatment with the brain blood barrier (BBB) penetrating neuronal nAChR

antagonist mecamylamine **12**, demonstrating that these actions of ABT-594 **1** were mediated via activation of neuronal nicotinic receptors [118]. At present, ABT-594 **14** is in Phase II clinical trials as analgesic.

Anabasine and Anabaseine

Anabasine **27** like nicotine **3** is a natural alkaloid present in tobacco plants. On the other hand, anabaseine **28**, whose structure resembles that of anabasine **27,** is an alkaloid isolated from an animal toxin (a marine worm, and in certain species of ants) [207](Fig. I/2.10). They differ structurally only at the 1,2 piperidine ring (anabaseine has a double bound) [208]. Anabaseine **28**, compared to (-)-nicotine **3** and anabasine **27**, displays the greatest efficacy and affinity at α7* receptors (efficacy EC_{50} = 6.7 μM, K_i = 58 nM rat brain, [^{125}I]α-Bgt) [209].

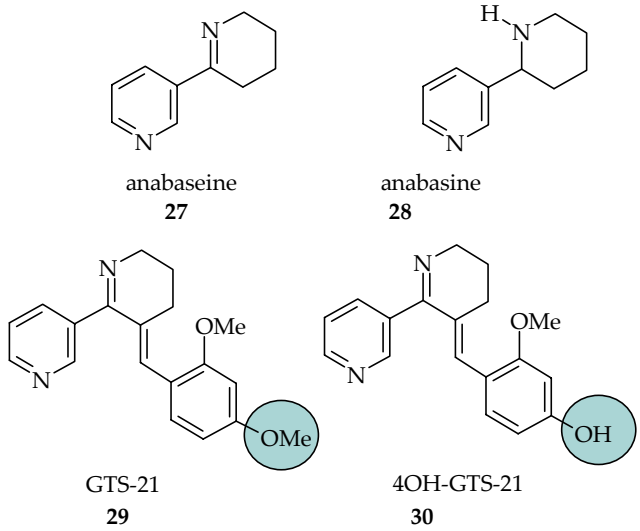

Figure I/2.10: Structures of anabasine **27** anabaseine **28** and its derivatives GTS-21 **29** and 4OH-GTS **30**[207]

GTS-21 **29** (DMXBA) *3-(2,4)-dimethoxybenzylidine)anabaseine* (Fig. I/2.10) is an anabaseine derivative, also known as DMXBA. It shows nanomolar affinities for both α4β2* (K_i = 85 nM) and α7* nAChRs (K_i = 212 nM) [75, 209]. GTS-21 **29** and its main metabolite in primates, 4-OH-GTS-21 **30** also known as HMBA [174] are both potent and selective agonists for the α7* type nicotinic acetylcholine receptor [174, 210, 211]. They appear to be neuroprotective through the selective activation of the α7* subtype nAChR [86]. GTS-21 **29** has recently passed through Phase I clinical trial for use in Alzheimer's disease as a cognition-enhancing agent [212].

(-)Lobeline

(-)Lobeline (α-lobeline) **31** *2-[6-((S)-2-Hydroxy-2-phenyl-ethyl)-1-methyl-piperidin-2-yl]-1-phenyl-ethanone* (Fig. I/2.11) is a lipophilic alkaloid from the Indian tobacco *Lobelia inflata*. In its structure (-)-Lobeline **31** contains a 2,5-disubstituted piperidine. It binds with high affinity to α4β2* nAChRs (K_i = 1.4 - 2 nM) and very low affinity to α7* nAChRs (K_i = 10,000 nM). In the past, it has been classified as an agonist at nAChRs. Despite its atypical structure, (-)-lobeline mimics some pharmacological effects of nicotine (self-administration by animals, antinociceptive effects and hypolocomotion) [213, 214]. There are indications that lobeline may be useful in memory and learning disorders and for the treatment of anxiety. Furthermore, (-)-lobeline **31** has been used in the treatment of smoking cessation [168,214]. However, more recent studies indicate that lobeline inhibits nicotine-evoked dopamine release and (-)-[^{3}H]nicotine binding, thus acting as a competitive, non-selective antagonist at α4β2* and α3β2* nAChRs [215] (Fig. I/2.11). SAR studies have shown that both aromatic rings are required for optimal affinity. Analogues lacking one oxygen atom bind with lower affinity to (-)-[^{3}H]nicotine binding sites [213]. The presence of the carbonyl oxygen, serving as a potential hydrogen bond acceptor, seems to be optimal for nACh receptor affinity [216].

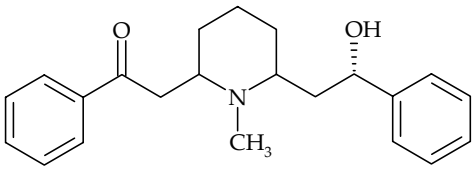

Figure I/2.11: Structure of lobeline **31**, a lipophilic alkaloid from the Indian tobacco *Lobelia inflata*.

I/2.2.1. Azabicyclic compounds

Epibatidine

The discovery of (±)-epibatidine **13** *(exo-2-(6-chloro-3-pyridyl)-7-azabicyclo-[2.2.1]heptane)* (Fig. /2.12) and its potent analgesic activity has had an enormous impact on research on nicotinic receptors and ligand development. However, (±)-

epibatidine **13** shows significant side-effect liabilities associated with potent activity at the ganglionic and neuromuscular nAChR subtypes, which limits its potential as a clinical entity. The presence of this alkaloid was revealed accidentally during a routine toxicity assay. The methanolic extract from an Ecuadorean frog (Fig. I/2.12), collected during an exploratory trip to Western Ecuador in 1974 by Daly and Myers, injected into a mouse, showed a drug reaction known as the Straub tail. These first assays led to the isolation of this alkaloid whose structure was revealed in 1992 by NMR analysis [217].

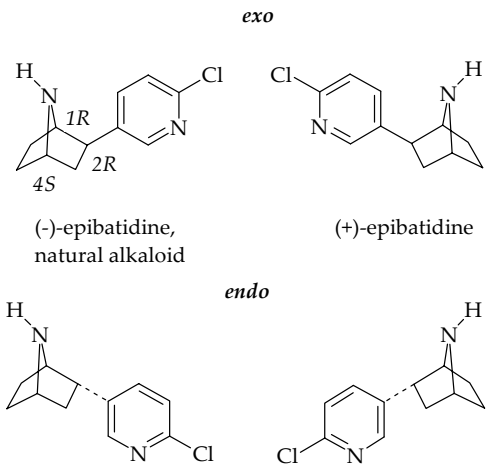

Figure I/2.12: The Ecuadorian frog and the structure of (±)-epibatidine **13** and its stereoisomers.

(±)-Epibatidine **13** is a potent nAChR modulator and possesses a 200-fold higher analgesic effect than morphine in the hot-plate test. The high analgesic activity is mediated through the nicotinic cholinergic receptor and was not due to an opioid or cholinergic muscarinic mechanism of action, as evidenced by the inability of naloxone and scopolamine to prevent it [218]. (±)-Epibatidine **13** binds to the α4β2* nAChR subtype in rat brain membranes with high affinity (K_i = 8 pM) [179]. In 1995, the binding of tritiated epibatidine was characterised. (±)-[^{3}H]Epibatidine has proved to be a very useful radioligand for monitoring a variety of defined nAChR subtypes in heterologous expression systems [173]. Zoli and colleagues identified, in a comparative analysis of nicotinic radioligand autoradiography, another high affinity (±)-[^{3}H]epibatidine binding site that persisted in mice lacking the β2 subunit, and assigned the subunit composition α3β4* [74]. (±)-[^{125}I]Epibatidine, in which the chlorine

atom of epibatidine is replaced by [^{125}I], has become available and provides a higher specific activity ligand for labelling minor populations of binding sites [219]. (±)-[^{125}I]Epibatidine possesses lower affinity in mouse brain homogenates when compared to (±)-[^{3}H]epibatidine (K_D = 50 and 8 pM, respectively) [179, 220]. The slight reduction in affinity presumably reflects the effect of substituting a ^{125}I for a chlorine atom. Nevertheless, the properties of the iodinate epibatidine in showing a slightly lower affinity than the tritiated form may be helpful in ameliorating ligand depletion problems associated with high affinity ligands [221].

Epibatidine analogues

Epiboxidine **32** *(exo-2-(3-methyl-5-isoxazolyl)-7-azabicyclo[2.2.1]heptane)* is an interesting synthetic analogue of the alkaloid (±)-epibatidine **13**. It represents a hybrid between (±)-epibatidine **13** and ABT-418 **10** [222] (Fig. I/2.13). Although not as potent as (±)-epibatidine **13**, epiboxidine has a higher affinity (K_i = 0.6 nM, α4β2*nAChRs) to nAChRs than nicotine (K_i = 0.838 nM, α4β2* nAChRs) [179] and ABT-418 **10** (K_i = 4.2 nM) [199]. In a hot-plate antinociceptive assay with mice, epiboxidine **32** was about 10-fold less potent but also 20-fold less toxic than (±)-epibatidine **13** [222].

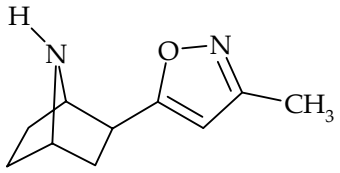

Figure I/2.13: Structure of epiboxidine **32,** a potent nicotinic receptors agonist.

Several analogues of (±)-epibatidine **13**, in which the azabicycloheptane ring has been expanded, have been synthesized and tested. These include, for example homoepibatidine (**33**) [223] and the analogue 3-(6-chloro-3-pyridazinyl)-3,8-diazabicyclo[3.2.1]octane **34** [224,225] (Fig. I/2.14). Interestingly, compound **33** possesses analgesic potency comparable to that of (±)-epibatidine **13** at doses 4-fold higher (40μg/kg) [223], and its binding affinity is in the picomolar range (K_i = 0.23 nM) [226]. Compounds **34**, bearing a diazabicyclo[3.2.1]octane skeleton, showed high affinity (K_i

= 4 nM, [^{3}H]cytisine, rat brain) for α4β2*nAChRs, an apparent high degree of selectivity (EC_{50} = > 1,000 μM, in muscle type cell line TE671) and also analgesic potency at low dose (1 mg/kg) [224]. The idea of synthesizing this compound originated partly from research aimed at discovering analgesics agents. As a final point, this study verified that the 8-azabicyclo ring system can substitute the 7-azabicyclo-heptane ring and can provide compounds with reduced binding affinities relative to (±)-epibatidine **13** but maintaining pharmacologically relevant potencies.

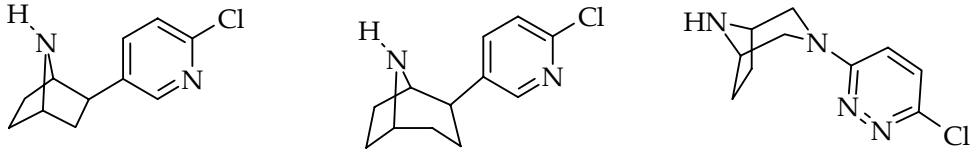

13 **33** **34**

Figure I/2.14: Structure of epibatidine **13** and homoepibatidines **33** and **34**.

Ferruginine

(+)-Ferruginine **Fe 1** is a potent neurotoxin containing an 8-azabicyclo[3.2.1]octene skeleton (Fig. I/2.15). This alkaloid was isolated from the arboreal species Darlingiana ferruginea (J. F. Bailey) and Darlingiana darlingiana (F. Muell). The unnatural enantiomer (-)-ferruginine, an analogue of anatoxin-a **An 1**, was used as a new lead compound for structure-activity relationships on nAChR agonist binding site and to develop new potent nAChR ligands bearing diazine moieties [227, 228].

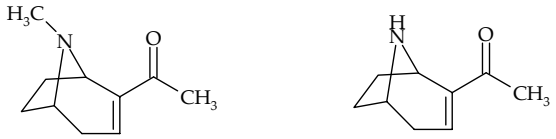

Fe 1 **Fe 2**

Figure I/2.15: Structures of ferruginine **Fe 1** and its demethylated analogue, nor-ferruginine **Fe 2**.

Anatoxin-a

Anatoxin-a **An 1** is a natural alkaloid; a toxin isolated from fresh-water cyanobacteria, Anabaena flos-aquae [198] (Fig. I/2.16). It is a small bicyclic compound, very soluble in water. Wright et al. developed an anatoxin-a/epibatidine hybrid **UB-**

165 [229], comprising the azabicyclononene bicycle of anatoxin-a **An 1** and the chloropiridyl moiety of (±)-epibatidine **13**.

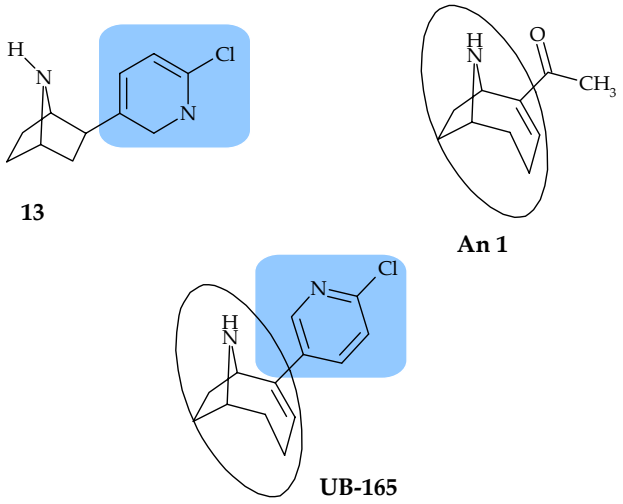

Figure I/2.16: Structures of anatoxin-a **An 1,** (±)-epibatidine **13** and the anatoxin-a/epibatidine hybrid **UB-165** [229]

UB-165 is a potent neuronal nicotinic acetylcholine receptor (nAChR) ligand that displays functional selectivity between nAChR subtypes. It shows intermediate potency, compared with the parent molecules (±)-epibatidine **13** and anatoxin-a **An 1,** at α4β2* and α3-containing binding sites.

I/2.2.2. Other nAChR ligands

Cytisine

(-)-Cytisine **Cy 1** *(1,2,3,4,5,6-hexahydro-1,5-methano-pyrido[1,2-a][1,5]diazocin-8-one)* is a chiral quinolizidine alkaloid composed of a tricyclic skeleton, including ring A und B forming a bispidine framework fused to a ring C representing a pyridin-2-one (Fig. I/2.17). In comparison with (-)-nicotine, (-)-cytisine **Cy 1** is a more potent nAChR ligand, displaying higher selectivity toward the α4β2* nAChR subtype combined with subnanomolar affinity (Ki = 0.122 nM) [230]. It has been found that the functional efficacy of (-)-cytisine **Cy 1** is dependent on the identity of the β subunit present in the nAChRs. This fact underlines the importance of the β subunit in determining

agonist interactions with neuronal nAChRs [231]. (-)-[^{3}H]cytisine labels specific sites in the brain with an affinity and distribution comparable to (-)-[^{3}H]nicotine [232].

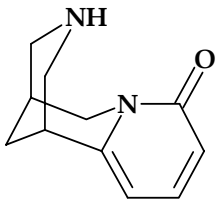

(-)cytisine Cy 1

Figure I/2.17: The structure of cytisine **Cy 1**

Mecamylamine

Mecamylamine **12** (*N-2,3,3-tetramethyl-bicyclo[2.2.1]heptan-2-amine)* is a competitive antagonist at nicotinic receptors in ganglia. It was introduced to the pharmaceutical market in 1956 as Inversene®, an antihypertensive agent. In early 1977, Merck, the company that owned the original patent, stopped producing mecamylamine **12** because of postural hypotension (due to a broad parasympathetic inhibition) and probably also because of the presence of many new drugs that were more effective in treating high blood pressure. In 2000, Layton BioScience Inc. received approval from the United States Food and Drug Administration to reintroduce Inversine ® (mecamylamine HCl) to the U.S. market for use in treating symptoms of Tourette's Syndrome, a condition which includes motor and vocal tics and mood disorders [233]. Recently, Targacep acquired the drug Inversine ® (Mecamylamine HCl) from Layton BioScience, and mecamylamine **12** is currently marketed for the management of moderately severe to severe essential hypertension [234].

Methyllycaconitine (MLA)

Methyllycaconitine (MLA) **35** (Fig. I/2.18) is a tertiary norditerpenoid alkaloid isolated from "Delphinium" species brownie. MLA **35** is a competitive antagonist (K_i =1 nM) at [^{125}I]α-Bgt binding site, in rat forebrain preparations [235]. It produces a

potent reversible blockade of α7* and it is > 30 fold less potent at the α3β4* or α4β2* and inactive at the muscle nAChRs [236].

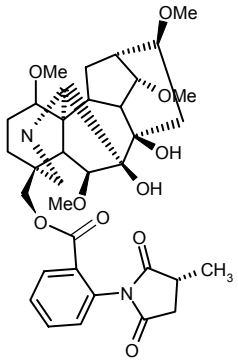

Figure I/2.18: Structure of the norditerpenoid alkaloid MLA **35**.

MLA **35** clearly differentiates between α-Bgt sensitive sites on neuronal and muscle nAChRs [235]. The use of MLA as an α7* selective antagonist should be applied with caution, especially in studies of nAChRs in basal ganglia. Recently, it was observed that MLA is able to inhibit the binding of a [^{125}I]α-CTx-MII binding site (a specific antagonist at nAChRs containing α3 and β2 subunits) [237] to striatum and nucleus accumbens with a K_i value of 33 nM [238]. Actually, MLA concentrations between 1 and 10 nM will reversibly block α7* type nAChRs, while at 100 nM it begins to block α3-type receptors (e.g. α3/α6β2β3), present at presynaptic terminals on DA neurons [238]. Since [^{3}H]MLA displays rapid association and dissociation kinetics, it has been developed as an alternative to [^{125}I]α-Bgt (slow dissociation kinetics) for labelling the *α7* subtype. This radioligand labels a single population of binding sites in the rat brain with low nanomolar affinity (K_D = 1-2 nM) [239].

Dihydro-beta-erythroidine (DHβE)

DHβE **(36)** (Fig. I/2.19) is an alkaloid found in seeds of plants of the genus *Erythrina*. In addition to its curare-like properties, it has been widely used as a classical, non-selective, competitive antagonist at neuronal nicotinic acetylcholine receptors. DHβE has nanomolar affinity at both α4β2* (Ki = 35 nM) and α3β2* receptor subtypes, but is a relatively weak antagonist at α3β4* (ganglionic-like) and muscle subtype (Ki = > 11,000 nM) [240,241].

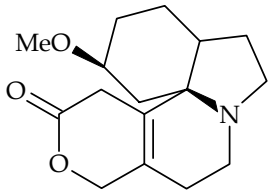

Figure I/2.19: Structure of dihydro-β-erythroidine **36**

I/2.3. Peptide toxins

I/2.3.1. Bungarotoxins

Snake neurotoxins have a very high affinity to nAChRs, they produce a potent receptor functional blockade at neuromuscular junctions and have been extremely useful in the characterization of structure and function of the nicotinic receptors. Snake neurotoxins can be divided into two subfamilies, "short" (60-62 residues) and "long" (64-72 residues), which have sequence homology and share the same 3D-structure [242]. The best-established snake neurotoxin is the α-Bungarotoxin α-Bgt **5**. It has been isolated from *Bungarus multicinctus* [239] (Fig. I/ 2.20).

Figure I 2.20: *Bungarus multicinctus.*

α-Bgt **5** is a 75 amino acid peptide, (8000 Da peptide), a highly potent and selective antagonist at α7* and muscle type nAChRs (K_i = 0.35 - 3.5 nM, respectively) [239,243]. It was the instrumental compound in the isolation and purification of *Torpedo* nAChRs (muscle type nAChR) [239]. Also avian α8* and the α9* subtype at cochlear hair cells interact with α-Bgt **5**. All other neuronal nACh receptors formed by the assembly of α2-α4 and β2-β4 subunits are completely insensitive to α-Bgt **5** [34]. [^{125}I]α-Bgt has been largely used for the exploration of the α7 channel structure and to investigate its

distribution in the PNS and CNS. [77,239]. [^{125}I]α-Bgt labels a single population of binding sites in the rat brain with low nanomolar affinity (K_D 1 = nM) [239]. However, [^{125}I]*α*-Bgt is not an ideal ligand in equilibrium binding studies because of its slow kinetics [244].

I/2.3.2. Conotoxins

Conotoxins are short peptides isolated from the venom of cone snails a carnivorous mollusk from tropical marine environments (genus *Conus*). Many of these toxins are selective inhibitors of ligand- and voltage-gated ion channels and are classified according to the type of channel to which they bind (Table I/2.1). They are small peptide toxins (14-17 amino acids) with a highly conserved disulphide-bonding pattern. They are structurally simpler than α-bungarotoxin **5** and other snake venom α-neurotoxins (constituted by 60-70 residues plus four or five disulphide bridges). **α-Conotoxin MII**, **α-Conotoxin IMI** and **α-Conotoxin AuIB** are important representatives of the neurotoxin family. **α-Conotoxin MII** is a potent, competitive antagonist, highly selective for neuronal nicotinic receptors containing **α3β2*** subunits [237]. Also **α6β2** nAChRs expressed in Xenopus oocytes are susceptible to inhibition by α-Conotoxin MII [237]. **Conotoxin IMI** is a selective antagonist of **α7*** nAChRs and also blocks the α9* subtype with an affinity 8-fold less than at α7* [245]. **α-Conotoxin AuIB** [246] belongs to the family of conotoxins isolated from *Conus aulicus*, including *α*-Conotoxin AuIA, AuIB, and AuIC [247]. Conotoxin AuIB partially inhibits nicotine-evoked [^{3}H]noradrenaline and [^{3}H]ACh release from rat brain and is a selective antagonist of **α3β4*** [246, 248]. Other conotoxin peptides, e.g. PnIA, PnIB showed in table I/2.1 might be used for selective inhibition of other specific nAChR subtypes [248].

Table I/2.1: Classification of selected α-Conotoxins

α-Conotoxins	**Species**	**Sequence**	**nAChR Targets**
AuIA	C. aulicus	GCCSYPPCFATNSDYC*	α3β4
AuIB	C. aulicus	GCCSYPPCFATNPDC*	α3β4
AuIC	C. aulicus	GCCSYPPCFATNSGYC*	α3β4
GI	C. geographus	ECCNPACGRHYSC*	muscle
ImI	C. imperialis	GCCSDPRCAWRC*	α7
MI	C. magus	GRCCHPACGKNYSC*	muscle
MII	C. magus	GCCSNPVCHLEHSNLC*	α3β2, α6 (chick), β3
PnIA	C. pennaceus	GCCSLPPCAANNPDYC*	α3β2
PnIB	C. pennaceus	GCCSLPPCALSNPDYC	α7
SI	C. striatus	ICCNPACGPKYSC*	muscle
* C-terminal amidation			

I/3. Pharmacophore models for nAChR ligands

The elucidation of the three-dimensional structure of the nAChRs at atomic level by X-ray crystallography or by NMR is very complex. This is because integral membrane proteins are not suited for crystallization and nAChRs are too large (wide) for NMR studies. Given that the experimental knowledge about the particular three-dimensional structure of nAChRs is still unavailable, corresponding hypothetical pharmacophore models represent key sources for understanding drug-receptor interaction on the molecular level and are useful tools that can be successfully employed in designing new nAChR modulators [249]. Data and structure activity relationships from binding studies of different chemical classes of modulators will be used to optimize and refine the pharmacophore model.

In the course of the pharmacophoric pattern identification process, the following limitations have to be taken into consideration: (1) The above reported inadequate characterization of the binding site on nAChRs, (2) the lack of a specific model for a subtype, despite the existence of ligands that interact with different receptor subtypes (3) and the existence of different pharmacophore models for every receptor state. In fact, the nAChR is an allosteric protein that exists in different conformational states [11]. In radioligand binding studies, the presence of the agonist stabilizes the receptor in a desensitized (high affinity) state. It is difficult to match radioligand-binding data coming from different laboratories. The use of different radioligands, the radioligand concentration, the buffer pH and composition and the method used to separate dissociated and bound ligand should be taken into account [188].

Since 1970, several investigations have been performed to define a pharmacophore model [185, 187, 249-257]. Beers and Reich developed the first model. It was characterized by two main structural elements: an onium group (N^+) and a hydrogen bond acceptor (HBA) atom, with the optimal distance between the onium site and the HBA acceptor atom of 5.9 Å. [258](Fig. I/3.1). One of the limitations of this first model was the use of a miscellaneous set of agonists and antagonists ((-)-cytisine, (S)-nicotine, trimethaphan, dihydro-β-erythroidine (DHβE) and strychnine).

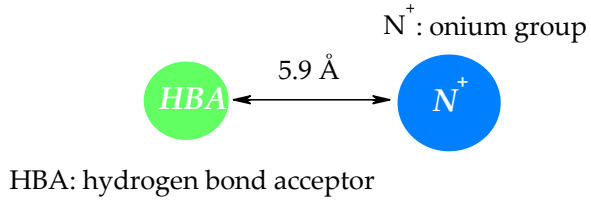

Figure I/3.1: Pharmacophore model of Beers and Reich, 1970.HBA can be an electronegative atom capable of accepting a hydrogen bond.

In 1986, Sheridan and co-workers using only nicotinic agonists refined this model. They formulated a new model based on three salient features: a protonable nitrogen atom (corresponding to the pyrrolidine nitrogen of nicotine), a hydrogen bond acceptor atom (HBA) (e.g. the carbonyl oxygen of cytisine or the pyridine nitrogen of nicotine) and a third point, representing the centroid of the pyridine ring of nicotine or the carbonyl carbon atom of cytisine (Fig. I/3.2) [259]. The optimal distances between the three points in the pharmacophore triangle were estimated to be (N^+-HBA) 4.8 Å (N^+-C) 4.0 Å (HBA-C) 1.2 Å (Fig. I/3.2). A limit is given by the fact that it was based on only four ligands, due to the paucity of ligands on nAChR at the time.

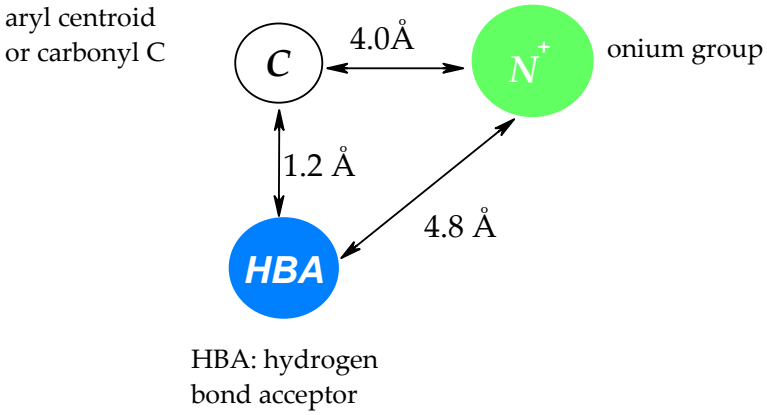

Figure I/3.2: Pharmacophore model of Sheridan (1986)

Barlow and Johnson (1989), whose model was based on X-ray crystallographic data of two nicotinic ligands ((-)-cytisine and (S)-nicotine), suggested that the agonist activity might depend on a charged nitrogen atom and a planar area on the receptor that

accommodates an aromatic ring (Fig. I/3.3). Tyrosine or phenylalanine residues [250] constitute this area. In some cases an unsaturated group, such as a carbonyl (ACh) or a double bond (anatoxin-a) can replace the aromatic ring.

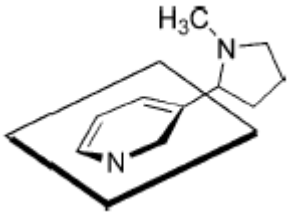

Figure I/3.3: Barlow and Johnson (1989) [255]

The elucidation of the structure of epibatidine and the discovery of its very high affinity at nicotinic acetylcholine receptors raised the issue of the role played by the internitrogen distance in binding affinity (See Table I/3.1). Glennon et al. [260] assumed that a relationship exists between N-N distance and affinity. They calculated that the internitrogen distance of the lowest energy conformation of epibatidine was 5.5 Å. Further studies demonstrated that other low-energy conformers of epibatidine were possible. Then the optimal internitrogen distance was considered to be 4 - 6 Å, [188, 202, 259, 261], given that nicotine and epibatidine showed an N-N distance of 4.8 and 5.5 Å respectively [216, 260, 261].

Table I/3.1: Different N-N distances found in literature

Reference	Compounds studied	N-N distance
1986 [259]	(S)-nicotine,(-)- cytisine, (-)-ferruginine methiodide, (-)-muscarone, (±)-epibatidine	4.8 Å
1994 [260]	(±)-epibatidine	5.5 Å
1996 [202]	A85380, (±)-epibatidine	4.6 - 6 Å
1998 [261]	A85380, (±)-epibatidine	4.5 Å
1999 [257]	(±)-epibatidine	> 5.5 Å

However, some high affinity nicotinic agents were identified, some of which were quite conformationally constrained, that possessed N-N distances > 5.5 Å [229, 257]. To account for the high affinity of these compounds, Tonder et al. assumed that the

distance between specific features of the ligand and the receptor is a parameter which predicts the affinity of a ligand for the nAChRs better than the internitrogen (N-N) distance [257].

Holladay et al. [13] extended the three-point model of Sheridan to a four-point pharmacophore model (Fig. I/3.4). In this model, the nitrogen atoms (1) and (2) are the pharmacophoric elements, while the elements presented in (3) and (4) are positions at the nAChR protein which optimally interact with (1) and (2). The optimal distance between the two N^+-N is approx. 4.85 Å [13].

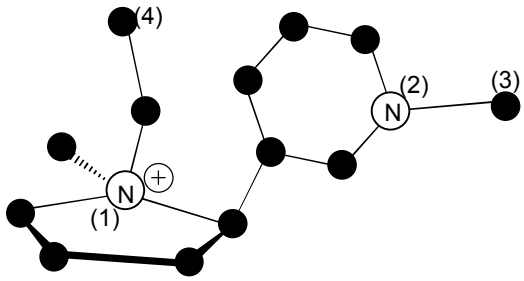

Figure I/3.4: Pharmacophore model proposed by Holladay et al. (1997)

Tonder et al. [257] proposed a vector model. They suggested that the distance between *site point a* and *site point b* define the binding to the nAChRs receptors (Fig. I/3.5 A), where *a* is a site selected to be 2.9 Å in length from a cationic head and *b* is a site selected to be 2.9 Å in length from a hydrogen bond acceptor moiety (Fig. I/3.5 A). An a-b distance of approximately 7-8 Å is thought to be optimal for the high affinity binding. Later, *Tonder et al.* modified the original model by the introduction of an aryl centroid (centre of a heteromatic ring or a carbonyl bond) [185, 256] (Fig. I/3.5 B). The authors assumed that a compound possesses high affinity for nAChRs if the following distances were present: **(a-b)** 7.3-8.0 Å and **(a-c)** 6.5-7.4 Å. The angle measured between the interatomic distance vectors should be 30°-35°. There is a certain appeal to the vector models because they account for the binding of agents with varying N-N distances, that is the distances between vectors and not the N-N

distances themselves [217]. The limitation of this pharmacophore model is due to the use of a mixed set of nicotinic ligands.

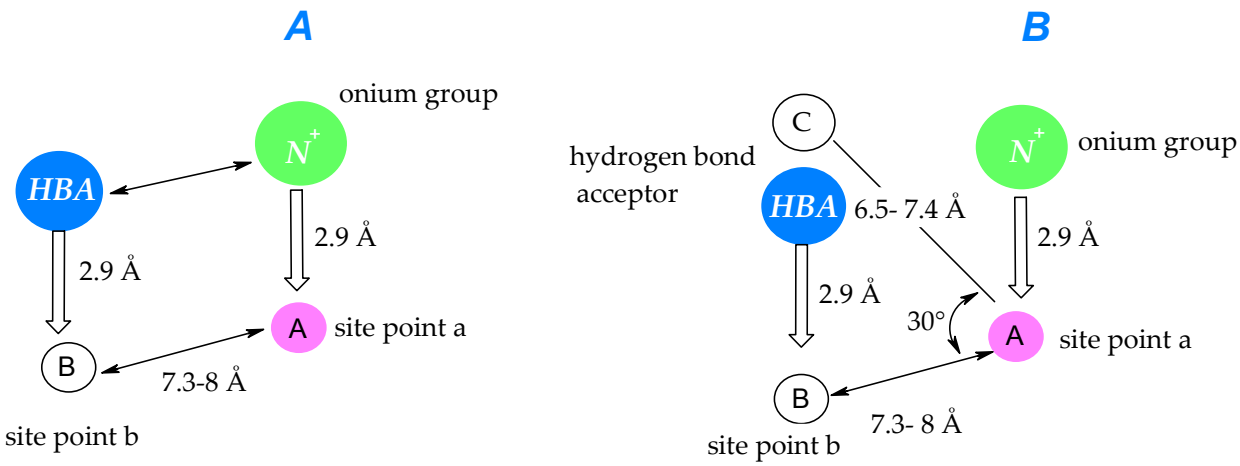

Figure I/3.5 (A) Original vector pharmacophore model [257]. (B) Improved vector model [256]

The assumption that nicotinic ligands must conform to three point pharmacophoric geometry cannot generally be accepted [188]. This issue is based on the fact that acetylcholine itself only bears two pharmacophoric features, a cation and HBA, and is an extremely flexible molecule. Schmitt [188] subdivided the nAChRs ligands in five classes (See Table I/3.2):

Class A: the cationic centre and the HBA/π are acyclic

Class B: the cationic moiety is acyclic, while the HBA/π is cyclic

Class C: the cationic and HBA/π are separated in non-fused rings

Class D: the cation moiety is cyclic and the HBA/π is acyclic

Class E: cationic and HBA/π sites are contained within a fused polycyclic or spiro ring system.

Table I/3.2: Schmitt's classification of nAChRs ligands

Class	Example	Reference
A Cationic centre acyclic HBA/π acyclic	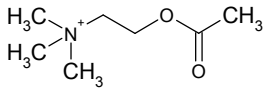 Acetylcholine	174
B Cationic moieties acyclic HBA/π cyclic	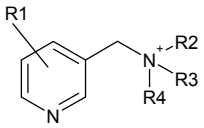 3-Pyridyl-methylamines	262
C Cationic and HBA/π are within separate non-fused rings	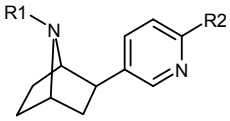 Epibatidine-Derivatives	157, 263
D Cation moiety is cyclic HBA/π acyclic	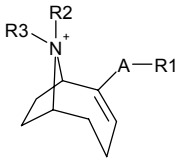 Anatoxin-a-Derivatives	264
E Cationic and HBA/π sites are in a fused polycyclic or spiro ring system	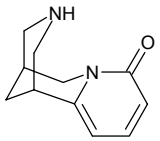 Cytisine	232

I/4. Radioligand binding studies

I/4.1. Introduction to *in vitro* pharmacology- Radioligand binding studies

The radioligand binding technique is an important tool in pharmacology. Radioligand binding assays are used to obtain information about a receptor (e.g. distribution, concentration, structure and function) and to evaluate potential agents by assessing their ability to interfere with the specific binding of radioligands to its receptor. The radioligand is a radioactively labelled drug that can associate with a receptor of interest [265]. Radioligand binding studies using both natively expressed and cloned receptors have been used extensively for the characterization of receptor modulators. There are two basic types of receptor binding experiments: saturation and competition [266].

Saturation studies are used to determine the affinity of a radioactive ligand for a receptor, known as K_D, as well as the B_{max} of the receptor in a specific tissue or sample. The K_D is the dissociation equilibrium constant of a drug for a receptor. The B_{max} is the density of the receptor site in a particular preparation [267].

Competition studies are used to determine the affinity of unlabelled ligands for a defined receptor. The K_i value, the equilibrium dissociation constant, for a competitive inhibitor of the receptor is a measure of how tightly a drug binds to a receptor. The higher the affinity (lower value of K_i) the tighter the drug binds to the receptor.

Basic concepts in receptor binding studies

Radioligand binding studies are based on a chemical equilibrium process (Fig. I/4.1) that is defined by the law of mass action (Eq. I/4.2).

$$\text{Receptor (R)} + \text{Ligand (L)} \underset{k_{off}}{\overset{k_{on}}{\rightleftharpoons}} \text{Ligand Receptor Complex (LR)}$$

Figure I/4.1: Radioligand binding experiments are based on the assumption that the receptor (R) interacts with a ligand (L) and forms a ligand-receptor complex (LR). This process is reversible.

The binding of a radioligand (L) to a receptor (R) to form a ligand-receptor complex (LR) is not a static process. It is viewed as a kinetic process of a ligand moving toward and away from receptors at different states. The equilibrium position is a position of minimum free energy within the force field of the receptors. It is reached when the rate constant of association equals the rate constant of dissociation.

$$[LR] \times k_{on} = [L][R] \times k_{off}$$

Equation I/4.1: Equation at equilibrium

In biological chemistry this equilibrium is expressed in terms of the dissociation reaction K_D rather than the association reaction K_a. The K_D is obtained by a rearrangement of the law of mass action:

$$K_D = \frac{k_{off}}{k_{on}} = \frac{[L][R]}{[LR]}$$

Equation I/4.2: The law of mass action, where K_D is the dissociation equilibrium constant, [L] is the concentration of the unbound ligand, [R] the concentration of the unbound receptor and [LR] the concentration of bound receptor-ligand complex. k_{on} is the rate constant for association and k_{off} is the rate constant of dissociation.

K_D is a measure of the affinity of a ligand for a receptor and is equal to k_{off} / k_{on}, where the k_{on} is the rate constant for association and k_{off} is the rate constant of dissociation, [L] is the concentration of the unbound ligand, [R] the concentration of the unbound receptor and [LR] the concentration of receptor-ligand complex. When the concentration of a ligand equals the K_D, half the receptors will be occupied at equilibrium. If the receptors have a high affinity for the ligand, the K_D will be low, as it will take a low concentration of ligand to bind half the receptors. The law of mass action is not useful in all situations. It can only be used in presence of certain conditions, that:

1. All receptors are equally accessible for the ligand;
2. Receptors are either free or bound by the ligand;
3. No more than one affinity state exists;
4. Binding is reversible and does not alter the ligand or receptor.

Basic steps in receptor binding studies

Radioligand binding studies consist of four basic steps (Fig. I/4.2).

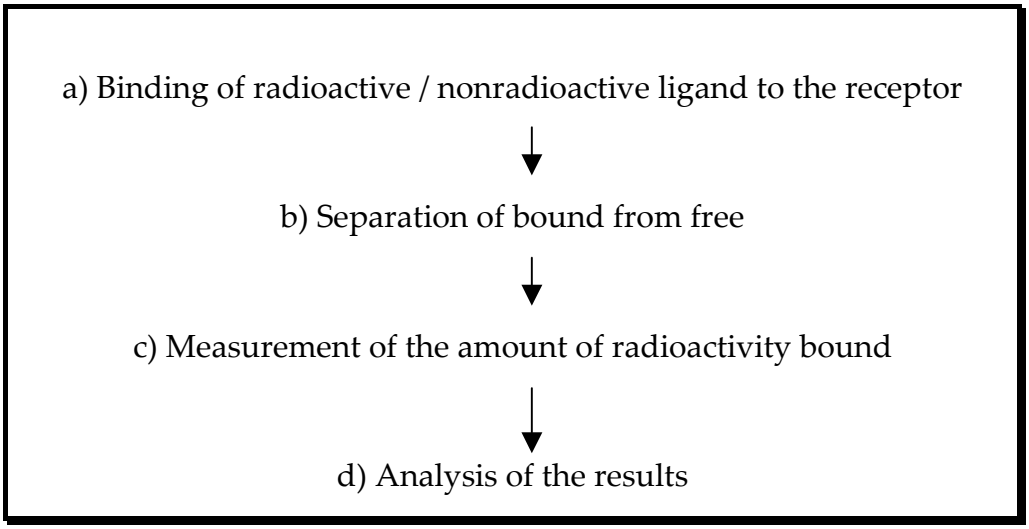

Figure I/4.2: Basic steps in receptor binding studies

a) Binding of radioactive / nonradioactive ligand to the receptor

The parameters that need to be optimised are:

1) radioligand (isotope, specific activity, stability),

2) protein concentration,

3) buffer (composition and pH),

4) incubation time (duration and temperature).

1) Radioligand

Selection of isotope: The most commonly used radioactive isotope in i*n vitro* pharmacological studies are ^{3}H and ^{125}I. They possess, as shown in Tab. 4.1, different physical properties. The Iodine-125 decays by electron capture, has a half-life of 60 days and gamma-ray (35 keV) and x-ray emission (27 keV). Tritium decays by

electron emission (β^-) with very low energy (18.6 keV) and has a half-life of 12.3 years. Tritium has some advantages in comparison with the iodine-125. Tritium is chosen to label small molecules in order not to influence the interaction of the ligand with the receptor. Moreover, the radioligand can maintain the biological structure and function without alteration. A very important property of tritium is its longer half-life, which does not require a correction for decay during the duration of the experiment. Furthermore, due to the low energy of the radiation, a tritium labelled ligand is much easier to handle than a iodine-125 radioligand. The only disadvantage consists in the fact that the low energy of the radiation (β^- particles) is responsible for the decomposition, by self-radiolysis of the radioligand. In fact, all the beta energy emitted is absorbed within the sample. On the other hand, iodinated radioligands have a higher specific activity (^{125}I maximum specific activity = 2,200 Ci/mmol vs. 30 - 100 Ci/mmol for ^{3}H) that reduces the amount of the ligand that should be set in the assays and makes them particularly useful if the density of the receptor is low.

Table I/4.1: Physical properties of the radionuclides ^{3}H and ^{125}I.

Nuclide ^{3}H	**Nuclide ^{125}I**
Mode of decay :β^- = 18,6 keV (100%)	Mode of decay: EC= γ (35 keV) and x-ray (27 keV)
Half-life = 12,4 years	Half-life = 60 days
maximum specific activity = 30 – 100 Ci/mmol	maximum specific activity = 2,200 Ci/mmol

Affinity, specific radioactivity and stability of the radioligand: The radioactive ligand used in radioligand assays should have a high affinity for the receptor being studied, low affinity for other receptors and a high specific radioactivity. The specific activity may be defined as the radioactivity per unit mass of a labelled compound. Usually, it is expressed as MBq/mmol (1 Bequerel, abbreviated Bq, equals one radioactive disintegration per second = 1 dps) or in Ci/mmol; Curies per mili mole (1 Curie = 3.17 * 10^{10} disintegrations per second, dps, or 2.22 * 10^{12} disintegrations per minute, dpm). The higher the specific activity of the labelled compounds, the less mass needs to be used in assays. On the other hand, high specific activity can cause radiolysis in the solution of a compound. Certain steps may be taken into consideration to minimize

chemical instability and radiolysis. The radioactive ligands should be dissolved in a suitable solvent such as ethanol (which act as radical scavenger) and should be stored cold (- 20 C°). It should not be frozen, since freezing the solution tends to locally concentrate the radioligand and increase its radiolytic destruction [268]. Further, exposure to UV light and rapidly changing temperature conditions should be avoided.

2) Protein Concentration

The right concentration of the receptor used in binding assays depends upon the amount, affinity and specific activity of the radioligand and on the density of the receptor in the tissue [269]. Approximately 100 to 500 cpm should be bound to the receptor of interest at the lowest concentration of the radioligand used in the assays. However, the cpm counts are suitable for detecting and measuring the interaction ligand-receptor depends upon the counter efficiency. The concentration of the protein is a very crucial factor in saturation and competition binding experiments. Indeed, it can cause the phenomenon of ligand depletion, thereby affecting the result of the assays. Ligand depletion occurs when the concentration of the protein in the tissue is so large that the binding of ligand to the receptor depletes the free concentration of ligand for binding to the available receptors. Ideally, the free concentration of the ligand should be equal to the concentration of the ligand that was added. If the difference between both these concentrations becomes too high, the law of mass action becomes invalid. In saturation assays the depletion of the radioligand is a very frequent phenomenon. In this case, the results can be corrected directy using an appropriate equation. In competition assays, ligand depletion can cause an underestimation of the affinity of high potent ligand. This concept was demonstrated by experiments performed by Gundisch et al. [179]. They investigated the effect of ligand depletion on the binding affinities of (-)-nicotine and (-)-epibatidine in competition assays with (-)-[^{3}H]cytisine. Various concentrations of rat brain membranes were used while keeping the same amount of radioligand. An increase in protein concentration caused an increasing K_i value for the high affinity ligand (-)-

epibatidine, whereas it had no effect on the binding affinity of (-)-nicotine (ligand with moderate affinity). The ligand depletion in competition assays can affect the results only if more than 10% of the radioligand binds. That is not true for the characterisation of ligands, which have higher affinities than the radioligands used in the assays [179]. To compensate the effect of depletion, some pratical procedures are required [270]:

1. Increase the incubation volume without changing the amount of tissue. In this case, it is necessary to increase the amount of the radioligand.
2. Reduce the amount of protein.
3. Use a high concentration of both the radioligand and the compound being tested to reduce a depletion of nonradioactive ligand with high affinity to the receptor.
4. Use an analysis procedure that can correct the difference between the concentration of the added ligand and the concentration of the free ligand.

3) Buffer Composition and pH

The choice of the buffer depends on the receptor type and the specific purpose of the experiments. The buffers usually used for binding studies are: HEPES or TRIS buffer at pH 7.4 (often used in the concentration of 20-50 mM) [269]. They contain ions that are present in physiological fluids (e.g. Mg^{2+}, Ca^{2+}, Na^{+}). Buffer solution containing heavy metal ions should be avoided because of the risk of reaction with sulphydryl groups in the receptors that may alter the structure-binding relationship [269].

4) Duration and temperature of the incubation

The tissue is incubated with the radioligand until the steady-state conditions are reached. The incubation time required is dependent upon the radioligand (concentration and affinity), receptors and temperature. The lowest concentration of radioligand will take the longest to equilibrate [267,271]. The incubation can be done on ice (ca. 4°C), at room temperature (22-25°C) or at 37 °C, depending on the stability of the radioactive ligand and the tissue [269]. The affinity of the radioligand may be temperature-dependent. In fact, *in vitro* binding affinity of some nAChR ligands is

affected by the change in incubation time and temperature [179,272]. The influence of these two parameters on the K_D value of (±)-[^{3}H]epibatidine binding were investigated in saturation binding assays. The P2 membrane preparations of rat brain were incubated in the presence of various concentrations of radioligand at 4 °C, 22° C, and 37 °C for different periods of time. Results of kinetic studies demonstrated that (±)-[^{3}H]epibatidine has a slow rate of dissociation ($t_{/2}$ = 220 ± 5 min at 22 °C) and, consistent with this slow dissociation, it also has a slow association ($t_{/2}$ = 110 ± 5 min at 22 °C for 8 pM (±)-[^{3}H]epibatidine). Based on this data, it was found that incubation of ca. 2h are required to get a precise affinity determination at 22 °C and 37 °C. In contrast, saturation assays carried out at 4 C° required more than 8 h incubation. Consequently, an insufficient incubation time may cause underestimation of the affinity of the radioligand [179].

b) Separation of bound from free radioactive ligand

Once the steady-state conditions have been reached, the bound radioactive ligand is separated from the free ligand using, for example filtration or centrifugation techniques. The suitable procedure is chosen upon the dissociation constant of the radioligand. Indeed, the filtration procedure is appropriate only for ligand receptor binding with K_D of approximately 10^{-8} M or less (Tab. I/4.2).

Table I/4.2: Relationship between allowable separation time and dissociation constant K_D [269]

K_D (M)	Allowable separation time
10^{-12}	1-2 days
10^{-10}	2.9 hours
10^{-11}	17 min
10^{-9}	1.7 min
10^{-8}	**10 sec**
10^{-7}	**0.1 sec**
10^{-6}	**0.01 sec**

The filtration method works by trapping the receptor-ligand complex in the filter. The procedure has to be very rapid so that the bound ligand does not dissociate from the receptor during separation [273]. Rapidity of the filtration depends on the K_D of the radioligands, e.g. for a radioligand with a K_D of 10 nM, the filtration time should be max. 10 sec (Tab. I/4.2). The rapid filtration technique presents some favourable aspects such as simplicity, rapidity, low non-specific binding and high reproducibility. Nevertheless, filtration possesses some disadvantages:

1. Loss of small size membrane particles during filtration.
2. Binding of the radioligand to the filter itself.
3. The filter may become clogged.

To solve the first problem, a suitable glass filter has to be used. Most of the particles will be captured by filter with pore size of 1 μm or pore size of 1.2 μm. The non-specific binding of the radioligand to the filter during the filtration can be reduced using different types of filters pre-soaked, for instance in 0.1 % polyethylenimine (PEI) [CH_3-(CH_2-CH_2)$_n$- CH=NH] for a short time before filtration [271,274]. The tissue concentration may be a critical factor in the filtration speed. In fact, in case of high concentrations of tissue homogenates (> 10 mg of tissue/tube), the filter may become clogged so that the filtration will be slow [269]. As anticipated, in case of a rapidly dissociating ligand, the filtration method cannot be used because a significant loss of the ligand receptor complex can occur. A good alternative in this case is the centrifugation technique. This method works by using a desktop microcentrifuge. The limitation of this procedure is the incomplete separation of the free ligand trapped in the pellets, the fair specific to non-specific ratio and the poor reproducibility [270].

c) Measurement of the amount of radioactivity bound

The amount of receptor-ligand complex formed can be estimated by measuring the amount of radioactivity on the filter using a liquid scintillation counter or gamma counter, depending on the isotope.

Liquid scintillation counter: ***The β^- counter***

A liquid scintillation counter is often used if the isotope being measured is tritium (low-energy β^- emitting nuclide, efficiency about 40-50 %). When a tritium atom decays (Eq. I/4.3), a neutron converts to a proton and the reaction shoots off an electron and antineutrino (beta decay).

$$\mathbf{n} \longrightarrow \mathbf{p} + \mathbf{e^-} + \mathbf{\Delta E} + \tilde{\upsilon}$$

Equation I/4.3: A neutron (n) converts to a proton (p) and the reaction shoots off an electron (e^-), an anti-neutrino ($\tilde{\upsilon}$) and energy (ΔE).

Electrons emitted by tritium decay have very low energy, (β-emission = 0.0186 MeV). Thus this signal is received only if the electron has sufficient energy to travel far enough to encounter a flour molecule in the scintillation fluid, which amplifies the signal received and gives a flash of light detected by the scintillation counter.

Solid scintillation counter: ***The γ-counter***

A gamma counter is suitable for detecting γ-rays emitted from isotopes such as ^{125}I (efficiency ca. > 90%). The gamma counter is provided with a sodium iodide crystal dot with a very small amount of thallium. The sodium iodide crystal shows great likelihood of absorbing part of the received energy. The task of the thallium is to transform part of the energy absorbed by the NaI crystal in light with different wavelengths that can go through the crystal. The choice of NaI crystals for γ-rays detection is due to their reasonable density and high atomic number of iodine (Z=53) that results in efficient production of light photons. When a nuclide such as ^{125}I decays (Eq. I/4.4), it emits energy in the form of high-energy photons (E = 35 keV for γ-rays and E = 27 keV for x-rays). The γ-rays hit the sodium iodide detector and light photons are re-emitted.

$$\mathbf{p} + \mathbf{e^-} \longrightarrow \mathbf{n} + \gamma + \mathbf{\Delta E}$$

Equation I/4.4: A proton (p) converts to a neutron (n) with emission of energy as electromagnetic radiation.

Light photons strike the photocathode of a photomultiplier (PM) tube. This photomultiplier (PM) amplifies the signal and generates an electric pulse that is proportional to the energy of the gamma rays. The resulting pulse will be measured in terms of counts/min (c.p.m.). The basic unit of radioactive emission is given variously as disintegrations per minute (d.p.m.), disintegrations per second (d.p.s.), or Curies (Ci). The ratio of measurement (c.p.m.) to emission (d.p.m.) is the counting efficiency (readily measured with the use of an external standard and quenched samples of known emission).

d) Analysis of the results

Receptor binding data can be analysed using different commercially available curve fitting programs, such as GraphPAD (supplied by GraphPAD software), CURVEFIT (supplied by IRL press software), LUNDON-1 and -2 KINETICS (supplied by Lundon software) [269]. Moreover, self-made programs using Excel are suitable for analysis of ligand binding data.

I/4.1.1.Saturation Binding Studies

Saturation radioligand binding experiments measure specific radioligand binding at equilibrium at various concentrations of the radioligand. They are based on several assumptions:

1. There is no cooperativity.
2. Experiment has reached the equilibrium.
3. Binding is reversible and follows the law of mass action.
4. Small fraction of radioligand binds. The free concentration is almost identical to the concentration added.

Such experiments are based on the one binding site equation (Eq. 4.5), where L is the free ligand, B_{max} (plateau of the curve) is a measure of the density of the receptor in the tissue preparation and the K_D is the concentration of radioactive ligand required to occupy 50% of the receptors.

$$RL = (L*B_{max})/(K_D + L)$$

Equation I/4.5: One site binding equation, where RL is the concentration of the drug-receptor complex, L is the concentration of the free radioactive ligand, K_D is the affinity of the radioactive ligand for the receptor and B_{max} is a measure of the density of the receptor in that tissue.

These experiments are called *saturation experiments* because at higher radioligand concentrations all the binding sites are occupied (saturated) by a radioactive ligand. In a typical saturation experiment, the radioligand concentration should be between 1/10 and 10 times the possible K_D (Fig. I/4.3) [267].

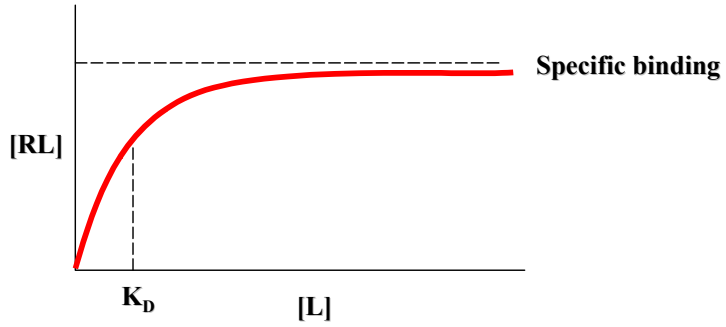

Figure I/4.3: Typical graph of a saturation hyperbole

Unfortunately, radioactive ligand binds also other sites (non specific sites) than that of interest. The whole amount of the radioactive ligand bound is referred to as total binding, whereas the specific binding is the difference between the total binding and the non-specific binding

Total binding (TB) –Non-Specific Binding (NS) = Specific Binding (S)

The non-specific sites may be other receptors from the same family or from a different class, other constituents of the tissue (they could be trapped in the lipid membrane) as well as the assay tools, such as glass fibre filters and test tubes. In order to distinguish specific and non-specific binding, a set of tubes containing a well-defined unlabelled ligand at a concentration sufficient to block the binding of the radioligand to the specific sites is conducted additionally. The inhibitory unlabelled ligand should be a competitive inhibitor, which is specific for the receptor and not the same ligand as the radioactive ligand [273]. The non-specific binding has to

be determined in each experiment. If it exceeds 50%, the experiment cannot be considered reliable. An optimal result is between 10% and 30% [266,271]. To reduce non-specific binding, following instructions are useful:

1. Achieve a very clean membrane homogenisation.
2. Optimise the filtration time.
3. Filter must be "pre-soaked" before the filtration.
4. Use the right radioligand concentration, namely a concentration ranging from 1/10 K_D to 10 K_D.

Analysis of saturation assays

The results of the saturation experiment are shown by plotting the "bound" vs. "free" as illustrated above (Fig. I/4.3). The resulting graph is a hyperbola. Since the equation I/4.5 is a nonlinear relationship, the binding parameters cannot be easily determined by graphical analysis. There are several linear transformations able to linearize binding data, including the methods of Lineweaver-Burk, Eadie-Hofstee (for enzyme kinetics), Scatchard and Rosenthal. All of them contain the same information given that they are achieved from the same equation (Eq. I/4.5). The prototype of a Rosenthal plot, the most popular linear transformation, is illustrated in figure 5 (Fig. I/4.4). In this plot, the X-axis presents the specific binding and the Y-axis the specific binding divided by the free radioligand concentration (Eq. I/4.6). The slope of the line is equal to $-1/K_D$ (K_D is the negative reciprocal of the slope). The B_{max} value is the X-intercept [275].

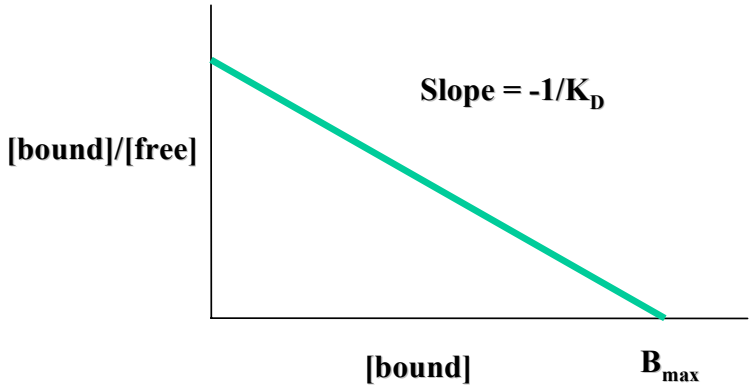

Figure I/4.4: Evaluation of saturation experiment with a Rosenthal plot [275]

$$B/L = -1/K_D * B + B_{max} / K_D$$

Equation I/4.6: Rosenthal equation [275], where B is the concentration of the bound radioactive ligand, L is the concentration of the free radioactive ligand, K_D is the affinity of the radioactive ligand for the receptor, and B_{max} is a measure of the density of the receptor in that tissue.

On the one hand, this graph permits a better and easier visualization of changes in K_D and B_{max} values [267]. On the other hand, the Rosenthal plot evaluates data points improperly and can therefore lead to errors. For this reason, nonlinear regression programs should be preferred to analyse binding data.

I/4.1.2 Competition Binding Studies

Competition experiments are aimed at determining the affinity of an unlabelled ligand for the receptor. The affinity is measured as the ability of a ligand to compete with (thus inhibit) the binding of a known radioactive ligand to the receptor of interest. In competition experiments, the concentration of the radioligand is fixed, while various concentrations of the unlabelled drug compete with it for the binding to the receptor. The binding parameter obtained from this experiment is the concentration of the unlabelled ligand that inhibits the binding of the radioligand by 50 %, namely the IC_{50} value. The IC_{50} is influenced by the concentration and the affinity of the radioligand for the receptor. The concentration of the radioactive ligand should be approximately 0.8-times the K_D. If the concentration of the radioactive ligand is too high, higher concentrations of unlabelled ligand will be required to compete with it. At the same time, it cannot be too low, because there

may not be sufficient binding to obtain reliable data. The IC_{50} can be converted into K_i using the Cheng Prusoff equation (Eq. I/4.7) [276].

$$K_i = IC_{50} / (1 + L / K_D)$$

Equation I/4.7: Cheng Prusoff equation [276] where IC_{50} is the concentration of the unlabelled ligand that inhibits the binding of the radioligand by 50%. L is the concentration of the radioactive ligand used, K_D is the affinity of the radioactive ligand for the receptor.

The K_i is defined as the equilibrium dissociation constant for a competitive inhibitor (agonist or antagonist) of the receptor. In simple terms, the K_i value for an unlabelled drug should be the same as the K_D value obtained from the same drug in radiolabelled form. If the K_i value is low, the affinity of the receptor for the inhibitor is high.

Affinity and efficacy of a ligand

A limitation of the binding studies is that they are not able to determine if a substance is an agonist or antagonist at the receptor. With this method we can only calculate the affinity of the unlabelled ligand, but nothing is known about the ability of these substances to evoke a biological response. The "occupation theory" formulated by Clark [277] was the first attempt to apply a mathematical principle to the measurement of the drug action at receptors. It assumed that the effect of a drug is proportional to the fraction of receptors occupied by the drug itself and that the maximal effect results when all receptors are occupied. Ariens formulated a theory in order to separate the binding phenomenon to the activation phenomenon and introduced a new term, intrinsic activity, to describe the relationship existing between the effects elicited by a drug and the concentration of drug receptor complexes (Eq. I/4.8)[278].

$$E = \alpha [LR]$$

Equation I/4.8: Equation to determine the agonist or antagonist effect of a ligand [278] where E is the effect, α is the intrinsic activity and LR is the concentration of the drug-receptor complex.

The intrinsic activity is a molecular property of a ligand and is related to its efficacy. The α value of 1 tells us that the ligand is a full agonist. When the α value is comprised between 0 and 1, the drug is a partial agonist. This means that it does not elicit a maximal response even at apparently maximal receptor occupancies. For α values equal to zero, the ligand is an antagonist and is not able to elicit any biological effect [278].

I/4.1.3.Protein Determination

The exact determination of the protein concentration in membrane preparation is a very important parameter for the realization of saturation and competition experiments. The methods used most often in *in vitro* pharmacology are the Bradford [279] and the Lowry test [280]. Both procedures are based on the differential colour change of a dye in response to various concentrations of protein. The Bradford method uses an acidic solution of Coomassie Brillant Blue G 250 which absorbance maximum shifts from λ= 465 to 595 nm when binding of the protein occurs (Fig. I/4.5). The Coomassie blue dye binds to primarily basic and aromatic amino acids residues. The absorption is measured with a spectrophotometer. The quantification of protein concentration is realized by comparison with a standard curve (obtained using a standard bovine serum albumin).

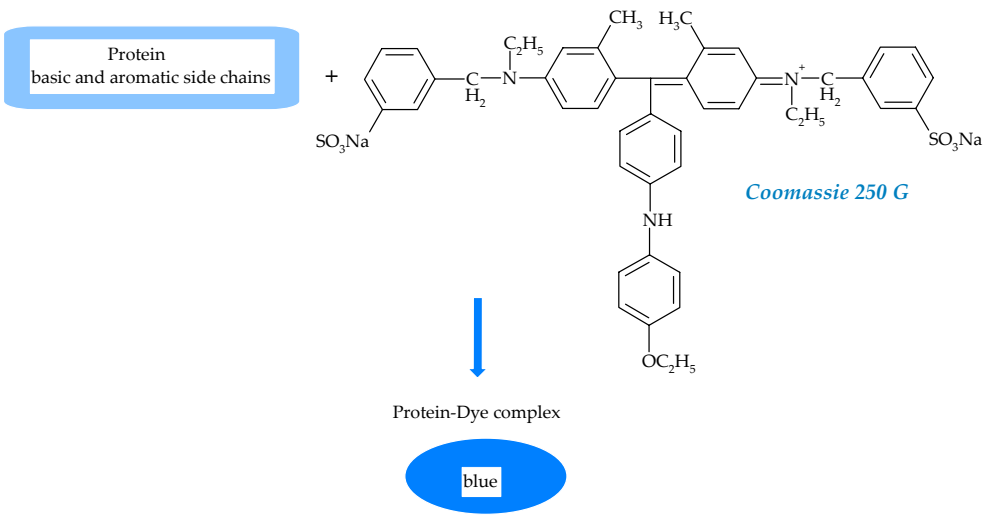

Figure I/4.5: Reaction schematic for the Coomassie dye based protein assays [391]

The Lowry's method involves reaction of protein with cupric sulfate and tartrate (Fig. I/4.6). Under alkaline conditions, the divalent copper ion forms a complex with peptide bonds in which it is reduced to a monovalent ion. Monovalent copper ion and the radical groups of tyrosine, tryptophane, and cysteine react with Folin reagent to produce an unstable, water-soluble product that is reduced to molybdenum/tungsten blue which can be measured at 750 nm. The protein selected as reference standard is bovine serum albumin. The Lowry procedure is a reliable and satisfactory method for quantification of proteins.

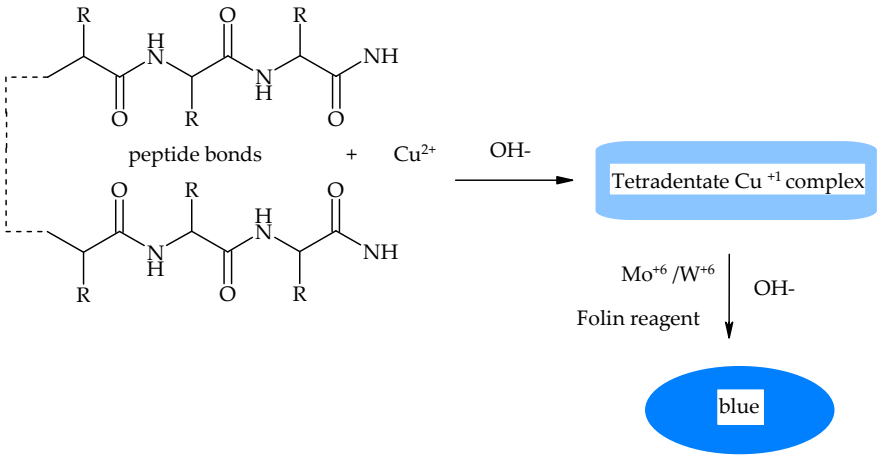

Figure I/4.6: Reaction schematic for Lowry's method [391]

II. Objectives

Over the past years, gradually interest is growing for the neuronal nicotinic acetylcholine receptors due to their involvement in a variety of brain functions, including neuronal development, learning and memory formation. (-)-Nicotine **3**, the natural alkaloid ligand of this receptor has been proved to be a cognitive enhancing agent with additional anxiolytic, analgesic and neuroprotective effects. Further interest in nAChR agonists has emerged since the discovery of (±)-epibatidine **13** as potent antinociceptive ligand. Unfortunately, the potential therapeutic use of both ligands is limited by their toxicity. Numerous investigations have focused on the synthesis and pharmacological evaluation of (±)-epibatidine **13** and (-)-nicotine **3** analogues in order to obtain novel ligands with low toxicity and improved selectivity. In the literature, the majority of *in vitro* SAR studies has been performed with the purpose to get information about the structural requirements for $\alpha4\beta2^*$ nAChRs. On the contrary, less or nothing is known about pharmacophore models for other subtypes, such as $\alpha7^*$, $\alpha3\beta4^*$ and $(\alpha1)_2\beta1\gamma\delta$. Other natural alkaloids, in addition to (-)-nicotine **3** and (±)-epibatidine **13**, like (-)-cytisine **Cy 1**, (+)-ferruginine **Fe 1**, and (+)-anatoxin-a **An 1** have been described as compounds with high affinity for $\alpha4\beta2^*$ nAChRs. However, structure-activity relationship studies for these ligands are missing for $\alpha7^*$, $\alpha3\beta4^*$ and $(\alpha1)_2\beta1\gamma\delta$. For this reason, in order to evaluate the affinities of the novel analogues of toxins, (-)-cytisine **Cy 1**, (+)-ferruginine **Fe 1**, and (+)-anatoxin-a **An 1**, in vitro radioligand binding studies are performed for four different nAChR subtypes: $\alpha4\beta2^*$, $\alpha7^*$, $\alpha3\beta4^*$ and $(\alpha1)_2\beta1\gamma\delta$. The structure-activity relationships of these novel toxin analogues will be examined with the aim to obtain more information about the structural requirements to achieve $\alpha4\beta2^*$ selectivity and at the same time to get insight into structural requirements for the $\alpha7^*$, $\alpha3\beta4^*$ and $(\alpha1)_2\beta1\gamma\delta$ nAChR. Beside the search and development of novel nAChRs ligands exhibiting selectivity for the $\alpha4\beta2^*$ nAChR, interest is growing to develop ligands

which are selective for the α7* and α3-containing subtypes. Since the recent discovery of choline as a selective ligand for α7* [284], novel choline analogues will be evaluated in radioligand binding to gain more information towards an α7* pharmacophore model.

The following items will be investigated:

1. Systematic evaluation of known and novel ligands for four different nAChR subtypes using radioligand binding technique

To address the issue of binding selectivity among nAChRs subtypes, affinities of known and novel toxin and choline analogues for α4β2*, α3β4*, α7*, and $(\alpha 1)_2\beta 1\gamma\delta$ nAChR subtypes are measured in four different competition assays. Previously described competition assays are revaluated in order to screen compounds. The radioligand binding studies are performed under the same buffer conditions (buffer contains ions that are present in physiological fluids with a pH of 7.4).

2. Establishment of a novel radioligand binding assay for α3β4* nAChR

Structure-activity relationship studies carried out with regard to α3β4* nAChRs are missing. It is due to the absence of native tissue with a suitable density of α3β4* nAChR [281]. In previous studies, it has been demonstrated that (±)-[^{3}H]epibatidine is an appropriate radioligand to label α3β4* nAChR and that this receptor subtype is present in sufficient density in rat adrenal glands [180] . Nevertheless, the poor availability and the small size of rat adrenal glands represent a drawback for the intention of screening compounds via radioligand binding assays using native tissue. In this study, pig or calf adrenal glands, as a source for α3β4* rich tissue obtained from a local slaughterhouse, are used for the evaluation of the affinities of novel derivatives in competition assays.

3. Structure-activity relationships of novel analogues of the toxic alkaloids (-)-cytisine Cy 1, (+)-ferruginine Fe 1, and (+)-anatoxin-a An 1 for different nAChRs

(In cooperation with Prof. Seitz, Department of Pharmaceutical Chemistry, University of Marburg, synthesis of novel cytisine, ferruginine and anatoxin-a derivatives)

Cytisine **Cy 1**, (+)-ferruginine **Fe 1**, and (+)-anatoxin-a **An 1** bind with high affinity to α4β2* nAChRs, but also interact more or less selective with the multifarious nAChRs. A better understanding of the steric and electronic requirements via SAR studies might be useful to identify novel ligands with high affinity and selectivity towards the central, heteropentameric *α*4β2* neuronal nicotinic receptors, eliminating interactions with the ganglionic and muscular subtypes, which are believed to mediate the toxic effects of these natural ligands.

Cytisine analogues

In previous studies, cytisine-based compounds either substituted with halogen atoms at position C-3, C-5 or C-3 and C-5 of the 2-pyridone fragment or characterised by a bioisosteric thiolactam pharmacophore (thiocytisine) instead of the lactam moiety have been evaluated *in vitro* for their affinities for *α*4β2* and *α*7* nAChRs and have been proved to be highly potent *α*4β2* and *α*7* nAChRs ligands {Imming, 2001 #383}. In the present study, the previously reported halogenated cytisines and novel thiocytisine analogues are evaluated in *in vitro* radioligand binding assays in order to determine their binding affinities to the ganglionic and muscular nAChR subtypes.

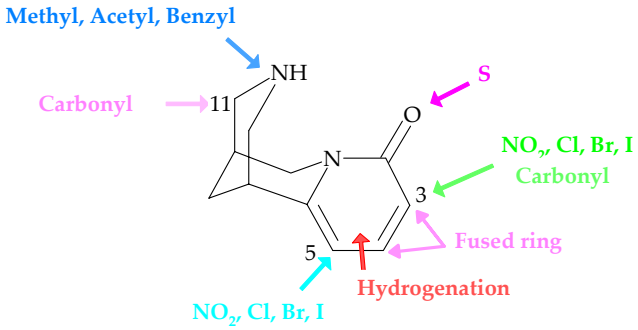

Aim of this study is also to investigate the influence of a nitro group at position C-3 or C-5 of the pyridine ring, the effect of hydrogenation of the pyridone ring or the introduction of a carbonyl moiety at position C-11 of the bispidine ring on the binding profile for $\alpha 4\beta 2^*$, $\alpha 7^*$, $\alpha 3\beta 4^*$ and $(\alpha 1)_2\beta 1\gamma\delta$ nAChR subtypes. Another point is to investigate the influence of a methyl, benzyl or acetyl substituent on the secondary amine function on the binding affinity in comparison to the lead compound.

Ferruginine and anatoxin-a analogues

The natural alkaloids, (-)-ferruginine **Fe 1** and (-)-anatoxin-a **An 1** are important natural nicotinic agonists, which possess nanomolar affinity for the central $\alpha 4\beta 2^*$ nAChR. Unfortunately, due to their poor selectivity for central versus peripheric nAChRs, they are proved to be too toxic to be useful therapeutic agents. Novel bioisosteric analogues might possess improved safety over the natural alkaloids, resulting from a higher discrimination between the multifarious receptor subtypes. In this study, the major structural modification, which is investigated, is the replacement of the acetyl moiety by heteroaromatic rings (diazines and pyridine moieties) in position C-2 as well as in position C-3 of the azabicyclic skeleton. N-demethylation of the amine moiety of (-)-ferruginine provides (-)-norferrugine **Fe 2**. It is known that the absence of a N-methyl group in the pyrrolidine ring of (-)-nicotine **3**, giving (-)-nornicotine **21**, [354] causes a decrease in binding affinity for nAChRs. On the contrary, replacement of the hydrogen on the NH group of (±)-epibatidine **13**, with a methyl group decreases by 2-fold the affinity [157]. On the basis of this controversial finding, it will be of great interest to investigate the influence of the N-methylation.

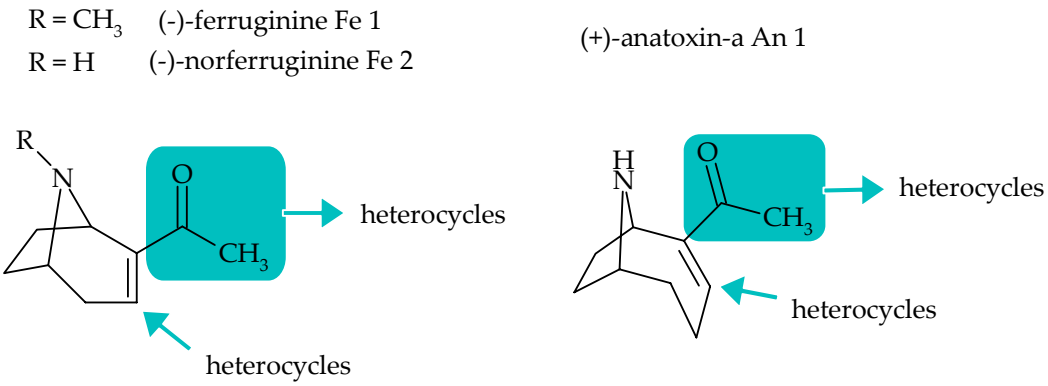

A series of enantiopure 9-diazabicyclo[4.2.1]nonanes, bioisosters of (+)-anatoxin-a **(An 1)**, will be evaluated for $\alpha 4\beta 2^*$, $\alpha 7^*$, $\alpha 3\beta 4^*$ and $(\alpha 1)_2\beta 1\gamma\delta$ nAChR subtypes: The novel compounds bear one structural part similar to the azabicyclo[4.2.1]nonene moiety of anatoxin-a **An 1** and a pyridine or diazine moiety (pyridazine, pyrimidine and pyrazine).

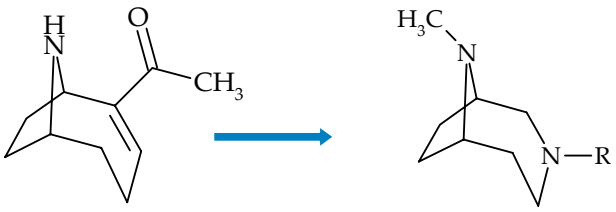

Anatoxin-a An 1 R = pyridine or diazine

basic structure of enantiopure
9-diazabicyclo[4.2.1.]nonane derivatives

The marine toxin, pinnamine **Pin**, can be regarded as a conformationally restricted variant of (+)-anatoxin-a **An 1**. Because of this evident similarity, it is used as a template to design novel structural analogues with probable similar affinity for the nAChRs. Two novel pinnamine derivatives *cis*-**Pin 1** and *trans*-**Pin 2** in which the 9-azabicyclo[4.2.1]nonane moiety is bioisosterically replaced by the 8-azabicyclo[3.2.1]octane moiety are evaluated in radioligand binding assays for their binding affinities to different nAChR subtypes.

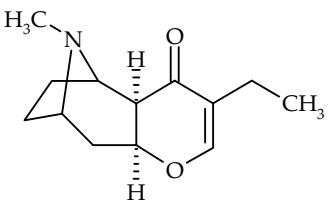

cis-Pin 1

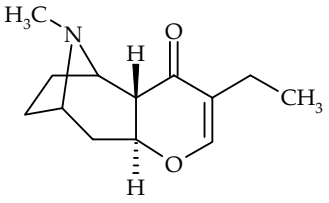

trans-Pin 2

Quinuclidin-2-ene derivatives

Other interesting novel nicotinic AChR ligands can be obtained from compounds developed as muscarinic agonists or antagonists [282, 387]. The quinuclidin-2-ene derivative with a 2–furanyl moiety **M1** showed a moderate affinity for the cortical muscarinic receptor (K_i = 300 nM) [282]. Interestingly, bioisosteric replacement of the furanyl moiety by a pyridine ring proved to be detrimental for the muscarinic activity of **M1.** The obvious structural relationship of this skeleton to the highly potent semirigid nAChRs agonists (±)-epibatidine **13** and **UB-165** leads to the evaluation of these quinuclidine analogues as novel nicotinic ligands.

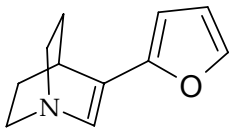

M1

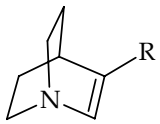

R = pyridine or chloropyridine

4. Structure activity relationships for known and novel choline analogues as α7* selective ligands

Ligands that are selective for the α7* subtype are gaining interest due to the implication of these latter subtypes in different diseases of the CNS and PNS. Recently, choline **4** has proved to be a selective ligand for the α7*, showing also neuroprotective actions [284].

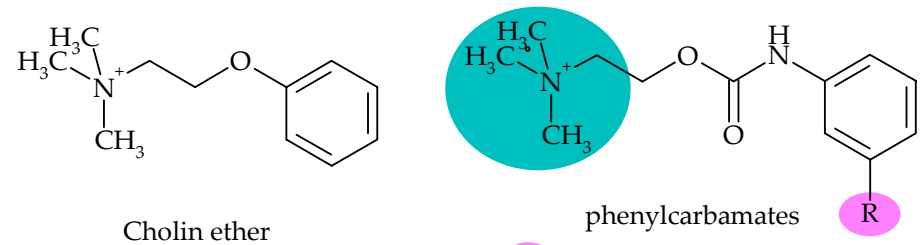

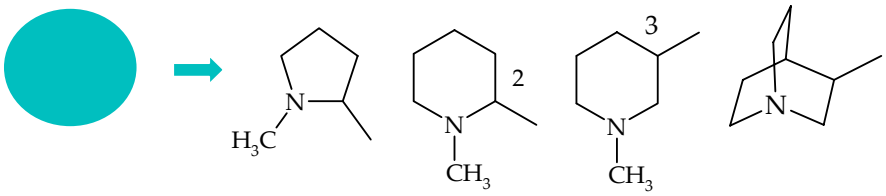

Extending choline **4** with an amide moiety to obtain the carbamate function leads to carbacholine, MCC and DMCC, which were proved to be nicotinic agonists [177]. Recently, compounds bearing a carbamate moiety showed a very selective interaction with the α7* nicotinic receptor versus α4β2* [178].

In this study, the phenylether of choline is used as lead structure. Further modification concerns the insertion of an amide to get a carbamate fragment and the incorporation of the nitrogen of the quaternary amine group into a cyclic system. These latter modifications are introduced in order to permit the penetration through the blood-brain barrier and to study the influence of the azacyclic moiety for the different nAChR subtypes. SAR studies of phenylcarbamate derivatives could give us more information about the structural requirements to enhance the selectivity for α7* versus the α4β2* nicotinic receptor.

III. Results

III/1. Radioligand binding studies for different nAChRs

(Results and experimental conditions used in saturation and competition assays)

III/1.1. α4β2* nAChR: Saturation and competition binding studies

(±)-[^{3}H]Epibatidine is a high affinity radioactive agonist able to label multiple nAChRs widely distributed in the brain as well as in the periphery. It is an excellent tool for studying neuronal nicotinic receptors and conceivably to distinguish between different subtypes that might exist in the central and peripheral nervous system [179, 261]. Several previous studies support the idea that the high affinity binding sites of epibatidine in the brain represent interactions with the α4β2* nAChRs subtype [77, 157, 285, 286]. Results of saturation experiments performed with (±)-[^{3}H]epibatidine in homogenates from rat forebrain and human cerebral cortex, in a concentration range of 1 pM to 15 nM, showed that this ligand bound with two binding sites in rat forebrain: a high affinity (K_D values of 15 pM) and low affinity site (K_D values 360 pM) [285]. Further studies performed in a concentration range of 1-500 pM permit a differentiation of the two binding sites. Indeed, over this concentration range, (±)-[^{3}H]epibatidine bound a single population of sites in the rat brain with K_D values of 8 pM and B_{max} of 180 fmol/mg protein [179]. This K_D value is in agreement with previously measured K_D (4-18 pM) for (±)-[^{3}H]epibatidine binding in rat brain [285, 286], human cerebral cortex [285], mouse brain [287] and M10 cells [173, 285]. Several indications, such as the similar pattern of distribution of (±)-epibatidine **13**, binding sites and the fact that the K_D value found for (±)-[^{3}H]epibatidine binding in M10 cells, stably expressing the α4β2 nAChRs [173, 285], similar to that found for (±)-[^{3}H]epibatidine binding in rat brain, corroborate the idea that these high affinity binding sites correspond to the α4β2* nAChRs subtype. Therefore, (±)-[^{3}H]epibatidine in an

optimal concentration between 1 and 500 pM with a K_D of 8 pM [179] is the ideal radioligand for characterizing neuronal $\alpha 4\beta 2^*$ nAChRs receptors.

Saturation binding studies

Based on these results, (±)-[^{3}H]epibatidine was used as a radioligand in saturation and competition binding assays for the $\alpha 4\beta 2^*$ nAChRs subtype. The concentration of (±)-[^{3}H]epibatidine set up in saturation assays was between 1 and 500 pM. Non-specific binding was determined using 300 μM (-)-nicotine hydrogen tartrate salt. The P2 membrane fraction was obtained from frozen Sprague-Dawley rat forebrain. To offset the effect of ligand depletion, 60-70 μg of protein pro vials were incubated at 22 °C for 4 h in a total volume of 4 ml HEPES-salt solution (HSS). A previous assay established for the $\alpha 4\beta 2^*$ nAChRs subtype was carried out using P2 membrane fraction from rat brains. The intention of this experiment was to verify whether frozen P2 membrane fraction stored in the freezer at –80 °C has the same characteristic of Fischer-344 rat brain used in earlier assays. The binding parameters obtained were consistent with previously published data [179].

Competition binding studies

In competition binding studies, a previously developed assay with (±)-[^{3}H]epibatidine and P2 membrane fraction of Sprague-Dawley rat brains (except the medulla and the cerebellum) was utilized [261]. Different concentrations of novel competitive ligands were incubated with 0.5 nM of (±)-[^{3}H]epibatidine. Rat membrane preparations were incubated at 22 °C for 90 minutes in a total volume of 0.5 ml of HSS. The concentration of the radioligand, the duration and temperature of incubation were established based on results obtained from kinetics studies [179].

III/1.2. α7* nAChR: Saturation and competition binding studies

Neuronal nicotinic receptors with high affinity for [^{125}I]α-bungarotoxin ([^{125}I]α-Bgt) are presumably composed of only α7* subunits and display a regional distribution distinct from that of the heteromeric nAChRs [86]. [^{125}I]α-bungarotoxin is recognised as a selective ligand for the homopentameric α7* nAChR (K_D =1.5 ± 0.7 nM, and B_{max} 63 ± 17 fmol/mg protein in rat brain) and has been widely used as a radioligand for

binding and autoradiographic studies of this receptor [76, 77] [75]. However, [^{125}I]α-Bgt presents some drawbacks, e.g. slow kinetics properties that affect the incubation time of the assay, and difficulty in separation of free radioligand from the assay media, resulting in high and poorly reproducible non-specific values. Moreover, it does not cross the blood brain barrier, limiting its use for in vivo binding and imaging studies for the α7* nAChRs [244]. A tritiated version of MLA, a selective antagonist at the α7* nAChRs subtype (affinity of unlabelled MLA for the α4β2* nAChRs subtype K_i =1.56 μM in rat brain [288]) has been developed as an alternative to [^{125}I]α-Bgt in radioligand binding assays [239]. Regional distribution of [^{3}H]MLA binding sites in rat brain shares the pattern of that of [^{125}I]α-Bgt [239]. In saturation binding studies, [^{3}H]MLA bound to a single population of binding sites exhibited a K_D value of 1.2 ± 0.2 nM [239].

Saturation binding studies

To confirm the binding parameters (K_D and B_{max}) reported in previous studies, the saturation of [^{3}H]MLA binding to α7* nAChR subtype in P2 membrane preparation of rat brain was re-evaluated. Saturation experiments were carried out in quadruplicates by incubating rat brain membranes (120 μg protein) at 22 °C for 2.5 h in HSS with concentrations of [^{3}H]MLA ranging from 0.1 to 40 nM. Non-specific binding was determined in the presence of MLA (50 μM). The binding parameters obtained were B_{max} = 147 fmol/mg protein and K_D = 1 nM which are consistent with previously published data [239].

Competition binding studies

[^{3}H]MLA is a tritium labelled ligand which is easier to handle than the iodine-125 labelled α-Bgt. [239, 244]. Therefore, [^{3}H]MLA was used as an alternative radioligand to [^{125}I]α-Bgt in competition binding assays. Membrane fractions isolated from the rat brain were incubated at 22 °C for 2 h in 250 μl HSS.

III/1.3. α3β4*nAChR: Saturation and competition binding studies

The affinity of novel ligands for the α3β4* nAChRs subtypes was assessed using a novel competition experiment procedure that involves the use of (±)-[^{3}H]epibatidine and calf or pig adrenal glands [289-292]. The specific binding of (±)-[^{3}H]epibatidine to

crude synaptic membranes of pig adrenals is characterized by a single population of binding sites and exhibited a K_D value of 54 pM (see Results III/2).

III/1.4. $(\alpha 1)_2\beta 1\gamma\delta$ nAChR: Saturation and competition binding studies

In previous experiments, the radioligand of choice to determine K_i values of novel ligand for muscle type nAChR was [^{125}I]α-Bgt. Unfortunately, [^{125}I]α-Bgt presents some drawbacks (see III/1.2). The incubation process had to be carried out on borosilicate glass tubes, instead of polypropylene tubes, to avoid the adherence of the radioligand to the walls of the tubes. Furthermore, in order to reduce the non-specific binding to filter material, the rinse buffer should contain 1% of nonfatty dry milk [180]. Based on the excellent properties of (±)-[^{3}H]epibatidine in radioligand binding studies [179] a novel assay was established using (±)-[^{3}H]epibatidine and membrane fractions isolated from the *Torpedo californica* electroplax [290, 291, 293, 294]. In saturation assays, [^{3}H]epibatidine binds to a single population of binding sites in *Torpedo californica* electroplax with a K_D value of 2 ± 0.2 nM.

III/1.5. Protein determination

In order to decide which methods, between those of Bradford [279] or Lowry [280], were the most reliable and satisfactory for the present studies, protein concentrations of P2 membrane fractions of rat brain and whole membranes of pig adrenal were determined following both procedures.

Table III/1.1: Comparison of the two methods (Lowry and Bradford) for the quantitative measurement of protein content in P2 membrane fraction from rat brain and whole membrane from pig adrenal.

Protein	Quantity of protein μg/ml		Ratio
	Bradford	Lowry	
rat brain (P2 fraction)	1.629 ± 269	2.407 ± 47	1.4
pig adrenal	1.112 ± 167	2.491 ± 260	2.2

The Bio-Rad Protein Assay, based on the method of Bradford, is a very simple procedure. It is rapid and also cheaper than the Lowry method. However, not every sample preparation is suitable for investigation with this method. Since the Coomassie dye reagent is highly acidic, a small number of proteins cannot be assayed with this reagent due to their poor solubility in the acidic reagent. In addition, Coomassie dye tinge the glass or quartz cuvettes used to hold the solution in the spectrophotometer. The Lowry method utilizes sodium dodecylsulfate (SDS) to facilitate the dissolution of relatively insoluble lipoproteins and to avoid a nonhomogeneous distribution of protein, responsible for errors in the protein determination [295]. The values listed in table III/1.1 show that the quantity of protein (expressed in μg/ml) determined with the Lowry method is ca. twice as large as the quantity measured with the Bradford method. This means that the Lowry procedure allows us to obtain a more accurate measurement of the protein present in the tissue. On the basis of these considerations, the protein concentration of other membrane preparations used in this study (*Torpedo Californica* electroplax and calf adrenal) was determined using the Lowry procedure.

III/2. Characterization of α3β4* nAChRs

III/2.1. Introduction

III/2.1.1. Distribution of α3-containing nAChRs

Nicotinic acetylcholine receptors containing α3 and β4 subunits are one of the major nicotinic receptor subtypes in post-synaptic neurons, in autonomic ganglia, sensory ganglia, and chromaffin cells of the adrenal medulla [40, 46, 296-299]. They are involved in mediation of cholinergic actions on the autonomic nervous system (ANS). Nicotinic receptors containing α3 and β4 nAChRs subunits are thought to be potential nicotinic receptor subtype in rat intracardiac neurons mediating the nicotine induced heart rate increase [91]. The α3-containing nAChRs are also present in several brain regions, in particular in the substantia nigra, the medial habenula and interpeduncular nucleus, hippocampus and ventral tegmental areas [113, 300, 301]. Although the exact subunit composition of these receptors in the CNS have not been unravelled yet, it is believed to be α3β4*, probably in association with α5 [299]. In 1995, some studies revealed that the pineal gland also contains nAChRs subunit mRNAs [302]. Recently, the pharmacological characteristic of nicotinic receptors present in rat pineal suggests that they are exclusively α3β4 nAChRs [312]. With regard to the nicotinic receptors present in the mammalian medial habenula (MHb), the lack of sensitivity to α-Bgt **5** and the high potency of (-)-cytisine **Cy 1** indicate the absence of α7 and the presence of β4 subunits. Currently, studies performed by Quick et al. provide evidence that the majority of functional receptors in the mammalian medial habenula (MHb) contain α3 and β4 nAChRs subunits [300]. The physiological role of α3β4* nAChR subtype in the CNS is not clear, but they seem to be involved in the control of norepinephrine and dopamine release [303, 304].

III/2.1.2. (±)-[³H]Epibatidine as radioligand to characterize α3β4* nAChRs

(±)-[³H]Epibatidine, due to its high affinity and low nonspecific binding represents a very broad-spectrum ligand for studying different subtypes of nicotinic acetylcholine receptors that might exist in brain and peripheral tissue [111, 285, 287, 305]. Currently, (±)-[³H]epibatidine is a suitable radioligand to investigate nicotinic receptors in peripheral neuronal tissues, including neurons of mammalian sympathetic and parasympathetic ganglia [87], sensory neurons, such as the trigeminal ganglia [83] and adrenal chromaffin cells [298]. Until the discovery of tritiated (±)-epibatidine **13** it was difficult to detect and measure the presence of nAChRs in such tissues. Indeed, compared to the α4β2* nAChR subtype in the CNS, receptors containing α3 subunits seem to possess a much lower affinity for other nicotinic ligands. In competition assays against (±)-[³H]epibatidine, the affinities of (-)-cytisine **Cy 1** and (-)-nicotine **3** for nAChRs in the adrenal gland, superior cervical ganglia and pineal, were between 85 nM and 325 nM [306]. Their low affinity limits the use of (-)-[³H]nicotine and (-)-[³H]cytisine as radioligands. In fact, in saturation assays, the binding of (-)-[³H]nicotine and (-)-[³H]cytisine in such tissues was characterized by a high non-specific binding [306], so that neither of these can be used to obtain reliable measurements of the density of these peripheric neuronal tissues. On the contrary, (±)-[³H]epibatidine binds with high affinity ganglionic-type receptors [83, 157, 219, 221, 286, 287] and is an appropriate radioligand for studying and characterizing α3β4* neuronal nAChRs in stably transfected cell lines [240, 281, 307]as well as receptors in rat adrenal glands [180, 285] and trigeminal ganglia [83]. Given that the α3β4* nAChRs subtypes are supposed to possess a lower affinity for (±)-[³H]epibatidine if compared to α4β2* nAChRs, a radioligand concentration higher than 500 pM is required to detect and measure the ganglionic nAChRs subtypes. In previous studies, epibatidine radiolabelled with tritium was replaced by its radioiodinate analogue, namely [¹²⁵I]IPH [111, 220, 221, 306]. The high specific radioactivity of [¹²⁵I]IPH greatly facilitated measurements in tissue with relatively low receptor density. However, the problem regarding the limited supply of the tissue still subsists.

III/2.1.3. Membrane preparations used to characterize α3β4* nAChRs

There are some difficulties which make the characterization of the pharmacology of α3β4* nAChR subtype complicated [281]. Firstly, the low density of nAChRs subtypes containing α3 subunits in peripheral neuronal tissue (autonomic ganglia and adrenal gland). A second critical aspect concerns the peripheral neuronal tissue that may contain more than one nAChR subtype. The novel recombinant technique permitted to study the pharmacological properties of recombinant rat, bovine and human α3β4 stably expressed in human embryonic kidney (HEK 293) cells. This technique has the advantage of working with nAChR of known subunit composition; on the other hand, is limited in that functional properties of recombinant receptors may not fully match those of the native AChRs. Nevertheless, it has proved to be useful in unravelling the pharmacological and functional characteristics of α3β4* receptors subtype located in the CNS as well as in the peripheral nervous system. In 1998, Xiao et al. [281] stably transfected human kidney embryonic 293 cell with the rat neuronal nicotinic acetylcholine receptor α3 and β4 subunit genes [281]. They found that this cell line contains a high level of the α3β4 receptor subtype and (±)-[^{3}H]epibatidine binds with a K_D value of 304 pM and a B_{MAX} value of 8942 fmol/mg protein (Tab. III/2.1). Staudermann et al. [308] also performed saturation binding experiments for the α3β4 nAChR receptor, but they preferred to use human recombinant α3β4 receptors stably transfected in embryonic kidney cells (HEK 293) and (±)-[^{3}H]epibatidine to determine the binding parameters (K_D = 236 pM and B_{MAX} = 2010 fmol/mg protein). Compared to Xiao et al., they found a lower receptor density. In 2002 and 2003, Free et al. made saturation and kinetics studies using both native bovine chromaffine cells (K_D = 52 pM and B_{MAX} =34 fmol/mg protein) [309] and recombinant bovine α3β4 nAChR expressed in HEK 293 cells (K_D = 66 pM and B_{MAX} =3500 fmol/mg protein) [310] in order to compare the difference in the pharmacological profile that might exist (based on difference in the subunit) (Tab. III/2.1). They found that the K_D values at BMα3β4 HEK cell and bovine adrenal medulla are nearly identical. On the other hand, the B_{MAX} value for (±)-[^{3}H]epibatidine to BMα3β4 HEK cell is > 100- fold higher than that

reported for (±)-[^{3}H]epibatidine binding to membranes from bovine adrenal cells [309, 310]. Only a few studies on native neuronal α3-containing nAChRs have been reported [285, 311] due to the lack of a specific native membrane preparation containing a high density of the α3β4* receptors subtype. The iodinated analogue of epibatidine, [^{125}I]IPH), due to its high specificy radioactivity, has been used to label α3β4 receptors in the superior cervical ganglia (K_D values of 443 pM and a B_{MAX} value of 272 fmol/mg protein [220] and in adrenal glands with a K_D value of 155 pM and a B_{MAX} value of 83 fmol/mg protein [306]. Like (±)-epibatidine **13**, the drawback of using [^{125}I]IPH is that it is not able to distinguish α4β2* nAChRs and the nicotinic receptors containing α3 and β4 subunit [83]. However, the K_D value found for the membrane preparation of rat adrenal glands using [^{125}I]IPH is 3-fold higher than that found by Mukhin et al. for (±)-[^{3}H]epibatidine using the same native tissue (K_D value of 55 pM, single population of binding sites) [180] (Tab. III/2.1). To exclude any possible interaction with the α7* subtype (also found in the adrenal gland), they proved that (±)-[^{3}H]epibatidine binding was not blocked (data not shown) by α-bungarotoxin (K_i = 1 nM) at concentrations as high as 10,000-times its affinity at α7* nAChRs [309 300]. These data are consistent with the view that (±)-[^{3}H]epibatidine binds nAChRs containing the α3 and β4 subunits. Nevertheless, these results do not exclude possible interactions with other subunits (e.g. α5) [83, 88, 89].

Table III/2.1: Comparison of K_D and B_{MAX} values obtained from different saturation binding experiments for α3β4*, using different membrane preparations and radioligands

Tissue used in radioligand binding assays (saturation assays)	**K_D (pM) (epibatidine radiolabelled)**	**B_{max} (fmol/mg protein)**	**References**
Rat brain α3β4 nAChR expressed in HEK 293 cells	**304** (±)-[^{3}H]EPI	**8942**	281
human recombinant α3β4 nAChR expressed in HEK 293 cells	**236** (±)-[^{3}H]EPI	**2010**	308
α3β4* nAChRs in native bovine chromaffine cells	**52** (±)-[^{3}H]EPI	**34**	309

recombinant bovine α3β4 nAChRs (BMα3β4) expressed in HEK 293 cells	**66** (±)-[^{3}H]EPI	**3500**	310
α3β4* nAChRs in the superior cervical ganglia	**443** [^{125}I]IPH	**272**	220
α3β4* nAChRs in native rat adrenal gland	**155** [^{125}I]IPH	**83**	306
α3β4* nAChRs in native rat adrenal gland	**55** (±)-[^{3}H]EPI	Data not shown	180
α3β4* nAChRs in native pineal gland	**100** (±)-[^{3}H]EPI	**300**	312

In 2004, Hernandez et al. [312] studied the nicotinic receptors expressed in the rat pineal gland. The pharmacology of these receptors and their function correspond to the defined α3β4 nAChRs subtype heterologously expressed in HEK 293 cells. They performed saturation studies for pineal glands and found that (±)-[^{3}H]epibatidine (concentration range: 5 – 3,000 pM) fits a model for a single binding site with a K_D value of 100 pM and a high density (B_{MAX} = 300 fmol/mg protein). Moreover, they performed immunoprecipitation studies with subunit-specific antibodies in order to definitively clarify the subunit composition of receptors in the pineal gland. These assays also corroborate the finding that the nAChRs receptor is apparently exclusively a α3β4 subtype. Previous mRNA analysis also indicated the presence of β2 subunits, but via western plot they did not find any evidence for the presence of such a subunit. Furthermore, autoradiographic studies of [^{125}I]α-Bgt binding in the pineal did not exceed the background level, indicating that the pineal gland does not express α7* or other subtype that binds [^{125}I]α-Bgt [312]. In future, the rat pineal glands may provide a suitable native tissue to perform studies about the channel properties, regulation and turnover of this subtype in native cells [312].

III/2.2. Project: establishment of a radioligand binding assay for α3β4*nAChRs using pig/calf adrenal glands

Saturation assays: Analysis of (±)-[^{3}H]epibatidine binding to α3β4 receptors in native adrenal glands*

Bovine adrenal chromaffin cells are supposed to contain at least two subtypes of neuronal nAChRs. One is thought to be the α7* nAChRs subtype, which binds α-Bgt **5** [313] and is present in the adrenal glands only in limited amounts. The precise subunit composition of the second neuronal nAChR is unknown so far, but it is likely to be composed of α3, α5 and β4 subunits. In fact, mRNAs for such subunits have been found in bovine adrenal cells [297-299]. Further studies with bovine adrenals confirmed that such glands were rich in nAChRs containing the α3 and β4 [309] subunits. Given that only limited amounts of tissue were available to carry out radioligand binding experiments, only few studies on native neuronal α3-containing nAChRs have been performed [180, 285, 309]. The use of a radio-iodinated version of (±)-epibatidine **13**, thought to give an acceptable numbers of counts, was not able to overcome the problem of a limited supply of tissue containing α3β4* nAChRs. On the other hand, the positive results obtained by Mukhin et al [180] using (±)-[^{3}H]epibatidine and rat adrenal glands suggest that tritiated epibatidine, due to its high affinity to the ganglionic-type nAChRs, is a suitable radioligand to detect α3β4* nAChRs in adrenal glands. Based on these considerations, larger and more easily obtainable pig or calf adrenal glands were used in this study to perform radioligand-binding assays. The intention of saturation binding assays was to determine the K_D and B_{max} of (±)-[^{3}H]epibatidine for the α3β4* nAChRs contained in pig or calf adrenal glands.

Competition assays

In order to validate a novel procedure for radioligand binding competition assays using α3β4* nAChRs in native adrenal glands, affinities of some standard ligands, such as (±)-epibatidine **13**, (-)-cytisine **(Cy1)** and (-)-nicotine **3** are assessed for the subtype under investigation. The results obtained in assays performed with known cholinergic drugs should confirm the utility of this novel protocol for screening the

affinities of novel ligands for the α3β4* nAChR. Moreover, for the first time, the affinities of the two enantiomers of epibatidine, (-)- and (+)-epibatidine are evaluated at the α3β4* nAChRs subtype (in the present study, (-)- and (+)-epibatidine refer to rotation of the salts).

III/2.3. Results

III/2.3.1. Analysis of (±)-[^{3}H]epibatidine binding to α3β4 receptors in pig adrenal glands*

Saturation experiments were carried out by incubating 60-90 μg protein of pig adrenal whole membranes at 22 °C for 4 h in a total volume of 2.2 ml of HSS with concentrations of (±)-[^{3}H]epibatidine ranging between 2 and 2400 pM. The results of saturation studies are shown in Fig. III/2.1. The binding parameters obtained from four independent experiments were: K_D = 54 ± 4.6 pM and B_{max} = 99 ± 11 fmol/mg protein. The nonspecific binding was determined in the presence of 600 μM (-) nicotine hydrogen tartrate salt.

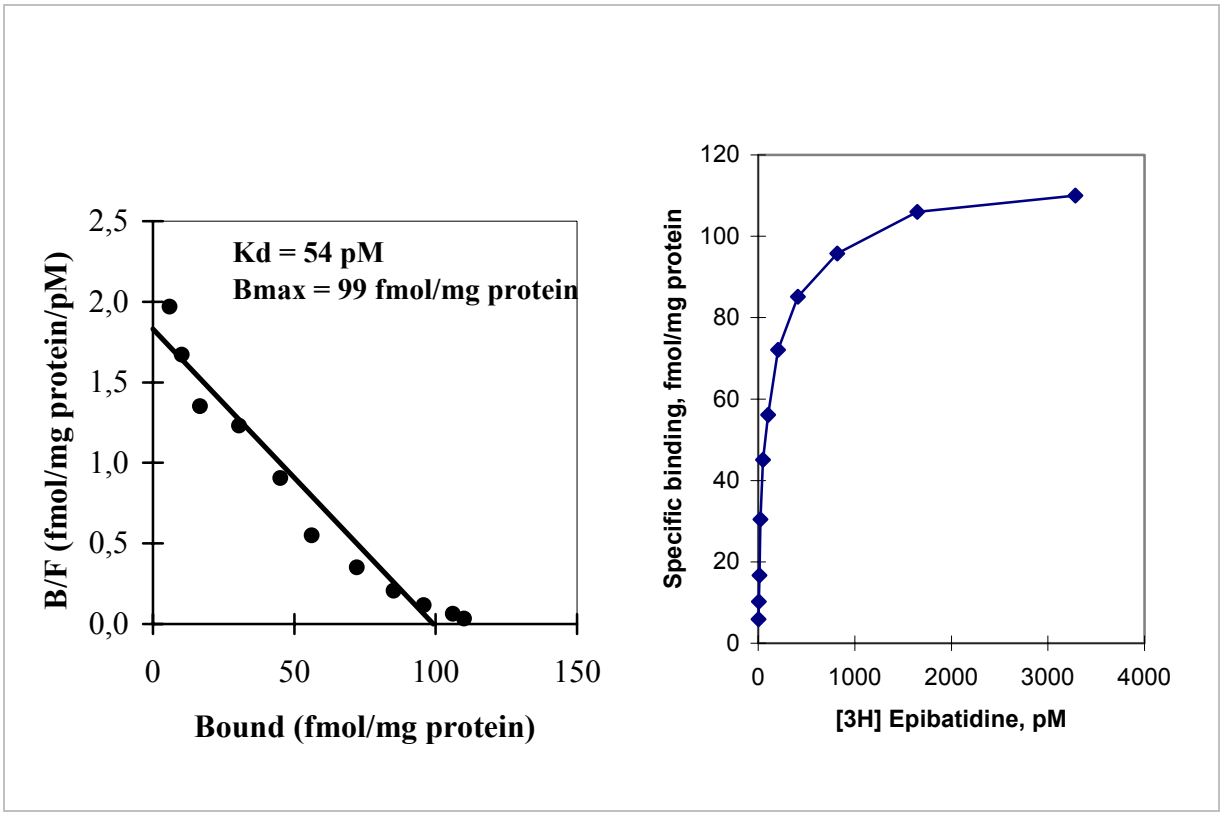

Figure III/2.1: Each graphs represents results of a single experiment performed in quadruplicates (S.E.M. < 10%). Similar results were obtained in three additional experiments.

III/2.3.2. Analysis of (±)-[^{3}H]epibatidine binding to α3β4 receptors in calf adrenal glands*

Saturation experiments were carried out by incubating whole membrane fractions of calf adrenals (60-90 μg protein) with different concentrations of (±)-[^{3}H]epibatidine (2-2400 pM) at 22 °C for 4 h in a total volume of 2.2 ml (HSS). Nonspecific binding was determined in the presence of 600 μM (-)-nicotine hydrogen tartrate salt. The results of saturation studies are shown in Fig. III/2.2. The Scatchard plot was linear in conformity with the presence of a single population of binding sites. The binding parameters obtained from two independent experiments were: K_D = 39 ± 5.3 pM and B_{max} = 91 ± 10 fmol/mg protein. These studies demonstrated that calf adrenal provides a simple and convenient model system to study native α3β4* nAChRs subtype.

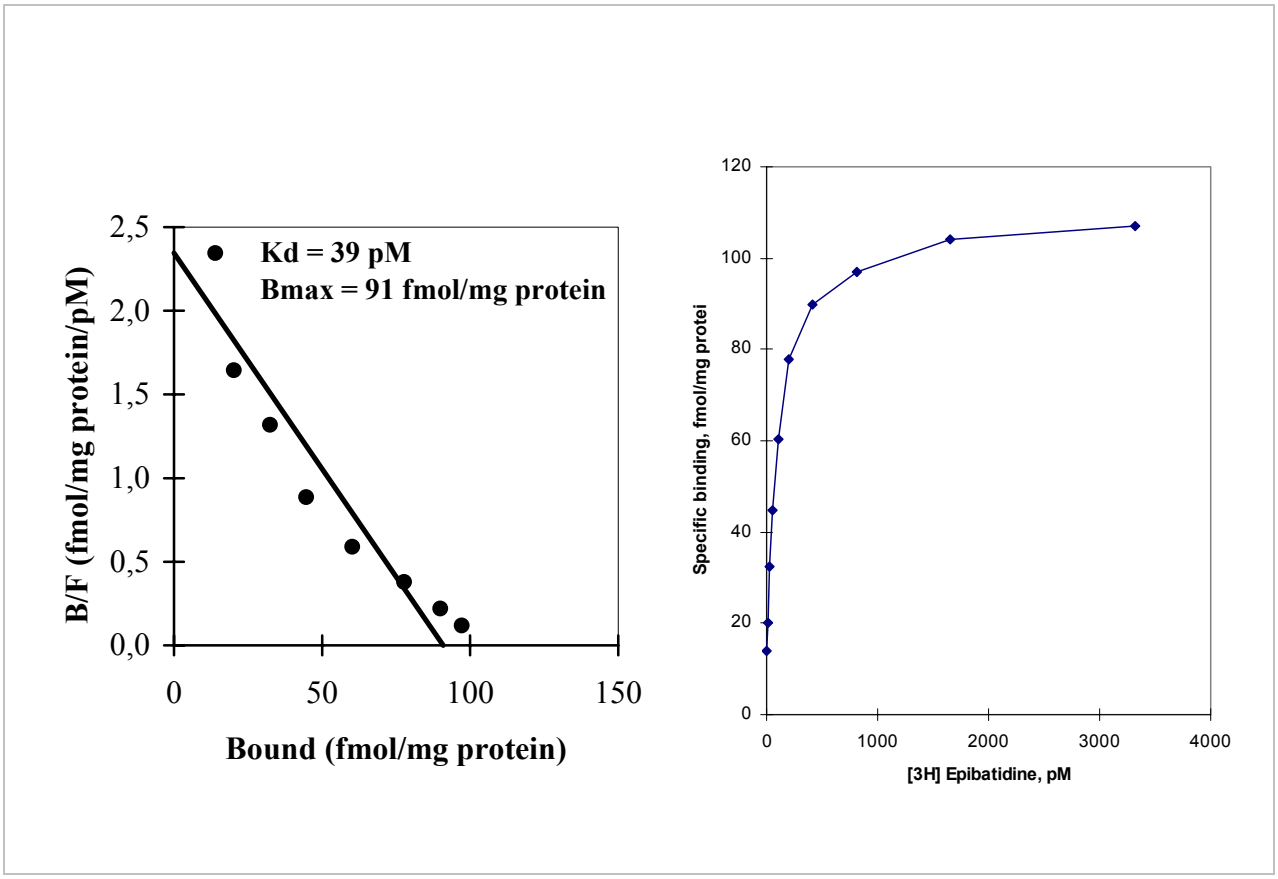

Figure III/2.2: Each graphs represents results of a single experiment performed in quadruplicates (S.E.M. < 10%). Similar results were obtained in three additional experiments.

III/2.3.3. A novel competition binding assay with (±)-[^{3}H]epibatidine and calf/pig adrenal glands

In competition assays with (±)-[^{3}H]epibatidine and pig adrenal glands the affinity of standard cholinergic ligands, such as (±)-epibatidine **13**, (+) and (-)-epibatidine, (-)-cytisine **Cy1** and (-)-nicotine **3** was assessed for α3β4* nAChRs [289-292]. (±)-[^{3}H]Epibatidine binds to crude synaptic membranes of pig adrenals with a K_D value of K_D = 54 ± 4.6 pM. Different concentrations of a competing drug were incubated in the presence of 0.5 nM of (±)-[^{3}H]epibatidine, at 22 °C for 90 min using whole membrane fractions of pig adrenal glands (60-90 μg). The rank order of potency of the agonists was (±)-epibatidine **13** >> (-)-cytisine **Cy 1** > (-)-nicotine **3** (Tab. III/2.2). (±)-Epibatidine **13** was by far the most potent drug in competing for α3β4* nAChRs (K_i = 0.03 nM). Among these ligands, (±)-epibatidine **13** was > 600 times more potent than (-)-cytisine **Cy 1** and 2200 times more potent than (-)-nicotine **3**. In the present study, the interaction of the two epibatidine enantiomers with the α3β4* nAChRs subtype was investigated for the first time. Results of competition binding assays carried out with (±)-[^{3}H]epibatidine in pig adrenal glands, revealed that (+)-epibatidine (K_i = 0.124 ± 0.02 nM) has a 3-fold lower affinity compared to the (-)-epibatidine (K_i = 0.042 ± 0.06 nM). Therefore, these values demonstrated that (-)-epibatidine binds to the α3β4* nAChRs subtypes with a certain degree of enantiomeric selectivity.

Table III/2.2: Comparison of binding affinities (K_i values) of nicotine **3,** (-)-cytisine **Cy1,** (±)-epibatidine **13** derived from binding competition studies against (±)-[^{3}H]epibatidine,using different tissue sources

Competing drugs	(±)-[^{3}H]EPI pig adrenal glands α3β4* nAChRs K_i (nM)	(±)-[^{3}H]EPI bovine adrenal medulla α3β4* nAChRs K_i (nM) [309]	(±)-[^{3}H]EPI recombinant bovine adrenal medulla expressed in HEK 293 cells K_i (nM) [310]	(±)-[^{125}I]EPI rat adrenal glands α3β4* nAChRs K_i (nM) Davila 2003	(±)-[^{3}H]EPI rat adrenal glands α3β4* nAChRs K_i (nM) [180]
(+)-EPI	0.124 ± 0.02	n.d.	n.d.	n.d.	n.d.
(-)-EPI	0.042 ± 0.06	n.d.	n.d.	n.d.	n.d.
(±)-EPI	0.03	0.3 ± 0.1	0.3 ± 0.02	0.30 ± 0.14	0.049 ± 0.02

(-)-Nicotine	67	215 ± 69	517 ± 9	236 ± 45	100 ± 20
(-)-Cytisine	18	401 ± 37	517 ± 27	325 ± 24	54 ± 9

III/2.4. Discussion

Neuronal nicotinic receptors in the brain can be labelled and studied with different radioactive agonists, including [^{3}H]ACh [75, 314], (-)-[^{3}H]nicotine [75], and (-)-[^{3}H]cytisine [232, 315]. However, these radiolabelled agonists, due to their low affinities towards non-α4β2* nAChRs, are not useful in detecting receptor subtypes in the adrenal glands or autonomic ganglia. The present study shows that (±)-[^{3}H]epibatidine, in addition to being an excellent radioligand for studying nAChRs present in rat brains (CNS)[179, 285, 286], is also a suitable ligand to characterize α3β4* nAChRs present in the peripheral neuronal tissues. This conclusion is based on results of saturation studies performed with (±)-[^{3}H]epibatidine and pi/calf adrenal glands. (±)-[^{3}H]Epibatidine (concentration range of 2-2400 pM) was shown to combine with a K_D = 54 ± 4.6 pM to nAChRs in pig adrenals (B_{max} of 99 ± 11 fmol/mg protein) and with a K_D of 39pM to nAChRs in calf adrenals (B_{max} of 91 ± 10 fmol/mg protein). The K_D values are consistent with the previously measured K_D value of 55 pM for (±)-[^{3}H]epibatidine binding with nAChRs in the rat adrenal gland membranes [180] and in native bovine adrenal α3β4* nAChRs (K_D = 52 pM and B_{MAX} =34 fmol/mg protein) [309, 310]. Pig and calf adrenal glands possess some advantages in comparison to rat adrenal glands, such as the large size and easy availability from a local slaughterhouse. Such characteristics make the preparation of whole membrane fraction from pig and calf adrenal glands uncomplicated and permit having enough native tissue, with a suitable density of α3β4* nAChRs at one´s disposal. Such considerations underlined that pig/calf adrenal glands represent a better tool for research purpose than other native tissue and sustain the classification of adrenal nAChRs as α3β4* nAChRs. In order to validate the experimental conditions for a novel competition binding assays for

α3β4* nAChRs subtypes, the binding affinities of standard cholinergic agonists were determined using (±)-[^{3}H]epibatidine and pig/calf adrenal glands [289-292]. In the present study, the binding affinity of (±)-epibatidine **13** for nAChRs in pig adrenal glands (K_i = 0.03 nM) was in accordance with the value found by Mukhin et al. 1[80] in competition binding assays using (±)-[^{3}H]epibatidine and rat adrenal glands (K_i = 0.049 nM). On the contrary, it is not possible to compare K_i values found in this project for (±)-epibatidine **13**, (-)-cytisine **Cy 1** and (-)-nicotine **3** for α3β4* nAChRs with previous values obtained from competition assays using (±)-[^{3}H]epibatidine and cultured bovine chromaffin cells or native bovine chromaffin cells (Tab. III/2.2) [309, 310]. The discrepancies may be related to the different protein concentration (10-fold higher) used by other research groups in radioligand assays [309,310]. Once the protocol of this novel competition assay had been validated, a series of experiments have been carried out, for the first time, to investigate the ability of the α3β4* nAChRs subtype to interact with a certain degree of enantiomeric selectivity. It has been previously reported that binding sites on the α4β2* nAChRs do not distinguish between the stereoisomers of (±)-epibaditine **13** [285]. In fact, competition assays using (-)-[^{3}H]nicotine and P2 membrane fraction of rat brain nAChRs showed that the natural enantiomer, (+)-epibaditine **13** (K_i = 0.045 nM) has nearly the same binding affinity of the synthetic enantiomer, (-)-epibaditine (K_i = 0.058 nM) for α4β2* nAChRs [157]. In order to determine whether the α3β4* nAChRs subtype is able to distinguish between the two isomers of (±)-epibatidine **13**, competition binding studies using (±)-[^{3}H]epibatidine and (+)-epibatidine, (-)-epibatidine in pig adrenal glands have been performed. The rank order of potency was (-)-epibatidine > (+)-epibatidine. Surprisingly, the (1R,2R,4S)-(-)-epibatidine (K_i =0.042 ± 0.06 nM) showed 3-fold higher affinity than the (+)-isomer of epibatidine (K_i =0.124 ± 0.02 nM) for the α3β4* nAChRs subtypes. This presence of stereospecificity probably indicates that a chiral centre of (±)-epibatidine **13** participates in a decisive way to its binding to α3β4* nAChRs.

III/3. Cytisine as a lead compound for novel nAChR ligands

III/3.1. Introduction

III/3.1.1. Cytisine: Structure and Origin

(-)-Cytisine **Cy 1** *(1,2,3,4,5,6-hexahydro-1,5-methano-pyrido[1,2-a][1,5]diazocin-8-one)* is a quinolizidine alkaloid composed of a tricyclic skeleton with a bispidine framework fused to a pyridone moiety (Fig. III/3.1). The absolute configuration of the two chiral centres was established by Okuda et al. to be 7R and 9S [316].

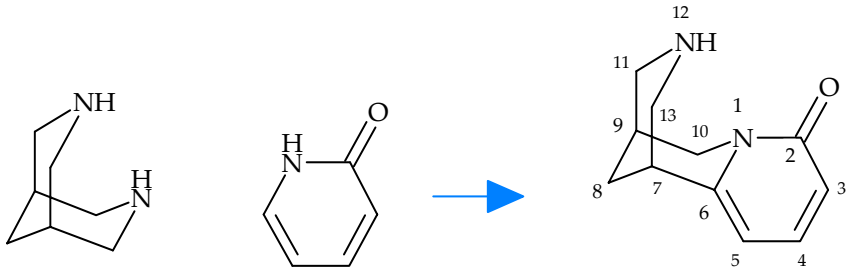

bispidine pyrid-2-one (-)-7R, 9S cytisine **Cy 1**

Figure III/3.1: Structure of cytisine **Cy 1**, composed of a bispidine framework fused to a pyridone moiety (an alternative numbering of atoms is used: 7,9,10,11,12,13-hexahydro-7,9-methano-pyrido[7,8][7,9]diazocin-2-one).

(-)-Cytisine **Cy 1** is easily accessible by extracting seeds from Laburnum anagyroides medicus (Fabaceae) (Fig. III/3.2) [317, 318]. This plant is poisonous with the greatest amount of the highly poisonous alkaloid found in the black seeds (up to 3%) [319]. They are toxic after ingestion (LD_{50} = 101 mg/kg p.o. in mouse) [319] and the symptoms are similar to those of (S)-(-)-nicotine **3** intoxication (LD_{50} = 25 mg/kg p.o in mouse) [319]. In fact, (-)-cytisine **Cy 1**, like (-)-nicotine **3**, can cause convulsions and death by respiratory failure [320, 321].

Figure III/3.2: Laburnum anagyroides medicus (Fabaceae). [322]

Barlow and Johnson determined the X-ray crystal structure of (-)-cytisine **Cy 1**. They noted that although **Cy 1** has a rigid structure, it occurs in the crystal in two distinct but very similar conformations. A comparison of the structure of (-)-cytisine **Cy 1** and (-)-nicotine **3** (Fig. III/3.3) shows that the quasi-aromatic ring in the (-)-cytisine **Cy 1** and the pyridine ring of (-)-nicotine **3** are tilted in a similar extent in relationship to the nitrogen atom in the bispidine ring and the nitrogen atom in the pyrrolidine ring, respectively [250] (Fig. III/3.3).

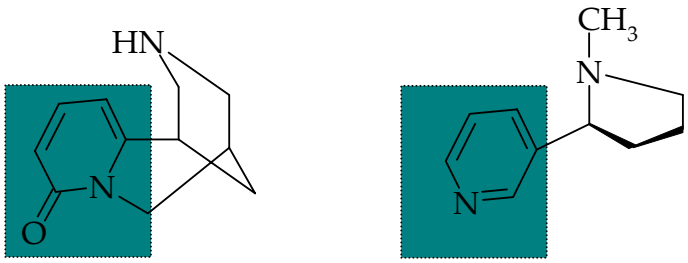

(7R,9S)(-)-cytisine Cy1 (S)(-)-nicotine (3)

Figure III/3.3: Structure of (-)-nicotine **3** and (-)-cytisine **Cy1.**

(-)-Cytisine **Cy 1** represents an important nAChR ligand, which could disclose new opportunities for developing new agonists or antagonists in this receptor family. In radioligand binding studies, (-)-cytisine **Cy 1** has demonstrated a very high affinity to neuronal nicotinic receptors (K_D = 0.15 - 0.98 nM) [43, 183, 231, 232, 315, 323] and a very high selectivity for nicotinic compared to muscarinic receptors (K_i = 0.16 nM (nAChRs) and K_i > 400,000 nM (mAChRs)) [183]. Recent studies showed that compared to (-)-nicotine **3**, (-)-cytisine **Cy 1** has a 7-fold higher affinity (K_i = 0.124 nM) [230] for the α4β2* subtype and only a 2-fold lower affinity for the α7* nAChR (K_i = 261 nM) [230].

Functional data showed that the effects of (-)-cytisine **Cy 1** on nAChRs are sensitive to receptor subunit composition. (-)-Cytisine **Cy 1** is a full and potent agonist at hα7 (EC_{50} = 83 μM) [324, 325] in the Xenopus oocytes expression system and an agonist at hα4β4 receptors. But it appears to be only a partial agonist when the α subunits are co-expressed with β2 instead of β4, constituting the hα4β2 subtype [183, 231, 325, 326]. (-)-Cytisine **Cy 1** has also been proved to be a relatively potent agonist at the α3β4* receptor but a poor agonist at the α3β2* [231]. In bovine adrenal chromaffin cells expressing the β4 subunit, (-)-cytisine **Cy 1** stimulates adrenal catecholamine release (EC_{50} = 41 μM), being less efficacious than either (-)-nicotine **3** or (±)epibatidine **13** (EC_{50} = 4 μM and 8.5 nM, respectively) [299]. These results are consistent with a partial agonist action of (-)-cytisine **Cy 1** on adrenal nAChRs. Tritiated (-)-cytisine **Cy 1** was used as radioligand largely due to its high affinity for α4β2* nAChRs (K_D = 0.15 - 0.98 nM) [183, 232]. The binding characteristics of (-)-[^{3}H]cytisine were investigated in whole rat brains as well as in different regions of the human brain (cortex, hippocampus, thalamus and cingulate). The highest density of cytisine binding sites was found in the thalamus (K_D = 0.147 nM and B_{max} = 48 fmol/mg protein) [315]. (-)-[^{3}H]Cytisine has the advantage to show a high selectivity for nicotinic over muscarinic receptors (eliminating the need to mask muscarinic receptors), a slow rate of dissociation and a chemical stability (it is not subject to hydrolysis, as ACh is) [183]. These features make it a suitable tool for studying neuronal nAChRs [315].

III/3.1.2. Cytisine: Potential Clinical Utility

(-)-Cytisine **Cy 1** has a remarkable combination of properties and shares various physiological effects with (-)-nicotine **3**. (-)-Cytisine **Cy 1** acts mainly at the ganglionic level where it exhibits more stimulating than blocking effects [327]. (-)-Cytisine **Cy 1** stimulates the nAChRs located on the postsynaptic membranes in the autonomic ganglia, chromaffins cells and sinocarotid reflexogenic zone. This results in an excitation of the respiratory centre, release of adrenaline by the suprarenal glands and a rise in the blood pressure.

Currently, (-)-cytisine **Cy 1** is on the market in Bulgaria as the main compound in a pharmaceutical preparation called Tabex®, intended for the treatment of tobacco dependence [319]. The mechanism of action of (-)-cytisine **Cy 1** is that of a nicotine-substitute able to reduce the smoker's mental and physical dependency on nicotine **3** [319]. The daily therapeutic saturating dose of Tabex® is from 1.5 to 9 mg. Each tablet contains 1.5 mg cytisine [319]. In the former Soviet Union, (-)-cytisine **Cy 1** was used as a respiratory analeptic for its stimulating activity on respiratory centres [328]. Japanese patents proposed (-)-cytisine **Cy 1** and its methyl derivative as hypoglycaemic and antinflammatory agents [329, 330]. Due to its high affinity to neuronal nicotinic receptors and its pharmacological similarities to (-)-nicotine **3**, (-)-cytisine **Cy 1** and some derivatives were patented in 1994 by Reynolds Tobacco CO (U.S.A.) for use in the treatment of neurodegenerative diseases [331]. More recently, Pfizer Company have filed patent applications that focus on the partial agonist profile of (-)-cytisine derivatives and their potential use in treating addiction and obesity (in conjunction with an anti-obesity agent) [332, 333]. In 2000, a Russian patent claimed phosphorus-containing derivatives of (-)-cytisine **Cy 1** as hepatoprotecting agents [334]. Moreover, (-)-cytisine **Cy 1** shows antinociceptive activity and is able to modulate locomotor activities [335, 336].

III/3.1.3. Cytisine: Previous Studies and Structural Modification

(-)-Cytisine **Cy 1** provides an interesting template for the design of novel nicotinic ligands [232]. Due to its semi-rigid structure, its high affinity towards neuronal nAChRs and its ability to discriminate among different receptor subtypes, it has been chosen as a lead compound for investigating the influence of various substituents on the affinity for different nAChR subtypes [230, 325, 327]. In the past, structural modifications of (-)-cytisine **Cy 1** were made to improve its respiratory analeptic property [337] or to develop new local anaesthetic agents [338]. In the past few years, structural modifications of (-)-cytisine **Cy 1** have been performed in order to obtain compounds of potential therapeutic interest in the central nervous system, with a particular focus on neurodegenerative disease [327]. One of the first chemical modifications on (-)-

cytisine **Cy 1** concerned the basic nitrogen atom of the bispidine ring. Boido et al. [327] investigated the effects of the introduction of saturated or unsaturated alkyl or arylalkyl residues and more complex moieties at the secondary amino group. Moreover, they prepared a set of compounds possessing two cytisine units connected by a polymethylene chain [327]. All these compounds were subjected to a broad pharmacological evaluation in order to clarify their affinities for a number of receptors (α1-adrenergic, dopaminergic (D_2), serotonin ($5HT_3$), histamine (H_3), kainate, muscarinic (M_1 and M_2), N-methyl-D-aspartic acid (NMDA), cholecystokinin A, vasoactive intestinal polypeptide (VIP)). The cytisine derivatives tested in binding experiments with (-)-[^{3}H]cytisine using brain cerebral cortices exhibited an affinity significantly lower than that of cytisine itself to the nAChRs. The K_i values are in the nanomolar range (between 30 and 4100 nM). The most active compound was the cytisine dimer 1,3-bis-(N-cytisinyl)-propane (K_i = 30 nM) [327]. The other compounds showed other biological effects such as anti-hypertensive, cardioionotropic, anti-inflammatory and hypoglycemic effects [327]. Recently, Boido et al. [339] studied structural modifications of (-)-cytisine **Cy 1** with the intention of reducing its affinity for ganglionic receptors. The chemical modification investigated in this work concerned mainly the secondary amino function rather than the pyridone ring (Fig. III/3.4.) [339]. These compounds were tested for their ability to displace (-)-[^{3}H]cytisine from rat brain membranes.

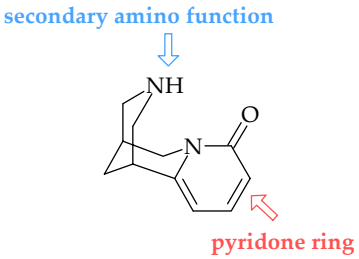

Figure III/3.4: Chemical modifications investigated in the structure of (-)-cytisine **Cy 1**

In 2003, Carbonelle et al. synthesized some cytisine derivatives whose amine function was substituted by aliphatic, alicyclic or chloroheteroaryl groups [340]. These cytisine derivatives were tested in competition binding studies using (±)-[^{3}H]epibatidine and [^{125}I]α-Bgt, respectively, and native neuronal nicotinic receptor

subtypes present in the rat central and peripheral nervous system. Furthermore, in order to assess the functional profile, all compounds were tested on the Ca^{2+} flux of native or transfected cell lines expressing the rat α7 or human α3β4 or α4β2 (using Ca^{2+} dynamics with a fluorescence image plate reader, FLIPR) [340]. Some derivatives were also electrophysiologically tested on *Xenopus* oocytes expressing rat α4β2; α3β4 and α7 subtypes. N-3-oxobutylcytisine was found being a partial agonist for α4β2 and α3β4 and only a weak antagonist at the α7 subtype. This derivative had the highest affinity for all three subtypes examined (K_i = 0.87 nM for α4β2, K_i = 552 nM for α3β4 and K_i = 1,240 nM for α7 nAChRs). The compound with an adamantin moiety at the bispidine nitrogen had the lowest affinity for all subtypes. Pfizer Company focused its interest on cytisine derivatives containing a halogen substituent at the pyridone ring. Data concerning biological evaluation has not been published [333]. In 2001, Imming et al. developed a new and simple synthetic method for preparing halogenated cytisine derivatives [230] and investigated the influence of halogen substituents, such as chlorine, bromine and iodine in position C-3, C-5 or C-3 and C-5 on the affinity for α4β2* and α7* nAChRs. They found that several of these halogenated cytisines proved to be highly potent nAChR ligands [230]. In addition, they reported the first synthesis and biological evaluation of the previously unknown thiocytisine, characterized by a bioisosteric replacement of the lactam moiety by a thiolactam [230]. In 2003, Slater et al. resynthesized and investigated the effects of bromination or iodination of the pyridone ring of (-)-cytisine **Cy 1** and N-methyl-cytisine **Cy 3** on recombinant human α7, hα4β2 and hα4β4 nAChRs expressed in Xenopus oocytes and clonal cell lines [341]. They found that halogenation at C-3 of the pyridone ring of (-)-cytisine **Cy 1** or N-methyl-cytisine **Cy 3** improves the binding affinities and efficacies of (-)-cytisine **Cy 1** on hα7 as well as on hα4β2 and hα4β4. The opposite effect was shown if (-)-cytisine **Cy 1** is halogenated at position C-5 or position C-3 and C-5 of the pyridone ring [341].

III/3.2. Project

(In cooperation with Prof. Seitz, Department of Pharmaceutical Chemistry, University of Marburg: synthesis of novel cytisine analogues)

(-)-Cytisine **Cy 1** has been chosen as a template to synthesize novel analogues due to its semi-rigid conformation and high affinity for the α4β2* neuronal nicotinic receptor. Although several derivatives have already been synthesized, there is still a need for other novel ligands that would interact with greater selectivity and more potency with different neuronal nAChRs. The focus of this project was to find out which steric and electronic requirements are necessary to obtain selective ligands for the α4β2* nAChR. The affinities of the novel (-)-cytisine derivatives were also assessed through radioligand binding assays for α7*, α3β4* and muscle nAChRs. The purpose of this study was to identify which moieties are responsible for the binding to ganglionic and muscular subtypes which are thought to mediate potential side effects on the cardiovascular and gastrointestinal systems. In order to gain further insight into the structure activity relationship (SAR) of (-)-cytisine derivatives, (Fig. III/3.5) a large number of structural modifications have been introduced such as:

1. The introduction of the following substituents on the secondary amine function: a methyl, benzyl or acetyl group.
2. The introduction of halogens (chlorine, bromine and iodine) in position C-3, position C-5 and in both positions C-3 and C-5 of the pyridone ring.
3. Variation of the pyridone ring by the introduction of the nitro group in position C-3 and in position C-5.
4. Conformationally constrained analogue.
5. Hydrogenation of the pyridone ring.
6. A carbonyl group in position C-11 of the bispidine ring.
7. The introduction of multiple oxygen functionalities in position N-12, in position C-6 of the bispidine moiety and in position C-3 of the pyridone ring.
8. Bioioisosteric replacement of the oxygen by sulphur: thiocytisine.

9. The introduction of halogens (chlorine, bromine and iodine) in position C-3, position C-5 and in both positions C-3 and C-5 of thiocytisine.

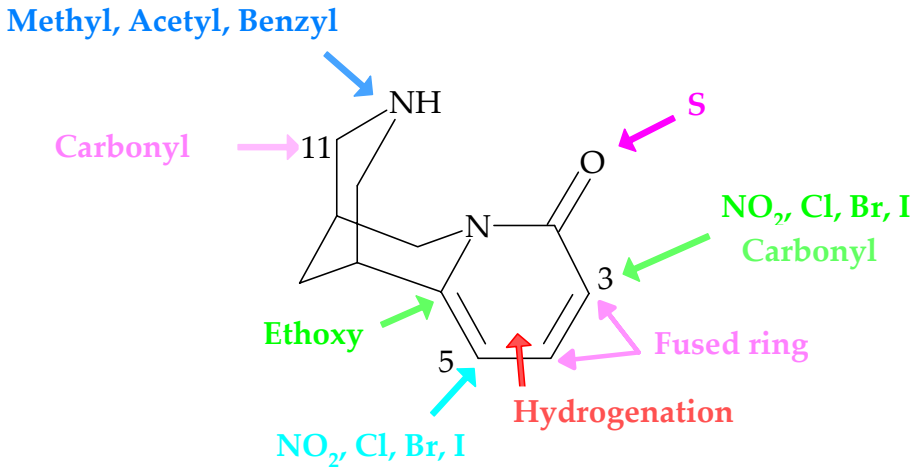

Figure III/3.5: Modifications on the structure of the natural alkaloid (-)-cytisine **Cy 1**

III/3.3. Determination of affinities and structure-activity relationships (SAR)

Cytisine

The affinities of (-)-cytisine **Cy 1** for the two major nAChR subtypes presumably present in the rat and human brain, α4β2* nAChRs and the α7* nAChRs, were previously determined by Imming et al. in radioligand binding studies on P2 membrane fraction of rat brain, using (±)-[^{3}H]epibatidine and [^{3}H]MLA, respectively [230]. In order to study the binding profile of (-)-cytisine **Cy 1** on receptors present in the autonomic nervous system (ANS) and neuromuscular junction (NMJ), its ability to displace binding of (±)-[^{3}H]epibatidine in α3β4* and $(\alpha1)_2\beta1\gamma\delta$ nAChRs was examined using whole membrane fractions from native pig adrenals and *Torpedo californica* electroplax, respectively. In competition binding experiments, (-)-cytisine **Cy 1** bound to the ganglionic receptor subtype with a K_i value of 18 nM which means a 145-fold lower affinity compared with α4β2* nAChR (K_i = 0.124 nM) [230]. The K_i value of (-)-cytisine **Cy 1** for the $(\alpha1)_2\beta1\gamma\delta$ subtypes was in the low micromolar range (K_i = 1,300 nM). Based on these results, the rank order of affinity of (-)-cytisine **Cy 1** for four nAChRs was: α4β2* > α3β4* > α7* > $(\alpha1)_2\beta1\gamma\delta$.

Influence of substituents at the secondary amine function

In previous studies, N–methylation of **Cy 1** (K_i = 0.124 nM) to caulophylline **Cy 3** caused a dramatic loss in affinity for α4β2* dropping into the nanomolar range (K_i = 5.7 nM) in comparison to the parent alkaloid **Cy 1** [230]. The dimethylated compound caulophylline-methiodide **Cy 5** disclosed only a two-fold lower affinity (K_i = 0.238 nM) for α4β2* nAChRs in comparison to (-)-cytisine **Cy 1** [230]. The introduction of a methyl moiety **Cy 3** or dimethyl moiety **Cy 5** at the secondary amine function proved to be unfavourable for the binding at α7* nAChRs (K_i = 15,000 nM and 1,100 nM, respectively) [230]. In the present study, N-methylation of (-)-cytisine **Cy 3** also proved to be detrimental for the binding affinity at the α3β4* nAChRs (83-fold lower in comparison with **Cy 1**) (Tab. III/3.1). The affinity of the N,N-dimethylated cytisine **Cy 5** for α3β4* nAChRs was not determined due to an insufficient amount of this compound. The influence of a voluminous group was investigated by the introduction of a benzyl group **Cy 8** on the bispidine nitrogen. Binding experiments demonstrated that this bulky moiety at N-position has a detrimental effect on the binding affinity for α4β2* nAChRs (11,000 fold decrease), α7* nAChRs (190 fold decrease) and also for α3β4* nAChRs (305 fold decrease) (Tab. III/3.1). Cytisine derivatives tested in this series do not possess affinity for the muscle type.

Tetrahydrocytisine and analogues

The hydrogenation of the pyridone ring of (-)-cytisine **Cy 1** leads to tetrahydrocytisine **Cy 2** (Tab. III/3.1). From the K_i value obtained is evident that tetrahydrocytisine **Cy 2** has a very low affinity for α4β2* nAChRs (170-fold lower than **Cy 1**), a 21-fold lower affinity for the α3β4* nAChRs (K_i = 385 nM), and a 14-fold lower affinity for the muscle type (K_i = 18,000 nM). Both N-methylation **Cy 4** and N-acetylation **Cy 7** of the secondary amino function of the tetrahydrocytisine **Cy 2** caused a further loss in affinity for α4β2* nAChRs (K_i = 10,000 and 20,000 nM, respectively). On the contrary, quaternization of the bispidine nitrogen gives compound **Cy 6** which shows a marked increase in affinity for α4β2* nAChRs (K_i = 35 nM) in comparison with **Cy 4** (K_i = 10,000 nM). The K_i value of **Cy 6** for α4β2*

nAChRs was also 2-fold higher than the affinity of tetrahydrocytisine **Cy 2** for this subtype (K_i = 17 nM) (Tab. III/3.1). A similar trend was observed for N-methylcytisine **Cy 3** and N,N-dimethylcytisine **Cy 5** compared to (-)-cytisine **Cy 1**. Interestingly, compound **Cy 6** showed a dramatic reduction for the α7* nAChR (K_i = 17,000 nM). In these series, the N-methyl-tetrahydrocytisine **Cy 4** is the only compound which maintains a modest affinity for α7* nAChRs (K_i = 2,450 nM). Its K_i value (K_i = 2,450 nM), is similar to the lead compound **Cy 2** (K_i = 2,000 nM), even if 7-fold lower compared to (-)-cytisine **Cy 1** (K_i = 250 nM). However, **Cy 4** showed only a weak interaction with α4β2* nAChRs (K_i = 10,000 nM) and no reasonable affinity for α3β4* nAChRs subtypes (K_i = > 50,000 nM) (Tab. III/3.1).

A carbonyl group in position C-11 of the bispidine ring

A carbonyl group in position C-11 of the pyridone moiety leads to a cytisine analogue **Cy 9** with an affinity 1,000-fold lower (K_i = 125 nM) than the lead compound for α4β2* nAChRs (Tab. III/3.1). The presence of the carbonyl group in position C-11 of the pyridone moiety is also detrimental to the affinity for α7* (K_i = 52,500 nM), α3β4* and muscle nAChRs (Tab. III/3.1).

Cytisine derivatives with multiple oxygen functionalities

The introduction of an acetyl substituent at position N-12, a carbonyl function in position C-3 of the pyridone ring and an ethoxy group in position C-6 of the bispidine moiety (**Cy 10**, 12-acetyl-6-ethoxy-3-oxo-dihydrocytisine) (Tab. III/3.1) result in a weak ligand for the nicotinic receptors, with K_i values in the micromolar range. It is difficult to predict which of these substituents are responsible for the loss of affinity because of the lack of analogues with similar moieties (Tab. III/3.1).

Variation at the pyridone ring by the introduction of a nitro group in positions C-3 and C-5

Interesting results were obtained with cytisine analogues bearing a nitro group in position C-3 and C-5 of the pyridone moiety. The compound containing a nitro group in position C-3 (**Cy 12)** presented a K_i value for the α4β2* nAChR in the picomolar range (K_i = 0.42 nM). On the contrary, introduction of the same moiety in

position C-5 led to a compound (**Cy 13)** 100-fold less potent than **Cy 12** for this subtype. The affinity of **Cy 12** for the α7* subtype was 65-fold higher than the lead compound **Cy 1**. The nitro group in position C-5 on the pyridine ring **Cy 13** is not well tolerated and is particularly detrimental to the affinity for the α7* subtype (300-fold decrease). The affinity of the analogue **Cy 12** for the α3β4* is similar to that of the lead compound (-)-cytisine **Cy 1** (Tab. III/3.1). Compound **Cy 13** showed only low affinity for α3β4* and $(\alpha 1)_2\beta 1\gamma\delta$ nAChRs.

Constrained analogues

A conformationally constrained analogue **Cy 11** possesses a low affinity for α4β2* nAChRs (K_i = 5,333 nM) (Tab. III/3.1), whereas it is not able to interact with α7* nAChRs subtypes.

Table III/3.1: Radioligand binding affinities of cytisine analogues for α4β2*, α7*, α3β4*and $(\alpha 1)_2\beta 1\gamma\delta$ nAChRs.

Structure	No.	α4β2* [^{3}H]EPI rat brain K_i (nM)	α7* [^{3}H]MLA rat brain K_i (nM)	α3β4* [^{3}H]EPI pig adrenals K_i (nM)	$(\alpha 1)_2\beta 1\gamma\delta$ [^{3}H]EPI Torpedo calif. Electroplax K_i (nM)
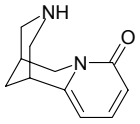	**Cy 1**	0.124 ± 0.014 [a]	261 ± 24 [b] 250 [n=1]	54 ± 9 [c] (rat adrenal) 18 (pig adrenal)	1,300
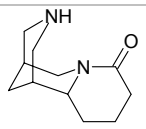	**Cy 2**	17	2,000	385 ± 6	19,000
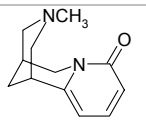	**Cy 3**	5.7 ± 1.5 [a]	15,000 [a]	1,500	n.d.
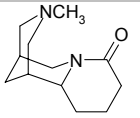	**Cy 4**	34	10,000	2,450 ± 420	> 50,000
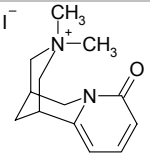	**Cy 5**	0.238 ± 0.046 [a]	1,100[a]	n.d.	>20,000

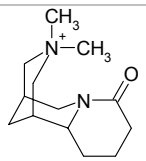	**Cy 6**	35	17,000	2,855 ± 6	> 50,000
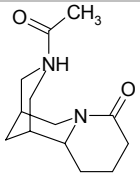	**Cy 7**	>20,000	> 50,000	> 50,000	> 50,000
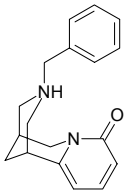	**Cy 8**	1,448 [n=1]	> 50,000[e]	5,500[e]	> 50,000
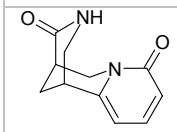	**Cy 9**	125 ± 17	52,500 ± 707[e]	1,600[e]	> 50,000
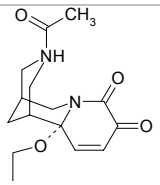	**Cy 10**	9,400	95,000[e]	50,000[e]	20,000
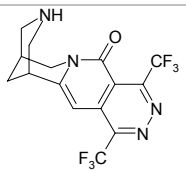	**Cy 11**	5,333	> 50,000	n.d.	n.d.
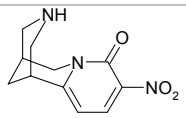	**Cy 12**	0.42 ± 0.07	40.7 ± 4.3 [e]	12 [e]	10,000 [d]
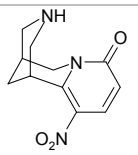	**Cy 13**	65.6 ± 0.28	12,000 [e]	1,000[e]	20,000 [d]

a =[230]
b = [^{125}I]-α-Bgt
c = [180]
d = [342]
e = [343]
n.d.= not determined

Halogen substitution

Halogen substitution at position C-3

In previous studies, halogenation at C-3 of (-)-cytisine **Cy 1** resulted in a marked improvement of affinity for α4β2* (K_i values from 0.01 to 0.022 nM) and for α7* nAChRs (K_i values from 1.5 to 2.5 nM) [230]. The most potent molecule of this series for α4β2* nAChRs was 3-bromocytisine **Cy 13** (K_i = 0.01 nM) which displayed a 10-fold higher affinity than the parent alkaloid (-)-cytisine **Cy 1** (K_i = 0.124 nM), similar to that of (±)epibatidine **13** (K_i = 0.008 nM) (Tab. III/3.2). Slater et al. [341] suggested that the favourable effects on affinity of halogenation of (-)-cytisine **Cy 1** at position C-3 might be due to the existence of a hypothetical hydrophobic-binding pocket located close to the hydrogen bond donor moiety which is thought to interact with the carbonyl oxygen of (-)-cytisine **Cy 1**. Within the halo-series, the size of the halogen atoms does not cause a significant influence on the binding affinity for α4β2* and the electronegativity of the halogens seems to possess small relevance too (K_i = 0.010 (Br) ≅ 0.017 (I) > 0.022 (Cl). However, when the halo-cytisine are compared to the lead compound (-)-cytisine **Cy 1**, the improvements in affinity are noteworthy. The presence of bromine in position C-3 is promising for a better interaction with the α4β2* nAChR. The size of the chlorine atom is smaller than that of bromine and, moreover, chlorine possesses a higher electronegativity. This causes a reduction of the negative charge on the carbonyl and thus a minor probability of hydrogen bond formation. Therefore, bromine emerges as the favourite halogen atom next to the carbonyl group. These considerations are also appropriate for α7* nAChRs. The affinity increases with an enhancement of the size of the halo substituent and with a diminution of the electronegativity. In fact, the 3-iodocytisine **Cy 22** possesses the highest affinity for the α7* nAChRs (K_i = 1.5 nM) [230] within the 3-halogenated analogues and shows a 174-fold higher affinity compared to the lead compound (-)-cytisine **Cy 1** (K_i = 261 nM). The halogenated analogues in position C-3 **(Cy 14**, **Cy 19** and **Cy 22)** were tested for their in vitro affinity at the α3β4* and $(\alpha 1)_2\beta\gamma\delta$ nAChRs (Tab. III/3.2). Compared to the parent alkaloid **Cy 1** (K_i = 18 nM) they showed a

higher affinity for the α3β4* nAChRs (K_i values from 0.35 -1.1 nM). The 3-iodocytisine **Cy 22** possesses the highest affinity, displacing (±)[^{3}H]epibatidine with a K_i value of 0.35 nM. The rank order of potency at α3β4* nAChR is: 3-I > 3-Br > 3-Cl (Tab. III/3.2). The same trend was found for the ability of the halogenated compounds to inhibit the binding of (±)[^{3}H]epibatidine at $(\alpha1)_2\beta1\gamma\delta$ nAChRs (K_i value from 413 to 1,332 nM). Actually, halogenation in position C-3 only slightly improves the binding affinity for the muscle type in comparison with the high influence on the binding affinity for the α4β2*, α7* and α3β4* nAChRs. Compared to (-)-cytisine **Cy 1**, the affinity of the halogenated analogues in position C-3 **(Cy 14**, **Cy 19** and **Cy 22)** for the α4β2* nAChRs is higher, but the selectivity to α7* nAChRs is lower. Halogenation in position C-3 provides a marked increase in affinity for the affinity for α7* nAChRs compared to α4β2* nAChRs, so that the selectivity for α4β2* over the α7* is lower than that for (-)-cytisine **Cy 1**.

Halogen substitution at position C-5

Compared with halogenation in position C-3, halogen substitution in position C-5 of the pyridone moiety exerts a smaller impact on the binding affinity for all subtypes under consideration. Nevertheless, the K_i values for α4β2* of compounds **Cy 16**, **Cy 20** and **Cy 24** are in the higher picomolar (5-iodocytisine **Cy 24**) and nanomolar ranges (5-chlorocytisine **Cy 20**) [230] (Tab. III/3.2). The 5-iodocytisine **Cy 24** shows the highest affinity (K_i= 0.23 nM) for α4β2* nAChRs. The potency scale is 5-I > 5-Br > 5-Cl. The 5-chlorocytisine **(Cy 20)** possesses the lowest affinity, with a K_i value being 10-fold lower (K_i= 2.5 nM) than the halogenated parent compounds **Cy 16** and **Cy 24**. Compared to the parent alkaloid **Cy 1** (K_i = 0.124 nM), the 5-iodocytisine and 5-bromocytisine (**Cy 24** and **Cy 16**, respectively) showed a similar affinity for the α4β2* nAChR (K_i values 0.23 nM and 0.38 nM, respectively). Even if the presence of a halogen at position C-5 of the pyridone fragment slightly reduces the affinity for α4β2* nAChR, it increases the affinity for the α7* nAChR subtype. The highest affinity was determined for the 5-iodocytisine **Cy 24** with a K_i value of 21 nM being two-fold higher than (-)-cytisine **Cy 1**. Surprisingly, the affinity of the 5-

chlorocytisine **Cy 20** for the α7* nAChRs subtype drops in the low micromolar range (K_i= 1,000 nM). The rank order of affinities is: 5-I > 5-Br > 5-Cl. The introduction of halogen substituents at position C-5 of the pyridone moiety proves to be favourable for α7* as well as for the interaction with the α3β4* nAChRs. It results in a 5-fold affinity increase compared to (-)-cytisine **Cy 1**. The ligand with the best affinity is again the 5-iodocytisine **Cy 24** with a K_i value in the low nanomolar range (K_i = 3.2 nM). In this series, although the 5-chloro analogue **Cy 20** possesses the lowest affinity for the ganglionic subtypes (K_i = 14.3 nM), it shows the highest K_i ratio between the α3β4* and α7* nAChR subtype. Interestingly, halogenation in position C-5 does not improve the affinity of cytisine derivatives for the muscle type. The K_i values are in the micromolar range (between 12,500 and 40,000 nM), thus 10 to 30-fold lower than that of (-)-cytisine **Cy 1** (K_i = 1,300 nM).

Halogen substitution at position C-3 and C-5

Given that a bulkier substituent at position C-5 of the pyridone fragment reduces the affinity for α4β2*, it is expected that the 3,5-dihalocytisine derivatives (**Cy 17**, **Cy 21** and **Cy 25**) also possesses a reduced affinity towards the four subtypes of the nicotinic receptors under investigation. Indeed, the K_i values of **Cy 17**, **Cy 21** and **Cy 25** ranged from 0.520 to 10.8 nM [230] (Tab. III/3.2). The 3,5-dichloro-cytisine **Cy 21** has the higher subtype selectivity for α4β2* nAChRs over α3β4* nAChRs (1:114). The introduction of two chlorine halogens in position C-3 and C-5 (**Cy 21)** causes a drastic reduction in affinity for the α3β4* nAChR (K_i = 287 nM), whereas disubstitution with iodine (**Cy 25)** leads to a marked affinity increase for the same nAChR subtype (K_i = 4.8 nM). Interestingly, the K_i value of **Cy 25** at the α3β4* nAChRs is 3-fold lower than that of (-)-cytisine **Cy 1** (K_i = 18 nM). The dihalogenation at position C-3 and C-5 causes a considerable decrease in affinity for $(\alpha 1)_2\beta\gamma\delta$ nAChRs (K_i = 8,000 to 15,000 nM) compared to (-)-cytisine **Cy 1** (K_i = 1,300 nM). The structure-affinity relationship of the dihalogenated cytisine derivatives indicates that introducing iodine at position C-3 and C-5 increases the affinity for the α3β4* nAChRs subtypes, whereas it has little impact on the affinity for $(\alpha 1)_2\beta\gamma\delta$ nAChRs. The disubstitution at positions C-3

and C-5 with two different types of halogen atoms (chlorine and bromine) leads to compounds **Cy 27** and **Cy 28**, with an even lower affinity for α4β2* in comparison to the previously tested dihalogenated derivatives (**Cy 17**, **Cy21** and **Cy 25**) (Tab. III/3.2). The K_i values of compound **Cy 27** and **Cy 28** for α4β2* nAChRs, clearly shows the positive influence on binding affinities of a bromine in position C-3. The electronic properties and the size of the halogen in position C-3 also appear to be important for the affinity at the α3β4* nAChRs. Compound **Cy 28** (3-Cl, 5-Br) (K_i = 869 nM) shows 3-fold lower affinity for the α3β4* nAChRs in comparison with the 3,5-dichlorocytisine derivative **Cy 21** (K_i = 287 nM), whereas the **Cy 27** (3-Br, 5-Cl) possesses 2-fold higher affinity than **Cy 21**. From these results we could hypothesize that an increase in size of the halogen atoms in position C-3, in combination with a reduced electronegativity, can have a positive influence on the affinity towards the α4β2*, α7* as well as α3β4* nAChRs subtype.

N-Methyl-halo-cytisines

N–methylation of 3-bromocytisine **Cy 14** (K_i = 0.010 nM) to **Cy 15** causes a dramatic loss in affinity **Cy 15** (Tab. III/3.2). In relation to **Cy 14**, the **Cy 15** has a 137-fold lower affinity for α4β2*, a 65-fold lower affinity for α7* and a 7.5-fold lower affinity for α3β4* nAChRs. Interestingly, compared to cytisine **Cy 1** (K_i = 260 nM), **Cy 15** retains a high affinity for the α7* nAChRs (K_i = 131 nM). It was observed that whilst N-methylation of the bispidine ring seems to encumber the binding to the α4β2* and with some less extent to α7*, it is not detrimental to the interaction with α3β4* nAChR. Indeed, the N-methyl-3-iodocytisine **Cy 23** shows subtype selectivity for α3β4* nAChR over α7* nAChR of a factor of 130 (Tab. III/3.2). N-methylation of 3,5-dibromocytisine **Cy 17** (K_i = 10.5 nM) to **Cy 18** causes a further loss of affinity for α4β2*, dropping it into the high nanomolar range (K_i = 485 nM). The same trend can also be observed for the N-methyl-3,5-iodo-derivative **Cy 26** (K_i = 656 nM). In fact, its binding affinity for the α4β2* is 1,300-fold lower than that of the 3,5-iodo-derivative **Cy 25** (K_i = 0.520 nM). The structure activity relationship (SAR) of these N-methyl

analogues shows that introducing a methyl moiety on the secondary nitrogen is detrimental to the affinity towards all subtypes under investigation.

Table III/3.2: Radioligand binding affinities of halo-cytisine analogues for α4β2*, α7*, α3β4* and $(\alpha1)_2\beta1\gamma\delta$ nAChRs.

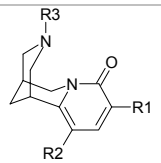

R1	R2	R3	No	α4β2* [³H]EPI rat brain K_i (nM)	α7* [³H]MLA rat brain K_i (nM)	α3β4* [³H]EPI pig adrenals K_i (nM)	$(\alpha1)_2\beta1\gamma\delta$ [³H]EPI Torpedo calif. electroplax K_i (nM)
Br	H	H	**Cy 14**	0.010 ± 0.001[a]	2 ± 0.3[a]	0.61 ± 0.8	627 ± 49
Br	H	CH_3	**Cy 15**	1.37 ± 0.28	131[c]	4.5[c]	n.d.
H	Br	H	**Cy 16**	0.308 ± 0.014[a]	28 ± 2[a]	5 ± 1.1	14,900 ± 2.3
Br	Br	H	**Cy 17**	10.8 ± 0.4[a]	1,500[a]	n.d.	n.d.
Br	Br	CH_3	**Cy 18**	485 [n=1]	> 10,000	n.d.	n.d.
Cl	H	H	**Cy 19**	0.022 ± 0.005[a]	2.5 ± 0.3[a]	1.1 ± 0.06	1,332 ± 108
H	Cl	H	**Cy 20**	2.5 ± 0.3[a]	1,000[a]	14.3 ± 2.5	40,000 [n=1]
Cl	Cl	H	**Cy 21**	2.5 ± 0.4[a]	1,000[a]	287 ± 6.3	>15,000
I	H	H	**Cy 22**	0.017 ± 0.002[a]	1.5 ± 0.1[a]	0.35	413 ± 22
I	H	CH_3	**Cy 23**	0.988 ± 0.008	260[c]	2[c]	n.d.
H	I	H	**Cy 24**	0.230 ± 0.02[a]	21 ± 2[a]	3.25 ± 0.7	12,500 ± 4.43
I	I	H	**Cy 25**	0.520 ± 0.015[a]	41 ± 2[a]	4.8 ± 0.1	8,032 ± 2.09
I	I	CH_3	**Cy 26**	656 ± 85	6,000[c]	1,568[c]	n.d.
Br	Cl	H	**Cy 27**	10.5 ± 0.5	420[c]	174[c]	2,744[b]
Cl	Br	H	**Cy 28**	27 [n=1]	1,328[c]	869[c]	15,000[b]

a = [230]
b = [342]
c = [343]
n.d. = not determined

Thiocytisine derivatives

The bioisosteric thioanalog of (-)-cytisine **Cy 1**, named thiocytisine, showed a seven-fold lower affinity compared with the parent alkaloid and subnanomolar binding affinity for the α4β2* receptor (Ki = 0.832 nM) **(Cy 29)** [230]. (Tab. III/3.3). Remarkably, the novel thiocytisine showed the best affinity-selectivity profile for α4β2* nAChRs with an affinity for the α7* in the μM range (K_i = 4,000 nM) [230]. In the present study, the affinity of thiocytisine **Cy 29** for the ganglionic nicotinic receptors α3β4* was in the nanomolar range (K_i = 632 nM), approximately 35-fold lower than that of the parent compound (-)-cytisine **Cy 1** (K_i = 18 nM). However, thiocytisine **Cy 29** shows the best K_i ratio between the α4β2* receptors and the α3β4* nAChRs (α4β2* / α3β4* = 1:790). Introduction of bromine or chlorine substituents at position C-3 of the pyridone moiety of thiocytisine **Cy 29** gives analogues **Cy 34** (K_i = 0.603 nM) and **Cy 32** (K_i = 1.48 nM) displaying affinities for α4β2* in the pico- and low nano-molar range. Compared to (-)-cytisine **Cy 1** and thiocytisine **Cy 29**, the improvement of the binding affinity of **Cy 34** was of great relevance towards all the neuronal nicotinic receptor subtypes under consideration. Indeed, the 3-bromothiocytisine **Cy 34** showed the highest affinity for α4β2* (K_i = 0.603 nM) as well as for α7* (K_i = 48 nM) and α3β4* (K_i= 11.8 nM) nAChRs. From these results it is evident that the introduction of a bromine or chlorine atom in position C-3 (**Cy 32** and **Cy 34,** respectively) adjacent to the hydrogen-bonding centre enhances the affinity of the ligand. The electronic effect of bromine on the pyridine ring, and more specifically on the hydrogen bond accepting oxygen atom, appears to be ideal for the interaction of **Cy 34** with the neuronal nicotinic receptor subtypes. The introduction of chlorine and bromine substituents at position C-5 of thiocytisine **Cy 29** gives analogues **Cy 33** and **Cy 36**, respectively. Compared to the thiocytisine **Cy 29**, both analogues possess lower affinity for α4β2* nAChRs. However, the 5-bromothiocytisine **Cy 33** displays a better affinity for α4β2* (K_i = 8.1 nM) compared to the 5-chlorothiocytisine **Cy 36** (K_i = 55 nM). Halogenation in position C-5 of the thiocytisine **Cy 29** slightly improves the binding affinity for the α7* nAChRs compared to the lead compound **Cy 29**. The 5-

halogenated thiocytisines were also tested for the ganglionic and the muscular type. The affinity of the 5-bromo derivative **Cy 36** (K_i = 141 nM) for the ganglionic type (α3β4*) is 8-fold higher than that for the α7* nAChRs and 4-fold higher than thiocytisine **Cy 29** (K_i = 3,390 nM) (Tab. III/3.3). The affinity towards the muscle type is in the high micromolar range and is similar for both 5-halogenated derivatives (**Cy 33** and **Cy 36**). Studying the influence of a methyl or acetyl moiety on the bispidine ring of thiocytisine, it was observed that the affinities of these derivatives follow the same trend of the cytisine derivatives. N-methylation of thiocytisine **Cy 30** caused a dramatic reduction in affinity, in particular towards α4β2* (K_i = 6,000 nM, which is 7000-fold lower than (-)-cytisine **Cy 1**). The affinity of **Cy 30** for the α7* and α3β4* nAChRs decreases by 10-and 5-fold respectively. N-acetylation of thiocytisine **Cy 29** leads to compound **Cy 31**. This substitution proved to be detrimental to the affinity towards α7*, α3β4* and muscle nAChRs. Interestingly, the introduction of an acetyl moiety on the byspidine ring **Cy 31** causes an enhancement of the affinity towards α4β2* compared to the N-methyl analogue **Cy 30**. Compound **Cy 35**, N-acetyl-3-bromo-thiocytisine, shows an increase in binding affinity for α4β2*, α7*, α3β4* subtypes with the exception of the muscle type (Tab. III/3.3). The **Cy 35** possesses a K_i value for α4β2* in the low nanomolar range (K_i = 2.4 nM), namely 357 times higher than the affinity measured for the N-acetyl-thiocytisine **Cy 31,** but almost 3-fold lower than the affinity of thiocytisine **Cy 29**. From these values it is evident that the affinity of **Cy 35** for the α4β2* is increased in comparison with the **Cy 31**, but not in comparison with the thiocytisine **Cy 29**. The opposite trend is observed for the affinities towards the other subtypes, namely the α7* and α3β4* nAChRs. Compared to thiocytisine **Cy 29**, **Cy 35** shows 10-fold higher binding affinity for α7* and 2-fold higher for α3β4* nAChRs.

Table III/3.3: Radioligand binding affinities of thiocytisine analogues for α4β2*, α7*, α3β4* and $(\alpha 1)_2\beta 1\gamma\delta$ nAChRs

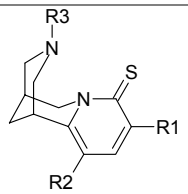

R1	R2	R3	No.	α4β2* [³H]EPI rat brain K_i (nM)	α7* [³H]MLA rat brain K_i (nM)	α3β4* [³H]EPI pig adrenals K_i (nM)	$(\alpha 1)_2\beta 1\gamma\delta$ [³H]EPI Torpedo calif. electroplax K_i (nM)
H	H	H	**Cy 29**	0.832[a]	4,000[a]	632 ± 62	95,000
H	H	CH_3	**Cy 30**	6,000	40,000	2,390	> 50,000
H	H	$COCH_3$	**Cy 31**	857	> 50,000	> 50,000	> 50,000
Cl	H	H	**Cy 32**	1.48 ± 0.4	50 [n=1]	248 ± 52	21,000 [n=1]
H	Cl	H	**Cy 33**	55 [n=1]	2,200 [n=1]	2,900 ± 208	> 50,000
Br	H	H	**Cy 34**	0.603	48 [n=1]	11.8 ± 0.35	11,150 ± 777
Br	H	$COCH_3$	**Cy 35**	2.4	412	307 ± 25	> 50,000
H	Br	H	**Cy 36**	8.1	1,400	141± 7	> 50,000
H	Br	CH_3	**Cy 37**	4,800	13,000	23,000	n.d.
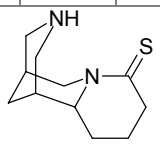			**Cy 38**	2,900	8,000	4,300 ± 458	> 50,000
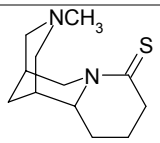			**Cy 39**	7,800 [n =1]	> 50,000	> 50,000	> 50,000

a= [230]
n= number of experiments

Structure-activity relationship (SAR) for α4β2* (Fig. III/3.6)

- The introduction of an acetyl or benzyl moiety at the secondary nitrogen of the bispidine ring of (-)-cytisine **Cy 1** results in a dramatic loss of affinity. A moderate loss of affinity was observed with the introduction of a methyl group. Interestingly, a dimethylation, determining the formation of a quaternary amino function, gives a compound with an affinity similar to the lead compound **Cy 1.**
- Bioisosteric thiolactam pharmacophore was found to retain much of the biological activity of the parent alkaloid with a subnanomolar affinity for the α4β2* subtype and displayed the best affinity-selectivity profile for α4β2* over α7* and α3β4*.

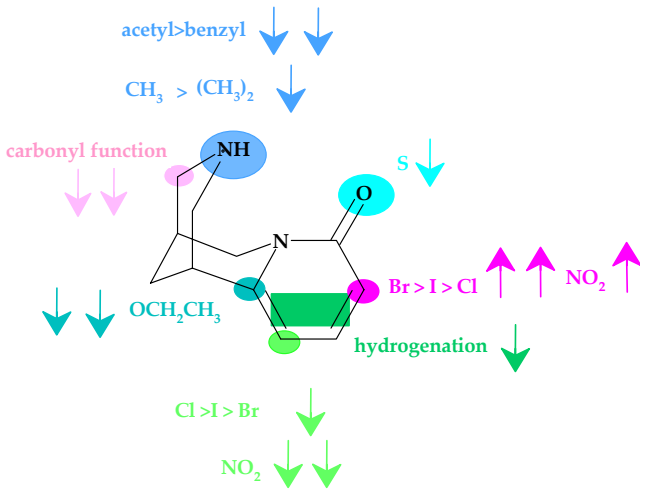

Figure III/3.6: Cytisine derivatives: structure activity relationship for the α4β2*nAChR

- Halogenation at position C-3 of the pyridone ring of (-)-cytisine **Cy 1** and thiocytisine **Cy 29** significantly increases the affinity.
- A nitro group in position C-3 as well as in position C-5 decreases the affinity. In particular, the nitro group in position C-5 causes a marked drop off in affinity compared to cytisine **Cy 1**.
- Hydrogenation of the pyridone ring reduces the affinity.
- Halogenation at position C-5 of the pyridone ring of (-)-cytisine **Cy 1** and thiocytisine **Cy 29** moderately decreases the affinity.

- Dihalogenation at position C-3 and C-5 of the pyridone ring of (-)-cytisine **Cy 1** and thiocytisine **Cy 29** decrease the affinity.
- Introduction of an ethyl moiety at position C-6 is detrimental to the affinity.

Structure-activity relationship (SAR) for α7* (Fig. III/3.7)

- The bulkiness of the N-substituent greatly reduces the affinity of the compounds for α7* nAChRs. The introduction of a methyl, acetyl or benzyl moiety on the secondary amine function results in a dramatic loss of affinity.
- A nitro group in position C-3 of the pyridone ring leads to a significant improvement of the affinity towards α7*, whereas in position C-5 it has a detrimental effect (binding affinity drops into the micromolar range).

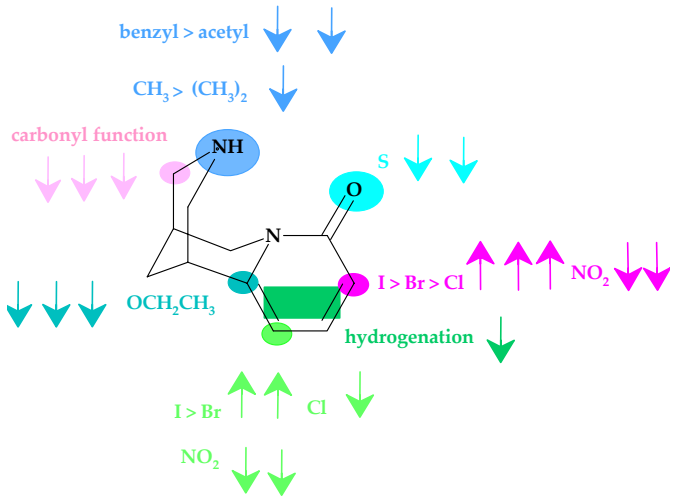

Figure III/3.7: Cytisine derivatives: structure activity relationship for the α7*nAChR

- 3-chlorine, 3-bromine, 3-iodine derivatives possess an appreciably higher affinity relative to (-)-cytisine **Cy 1**. The K_i values range from 1.5 to 2.5 nM.
- The introduction of a halogen in position C-5 of the pyridone ring may exert different effects, depending upon the nature of the halogen introduced. The 5-chlorocytisine has a K_i value in the micromolar range, whilst 5-bromine and 5-iodine possess an affinity for the α7* nAChRs of 21 and 28 nM, respectively. These latter compounds are more potent at α7* nAChRs than (-)-cytisine **Cy 1** (K_i value of 261 nM).
- The dihalogenation in positions C-3 and C-5 is detrimental for the affinity.

Structure-activity relationship (SAR) for α3β4*nAChR (Fig. III/3.8)

- The bulkiness of the N-substituent greatly decreases the affinity of the compounds.
- The introduction of halogens on the pyridone ring in position C-3 or in position C-5 causes a marked increase in affinity. The rank order was for both positions: I > Br > Cl.

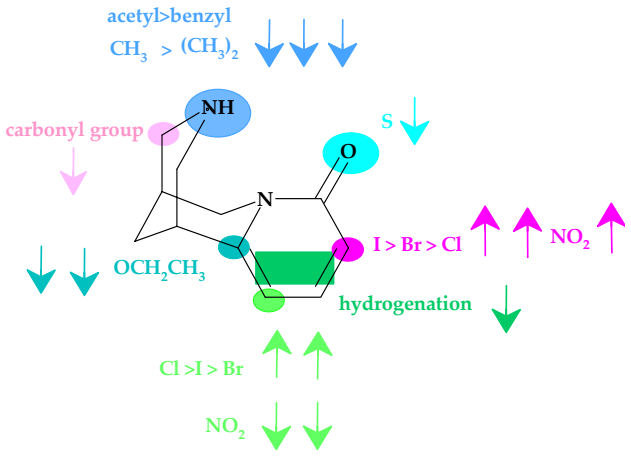

Figure III/3.8: Cytisine derivatives: structure activity relationship for the α3β4* nAChR

- A nitro group in position C-3 or C-5 of the pyridone ring shows different effects: the 3-nitro derivative has an affinity similar to the lead compound (-)-cytisine **Cy 1**. In contrast, the 5-nitro derivative shows reduced affinity compared to (-)-cytisine **Cy 1**.
- The hydrogenation, as well as the bioisosteric replacement of oxygen by sulphur, in the pyridone ring leads to compounds with very low affinity.

Structure-activity relationship (SAR) for muscle type (Fig. III/3.9)

- All modifications introduced at the structure of the lead compound resulted in being detrimental to the affinity to muscle type.

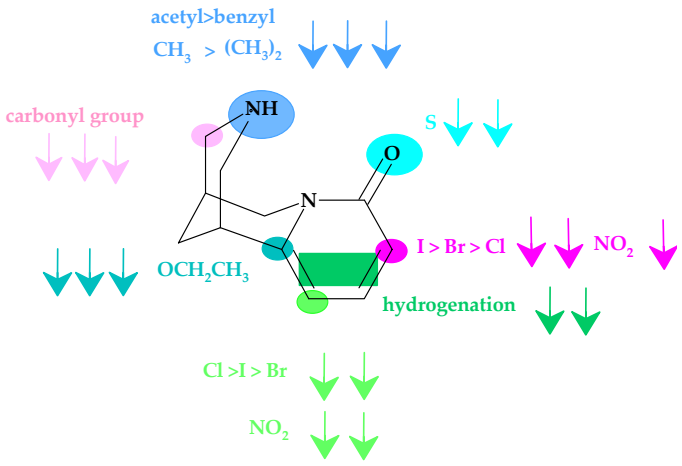

Figure III/3.9: Cytisine derivatives: structure activity relationship for the $(\alpha 1)_2\beta 1\gamma\delta$ nAChR

- The 3-iodo derivative with a Ki value of 413 nM (2-fold lower than cytisine **Cy 1**) was the compound with the best affinity in this series.

Summary of structure-activity relationschips (SAR)

- ✓ Substituents in the secondary amine function of cytisine decrease the affinity towards the nAChRs under consideration (**Cy 3**).
- ✓ Cytisine and thiocytisine analogues with a bromine atom as a substituent at position C-3 are the most potent nAChR ligands for the $\alpha 4\beta 2^*$ (**Cy 14-Cy 34**).
- ✓ Bioisosteric replacement of oxygen by sulphur resulted in thiocytisine, a very selective ligand for $\alpha 4\beta 2^*$ nAChRs (**Cy 29**).

III/3.4. Discussion

(-)-Cytisine **Cy 1,** due to its structural rigidity and its high affinity for the nAChRs, has been chosen as a reference compound to design and synthesize new ligands for nAChRs [231]. In preliminary studies, it was found that (-)-cytisine **Cy 1** exhibited a high affinity (K_i = 0.124 nM) for the α4β2* subtype and a moderate affinity for the α7* subtype (K_i = 261 nM) [230].

The binding affinity of (-)-cytisine **Cy 1** has been evaluated for the muscle type $(\alpha 1)_2\beta 1\gamma\delta$ and the ganglionic type α3β4* nAChRs. The K_i value of (-)-cytisine **Cy 1** for the $(\alpha 1)_2\beta 1\gamma\delta$ nAChRs was in the high nanomolar range (K_i = 1,300 nM). The binding affinity at α3β4* nAChRs, using (±) [^{3}H]epibatidine and pig adrenals (K_i = 18 nM) was slightly higher than that assessed in a competition experiment performed with (±)[^{3}H]epibatidine and rat adrenals (K_i = 54 nM) (Tab. III/3.1) resulting in a moderate species dependency. On the basis of these data, (-)-cytisine **Cy 1** shows a high subtype selectivity for α4β2* nAChRs over the α7*, α3β4* and $(\alpha 1)_2\beta 1\gamma\delta$ nAChRs.

To evaluate the affinity of a high affinity ligand such as (-)-cytisine **Cy 1**, it is necessary to take into account the conditions used in the assays. There are some parameters that are essential to prevent the underestimation of the affinity of the competitors. Such parameters are: radioligand concentration, protein concentration, temperature and duration of the incubation time. For example, an increase in protein concentration can result in an increase of the K_i value of a high affinity ligand. In studies of Boido et al. [339], the use in assays of too high protein concentration (i.e. 600 mg of protein in contrast to 60 mg [179]) could give incorrect values (ligand depletion, K_i = 2.3 nM using (-)[^{3}H]cytisine in rat brain, [339]). In addition, K_i values found by Gündisch et al. [179] are not even comparable to the other K_i values that have been found in literature, due to the fact that the latter ones were determined using different membrane preparations, such as human recombinant α4β2 expressed in SHSY5Y cells [325] or in Xenopus oocytes [341]. Binding studies [230, 251, 325, 327, 339] demonstrated that halogenation of (-)-cytisine **Cy 1** in position C-3 provides a higher affinity for nAChRs. In 2001, Imming et al.[230] performed a further structural

modification of (-)-cytisine **Cy 1** by replacement of a hydrogen atom of the pyridine moiety with a halogen (such as a chlorine, bromine and iodine) in one or more positions (C-3 and/or C-5) and investigated the influence of these substitutions on in vitro affinity for α4β2* and α7* nAChR. They found 3-bromocytisine **Cy 14** to be the most potent molecule of this series (for α4β2* nAChRs) (K_i = 0.01 nM) with an affinity 10-fold higher than the parent alkaloid (-)-cytisine **Cy 1** (K_i = 0.124 nM). Furthermore, performing binding assays for the α7* nAChR using [^{3}H]MLA and native α7* nAChR [230], they also found that the introduction of a halogen in position C-3 causes a remarkable increase in affinity compared to (-)-cytisine **Cy 1** with the following order of potency: I > Br > Cl. These results are in agreement with the ones performed by Houlihan [325] who compared the binding affinity of brominated cytisine analogues in position C-3, position C-5 and in both position C-3 and C-5 using human recombinant hα4β2 and hα7 expressed in SH-EP1 and SH-SY5Y cells as well as the ones from Slater et al. [341] who also tested the 3-iodocytisine and 5-iodocytisine using recombinant hα4β2 and hα7 nAChR [325].

In the present study, the binding affinities of the halogenated compounds were determined for the naturally expressed α3β4* and $(\alpha 1)_2\beta 1\gamma\delta$ nAChRs. The introduction of a halogen substituent in position C-3 of the pyridine ring improves the ability of the (-)-cytisine **Cy 1** derivatives to interact with the ganglionic nicotinic receptors α3β4* nAChRs. Interestingly, the ability of 3-halogenated cytisine to interact with the nicotinic neuromuscular receptors is only slightly enhanced. Halogenation (bromine, chlorine and iodine) of cytisine at position C-5 reduces affinity for (±)-[^{3}H]epibatidine binding site for α4β2* nAChRs [230], whereas 5-iodine and 5-bromine have an affinity higher than that of (-)-cytisine **Cy 1** for α7* nAChRs [230]. Again, 5-halogenation on the pyridone ring of (-)-cytisine **Cy 1** resulted favourably for the interaction with the α3β4* nAChRs naturally expressed in pig adrenals, whereas is unable to improve the affinity for the muscle type.

Furthermore, the effects of the simultaneous halogenation either in position C-3 and position C-5 on the affinity for α3β4* and muscle nAChRs were investigated. The

introduction of two chlorine atoms in position C-3 and C-5 causes a drastic reduction in affinity for the α3β4* nAChRs, while disubstitution with iodine leads to a notable increase in affinity. The large size of the halogen atom may be favourable for the interaction with the α3β4* nAChR subtype. This trend does not subsist for $(\alpha 1)_2\beta\gamma\delta$ nAChRs. The disubstitution in positions C-3 and in C-5 with two different types of halogen atoms (chlorine and bromine) showed that a bromine halogen in position C-3 rather than a chlorine halogen at the same position have a preference for a higher interaction at α4β2*, α3β4* and α7* nAChRs. From these results it follows that the halogen atom has different effects at the different receptor subtypes. In particular, the increase of the size of the halogen atom and the decrease of its electronegativity can enhance the affinity toward the ganglionic nicotine receptors subtype. Thus, the size of the halogen substituent may be a limiting factor at α4 subunit containing receptors, but not for α7* and α3β4* nAChRs.

In literature, the influence of a variety of substituents on the amine nitrogen of (-)-cytisine **Cy 1** have been deeply investigated [327,340,339]. In 2001, it was demonstrated that the introduction of a methyl group on the secondary nitrogen of (-)-cytisine **Cy 1** is generally unfavourable for the affinity to all the nAChRs subtypes [230]. Moreover, the introduction of a pentyl moiety leads to a compound showing a lower affinity for the neuronal nAChRs (K_i = 43.4 nM, using (-)[^{3}H]cytisine and rat brain preparation) [339]. Slater et al. [341] tested on α4β2 and α7 nAChRs expressed in human recombinant Xenopus oocytes, the N-methyl-3-bromocytisine and the N-methyl-5-bromocytisine [341], demonstrating that halogenation of the N-methylcytisine in position C-3 as well as in position C-5 is favourable to the interaction with the α4β2 and α7 nAChRs. A similar trend has been observed in our binding experiments performed on native α4β2* and α7* nAChRs. Interestingly, a quaternization of the bispidine nitrogen improves the affinity for the α4β2* and α7* nAChRs, except for the muscle type (K_i value for α3β4* was not determined). In addition, in the course of this study it has been demonstrated that N-substitution (e.g. with a methyl, acetyl, benzyl, or carbonyl moiety) dramatically decreases the affinity for all nAChRs subtypes under

investigation. Such tendency is also corroborated from binding studies carried out by Slater et al. on α4β2 and α7 nAChRs expressed in human recombinant Xenopus oocytes [341]. Furthermore, in order to unravel the influence of halogenation in the N-methylcytisine skeleton on the affinities for other subtypes, the K_i values of these novel analogues have been evaluated for α3β4* and muscle nAChRs. Compared to the N-methyl analogue (K_i = 5.7 nM), the introduction of a bromine or an iodine atom at position C-3 of the N-methylcytisine produces an increase in the affinity for α4β2* nAChRs (K_i = 1.37 (Br) and K_i = 0.959 nM (I)). Moreover, the introduction of a bromine or an iodine atom at position C-3 of the N-methylcytisine is responsible for a significant increase in the affinity for native α3β4* (333- and 750–fold higher affinity, respectively) and α7* nAChRs (114- and 57–fold higher affinity, respectively). The binding affinity of N-methyl-3-bromocytisine and N-methyl-3-iodocytisine for the α7* is similar to that of (-)-cytisine **Cy 1** (K_i = 131 and 260 nM, respectively), whereas it was observed as an improvement, in comparison to the lead compound, for their ability to displace (±)[^{3}H]epibatidine on α3β4* nAChRs (4 and 9-fold, respectively). The affinity decreases remarkably for all the subtypes under investigation when the iodine or the bromine atoms are introduced at both positions C-3 and C-5 at the pyridone ring of N-methyl-cytisine.

Interesting results have been obtained with compounds derived from the introduction of a nitro group in position C-3 or C-5 of the pyridone moiety of (-)-cytisine **Cy 1**. The replacement of hydrogen in position C-3 by a nitro group enhanced the affinity for all types of nAChRs. On the contrary, the introduction of the same group in position C-5 strongly reduced the affinity. Bodio et al. [339] reported a similar pattern in a radioligand binding experiment using (-)-[^{3}H]cytisine and whole membrane preparation from rat brain.

The thiocytisine analogues representing a novel series of (-)-cytisine **Cy 1** which have not been investigated so far. Here, for the first time, the affinity of these analogues was determined for four different nAChRs subtypes, namely: α4β2*, α7*, α3β4* and muscle type nAChRs. Bioisosteric replacement of the carbonyl oxygen by sulphur

resulted in a drastic decrease of affinity for the α7* subtype. On the basis of this finding, the novel thiocytisine may be used as a very selective ligand for α4β2* nAChRs. Unfortunately, none of the structural modifications of the thiocytisine were able to enhance the selectivity for subtypes under investigation. Furthermore, the influence of hydrogenation of the pyridine moiety was investigated. The tetrahydrocytisine **Cy 2** showed affinity in the nanomolar range for α4β2* nAChR. Binding studies performed in our laboratory showed that structural modifications of the skeleton of the tetrahydrocytisine, such as N-methylation or N-acetylation are detrimental to the binding to α3β4*, α7* and muscle nAChRs. In a successive study, Boido et al. also tested the affinity of tetrahydrocytisine for the central neurons in the brain, finding a value (K_i = 138 nM) notably higher than the value found in the present study (K_i = 17 nM). This difference is probably due to the different conditions used in the competition radioligand binding assays.

Such chemical modifications were of particular importance for unravelling the characteristics of the binding site and the development of a pharmacophore model (I/3).

In conclusion, it would be interesting to discover which kind of substituent in the cytisine and thiocytisine template would be able to improve the selectivity towards α4β2* nAChRs and reduce or abolish the affinity towards the ganglionic and peripheral subtype. At the same time further modifications could lead to analogues with an improved selectivity for other nAChR subtypes.

III/4. Ferruginine as a lead compound for novel nAChRs ligands

III/4.1. Introduction

(+)-Ferruginine, a potent neurotoxin, is a natural alkaloid isolated from the arboreal species *Darlingia ferruginea* (J. F. Bailey) [344] and *darlingiana* (F. Muell) [345]. The *Darlingia darlingiana* and *ferruginea* (common name Silky Oak) belong to the family of the *Proteaceae* (Fig. III/4.1) and contain (+)-ferruginine as their major alkaloid.

Figure III/4.1: Flowers of the trees of *Darlingia darlingiana* and *ferruginea* [346]

The unnatural enantiomer of (+)-ferruginine, (-)-ferruginine **Fe 1** as well as the demethylated analogue (-)-norferruginine **Fe 2** [347] (Fig. III/4.2), characterized by an 8-azabicyclo[3.2.1.]octene-skeleton, have attracted considerable attention as potential modulators of the nicotinic acetylcholine receptors [348]. The structure of (-)-ferruginine **Fe 1** is similar to that of (+)-anatoxin-a **An 1**, a potent ligand on nAChRs. They differ only in the number of carbon atoms constituting the azabicyclic skeleton.

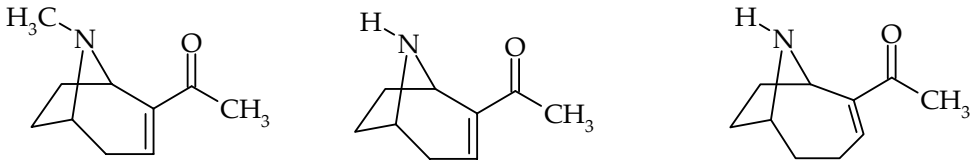

(Fe 1) **(Fe 2)** **(An 1)**

Figure III/4.2: Structures of (-)-ferruginine **Fe 1**, its demethylated analogue (-)-norferruginine **Fe 2** and (+)-anatoxin-a **An 1**

As shown in Fig. III/4.2, (+)-anatoxin-a **An 1**, (-)-ferruginine **Fe 1** and (-)-norferruginine **Fe 2** have common structural characteristics. All of them possess a protonable nitrogen function and an acetyl side chain. Despite their similar structure,

(-)-ferruginine **Fe 1** and its demethylated analogue **Fe 2** possess a lower affinity for the central α4β2* nAChRs subtypes (K_i = 110 and 94 nM, respectively) compared to anatoxin-a **An 1** (K_i = 1.1 nM) [228]. In addition, (-)-norferruginine **Fe 2** shows remarkably low affinity for the α7* nAChRs subtypes (K_i = 110,000 nM) [228]. On the basis of the structural correlation of (-)-norferruginine **Fe 2** to (+)-anatoxin-a **An 1** as well as of the discovery of the racemic pyrido[3.4b]homotropane **PHT**, which is a bioisosteric and conformationally constrained variation of (+)-anatoxin-a **An 1**, the conformationally restricted pyrido[3.4-b]tropane **P1**, a bioisosteric variant of (-)-norferruginine **Fe 2**, has been synthesized [349] (Fig. III/4.3).

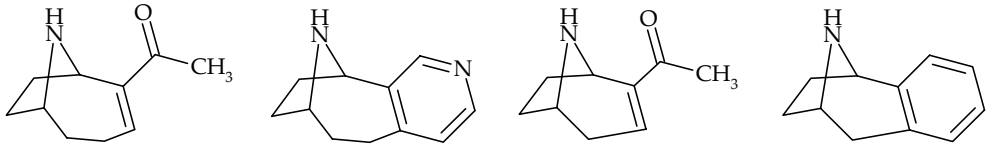

Figure III/4.3: Structure of anatoxin-a **An 1**, its conformationally restricted analogue **PHT,** (-)-norferruginine **Fe 2** and its conformationally restricted analogue **P1**

In order to obtain more information about the SAR of this structure for the nAChRs, the pyridino[3.4-b]tropane **P1** has been used as lead compound to synthesize new variants, whereas the pyridine element is bioisosterically replaced by other nitrogens containing heteroarenes such as 1,2 and 1,3 diazines [349] (Fig. III/4.4). These constrained analogues were tested for their *in vitro* affinity for α4β2* and α7* nAChRs using (±)-[^{3}H]epibatidine and [^{3}H]MLA in P2 membrane fraction from rat brains.

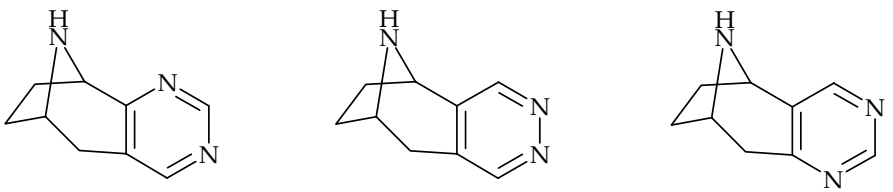

pyrimidino[4.5-b]tropane **P2** pyridazino[4.5-b]tropane **P3** pyrimidino[5.4-b]tropane **P4**

Figure III/4.4: Conformationally restricted diazine bioisosteres of pyrido[3.4-b]tropane.

The pyridazino[4.5-b]tropane **P3** (Ki = 76 nM) [349] has the highest affinity for α4β2* nAChRs. The dramatic decrease in affinity observed for the pyrimidine annulated isomer **P2** (K_i value higher than 10,000 nM) is considered due to the less favourable orientation of the nitrogen atoms in position C-3. In contrast, the isomeric racemic pyrimidino[5.4-b]tropane **P4** binds with a significantly higher affinity than **P2** (although it is 9-fold lower in comparison with the pyridazine annulated species **P3**). As observed for (-)-norferruginine **Fe 2**, none of these pyridazine or pyrimidine annulated ligands possess any affinity for the α7*, demonstrating an increased selectivity for the α4β2* over the α7* nAChRs. The structural modifications introduced on the skeleton of (±)-epibatidine **13,** the potent agonist at α4β2* nAChR subtype, were taken as a model in order to improve the binding affinity of the lead compound (-)-ferruginine **Fe 1**. In previous studies, the bioisosteric replacement of the chloropyridyl moiety of (±)-epibatidine **13** [350](with e.g. methylisoxazole, [222] pyrimidine [351] or pyridazine [352]) produced novel agonists which retained a good or improved affinity towards neuronal nAChRs receptors. Hence, novel diazine analogues of (-)-ferruginine **Fe 1** were synthesized and tested in radioligand assays in order to examine the limits of the nicotinic pharmacophore [228, 258, 224, 260, 353, 259]. These novel ligands are characterized by the azabicyclo[3.2.1]octane moiety of (-)-ferruginine **Fe 1** and by the replacement of the acetyl moiety in position C-2 with a diazine, such as pyridazine, pyrimidine and pyrazine. They were tested for *in vitro* affinity to central nAChRs such as α4β2* and α7* subtype [228]. Interestingly, the pyrimidine analogue was revealed to be the most active compound with a K_i value of 3.7 nM (**Fe 20)**. The structure of this analogue was verified by X-ray crystallography, revealing an internitrogen distance close to that of (±)-epibatidine **13** [228]. In general, both the pyridazine and pyrimidine derivatives proved to be more efficacious to the α4β2* compared to the lead compound (-)-ferruginine **Fe 1.** Moreover, it was discovered that these ligands have only a weak binding affinity for the α7* subtype [228].

III/4.2. Project

(In cooperation with Prof. Seitz, Department of Pharmaceutical Chemistry, University of Marburg: synthesis of the novel ferruginine analogues)

Only few structure-activity relationship (SAR) studies have been carried out with regard to the (-)-ferruginine-type nAChRs ligands so far. In 2001, an initial study was performed to determine the binding affinities of some diazine derivatives of (-)-norferruginine (**P2, P3, P4**) for α4β2* and α7* nAChRs [228] (see above, introduction). In order to gain more information about the SAR of (-)-ferruginine **Fe 1**, some structural modifications have been introduced in the azabicyclic skeleton of (-)-ferruginine **Fe 1** by varying the nature of the two main elements of the general nAChR pharmacophore: the positively charged sp^3 hybridised nitrogen in the azabicycle and the hydrogen bond acceptor group (HBA) [257-259,261]. The (-)-ferruginine analogues are structurally similar to the (-)-norferruginine series recently published [228]. In a previous study, it has been seen that the introduction of a N-methyl group, as in the case of (-)-nicotine/(-)-nornicotine [354] could increase affinity to the nAChRs. Therefore, it was of interest to study the influence of this modification on an 8-azabicyclo[3.2.1.]octene-skeleton. To address the topic of binding selectivity among the nAChR subtypes, the affinities of these novel (-)-ferruginine and (-)-norferruginine analogues will be measured in competition-binding assays for four different nAChRs. Below, (Fig. III/ 4.5) a list of the structural variations of the (-)-ferruginine **Fe 1** which have been developed is enumerated:

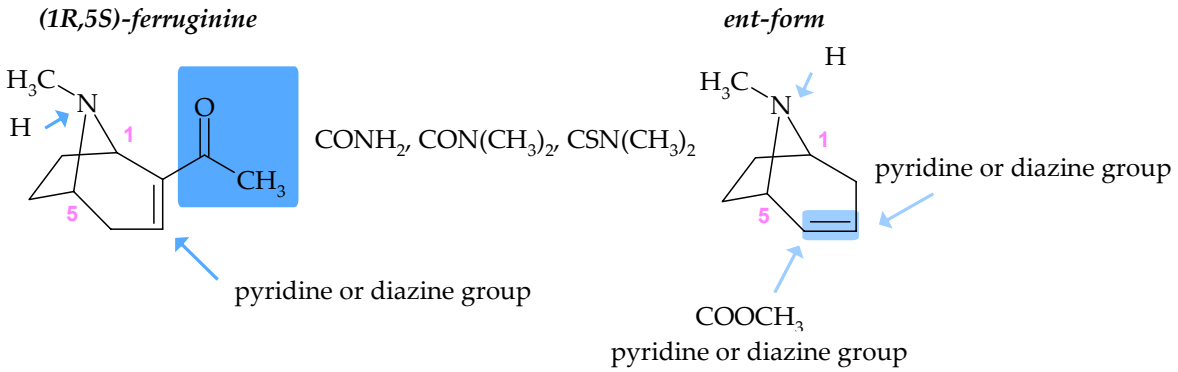

Figure III/4.5: Structural modifications of (1R,5S)(-)-ferruginine **Fe 1** and the corresponding (1S,5R)(-)-*ent*-form.

- ✓ Replacement of the acetyl group of (1R,5S)(-)-ferruginine **Fe 1** with an amide, dimethylamide, or thioamide moiety
- ✓ Replacement of the acetyl group of (-)-ferruginine **Fe 1** with a pyridine or diazine group at position C-2 of the azabicycle.
- ✓ Introduction of a pyridine or diazine group at position C-3 of the azabicycle.
- ✓ Novel analogues of (-)-norferruginine with similar structural modifications performed on the (-)-ferruginine structure.
- ✓ Novel enantiopure *ent*-(-)-ferrugininoids (1S,5R) with a pyridine or diazine group
- ✓ Double substitution of the *ent*-azabicyclic skeleton with an ester and a diazine group.

III/4.3. Determination of affinities and structure-activity relationships (SAR)

The (-)-norferruginine derivatives were evaluated in previously described competition assays for their possible interaction with different nAChR subtypes using (±)-[^{3}H]epibatidine and [^{3}H]MLA as radioligands and P2 membrane fractions of Sprague-Dawley rat forebrain (α4β2* and α7* nAChRs) [179,294,349,355]. To estimate the binding affinities of the novel (-)-ferruginine and (-)-norferruginine analogues for the α3β4* nAChRs, a novel assay using pig adrenals and (±)-[^{3}H]epibatidine was established [290, 292, 294]. To characterize binding of each of the ferrugininoids to the $(\alpha1)_2\beta1\gamma\delta$ nAChRs, (±)-[^{3}H]epibatidine and *Torpedo californica* electroplax were used. (±)-[^{3}H]Epibatidine bound to a single population of binding sites with $K_D = 2 \pm 0.3$ nM [289, 290].

Replacement of the acetyl moiety by an amide or thioamide group

The replacement of the methyl group next to the carbonyl function with an amine, methylamine or dimethylamine moiety leads to compounds **Fe 3, Fe 4** and **Fe 5**. These modifications have been performed based on the hypothesis that an increase of the hydrogen bond acceptor (HBA) capability of (-)-ferruginine **Fe 1** might enhance the binding affinity for α4β2* nAChRs. In contrast, each of the amides **Fe 3, Fe 4** and **Fe 5** were weaker ligands for the nAChRs than the lead compound **Fe 1**. These derivatives (**Fe 3, Fe 4, Fe 5**) exhibited low affinity for α4β2* nAChRs (K_i values in the μM range) and no interaction with α7*, α3β4* and $(\alpha1)_2\beta1\gamma\delta$ nAChRs (Tab. III/4.1). Furthermore, the exchange of the oxygen atom with a sulphur led to weaker ligands for the α4β2* nAChR, with K_i values in the higher μM range (**Fe 6**, **Fe 7**) (Tab. III/4.1). The derivatives **Fe 6** and **Fe 7** showed no interaction with other nAChR subtypes examined.

Table III/4.1: Radioligand binding affinities of (-)-ferruginine **Fe 1** and (-)-norferruginine **Fe 2** analogues bearing an amide moiety for α4β2*, α7*, α3β4* and $(\alpha1)_2\beta1\gamma\delta$ nAChRs.

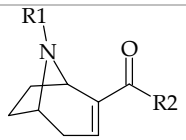

R1	R2	No	α4β2* [³H]EPI rat brain K_i (nM)	α7* [³H]MLA rat brain K_i (nM)	α3β4* [³H]EPI pig adrenals K_i (nM)	$(\alpha1)_2\beta1\gamma\delta$ [³H]EPI Torpedo calif. electroplax K_i (nM)
CH_3	CH_3	**Fe 1**	120 ± 2 [a]	330 ± 23 [a]	1,455 ± 319	> 50,000
H	CH_3	**Fe 2**	94 ± 5 [a]	> 100,000	2,300 [n=1]	5,300 [n=1]
CH_3	NH_2	**Fe 3**	3,790	> 50,000	> 50,000	> 50,000
CH_3	$NHCH_3$	**Fe 4**	1,490 ± 252	> 10,000	> 50,000	> 50,000
CH_3	$N(CH_3)_2$	**Fe 5**	2,027 ± 40	7,500 [n=1]	n.d.	n.d.
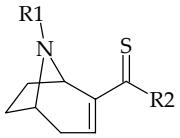						
CH_3	$N(CH_3)_2$	**Fe 6**	20,000	50,000	n.d.	n.d.
H	$N(CH_3)_2$	**Fe 7**	2460 [n=1]	39,000 ± 1414	13,650 ± 3323	n.d.

n.d. = not determined
n = number of experiments
a = [228]

Pyridine analogues

The substitution of the 2-acetyl moiety with a 3-pyridyl moiety seems to be of particular interest in the search for compounds with an improved affinity for neuronal nAChRs [202] [203] [356,357]. Hence, in these series, the acetyl moiety of **Fe 1** and **Fe 2** was substituted with a 3-pyridyl moiety, giving the analogues **Fe 8** and **Fe 10,** respectively. The introduction of a 5-chloro-pyridyl moiety at position C-2, according to the structure of (±)-epibatidine **13**, led to the ferruginine analogue **Fe 11** (Tab. III/4.2). In addition, in order to obtain more information about the stereodiscrimination, *ent*-**Fe 8**, *ent*-**Fe 9** and *ent*-**Fe 10** were investigated for the multifarious nAChRs subtypes

Substitution at position C-2

The azine analogues **Fe 8-Fe 11** proved to be very high affinity bioisosters of **Fe 1** with a significant influence of the heteroaryl moiety on the binding affinity and selectivity towards the nAChRs examined. The novel ferrugininoids proved to be more potent than the lead **Fe 1** and the analogue **Fe 2**. The (-)-norferruginine derivative **Fe 8** showed the highest affinity for the α4β2* nAChR subtype with a K_i value of 1.6 nM being twice as potent as (1S,5R) *ent*-**Fe 8** (K_i = 3.8 nM). Interestingly, the stereodiscrimination found for **Fe 8**/*ent*-**Fe 8** towards the α4β2* nAChRs subtype was not observed towards the α7* and α3β4* nAChRs subtypes. The 5-iodo-pyridyl-containing modification (1S,5R) *ent*-**Fe 9**, exhibited a ca. 6-fold lower affinity (K_i = 1,724 nM) for the α7* nAChRs compared to both **Fe 8** and *ent*-**Fe 8** (K_i = 396 and 365 nM, respectively). Probably, the presence of a bulky substituent distorts the molecular conformation of the ligands and also affects the intramolecular N-N distance that seems to be important for the binding to neuronal nAChRs. On the contrary, the introduction of the iodine atom does not seem to disturb the interaction of (1S,5R) *ent*-**Fe 9** with the α3β4* nAChRs, given that its affinity (K_i = 224 nM) is similar to that of the pyridyl analogue *ent*-**Fe 8** (K_i = 198 nM). With regard to the ferruginine analogues, **Fe 10, Fe 11** and their corresponding compounds *ent*-**Fe 10** and *ent*-**Fe 11,** the most active ligand at the α4β2* and α3β4* nAChRs (Tab. III/4.2)

was the 5-chloropyridyl-containing ligand **Fe 11**. The binding affinity of this compound for the α4β2* nAChRs (K_i = 1.1 nM) is 100-fold higher than the affinity of the lead **Fe 1**. Further, **Fe 11** is able to differentiate between different nAChRs subtypes. In fact, it binds to the ganglionic α3β4* subtype with a 18-fold lower affinity than to the α4β2* nAChRs. One aspect that should be highlighted is the influence of the N-methyl moiety on the binding affinity of these ferrugininoids towards α7* nAChRs. On the one hand, N-methylation decreases (even if slightly) the affinity for the α4β2*, on the other hand it has been shown to increase significantly the affinity for α7* nAChRs. The results listed in the Table III/4.2 show that the ferruginine analogues, **Fe 10** and **Fe 11,** exhibited the highest affinity for the α7* nAChRs in this series (K_i = 53 and 56 nM, respectively), which is ca. 7- to 30-fold higher than the affinities of its demethylated analogues (**Fe 8,** *ent*-**Fe 8**). The novel compounds **Fe 10** and **Fe 11** possess an even greater affinity for the α7* nAChR than the lead compound (-)-ferruginine **Fe 1** (K_i = 330 nM). Interestingly, both correspondent analogues *ent*-**Fe 10** and *ent*-**Fe 11** showed reduced affinity for the α7* nAChRs (K_i =237 and 371 nM, for the *ent*-**Fe 10** and *ent*-**Fe 11,** respectively). The same tendency is observed for the α3β4* nAChRs. The ferruginine analogues **Fe 10** and **Fe 11** bind with 3- and 7-fold higher affinity to the ganglionic α3β4* nAChRs (K_i = 44 and 20 nM, respectively) compared to the (-)-norferruginine analogue **Fe 8** (K_i =139 nM). Both analogues *ent*-**Fe 10** and *ent*-**Fe 11** lose their affinities towards α3β4* nAChRs compared to the corresponding form **Fe 10** and **Fe 11.** Whereas the α7* and α3β4* nAChRs are affected by the stereodiscrimination, the muscle type nAChRs does not seem to be influenced by the stereospecificity of the compounds. The K_i values found for **Fe 10** and its corresponding analogue for muscle type nAChRs are nearly similar, as well as the affinities of **Fe 11** and *ent*-**Fe 11**. It is interesting to notice that the introduction of a chlorine atom on the pyridine ring is correlated to an increase of 4-6 fold of the affinity of **Fe 11** in comparison to **Fe 10** for the muscle type nAChRs (Tab. III/4.2).

Influence of the methylisoxazole group

It is known that the replacement of the pyridine ring of (S)(-)-nicotine **3** by an methylisoxazolyl moiety leads to a potent nicotinic ligand (ABT-418) **10** which possesses a high affinity binding for α4β2* nAChRs receptors [200]. The replacement of the 2-chloro-pyridinyl unit of (±)-epibatidine **13** with a methylisoxazolyl moiety results in epiboxidine **32**, an (±)-epibatidine **13** analogue also with very potent antinociceptive activity and a very high affinity for the neuronal nAChRs [222]. Based on these results, the methylisoxazole ring appears to be a useful bioisosteric moiety, and it was used for the synthesis of the ferruginine analogue, **Fe 12.** Interestingly, this analogue possesses ca. 4-fold higher affinity for the α4β2* receptor compared to the lead compound **Fe 1**. Moreover, it is slightly more potent at the α7* receptor in comparison to the (-)-ferruginine **Fe 1** (Tab. III/4.2).

Table III/4.2: Radioligand binding affinities of ferruginine analogues bearing different pyridine moieties or a methylisoxazole for $\alpha4_2\beta2_3$, α7*, α3β4*and $(\alpha1)_2\beta1\gamma\delta$ nAChRs.

Pyridine moieties (substitution at position C-2)						
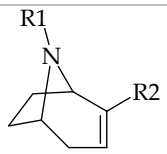				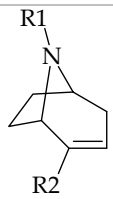 *ent*-form		
R1	**R2**	**No.**	**α4β2* [³H]EPI rat brain K_i (nM)**	**α7* [³H]MLA rat brain K_i (nM)**	**α3β4* [³H]EPI pig adrenals K_i (nM)**	**$(\alpha1)_2\beta1\gamma\delta$ [³H]EPI Torpedo californica electroplax K_i (nM)**
H	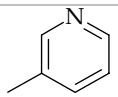	**Fe 8**	1.6 ± 0.2	396 [n=1]	139 ± 16	n.d.
H	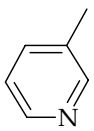	*ent*-**Fe 8**	3.8 ± 0.8	365 ± 45	198 ± 72	n.d.
H	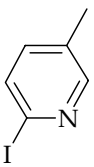	*ent*-**Fe 9**	6.3 ± 0.9	1,724 ± 189	224 ± 45	n.d.

CH_3	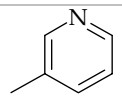	**Fe 10**	3.4 ± 1.4	53.3 ± 9.3	44 ± 5.7	4,390 ± 50
CH_3	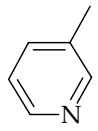	*ent*-**Fe 10**	9.6 $^{n=1}$	273 $^{n=1}$	305 ± 7	6,323 $^{n=1}$
CH_3	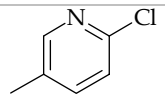	**Fe 11**	1.1 ± 0.2	56.6 ± 3	20.7 ± 2	1,361 $^{n=1}$
CH_3	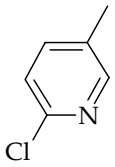	*ent*-**Fe 11**	13.2 ± 3.7	371 ± 31	156 ± 3.5	1,430 ± 24
Methylisoxazole analogue of (-)-ferruginine						
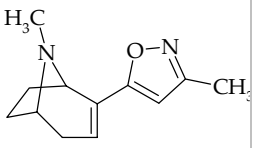		**Fe 12**	30 ± 1.2	234	n.d.	n.d.
n.d. = not determined n = number of experiments						

Substitution at position C-3

The introduction of a pyridine or chloropyridine ring at the position C-3 of the 8-azabicyclo[3.2.1.]octene-skeleton leads to (-)-ferruginine/(-)-norferruginine analogues **Fe 13, Fe 14** and **Fe 15** bearing a structure similar to (±)-epibatidine **13**. In previous studies, it has been shown that the 3-pyridyl unit is an important requisite for high affinity binding. As expected, these analogues showed an improved affinity for α4β2*, α7*, α3β4* and muscle nAChRs compared to the lead compounds **Fe 1** and **Fe 2.** The SAR observed for **Fe 13, Fe 14** and **Fe 15** confirmed the importance of an optimal distance between the cationic nitrogen of the azabicyclic skeleton and the pyridyl nitrogen for the binding affinity at α4β2* nAChRs. In this series, the (-)-norferruginine derivative **Fe 13** showed the highest affinity for α4β2* (K_i = 0.257 nM), being 376- and 466-fold more potent than (-)-norferruginine **Fe 2** (K_i = 94 nM) and (-)-

ferruginine **Fe 1** (K_i = 120 nM), respectively. **Fe 13** also showed a moderate selectivity for α4β2* over α3β4* nAChR subtypes (1:54). With regard to the (-)-ferruginine analogues, **Fe 14** is slightly less potent than **Fe 13** with respective decrease in binding affinities of 4.5 and 2-fold at α4β2* and α3β4*nAChRs. Chlorination of the pyridyl ring, as in compound **Fe 15,** exerts different effects on the binding affinity depending upon the subtype under consideration: it slightly decreases the affinity for α4β2* nAChR, whereas it has a detrimental effect for the affinity to α7* nAChRs (4-fold lower). An opposite tendency is observed for the ability of **Fe 14** and **Fe 15** to interact with the α3β4* nAChRs. Actually, analogue **Fe 15** turned out to be the most active ligand at α3β4* nAChRs (K_i = 5.5 nM). The 5-chloropyridine moiety in position C-3, has been shown to improve the binding affinity toward α3β4* and muscle type to a similar extent (4-fold). This observation suggests that a chlorine atom on the pyridine ring improves the affinities for α3β4* and muscle type nAChRs (Tab. III/4.3).

Influence of a double substitution at the azabicyclic skeleton

The drop in affinity observed for the (-)-ferruginine analogues (*ent*-**Fe 16** and *ent*-**Fe 17)** (Tab. III/4.3) clearly indicates that a double substitution, such as an introduction of an ester moiety in position C-2 and a pyridine or chloropyridyl moiety at position C-3 of the (1S,5R)-8-azabicyclo-[3.2.1]octene-skeleton is significantly detrimental to the affinity for all subtypes examined. The K_i values have been detected in the micromolar range (Tab. III/4.3). The presence of bulkier substituents close to the HBA moiety appears to dramatically influence the affinities for neuronal nAChR. This observation inspires a hypothesis, namely that the ester group at position C-2 orientates the substituent in a disfavoured region. In addition, the loss of affinity could be attributed not only to steric effects but also to the reduced electron density of the aromatic chloropyridine moiety.

Table III/4.3: Radioligand binding affinities of pyridine analogues of (-)-ferruginine, *ent*-(-)-ferruginine and (-)-norferruginine for α4β2*, α7*, α3β4* and $(\alpha1)_2\beta1\gamma\delta$ nAChRs.

Pyridine moieties at position C-3							
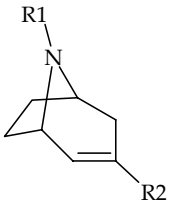				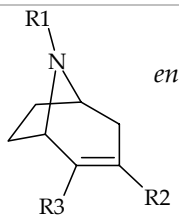 *ent*-form			
R1	**R2**	**R3**	**No.**	**α4β2* [³H]EPI rat brain K_i (nM)**	**α7* [³H]MLA rat brain K_i (nM)**	**α3β4* [³H]EPI pig adrenals K_i (nM)**	**$(\alpha1)_2\beta1\gamma\delta$ [³H]EPI Torpedo calif. electroplax K_i (nM)**
H	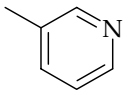	H	**Fe 13**	0.257 ± 0.06	n.d.	14 ± 3.5	n.d.
CH_3	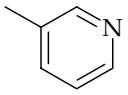	H	**Fe 14**	0.96 ± 0.14	73.6 ± 7.7	24 ± 3.5	$341^{n=1}$
CH_3	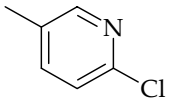	H	**Fe 15**	1.54 ± 0.02	256 ± 26	5.5 ± 0.9	80.3 ± 10
CH_3	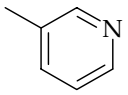	$COOCH_3$	*ent*-**Fe 16**	4,931 ± 144[a]	> 50,000	> 30,000	> 50,000
CH_3	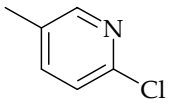	$COOCH_3$	*ent*-**Fe 17**	1,659 ± 354	20,311 ± 185	13,340 ± 58	> 50,000
n.d.= not determined n= number of experiments							

Diazine analogues

The bioisosteric potential of diazine moieties on binding affinities was investigated in the field of (-)-ferruginine/(-)-norferruginine type structures. The novel ligands **Fe 18-Fe 34** are characterized by the azabicyclo[3.2.1]octene pharmacophore and by the replacement of the acetyl group of **Fe 1** and **Fe 2** with a diazine nucleus such as pyridazine, pyrimidine and pyrazine. The diazine moiety was introduced at position C-2 as well as positions C-3 of the azabicyclic skeleton. All these novel analogues were analysed for their *in vitro* affinity for α4β2*, α7*, α3β4* and $(\alpha1)_2\beta1\gamma\delta$ nAChRs. Generally, the incorporation of an additional nitrogen atom into the heteroaromatic HBA pharmacophoric element has a deleterious effect on the binding affinity. This effect is well-known in literature, e.g. for the diazine substituted variants of (±)-epibatidine **13** and anatoxin-a **An 1** [352]. In the present study, the diazine substituted ferrugininoids and norferrugininoids are approximately 10-times less potent than the chloropyridyl/pyridyl substituted ligands **Fe 8** and **Fe 11** and **Fe 13** and **Fe 15** for the neuronal nAChRs subtypes.

Influence of diazine substituents at position C-2

The binding affinities (K_i values) of compounds **Fe 18, Fe 20** and **21** for α4β2* and α7* have already been reported [228]. It was demonstrated that the three isomeric diazine heterocycles are suitable bioisosteres of the acetyl moiety of **Fe 1** [228]. Although the inter-nitrogen distance for the three bioisosteres is approximately equal, the presence of another nitrogen in the heteroaryl moiety obviously results in modifications of the electronic density in the diazine ring. As a consequence, the hydrogen bond acceptor ability, which is crucial for nAChR affinity, decreases. The most potent analogue for α4β2* was the chloro-pyrimidine derivative of (-)-norferruginine **Fe 19** with a K_i value of 2 nM. Compounds **Fe 18** and **Fe 19** differ by the presence of a chlorine atom in the pyridine ring. This halogenation has small influence on the binding potency of **Fe 18** and **Fe 19** at α4β2* nAChRs. On the contrary, it seems to be favourable for the binding to the α7* nAChRs. Compound **Fe 19** exhibited a 5-fold higher affinity at the α7* nAChRs compared to the deschloro analogue **Fe 18**. The **Fe 19** shows the highest

affinity in these series for the α3β4* nAChRs (K_i= 71 nM) (Tab. III/4.4). Compound **Fe 22,** bearing chloropyrazine moiety displays the lowest affinity for α4β2* nAChRs within the (-)-norferruginine derivatives (K_i = 4,100 nM). In this case, the marked decrease in affinity could be caused by steric interactions between the chloro-substituent and the bicyclic ring system that leads to an unfavourable orientation of the pyrazine ring [358]. The **Fe 18** and **Fe 20** possess no affinity for the α7* nAChR. It is of interest to notice that for the (-)-ferruginine analogues **Fe 24** and **Fe 25** the influence of the diazine moiety on binding affinities is similar to that observed in the (-)-norferruginine series. The order of potency is the following: 5-pyrimidinyl > 4-pyridazinyl > 2-pyrazinyl. Among the series of diazine containing compounds, the favourable influence of the pyrimidine moiety is due to its electrostatic properties. In fact, pyrimidine has been shown to possess by far the most negative atomic density compared to pyridazine or pyrazine substituents [358]. Thus, the analogue **Fe 23**, having a pyrimidine moiety as a substituent, has turned out to be the most active ligand among the ferrugininoids (Tab. III/4.4). However, in comparison to its (-)-norferruginine analogue **Fe 18**, it possesses a 4-fold lower affinity for the α4β2* nAChR. On the contrary, the presence of a methyl moiety in compound **Fe 23** results in an increase of affinity for the α7* nAChRs (K_i = 500 nM). The analogue **Fe 25**, bearing a pyridazine moiety proved to be the weakest ligand in the series of diazine analogues (C2-substitution at the (-)-ferruginine skeleton). Probing the issue of enantioselectivity, an investigation was made whether the pyridazine substituted ferruginine analogues **Fe 24**/*ent*-**Fe 24** and **Fe 23**/*ent*-**Fe 23** have the same stereochemical bias observed with **Fe 10**/*ent*-**Fe10** and **Fe 11**/*ent*-**Fe11** ferruginine analogues. Surprisingly, the analogues **Fe 24**/*ent*-**Fe 24** showed no stereo-discrimination toward the α4β2*. A certain degree of stereoselectivity was observed for their interaction with the ganglionic type. Indeed, the binding potency of *ent*-**Fe 24** (K_i= 305 nM) was 5-fold better than the corresponding analogue **Fe 24** (K_i= 1,559 nM). On the contrary, the ligands **Fe 23**/*ent*-**Fe 23** (Tab. III/4.4) interact in a

stereoselective manner with α4β2*, α7* and α3β4* nAChRs subtypes, but not with the $(\alpha1)_2\beta1\gamma\delta$ nAChRs.

Table III/4.4: Radioligand binding affinities of diazine analogues (substituted at position C-2) of (-)-ferruginine **Fe 1**, its *ent*-form and (-)-norferruginine **Fe 2** for α4β2*, α7*, α3β4*and $(\alpha1)_2\beta1\gamma\delta$ nAChRs.

Diazine analogues (substitution at position C-2)						
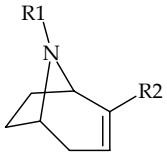				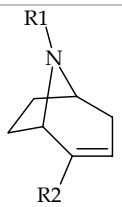 *ent*		
R1	**R2**	**No**	**α4β2* [³H]EPI rat brain K_i (nM)**	**α7* [³H]MLA rat brain K_i (nM)**	**α3β4* [³H] EPI pig adrenals K_i (nM)**	**$(\alpha1)_2\beta1\gamma\delta$ [³H] EPI Torpedo calif. electroplax K_i (nM)**
H	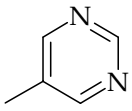	**Fe 18**	3.7 ± 0.6 [a]	5,000 ± 230	n.d.	n.d.
H	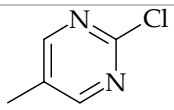	**Fe 19**	2 ± 0.5	1,000	71.6	n.d
H	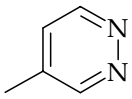	**Fe 20**	113 ± 4.7 [a]	> 50,000	n.d.	n.d.
H	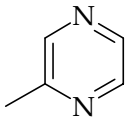	**Fe 21**	400 ± 17 [a]	13,500 ± 244	n.d.	n.d.
H	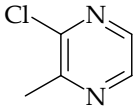	**Fe 22**	4,100 ± 300	> 50,000	n.d.	n.d.
CH_3	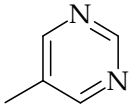	**Fe 23**	12.6 ± 0.07	500 ± 28	234 ± 16	15,269 [n=1]
CH_3	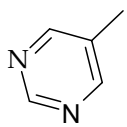	*ent*-**Fe 23**	43.2 [n=1]	4,215 ± 90	906 [n=1]	25,300 [n=1]

CH_3	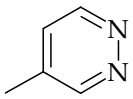	**Fe 24**	29.7 ± 0.7	1,300 [n=1]	1,559 ± 297	> 50,000
CH_3	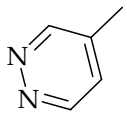	*ent*-**Fe 24**	29.5 ± 4.7	2,862 ± 353	305 ± 14.8	> 50,000
CH_3	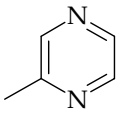	**Fe 25**	713 ± 49	10,000 [n=1]	6,444 ± 50	n.d.
a =[228]						

Influence of diazine substituents at position C-3

In this series, the influence on the binding affinity of an introduction of a diazine moiety at position C-3 of the azabicyclic system of (-)-ferruginine **Fe 1** and (-)-norferrugine **Fe 2** was investigated. The results of radioligand binding studies for these novel analogues are listed in Tab. III/4.5. As already observed in the pyridine series, the introduction of a diazine moiety at the same position would be expected to have a positive influence on the binding affinity for the central nAChRs. Indeed, **Fe 26** and **Fe 27** showed affinity values for the α4β2* nAChRs in the picomolar range (K_i value of 0.66 and 0.70 nM, respectively). Thus, having an affinity ca. 140-fold higher than that of ferruginine **Fe 1**, they represent the more potent analogues tested for α4β2* nAChRs. The introduction of a chlorine atom into the pyrimidine moiety, as in compound **Fe 27**, does not influence the affinity towards the α4β2* nAChRs. On the other hand, it increases the selectivity for α4β2* over α7* (1/5100). The analogues **Fe 28** and **Fe 29,** bearing a pyridazinyl and pyrazinyl moiety at position C-3 of the (-)-norferruginine skeleton, are 15- and 46-fold less potent at the α4β2* nAChRs respectively (K_i value of 10 and 31 nM, respectively) than the pyrimidine substituted analogue **Fe 27.** The introduction of a chlorine atom in the pyrazine moiety, such as in compound **Fe 30,** further decreases the affinities for the neuronal receptor, α4β2* (K_i= 210 nM). This compound also displays the lowest affinity for α7* and α3β4* within the series of (-)-norferruginine analogues (K_i= 50,000 and 1,738 nM, respectively). As far as diazine substituted ferruginine analogues are concerned, the

Fe 31 shows a slightly lower affinity for the α4β2* nAChRs and an improved affinity for α7* nAChRs. N-methylation, as already observed for other ferrugininoids analogues (e.g. **Fe 23, Fe 10, Fe 11),** leads to an enhancement of the binding affinity for α7* nAChRs. Interestingly, the **Fe 31** showed the highest affinity for α3β4* (K_i= 54 nM) and muscle type nAChRs (K_i = 847 nM). The K_i value for the muscle type was 18-fold lower than the K_i value of the analogue bearing the pyrimidine group in position C-2, **Fe 23** (K_i = 15,269 nM). As expected, the introduction of an ester group at position C-2 of the azabicyclic skeleton *ent*-**Fe 32** has a negative impact on the affinity. This modification markedly diminishes binding affinities for all nAChR subtypes investigated. The pyrazine moiety at position C-3, **(Fe 33)** showed lowest affinities towards all subtypes under consideration (K_i = 171 nM, 2,667 nM and 2,754 nM for α4β2*, α7* and α3β4*, respectively) in the diazine series.

Table III/4.5: Radioligand binding affinities of diazine analogues (substitution at C-3) of (-)-ferruginine **Fe 1**, *ent*-(-)-ferruginine and (-)-norferruginine **Fe 2** for α4β2*, α7*, α3β4*and $(\alpha1)_2\beta1\gamma\delta$ nAChRs.

Diazine moieties at position C-3							
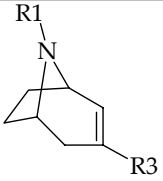				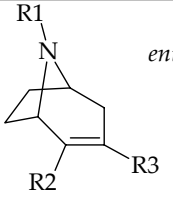 *ent*-form			
R1	**R2**	**R3**	**No.**	**α4β2* [³H]EPI rat brain K_i (nM)**	**α7* [³H]MLA rat brain K_i (nM**	**α3β4* [³H] EPI pig adrenals K_i (nM)**	**$(\alpha1)_2\beta1\gamma\delta$ [³H] EPI Torpedo calif. electroplax K_i (nM)**
H	H	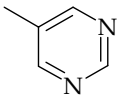	**Fe 26**	0.66 ± 0.04	2,500	n.d.	n.d.
H	H	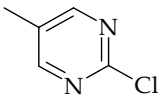	**Fe 27**	0.708 ± 0.04	3,600	114	n.d.
H	H	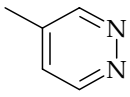	**Fe 28**	10 ± 2.3	20,000	n.d.	n.d.

H	H	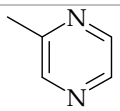	**Fe 29**	31 ± 2.4	7,000	n.d.	n.d.
H	H	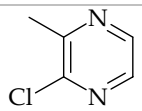	**Fe 30**	210 ± 25	50,000 [b]	1,738[b]	20,000[b]
CH_3	H	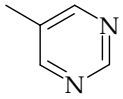	**Fe 31**	1.25 [n=1]	1,100 ± 36	54.3 ± 10.3	847 [n= 1]
CH_3	$COOCH_3$	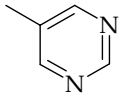	*ent-* **Fe 32**	212 ± 50	> 50,000	5,796 [n=1]	31,865 ± 456
CH_3	H	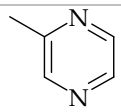	**Fe 33**	171	2,667	2,754	n.d.
n= number of experiments n.d.= not determined							

Further modifications on the azabicyclic skeleton

The structural modifications introduced in compounds **Fe 34** and **Fe 35** were the reduction of the double bond on the azabicyclic ring by introduction of a hydroxy moiety at the same position as pyrazine ring (Tab. III/4.6). This structural alteration concerns the positions C-2 for **Fe 34** and position C-3 for **Fe 35**. The introduction of a hydroxyl moiety at the position C-3 markedly diminishes the binding affinity for the α4β2* subtype (K_i = 8,116 nM). The K_i value is 50-fold lower in comparison with the pyrazine analogue **Fe 33** (K_i = 171 nM). An equivalent substitution at position C-2 of the azabicyclo skeleton also results in a marked decrease of affinity (K_i = 5,800 nM) compared to the (-)-ferruginine analogue **Fe 25** (K_i = 713 nM). The additional hydroxyl group seems to disturb the interaction with all subtypes investigated.

Table III/4.6: Radioligand binding affinities of hydroxylated analogues of (-)-ferruginine **Fe 1** for α4β2*, α7*and α3β4* nAChRs.

Structure	No.	α4β2* [³H]EPI rat brain K_i (nM)	α7* [³H]MLA rat brain K_i (nM	α3β4* [³H] EPI pig adrenals K_i (nM)
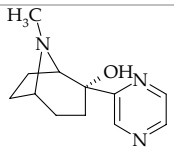	**Fe 34**	5,800 ± 1,008	~20,000	20,885 $^{n=1}$
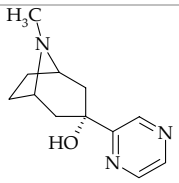	**Fe 35**	8,116 $^{n=1}$	~ 20,000	26,535 $^{n=1}$

III/4.4. Discussion

The affinity profiles of novel (-)-ferruginine **Fe 1** and (-)-norferruginine **Fe 2** ligands (which have heteroaromatic rings at position C-2 or C-3), with the exception of some compounds, shows the following sequence of binding potency (in order of decreasing affinities) (Fig. III/4.6):

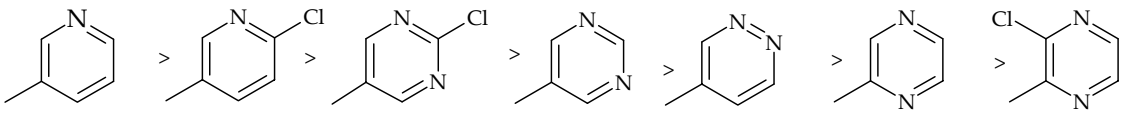

Figure III/4.6: Decreasing order of binding potency for (-)-ferruginine **Fe 1** and (-)-norferruginine **Fe 2** derivatives related to the N-heterocycle introduced.

The affinities of the novel ferrugininoids and norferrugininoids will decrease by increasing the number of nitrogen atoms in the heteroaromatic moiety thereby reducing the electron density in the ring. It is clear that decreasing the electron density, the hydrogen bond acceptor capability of the heteroaromatic atom will diminish too. Another crucial factor seems to be the position of the halogen in the pyridine or diazine ring. There is a special region that may be particularly interesting for substitution: the para position to the pivot bond of the aromatic moiety. Indeed, the introduction of a chlorine-substituent in position C-2 of the pyridine **Fe 11** or pyrimidine ring **Fe 19** and **Fe 27** results in compounds with an improved affinity towards the nAChRs. On the contrary, the introduction of a chlorine atom in the C-5 of the pyrazine moiety, in ortho position to the pivot bond, caused a remarkable decrease in affinity **Fe 22**. One other parameter that seemed to be important for the affinity is the position of the heterocycle at the azabicyclic system. The pyridine and the diazine moiety were introduced at position C-2 as well as at position C-3. Results of structure-affinity-relationship studies show that substitution at position C-3 seems to be the one preferred for high affinity binding of the ligands (Fig. III/4.7).

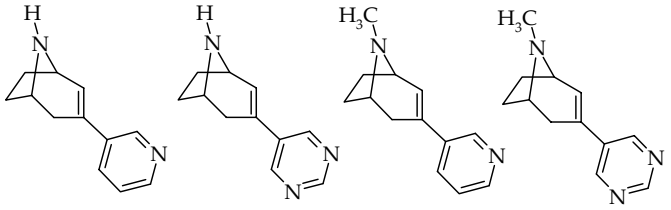

Fe 13 **Fe 26** **Fe 14** **Fe 31**

Figure III/4.7: Structures of (-)-ferruginine **Fe 1** and (-)-norferruginine **Fe 2** analogues with a pyridine or pyrimidine moiety introduced at position C-3 of the azabicyclic skeleton.

It has been found that, within the (-)-norferruginine analogues, compound **Fe 13**, having a pyridine moiety at position C-3, shows the highest affinity for α4β2* nAChRs (K_i = 0.25 nM), followed by **Fe 26** (K_i = 0.66 nM) containing a pyrimidine moiety. As far as (-)-ferruginine analogues are concerned, the most potent ligands for α4β2* nAChRs were **Fe 14**, with a pyridine moiety at position C-3 (K_i = 0.96 nM) and **Fe 31** (K_i = 1.2 nM) with a pyrimidine moiety in the same position. The chlorine atom has been shown to increase the affinity of (-)-ferruginine analogues for the ganglionic α3β4* nAChR. The affinity of **Fe 15** (K_i = 5.5 nM) increases in comparison to **Fe 14** (K_i = 24 nM) (ca. 5-fold), as well as the affinity of **Fe 11** in comparison to **Fe 10** (ca. 2-fold) (Fig. III/4.8).

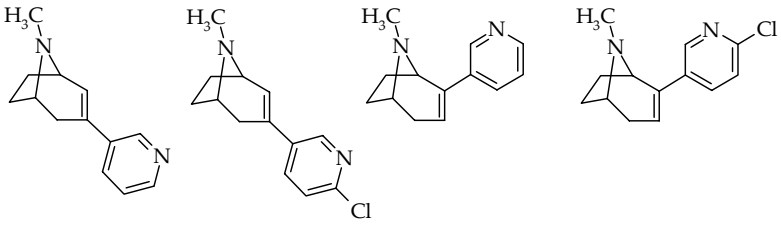

Fe 14 **Fe 15** **Fe 11** **Fe 10**

Figure III/4.8: Structures of the pyridine derivatives **Fe 14** and **Fe 11** and chloropyridine derivatives **Fe 15** and **Fe 10.**

The effect of the azabicyclic moiety with respect to N-methylation in tropane analogues was investigated. In binding assays, typical nicotinic ligands exhibit diverse structure-activity patterns with respect to N-substitution. The affinity of (-)-nicotine **3**, e.g. is 20-fold higher than that of its nor-analogue [354]. On the contrary, N-methylation decreases by 2-fold the affinity of (±)-epibatidine **13** [157] and by several

hundreds that of anatoxin-a **An 1** [359]. In the present study, N-methylation influences the affinities in different ways, depending upon the subtypes investigated. On the one hand, the presence of a methyl moiety in the azabicyclic system decreases the affinity for the α4β2* nAChR subtype, on the other hand, it improves the affinity for α7* and α3β4* nAChRs subtypes (e.g. **Fe 8** in comparison to **Fe 10** or **Fe 11)**. These trends are contrary to those found for (-)-nicotine / (-)nornicotine and more similar to those found for (-)-cytisine / (-)-caulophylline (N-Methyl-cytisine) [230]. The enantiomeric analogues of **Fe 10** as well as of **Fe 11, Fe 23** and **Fe 24** have been synthesized in order to probe the issue of enantioselectivity that is also important for refining the concept of the nicotinic pharmacophore. The binding affinities of (-)-ferruginine analogues **Fe 10, Fe 11, Fe 23** and **Fe 24** and their correspondent enantiomeric form have been evaluated for all the subtypes under consideration. Interestingly, **Fe 10, Fe 11, Fe 23** resemble (S)(-)-nicotine **3** with respect to the enantioselectivity. Binding results listed in Tab. III/4.2 and III/4.4 reveals that the (1R,5S) enantiomers **Fe 10, Fe 11** and **Fe 23** exhibit a ca. 3 –to 12-fold higher affinity towards the α4β2* nAChRs subtypes than the corresponding (1S,5R) form. This stereodiscrimination is more or less true in regard to the different nAChRs examined. The only exception concerned the pyridazine-substituted analogue **Fe 24.** This compound interacts with the α4β2* nAChRs subtypes in a non-stereoselective manner. However, (1S,5R) *ent*-**Fe 24** exhibited a certain degree of enantioselectivity in the interaction with α3β4* nAChRs. In conclusion, the bioisosterism approach led to the discovery of novel ligands with higher affinity and improved selectivity in comparison to the lead compound (-)-ferruginine **Fe 1.**

III/5. Pinnamine variants

III/5.1. Introduction

In 2000, a novel marine alkaloid, called pinammine, was isolated from the Okinawan bivalve *Pinna Muricata*. It is characterized by a 9-azabicyclo[4.2.1]nonane moiety like anatoxin-a and a transannulated with a dihydro-4-pyrone ring (Fig. III/5.1). The absolute configuration of the four-stereogenic centres in the pyrano-anatoxinoid core was determined to be 1R, 2R, 7S, 10S [360]. A total synthesis of enantiopure pinnamine was published in 2001 [361].

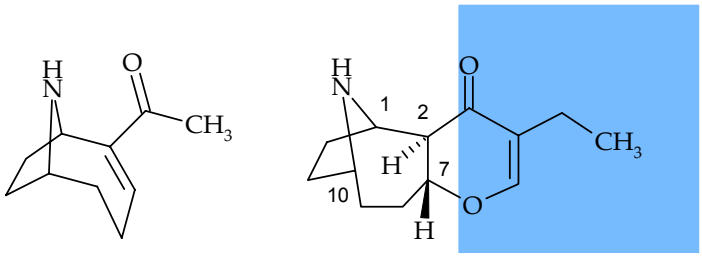

anatoxin-a An 1 **pinnamine Pin**

Figure III/5.1: Structures of anatoxin- a **An 1** and pinnamine **Pin**.

According to the Schmitt's classification scheme (see chapter I/3), pinnamine **Pin** belongs to the E-class of nAChRs ligands where both the cationic and the HBA/π (hydrogen bond acceptor π moiety) sites are placed within a fused polycyclic ring system.

III/5.2. Project

(In cooperation with Prof. Seitz, Department of Pharmaceutical Chemistry, University of Marburg: synthesis of the novel pinnamine analogues)

The structural resemblance between pinnamine **Pin** and (+)-anatoxin-a **An 1**, a potent nAChR ligand, turns this novel alkaloid into an attractive lead for the design of interesting structural analogues. Pinnamine could be considered as a conformationally restricted variant of dihydro-anatoxin-a which ring is already known as an element of the structure of alkaloids contained in the *Darlingia darlingiana* [344]. One other alkaloid isolated from this arboreal plant is the (+)-

ferruginine **Fe 1** whose unnatural enantiomer has been used as a lead compound for developing new nAChRs ligands. On the basis of the structural correlation of (+)-anatoxin-a **An 1** and (-)-ferruginine **Fe 1**, this latter alkaloid was chosen as a component of novel synthetic pinnamin derivatives. The new ligands *cis*-**Pin 1** and *trans*-**Pin 2** (Fig. III/5.2) can be regarded as a hybrid of the azabicyclic skeleton of (-)-ferruginine **Fe 1** and the dihydropyrano skeleton of pinnamine **Pin**. *Cis*-**Pin 1** and *trans*-**Pin 2** were tested for their *in vitro* affinities for α4β2* and α7* nAChR subtypes by radioligand binding assays (Fig. III/5.2).

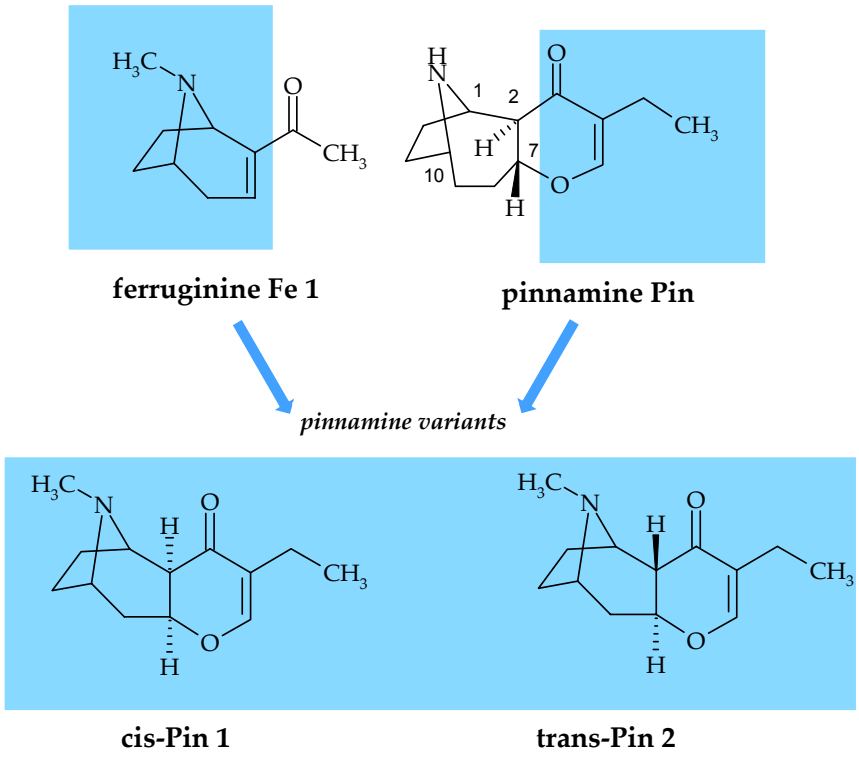

Figure III/5.2: Structures of (-)-ferruginine **Fe 1**, pinammine **Pin** and the corresponding hybrid pinammine variants *cis*-**Pin 1** and *trans*-**Pin 2.**

III/5.3. Determination of affinities and structure-activity relationships (SAR)

The results of radioligands binding studies for the two stereoisomer *cis*-**Pin 1** and *trans*-**Pin 2** are listed in Table III/5.1 Neither *cis*-**Pin 1** nor *trans*-**Pin 2** retain the affinity of the lead compound (-)-ferruginine **Fe 1** for the α4β2* nAChR. The K_i values for both pinammine variants are in the high nanomolar (K_i = 961 nM, *trans*-**Pin 2)** or low micromolar range (K_i = 4,800 nM, *cis*-**Pin 1**). Compound *cis*-**Pin 1** is devoid of

affinity at the α7* nAChRs subtype, whereas *trans*-**Pi 2** binds with significant affinity in the low micromolar range (K_i = 1,360 nM *trans*-**Pin 2**).

Table III/5.1: Radioligand binding affinities of pinnamine and its variants for α4β2*, α7*, α3β4*and $(\alpha1)_2\beta1\gamma\delta$ nAChRs.

Pinnamine variants	**No.**	**α4β2* [³H]EPI rat brain K_i (nM)**	**α7* [³H]MLA rat brain K_i (nM)**	**α3β4* [³H]EPI pig adrenals K_i (nM)**	**$(\alpha1)_2\beta1\gamma\delta$ [³H]EPI Torpedo calif. Electroplax K_i (nM)**
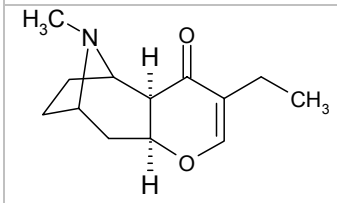	*cis*-**Pin 1**	4,800 ± 1,630	22,470 ± 680	> 50 000	> 50 000
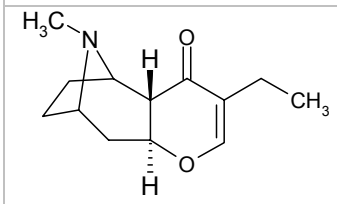	*trans*-**Pin 2**	976 ± 62	1,360 ± 675	7071 $^{n=1}$	> 50 000
n= number of experiments					

III/5.4. Discussion

The pinnamine variants, characterized by a pyranotropane skeleton have been synthesized with the aim of a more rigid template for potent nAChR ligands. Surprisingly, despite its resemblance to (+)-anatoxin-a **An 1**, (-)-ferruginine **Fe 1**, the novel compounds *cis*-**Pin 1** and *trans*-**Pin 2** only exhibited affinities in the lower micromolar range for the α4β2* and α7* nAChR subtypes. The reasons for their lack of affinities may be different. The orientation of the pharmacophoric element could be unfavourable, or maybe the ethyl moiety cannot be sterically tolerated. Therefore, it will be interesting to investigate whether the presence of a substituent smaller or larger than the ethyl moiety could increase the affinity.

III/6. Anatoxin-a as a lead compound for novel nAChR ligands

III/6.1. Introduction

The anatoxins are a group of neurotoxic alkaloids produced by a number of cyanobacterial genera including *Anabaena*, *Oscillatoria* and *Aphanizomenon* that occur naturally in freshwater [362].

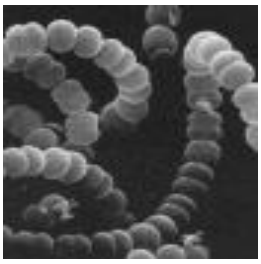

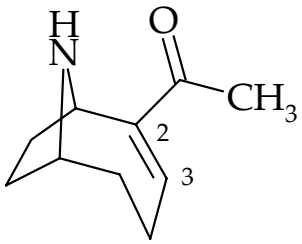

Figure III/6.1: Structure of (+)-anatoxin-a **An 1**, a toxin produced by the Anabaena flos-aquae (cyanobacteria) [363].

(+)-Anatoxin-a **An 1** is a low molecular weight alkaloid produced by the blue green alga *Anabaena flos-aquae* (Fig. III/6.1). It is commonly found as a bright green layer of stagnant water [362]. (+)-Anatoxin-a **An 1** is known as "very fast death factor", since ingestion of it can be lethal within 4 minutes (in mice, LD_{50} = 368 μg/kg intravenous, 200-250 μg/kg intraperitoneal) [362]. (+)-Anatoxin-a **An 1** exerts its action by depolarising the postsynaptic nicotinic acetylcholine receptors [364] [365]. The victim suffers from twitching, muscle spasm, paralysis and respiratory arrest. The toxic dose in humans is not known but is estimated to be less than 5 mg for an adult male [366]. Despite its poisonous nature, (+)-anatoxin-a is of interest because of its high affinity and intrinsic activity at nicotinic synapses [264] [364] [367]. (+)-Anatoxin-a **An 1** having a semirigid bicyclic structure containing a cyclic HBA/π moiety and a cyclic cationic site (Fig. III/6.1) is classified as a member of class D in Schmitt's scheme (see chapter I/3). Radioligand binding studies using [^{125}I]αBgt and tritiated perhydrohistrionicotoxin ([^{3}H]H_{12}-HTX) revealed the existence of two discrete binding sites for (+)-anatoxin-a. The radioiodinated α-Bgt **5** was used for the high affinity agonist site [365], while [^{3}H]H_{12}-HTX (known as an ion channel blocker, acting inside the channel) was used for the low affinity site, associated with the ion channel

[368]. (+)-Anatoxin-a **An 1** has a relatively low affinity for muscarinic acetylcholine receptors in rat brain [364]. On the contrary, it is a potent agonist at neuronal nAChRs, with 1000-fold selectivity for nAChRs compared to mAChRs [364] [264]. The naturally occurring (+)-anatoxin-a **An 1** binds with very high affinity to $\alpha4\beta2^*$ receptors (K_i = 1.1 nM) [228], and with minor affinity to $\alpha7^*$ receptors (K_i = 90 nM) [349]. On the basis of its semirigid bicyclic structure, limiting its possible conformations and its flexible functional group chemistry [264], (+)-anatoxin-a **An 1** is a useful lead compound. Determination of the bioactive conformation of anatoxin-a **An 1** could provide valuable information concerning the conformational requirements for binding to the receptor. Therefore, the pyrido[3,4-b]homotropane (PHT), a bioisosteric and conformationally constrained variation of (+)-anatoxin-a **An 1,** was synthesized and evaluated pharmacologically [369]. Pyrido[3,4-b]homotropane **(PHT)** (Fig. III/6.2) is a combination of (+)-anatoxin-a **An 1** and nornicotine **21**. Results from *in vitro* and *in vivo* assays have revealed that PHT retains much of the potency (IC_{50} = 2 nM) of the natural compound (+)-anatoxin-a **An 1** (IC_{50} = 5 nM) [369].

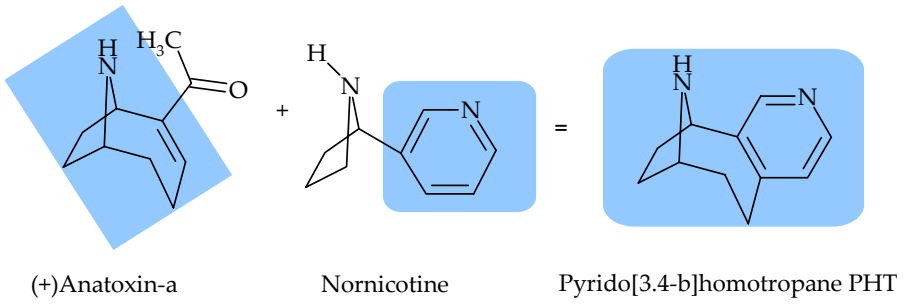

(+)Anatoxin-a Nornicotine Pyrido[3.4-b]homotropane PHT

Figure III/6.2: Structure of pyrido[3.4-b]homotropane **PHT,** a combination of (+)-anatoxina **An 1** and nornicotine **21.**

Swanson et al. [365] designed novel anatoxin-a analogues in order to evaluate the importance of hydrogen-binding strength, planarity, size and steric configuration of the chain moiety of (+)-anatoxin-a **An 1** for the binding peripheral AChRs. The structural modifications on the side chain involved three chemical categories: carbonyls, alcohols and amides (Tab. III/6.1). It has been found that steric crowding or perhaps hydrophilicity is more important than H-bonding strength for the interactions with peripheral AChRs [264]. Analogues that retain planar carbonyl moiety

and unbranched side chain structures were the more potent compound of this series for the muscular type. Therefore a limited size of the side chain might be important for the interaction with the peripheral nAChRs.

Table III/6.1: Structures of (+)-anatoxin-a and the different side chains of the corresponding anatoxin-a analogues.

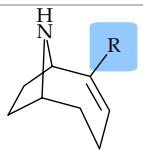

R = from R1 -to R12

R = Carbonyls	**R 1**		**R 2**		**R 3**		**R 4**	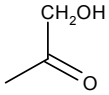
R = Alcohols	**R 5**		**R 6**		**R 7**		**R 8**	
R = Amide	**R 9**	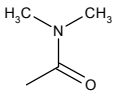	**R 10**	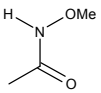	**R 11**	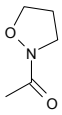	**R 12**	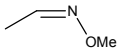

In 1991, Wonnacott et al. [264] considered the interactions of the same analogues with neuronal nicotinic AChRs, α4β2* and α7*, identified by (-)-[^{3}H]nicotine and [^{125}I]α-Bgt, respectively. They found that the isoxazolidide acid **(R 11)** and methoxyamide acid **(R 10)** derivatives were the most potent substances for the interaction with nicotinic receptors in the brain. Moreover, compounds **(R 11)** and **(R 10)** present selectivity for α7* over α4β2* (1111-fold for **(R 11)** and 756-fold for **(R 10))** [264]. Modification of the side chain with hydrophobic moieties (ethyl or methoxy group) maintains the affinity for the α4β2* nAChRs receptor, whereas substitution with a more polar function elicits severe reduction of the affinity for α4β2* nAChR [264]. Reduction of a carbonyl to an alcoholic group caused a drastic decrease of the binding affinities for α4β2* and α7* nAChRs (Ki = 4600 and > 10 µM, respectively) [264,370]. In the search for a novel analogue with enhanced affinity and selectivity for α4β2* nAChR over the α3β4*, the novel ligand **UB-165** was designed (Fig. III/6.3) [229]. It represents a novel (+)-anatoxin-a **An 1** /(±)-epibatidine **13** hybrid in which the bulky

azabicyclo[4.2.1]nonene moiety of (+)-anatoxin-a **An 1** is combined with the chloropyridyl pharmacophoric element (HBA component of (±)-epibatidine **13** [371]). Interestingly, in contrast to (±)-epibatidine **13**, **UB-165** interacts in a stereoselective manner with the receptors [229]. Its enantioselectivity is associated with the azabicyclo[4.2.1]nonene moiety of (+)-anatoxin-a **An 1.** Sharples et al. measured the affinities of UB-165, (±)-epibatidine **13**, and (+)-anatoxin-a **An 1** for radioligand binding sites corresponding to various nAChRs subtypes using (-)-[^{3}H]nicotine and [^{125}I]α-Bgt in native and recombinant membrane preparations, **UB-165** was identified as a potent nicotinic ligand. In competition assays with (-)-[^{3}H]nicotine using rat brain membranes it showed a binding affinity for the α4β2* nAChR (K_i = 0.27 nM) that was intermediate between (±)-epibatidine **13** (K_i = 0.021 nM) and (+)-anatoxin-a **An 1** (K_i = 1.25 nM) [371]. Comparable K_i values were found for the inhibition of (±)-[^{3}H]epibatidine binding to α4β2* nAChR in M10 cells. In competition assays with [^{125}I]α-Bgt in rat brain membrane preparations, **UB-165** (K_i = 2790 nM) showed a slightly lower potency than anatoxin-a (K_i = 1840 nM). Results from competition binding assays with (±)-[^{3}H]epibatidine at the human α-3 containing nAChRs subtypes showed that the rank order of potency was similar to that established for the α4β2* nAChR, namely (±)-epibatidine **13** > **UB-165** > (+)-anatoxin-a **An 1**. In contrast, **UB-165** was less potent at α7* and muscle nAChRs. The rank order of potency is: (±)-epibatidine **13** > (+)-anatoxin-a **An 1** > **UB-165**. Therefore, the (±)-**UB-165** resembles (±)-epibatidine **13** in its preference for α4β2* nAChR compared with the α7* and muscle nAChR. They also characterized this compound functionally for different nAChRs subtypes [371]. Functional studies demonstrated that **UB-165** is a full agonist at α3β2* nAChRs but only a weak partial agonist at α4β2* nAChRs. In fact, it failed to elicit significant currents in Xenopus oocytes expressing α4β2* or α2β2* nAChRs and produced very little response when tested in the [^{3}H]dopamine release assays. On the contrary, it was more potent than (+)-anatoxin-a **An 1** in activation of Ca^{2+} fluxes in the SH-SY5Y cell line expressing the α3 nAChR subunit [371]. In a later publication by Slater et al., the structure of **UB-165** was the subject of structure-

activity-relationship studies with pyridyl-analogues and with a series of diazines variants, having been prepared and evaluated [357].

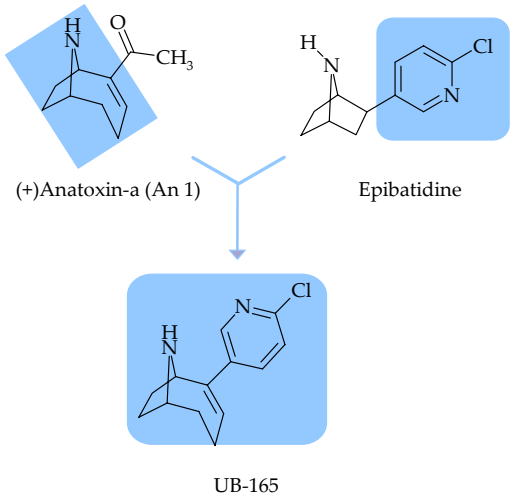

Figure III/6.3: Structure of **UB-165**, a hybrid molecule composed of the azabicyclo[4.2.1]nonene moiety of (+)-anatoxin-a **An 1** and the chloropyridyl unit of (±)-epibatidine **13** [371].

III/6.2. Project

(In cooperation with Prof. Seitz, Department of Pharmaceutical Chemistry, University of Marburg, synthesis of the novel anatoxin-a analogues)

The azabicyclo[4.2.1]nonene ring of (+)-anatoxin-a **An 1** was used as a lead structure to develop novel potent ligands on the basis of its semirigid structure which limits the number of stable conformations and its accessibility to structural modifications. The aim of the project was to investigate whether the replacement of the acetyl moiety of (+)-anatoxin-a **An 1** by pyridine (giving the deschloro analogue **DUB-65**) or diazine rings, such as pyrazine, pyrimidine and pyridazine could give novel potent ligands with the ability to discriminate further between nAChR subtypes. A schema of the structural variations is shown in Fig. III/6.4.

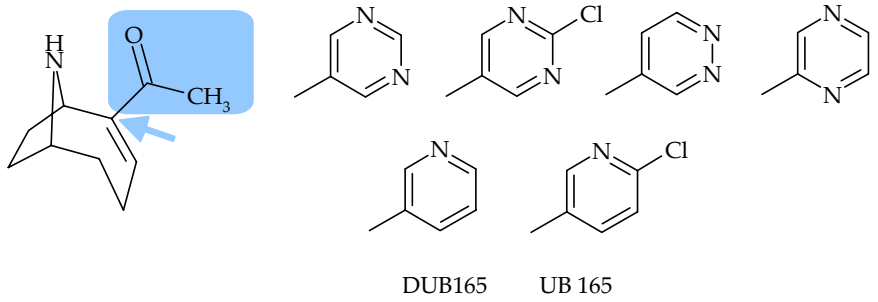

DUB165 UB 165

Figure III/6.4: Structural variations of (+)-anatoxin-a **An 1.**

On the basis of the high affinities for the neuronal nAChRs of (±)-epibatidine **13**, characterized by a 7-azabicyclo[2.2.1]heptane, and (+)-anatoxin-a **An 1**, with an azabicyclo[4.2.1]nonene ring, great interest has been shown for analogues having an azabicyclic core. Barlocco et al. reported the synthesis and the pharmacological characterization of a novel class of 3,8 disubstituted 3,8-diazabicyclo[3.2.1]octane analogue [224]. Among them, the 3-(6-chloro-3-pyridazinyl)3,8-diazabicyclo[2.2.1]octane (Fig. III/6.5), showed a nanomolar affinity for $\alpha 4\beta 2^*$ nAChRs (K_i = 4.1 ± 0.21 nM) and retained antinociceptive properties at doses of 1 mg/Kg in mouse hot plate test [224].

3-(6-chloro-3-pyridizanyl)3,8-diazabicyclo[2.2.1]octane epibatidine 13

Figure III/6.5: Structures of 3-(6-chloro-3-pyridazinyl)3,8-diazabicyclo[2.2.1]octane and (±)-epibatidine **13.**

Following the bioisosterical approach, a series of enantiopure 3,9-diazabicyclo[4.2.1]nonane derivatives were synthesized as potential analogues of the nicotinic agonist (+)-anatoxin-a **An 1** (Fig. III/6.6). These novel ligands are structurally related to (+)-anatoxin-a **An 1** in that they both incorporate an azabicyclic core. However, they show some modifications concerning the bulky azabicyclo[4.2.1]nonene moiety of anatoxin-a such as:

1. Saturation of the bicyclic ring.

2. Additional nitrogen in position C-3.
3. Methylation of the sp^3 nitrogen.

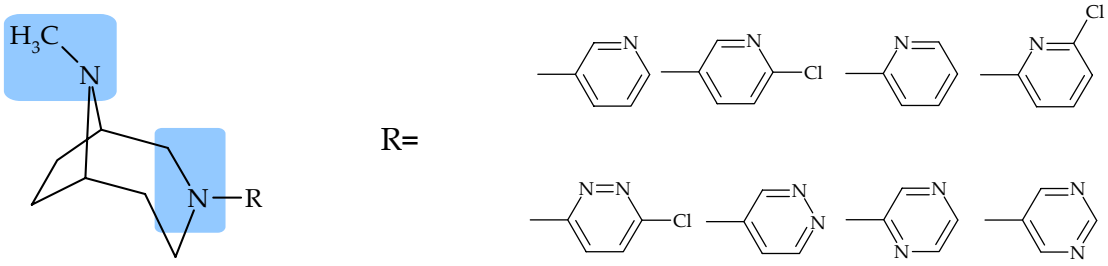

Figure III/6.6: Different substituents introduced at position N-3 on the bulky 3,9-diazabicyclo[4.2.1]nonane moiety.

The enantiopure 3,9-diazabicyclo[4.2.1]nonane derivatives are classified according to Schmitt's classification, as class-C compounds (see chapter I/3). They are characterized by the requisite pharmacophoric elements typical of nAChR ligands, namely the N-bicycle and the HBA–π system within separate non-fused rings. A pivot bond joins the two pharmacophoric elements. In this series, further modifications of the lead compound e.g. introduction of pyridine, chloro-pyridine and diazines group at position C-3 of the more flexible 3,9-diazabicyclo[4.2.1]nonane ring (Fig. III/6.6) have been performed. *In vitro* radioligand binding assays were carried out with the aim of exploiting the scope and potential offered by the resulting ligands in the CNS and peripheral nervous system. The binding affinities and selectivity among different nAChRs were measured in four different competition assays for the α4β2*, α7*, α3β4* and the muscle type nAChRs.

III/6.3. Determination of affinities and structure-activity relationships (SAR) UB-165 and DUB-165

To assess the issue of binding selectivity among nAChR subtypes, affinities of the chloro-pyridine/pyridine analogues, UB-165 and DUB-165 and diazine analogues **An 2, An 3, An 4** and **An 5** listed in Tab. III/6.2, were measured in four different competition assays and compared with those of (±)-epibatidine **13** and (+)-anatoxin-a **An 1**. (+)-Anatoxin-a **An 1** binding affinities for α4β2* and α7* nAChR subtypes, using (±)-[^{3}H]epibatidine and [^{3}H]MLA and P2 membrane fractions of Sprague-Dawley rat forebrain, were evaluated in previously described competition assays [349]. Compared to (±)-epibatidine **13**, (+)-anatoxin-a exhibited ca. 140-fold lower affinity for α4β2* (K_i = 1.1 nM) and approximately 20-fold lower affinity for α7* (K_i = 90 nM). In the present study, the affinity of (+)-anatoxin-a **An 1** for nAChRs containing α3 and β4 subunits has been estimated to be in the nanomolar range (K_i = 19 nM), 45-fold lower than (±)-epibatidine **13** (Tab. III/6.2). Remarkably, **UB-165** and **DUB-165** potently interact with all three nAChRs subtypes under consideration with comparable high affinities, demonstrating that the electron-withdrawing chlorine atom of **UB-165** has only little effect on binding affinity. The replacement of the acetyl moiety by a pyridine heterocycle **(DUB-195)** increased the affinity for α7* nAChR by a factor of 94. Compared to (+)-anatoxin-a **An 1** and **UB-165**, **DUB-165** exhibits the highest affinity for the α7* nAChR subtype (K_i = 0.95 nM). This affinity enhancement can be caused by the loss of the halogen atom. On the contrary, the presence of the halogen in the pyridyl ring of **UB-165** seems to be favourable for the affinity to the α3β4* subtype (K_i = 1.3 nM). **UB-165** is more selective for α4β2* nAChRs over α7* nAChRs than (+)-anatoxin-a **An 1** and **DUB-165**.

Diazine analogues

The bioisosteric replacement of the acetyl moiety as a structural part of (+)-anatoxin-a **An 1** by a 4-pyridazinyl **(An 4)**, 5-pyrimidinyl **(An 2)**, 3-chloro-5-pyrimidinyl **(An 3)**, or 2-pyrazinyl **(An 5)** pharmacophoric element led to anatoxinoids (Tab. III/6.2) that interact with all four nAChRs subtypes under consideration**.** In this series, analogue **An 2**, having a 5-pyrimidinyl moiety, turned out to be the most active ligand for the α4β2* nAChR (K_i = 0.14 nM). For this subtype, **An 2** showed an affinity similar to that of the chloro-pyrimidinyl analogue **An 3** (K_i = 0.15 nM). Thus, replacement of the acetyl moiety by a pyrimidine or chloro-pyrimidine moiety (**An 2** and **An 3**) leads to compounds that are ca. 8-fold more active than (+)-anatoxin-a **An 1** and slightly less potent (2.7- and 3.5-fold) for the α4β2* nAChR compared to **DUB-165** and **UB-165**, respectively. The introduction of a pyridazinyl moiety **(An 4),** resulted in being deleterious for the affinity for the α4β2* nAChR, causing a significant drop by a factor of ca. 370 (K_i = 19 nM) compared to **DUB-165** and a factor of ca. 475 compared to **UB-165**. A similar decrease in affinity was observed for the pyrazine analogue **An 5**, with a K_i value of 12 nM for the α4β2* nAChR. Summing up, the rank order of potency towards α4β2* nAChR for the diazine derivatives of anatoxin-a is: pyrimidine > pyridazine > pyrazine. This affinity profile was observed for analogues **An 2**, **An 4** and **An 5** and is found to be the same for α3β4* and α7* nAChRs. In fact, the analogue **An 4**, having the pyrazine moiety, possesses the lowest binding affinity for α4β2*, α7* and α3β4* nAChRs.

Table III/6.2: Radioligand binding affinities of (+)-anatoxin-a **An 1**, **UB-165**, **DUB-165** and diazine analogues for α4β2*, α7*, α3β4*and $(\alpha 1)_2\beta 1\gamma\delta$ nAChRs.

Structure	No.	α4β2* [³H]EPI rat brain K_i (nM)	α7* [³H]MLA rat brain K_i (nM)	α3β4* [³H]EPI pig adrenals K_i (nM)	$(\alpha 1)_2\beta 1\gamma\delta$ [³H]EPI Torpedo calif. electroplax K_i (nM)
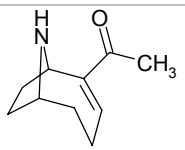	**An 1**	1.1 ± 0.2	90 ± 4	19 ± 1	n.d.
Pyridine analogues					
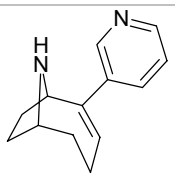	**DUB-165**	0.051 ± 0.0006	0.95 ± 0.05	6.2 ± 0.5	>50,000
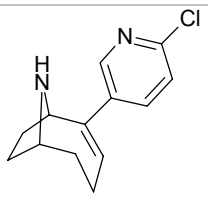	**UB-165**	0.04 ± 0.004	12 ± 2.5	1.3 ± 0.1	>50,000
Diazine analogues					
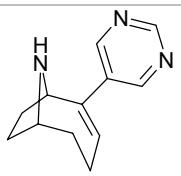	**An 2**	0.14 ± 0.03	10.7± 1.3	20 ± 1	n.d.
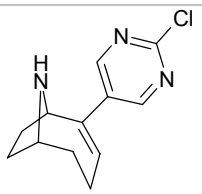	**An 3**	0.151 ± 0.02	n.d.	n.d.	n.d.
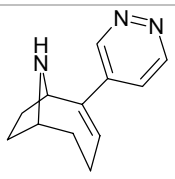	**An 4**	19 ± 2.5	> 10 000	2 500 ± 150	n.d.
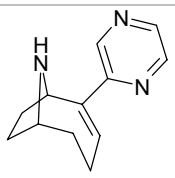	**An 5**	12 ± 1.8	250 ± 7.6	259 ± 21	n.d.
n.d.= not determined					

3,9-Diazabicyclo[4.2.1]nonane-diazine-derivatives

*Structure activity relationshisp for α4β2*nAChRs:*

Among the pyridine derivatives tested, **An 8** (pyridine analogue) exhibited the most potent binding affinity for α4β2* nAChRs (K_i = 0.62 nM). The **An 8** was found to be more potent than (+)-anatoxin-a **An 1** (K_i = 1.1 nM). The structural isomer 9-ethyl-3-(2-pyridine)-3,9-diazabicyclo[4.2.1]nonane, **An 6** (K_i = 2.09 nM) was 3-fold less potent than the **An 8** (K_i = 0.62 nM) analogue for the binding at α4β2* nAChRs. The affinity drop-off could be attributed to a different distance between the bicyclic nitrogen atom and the heterocyclic nitrogen atom, which is considered important for the binding affinity [259]. The chlorine analogue of **An 6 (An 7)** as well as of **An 8 (An 9)** are almost equipotent for their binding affinity for α4β2* nAChRs (ca. 2-fold difference in affinity) corroborating the finding that a chlorine atom has only little effect on binding affinity. Except for **An 13**, (a pyrazine analog, Fig. III/6.7), the introduction of another diazine moiety can enhance the affinity for α4β2* nAChRs in comparison to (+)-anatoxin-a **An 1**. Analogues **An 10** and **An 11**, with a pyridazine and chloropyridazine moiety respectively, showed affinities in the picomolar range (K_i = 0.55 and 0.52 nM, respectively), thus emerging as the most potent derivatives of this series. The introduction of pyrimidine led to analogue **An 12** (K_i = 2.8 nM) which retained almost the same affinity of the pyridine analogue **An 6** (K_i = 2.09 nM) for the α4β2* nAChR subtype.

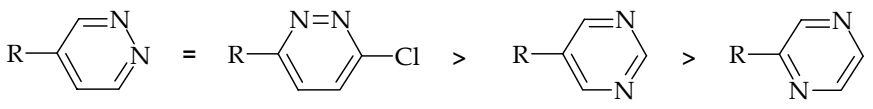

Figure III/6.7: The affinity rank order for α4β2* nAChRs of the diazine analogues in the 3,9-diazabicyclo[4.2.1]nonene series.

Structure activity relationships for α7 nAChRs:*

The affinities of the enantiopure 3,9-diazabicyclo[4.2.1]nonane derivatives for α7* nAChRs, with the exception of **An 13** (K_i > 50,000 nM), are in the higher nanomolar range, between 90 and 900 nM (Tab. III/6.3). The analogue **An 7** with a 6-chloro-3-pyridine moiety exhibited the highest affinity for α7* (K_i = 92 nM). Interestingly, the introduction of the chlorine atom in position C-6 on the pyridine ring leads to an increase in affinity by a factor of 100 compared to the deschloro analogue **An 6** (K_i = 950 nM). The diazine derivatives, **An 10** and **An 11**, even though less potent than **An 7,** possess an affinity for α7* nAChR (K_i = 190 and 157 nM, respectively) that is about 2-fold lower to the one shown by (+)-anatoxin-a **An 1** (K_i = 90 nM). The pyrimidine analogue, **An 12** (K_i = 982 nM), as already observed for the affinity for α4β2*, possesses a very similar K_i value to the pyridine analogue **An 6** (K_i = 950 nM).

Table III/6.3: Radioligand binding affinities of 3,9-diazabicyclo[4.2.1]nonane derivatives for α4β2*, α7*, α3β4*and $(\alpha1)_2\beta1\gamma\delta$ nAChRs.

Pyridine and Diazine analogues of 3,9-diazabicyclo[4.2.1]nonane					
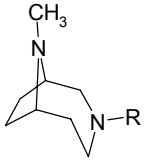					
R	**No.**	**α4β2* [^{3}H]EPI rat brain K_i (nM)**	**α7* [^{3}H]MLA rat brain K_i (nM)**	**α3β4* [^{3}H]EPI pig adrenals K_i (nM)**	**$(\alpha1)_2\beta1\gamma\delta$ [^{3}H]EPI Torpedo calif. electroplax K_i (nM)**
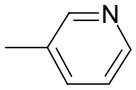	**An 6**	2.09 ± 0.43	950 ± 134	81.4 ± 0.70	11,900 ± 3.9
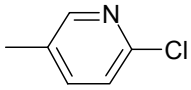	**An 7**	0.873 $^{n=1}$	92.1± 13	30.6± 1.13	2,326 $^{n=1}$
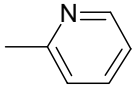	**An 8**	0.62 ± 0.15	138± 8.2	23 $^{n=1}$	3,050 ± 0.55
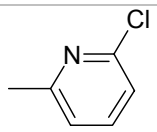	**An 9**	1.4 ± 0.07	486 ± 11.9	42.8 ± 4.6	8,467 ± 338
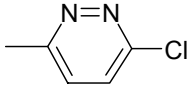	**An 10**	0.55 ± 0.15	190 ± 17	30± 0.5	2,540 ± 0.7
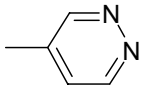	**An 11**	0.52 ± 0.11	157 ± 10	9.5 ± 2	2,330 ± 0.44
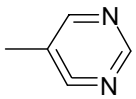	**An 12**	2.08 ± 0.14	982 ± 0.08	156 ± 7.1	15,480 ± 2.5
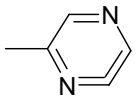	**An 13**	265 $^{n=1}$	> 50 000	> 50 000	> 50000
n= number of experiments					

Structure activity relationships for α3β4 and $(\alpha 1)_2\beta 1\gamma\delta$ nAChRs:*

Compound **An 11**, containing a pyridazinyl moiety, exhibited the highest affinity for the α3β4* nAChRs (K_i = 9.5 nM), even higher than (+)-anatoxin-a **An1** (K_i = 19 nM). The analogues **An 7, An 8, An 9** and **An 10** possess similar affinities for the α3β4* nAChR, with K_i values ranging from 23 to 40 nM (Tab. III/6.3). Analogue **An 12** possesses the lowest affinity for α3β4* nAChRs with a K_i value of 157 nM, namely 8-fold less potent than (+)-anatoxin-a **An 1** (K_i = 90nM). The highest affinity for the muscle type was found for the analogues containing a pyridazinyl (**An 11;** K_i= 2,330 nM) and chloropyridine moiety (**An 7;** K_i= 2,326 nM) (Tab. III/6.3). Pyridine and pyrimidine carrying derivatives **An 6** and **An 12,** showed a drastic drop in affinity for the $(\alpha 1)_2\beta 1\gamma\delta$ nAChR subtype with a K_i value in the higher micromolar range (K_i = 11,900 and 15,480 nM, respectively). Analogue **An 13** did not interact with either α3β4* nor with $(\alpha 1)_2\beta 1\gamma\delta$ nAChRs (K_i > 50,000 nM).

III/6.4. Discussion

The alkaloid (+)-anatoxin-a **An 1** is known as a potent but not selective modulator of nAChRs. Unfortunately, based on its poor ability to discriminate between neuronal and peripheral nAChRs and its toxic effects, this ligand can not be used therapeutically. It was anticipated that bioisosteric analogues might possess less toxicity resulting from higher discrimination between the multifarious receptor subtypes. (+)-Anatoxin-a **An 1** possesses a semirigid skeleton, which limits the number of low-energy conformations and a side chain readily amenable to structural modifications. Based on these characteristics, it has been chosen as a useful lead compound for the design of potent novel ligands and for structure activity relationship studies on nAChRs. In the present study, the influence on the binding affinity of the replacement of the acetyl group by a pyridine or chloropyridine fragment and by N-heterocycles (pyridine, pyridazinyl, pyrimidinyl or pyrazinyl moieties) was investigated. The affinities of **UB-165**, an already known nAChR ligand [357], and its deschloro analogue were evaluated for four different subtypes. The K_i values found reveal that both analogues potently interact with the $\alpha4\beta2^*$ with comparable affinities. The rank orders of potency is: (±)-epibatidine **13** > (+)-anatoxin-a **An 1** > **UB-165** = **DUB-165**. These results confirm that the chlorine atom has only small influence on the binding potency at the $\alpha4\beta2^*$ nAChR subtype. Relative to $\alpha4\beta2^*$, **UB-165** has a 300- and 32-fold difference in potency at the $\alpha7^*$ and $\alpha3\beta4^*$ nAChRs. Therefore, **UB-165** turned out to be the most selective compound for $\alpha4\beta2^*$ nAChRs over $\alpha7^*$ nAChRs (1:300). The replacement of the acetyl moiety by pyridine, given **DUB-165**, increases by 94-fold the affinity for the $\alpha7^*$ nAChR (K_i = 0.95 nM). In addition, **DUB-165** possesses an improved selectivity for $\alpha4\beta2^*$ nAChRs over $\alpha3\beta4^*$ nAChRs (1:124). In a later study by Sharples et al. [357], binding studies showed the same rank order of potency for binding to $\alpha4\beta2^*$: (±)-epibatidine > (+)-anatoxin-a > **UB-165** = **DUB-165** and for $\alpha7^*$: (±)-epibatidine > **DUB-165** > **UB-165** > (+)-anatoxin-a in competiton assays. However, the K_i values that they found for the $\alpha7^*$ nAChRs

subtypes are very high. This discrepancy in values is possibly being attributed to the different amount of protein used in their assays.

In order to investigate whether a bioisosteric replacement of the acetyl moiety of (+)-anatoxin-a **An 1** by diazines can be favourable for binding to each nAChR subtypes, the diazine analogues **An 2**, **An 3, An 4** and **An 5** were synthesized and evaluated in competition binding assays. The main finding of SAR studies performed on this series was that the pyrimidine **An 2** and chloro-pyrimidine **An 3** moiety are the most appropriates substituents at the azabicyclic core of (+)-anatoxin-a **An 1**. Indeed, they showed an affinity for the α4β2* nAChRs in the picomolar range (K_i = 0.14 nM **An 2** and 0.15 nM **An 3**). Based on these data, it was pointed out that the electron-withdrawing chloro atom of ligand **An 3** has no effect on the binding affinity for α4β2* nAChRs. The same trend was observed for **UB-165** and **DUB-165**. As compared to the lead compound, analogue **An 2** has a 7.8- and 9-fold higher affinity for α4β2* and α7* nAChRs. In addition, the pyrimidine moiety seems to increase the selectivity for α4β2* given that, relative to α4β2* nAChRs, **An 2** has a 142-fold difference in potency at the α3β4* nAChRs. On the contrary, the introduction of a pyrazine or pyridazine moiety, decreases the binding affinity for all subtypes examined. This affinity profile closely agrees with the data published in 2002 by Sharples et al. [357]. They described the synthesis of two classes of **UB-165** analogues. One class includes positional isomers of the pyridyl moiety and the other one consists of selective diazines variants [357]. For the diazine variants, they reported similar binding profiles for α4β2* and α7* nAChRs. They carried out competition studies using α3β4 nAChR stably expressed in Lα3β4* cell line and (±)-[^{3}H]epibatidine. According to our assessment, they observed that the presence of an additional nitrogen atom produces a more π-electron deficient aromatic ring, and this exerts a significant effect on the pKa of the nitrogen atom representing the hydrogen bond acceptor associated with the ligand-receptor interaction. Thus underlining that the high affinity binding of these analogues is significantly dependent on the HBA ability of the nitrogen in the pyridyl and diazine rings [357].

Following the idea that bioisosteric alterations in the azabyclic core might generate ligands that are subtype selective with a minimum of side effects, a novel series of diazabicyclo[4.2.1]nonane analogues were synthesized. They are structurally related to (+)-anatoxin-a **An 1**, with some modification concerning the saturation of the azabicyclic core, the introduction of an additional nitrogen in position C-3 and methylation of the sp^3 nitrogen. On the basis of the SAR, it turned out that, with the exception of the pyridazine analogue **An 13**, all new ligands **An 6-An 12** retained affinity for $\alpha4\beta2^*$, $\alpha7^*$, $\alpha3\beta4^*$ and muscle type nAChRs. Recently, in a study of Sharples et al. [357] is has been found that the 2-pyridyl analogue of **UB-165**, with a reduced distance between the cationic nitrogen and pyridyl nitrogen, had a deleterious effect in binding affinity at $\alpha4\beta2^*$. The same effect was observed with the 2-pyridyl analogue of **DUB-165**, wich showed a 3581-fold lower potency at the $\alpha4\beta2^*$ than the 3-pyridyl analogue**.** Analogues **An 6** and **An 8** (Fig. III/6.8) have been characterized in *in vitro* binding experiments in order to explore the effect of translocation of the pyridyl nitrogen which is proposed to act as a hydrogen bond acceptor in pharmacophore models.

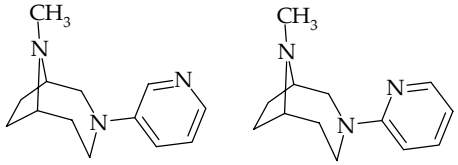

An 6 An 8

Figure III/6.8: Structures of the diazabicyclo[4.2.1]nonane analogues **An 6** and **An 8.**

In the present study, both the 2- and 3-pyridyl moiety are suitable moieties for high affinity binding at the $\alpha4\beta2^*$ nAChRs (K_i values ranging between 0.62 to 2.09 nM). On the contrary, results of binding studies performed at $\alpha7^*$ nAChRs have shown that they possess only moderate affinity for these neuronal nAChR subtypes. Hence showing that this novel series of diazabicyclo[4.2.1]nonane analogues exhibited a certain degree of preference for the $\alpha4\beta2^*$ compared to the $\alpha7^*$ nAChRs. Interestingly, they also showed a modest affinity in the low micromolar range for the muscle nAChR.

III/7. Quinuclidin-2-ene based derivatives as ligands for nicotinic acetylcholine receptors

III/7.1. Introduction

The semirigid ring of the quinuclidine moiety has been extensively used to design novel muscarinic receptors ligands. One of the most potent and efficacious ligand within the series of the 3-heteroaryl-substituted quinuclidin-3-ol was the 1,2,4-oxadiazole analogue **n 1.** It has been observed that the introduction of a double bond between C-2 and C-3 in the quinuclidine ring **n 1,** affording a quinuclidin-2-ene derivative **n 2**, was detrimental (444-fold) for the efficacy and affinity for muscarinic receptors [373].

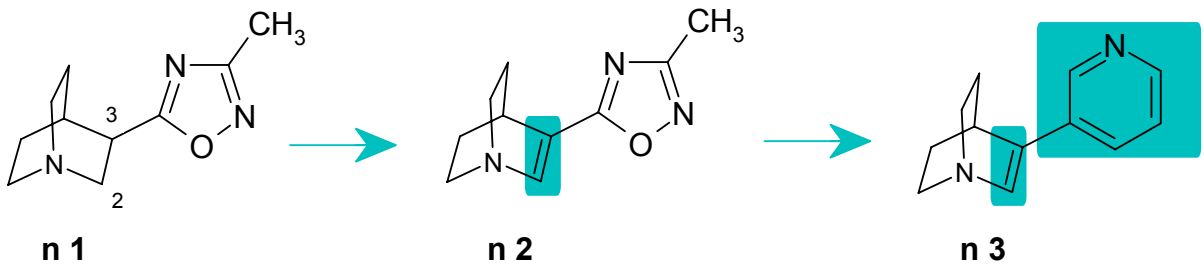

Figure 7.1: Structures of the muscarinic agents **n 1, n 2, n 3**

Bioisosteric replacement of the 1,2,4-oxadiazole moieties by a pyridine ring **n 3** proved to be unfavourable for the affinity to muscarinic receptors [202]. The evident structural correlation of **n 3** to the highly potent semirigid nAChRs agonist (±)-epibatidine **13** and **UB-165** gave rise to investigate compounds of type **n 3** as novel nicotinic nAChRs ligands (Fig. III/7.1).

III/7.2. Project

(In cooperation with Prof. Seitz, Department of Pharmaceutical Chemistry, University of Marburg, synthesis of the novel quinuclidine analogues)

Based on the obvious similarity of the pyridine derivative of the quinuclid-2-ene with the structure of (±)-epibatidine **13** and **UB-165**, other quinuclid-2-ene analogues containing the 2-choropyridine and a pyrimidine moiety have been synthesised (Fig. III/7.2).

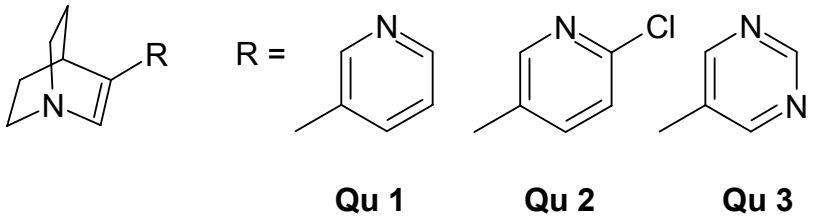

Figure III/7.2: Structure of the novel ligands **Qu 1, Qu 2, Qu 3.** One pharmacophoric element is represented by a quinuclidin-2-ene moiety.

The quinuclidine analogues **Qu 1**, **Qu 2** and **Qu 3** were evaluated for their ability to compete for (±)-[^{3}H]epibatidine and [^{3}H]MLA binding sites in membrane fraction of rat forebrain (α4β2*, α7*), pig adrenals (α3β4*) and *Torpedo californica* electroplax ($(\alpha1)_2\beta1\gamma\delta$) using radioligand binding assays.

III/7.3. Determination of affinities and structure-activity relationships (SAR)

Results of radioligand binding assays demonstrated that a quinuclidin-2-ene skeleton, substituted in position C-3 by a pyridine moiety, could be considered as a suitable nicotinic ligand. The novel analogues **Qu 1, Qu 2** and **Qu 3** showed affinity in the low nanomolar range for neuronal and peripheral nAChRs and a subtype selectivity for α4β2*. The chloropyridine containing ligand **Qu 2** turned out to be the most active analogue for α4β2*, α7*, α3β4* and muscle nAChRs. The chlorine atom seems to produce a positive effect on the binding affinities of this series for nAChRs under investigation. Indeed, the chloropyridine analogue **Qu 2** has ca. 4-fold higher affinity for α4β2* compared to the pyridine analogue **Qu 1.** The pyrimidine derivative **Qu 3,** although 5-fold less potent than **Qu 2** for α4β2* (K_i = 12.2 nM) shows the highest subtype selectivity for α4β2* over α7* and α3β4* nAChRs.

Table III/7.1: Radioligand binding affinities of quinuclidin-2-ene based ligands for α4β2*, α7*, α3β4*and $(\alpha1)_2\beta1\gamma\delta$ nAChRs.

Structure	No.	α4β2* [^{3}H]EPI rat brain K_i (nM)	α7* [^{3}H]MLA rat brain K_i (nM)	α3β4* [^{3}H]EPI pig adrenals K_i (nM)	$(\alpha1)_2\beta1\gamma\delta$ [^{3}H]EPI Torpedo calif. electroplax K_i (nM)
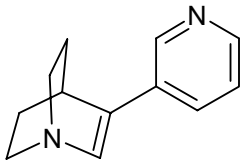	**Qu 1**	7.5 ± 0.49	85.2 ± 2.7	103 ± 13	237 ± 12
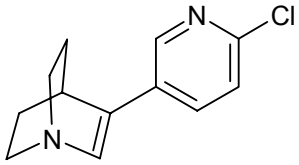	**Qu 2**	2.2 ± 0.52	26.8 ± 4.1	19.2 ± 1.1[a]	49 [n=1]
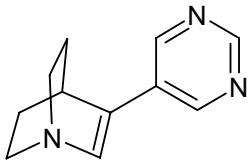	**Qu 3**	12.2 ± 0.18	751 ± 52.3	112 ± 41	100 [n=1]
n= number of experiments					

III/7.4. Discussion

In previous studies [373] [282], the quinuclidine nucleus was used as a template to design ligands for the muscarinic acetylcholine receptor. However, the introduction of a pyridine moiety in position C-3 of a quinuclidin-2-ene skeleton proved to be detrimental to the affinity to muscarinic receptors. On the contrary, this modification leads to a pyridine analogue **Qu 1** with nanomolar affinities for the α4β2* (K_i = 7.5 nM) and α7* nAChR (K_i = 85.2 nM) and subtype selectivity for α4β2*. The quinuclidin-2-ene skeleton substituted with a pyridine ring possesses all the structural elements required in order to be a potent nicotinic agonist. Indeed, it has basic nitrogen, which can be protonated to provide a cationic centre and π-HBA system. Novel analogues have been synthesized bearing a choropyridine and pyrimidine moiety. The analogue **Qu 2** with the 2-chloropyridine moiety is the most potent ligand for all subtypes under consideration. It also showed subtype selectivity for α4β2* over α7* and α3β4* nAChRs. The pyrimidine derivative **Qu 3** showed

similar affinity to **Qu 1** and **Qu 2** for the α4β2* and α3β4* but it has a lower affinity for the α7* nAChR (K_i = 751 nM). Therefore, **Qu 3** showed the highest subtype selectivity for α4β2* over α7* and α3β4* nAChRs.

III/8. Choline analogues as ligands for nicotinic acetylcholine receptors

III/8.1. Introduction

Choline **4** (2-hydroxyethyltrimethylammonium) is a metabolic product of ACh hydrolysis by cholinesterases (Fig. III/8.1). It is taken back into the cholinergic terminals by a high affinity transporter and then reused in transmitter synthesis.

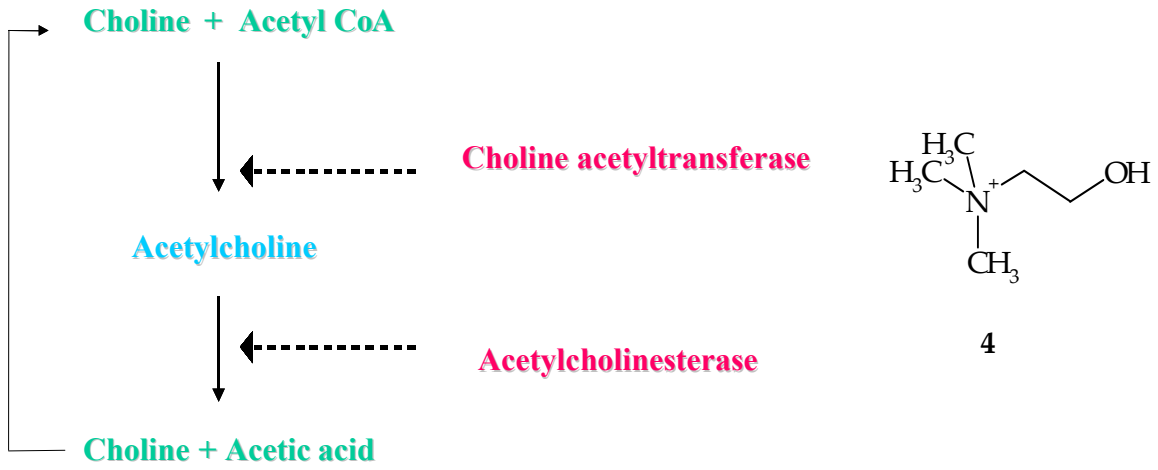

Figure III/8.1: Metabolism of choline **4**. Structure of choline **4.**

Choline **4** is a physiological component of the cerebral spinal fluid (CSF) and is important for the structural integrity of the membrane. It plays a key role in lipid and cholesterol transportation [171]. The choline **4** concentration in the brain is ca. 10 μM but it increases up to 100 μM in a number of pathophysiological conditions due to an abnormal phospolipid metabolism occurring in chronic degenerative disorders, like Alzheimer's disease [375]. Choline **4** is also an important component in the human diet and therefore the Food and Drug Administration (FDA) Modernization Act, [376], recognized it as essential in 2001. A supplementation of choline **4** in adult diet has been shown to have benefits in both verbal and visual memory [377]. Choline **4** crosses the blood brain barrier (BBB) via a specific carrier [375] that has also been thought to play a significant role in the brain's uptake of choline derivatives [378] (Fig. III/8.2).

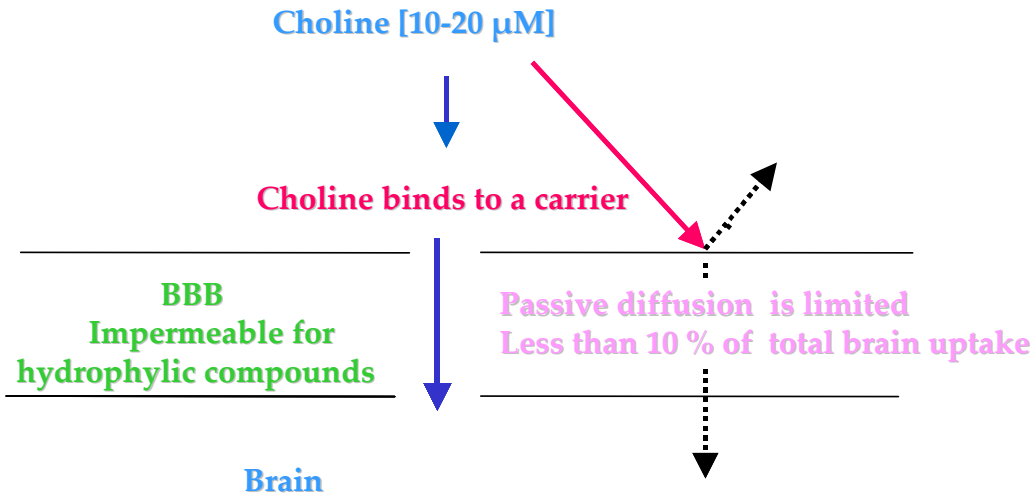

Figure III/8.2: Choline carrier: the transport mechanism from plasma to brain.

Choline **4** has been shown to be a full and highly selective, but not potent, agonist at the α7* subtype of the nicotinic acetylcholine receptors in neurons cultured from rat hippocampus, olfactory bulb and thalamus as well as in PC12 cells [171,284]. In functional assays, choline **4** acts as a partial agonist at α3β4-containing nAChRs in PC12 cells and does not activate α4β2 nAChRs on hippocampal neurons [284]. Choline **4**, like (-)-nicotine **3**, has been shown to protect neural cells from cytotoxicity induced by growth factor deprivation [379]. Unfortunately, the mechanism for the cytoprotective effect has not been fully elucidated [380]. The structure of choline (2-hydroxyethyltrimethylammonium) (Fig. III/8.3) **4** can be found in a multiplicity of substances with different pharmacological effects, e.g. in drugs with antihistaminic and analgesic effects, like diphenhydramine **37** and nefopam **38**, which display affinities in the micromolar range for neuronal nicotinic AChRs [374].

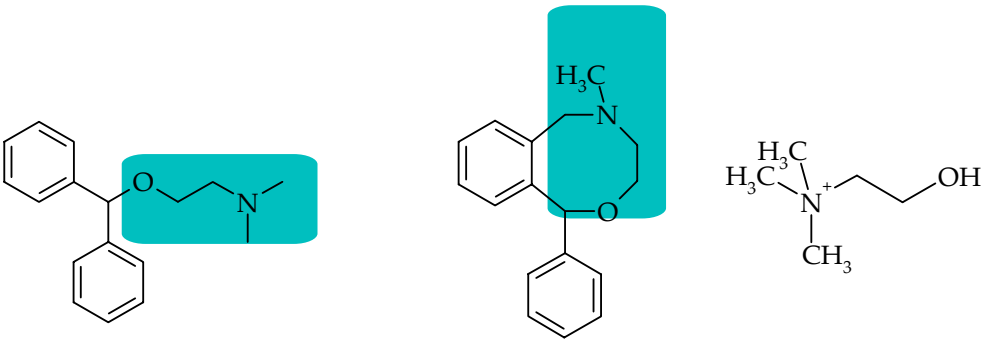

diphenhydramine (37) nefopam (38) choline (4)

Figure III/8.3: Structures of diphenhydramine **37,** nefopam **38** and choline **4.**

The pharmacological properties of choline phenyl ether analogues are of some interest. They were studied by Hunt and Renshaw (1929) [381] as powerful ganglionic stimulants. Further studies on aryl ether analogues of choline **4** demonstrated their amine-oxidase-inhibitory activity [382,383]. The substitution at the ortho-position and the para-position in the choline phenyl ether increases the amine-oxidase-inhibitory activity, whilst a meta-substitution decreases it [382,383]. In 2003, Simsek and co-workers [384] showed that several 3-pyridyl ether analogues of choline **4** (Fig. III/8.4) display antinociceptive properties and also nanomolar affinities for (-)-[^{3}H]nicotine sensitive binding sites.

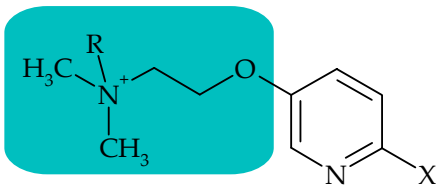

R= CH_3, CH_2CH_3 , $CH_2CH_2CH_3$

X = Cl, Br or OCH_3

Figure III/8.4: Structure of the lead compound used by Simsek et al. to investigate the 3-pyridyl ether analogues of choline as antinociceptive agents. In the coloured rectangle the structure of choline **4** is represented.

Abreo et al. described similar analogues of choline with a very high affinity for the $\alpha 4\beta 2^*$ and the amine function being incorporated in a cyclic carbon skeleton which can be an azetidine or a pyrrolidine ring (Fig. III/8.5) [202].

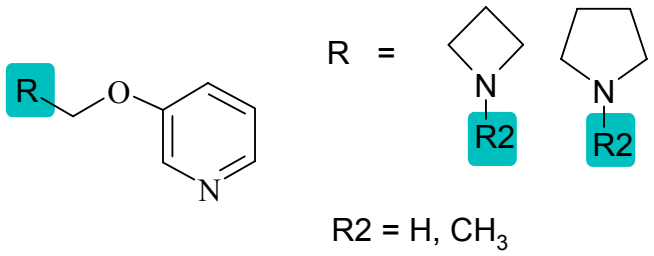

Figure III/8.5: Analogues of choline with the amine function incorporated in a cyclic carbon skeleton.

Extending choline **4** with an amide moiety to obtain the carbamate function leads to carbacholine, a known muscarinic ligand. In 1988, Abood et al. described carbamate esters of choline [385] and used radioligand binding studies to evaluate their possible interaction with (-)-[^{3}H]nicotine sensitive and [^{3}H]MCC sensitive binding sites. They reported that the introduction of one or two methyl substituent on the amide function of carbamylchloride, producing 2-dimethylaminoethyl **(DMAE)** and 3-trimethylaminoethyl **(TMAE)** phenylcarbamate, increased the affinity for neuronal nicotinic receptors. Recently N-methylated and dimethylated analogues of carbacholine Cch **17** were evaluated for their nicotinic activity [177]. N,N-dimethylcarbachol (DMCC) **19** proved to possess the highest selectivity for nicotinic over muscarinic acetylcholine receptors within this series [177]. Recently, the carbamate derivative containing an azabicyclic system was claimed in a patent from Astra Laboratories [389] as an α7* selective compound. During the past few years, choline and its derivatives has not received much attention as selective for α7* nAChRs. Agonists for the α7* nAChRs are thought to be useful in the treatment or prophylaxis of psychotic disorders (schizophrenia, mania, maniac depression and anxiety) and intellectual impairment disorders (Parkinson's disease, Alzheimer's disease, memory loss, autism and Attention Deficit Hyperactivity Disorder (ADHD)). They might also be useful in the treatment of inflammatory bowel diseases, for example ulcerative colitis [386].

III/8.2. Project

(Matthias Andrä, Lenka Munoz, Department of Pharmaceutical Chemistry, University of Bonn: synthesis of novel phenylcarbamate analogues)

In order to achieve greater insight into structural requirements for nAChRs, especially for the α7* nAChR, the binding affinities of known and novel choline derivatives have been evaluated for different nAChR subtypes. The phenyl ether of choline was investigated for its in vitro binding affinity for different nicotinic nAChR subtypes for the first time. Extending choline **4** with an amide moiety to obtain the carbamate leads to a phenylcarbamate derivative. DMAE and TMAE were re-synthesized and their affinity evaluated for the α4β2* α7*, α3β4* and muscle types nAChRs. Since the ortho and para positions at the phenyl moiety in phenylcarbamate derivatives have proved to strongly increase the affinity for muscarinic receptors as well as to increase the anesthetic effect [387], the meta position of the phenyl ring was selected for the introduction of various substituents, such as bromine, fluorine, methyl and trifluoromethyl moiety (Fig. III/8.6).

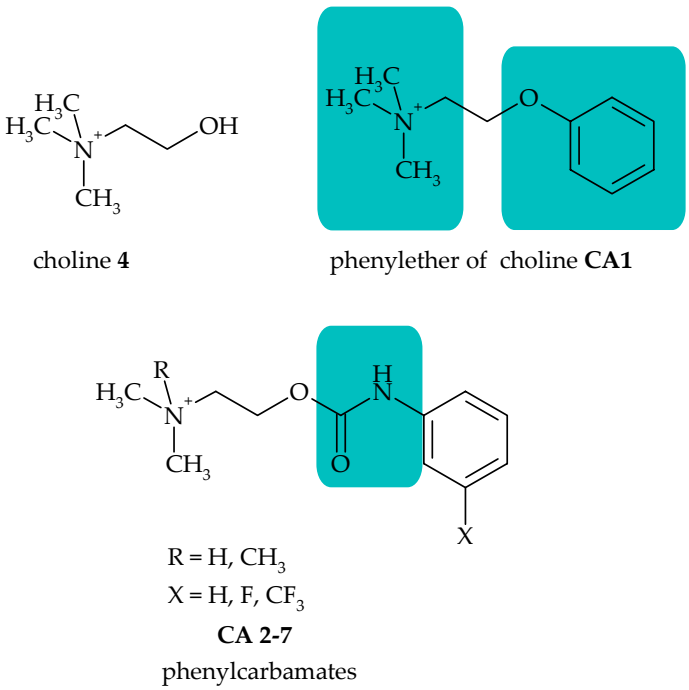

Figure III/8.6: Structures of choline **4,** phenyl ether of choline **CA 1** and phenylcarbamate derivatives **CA 2-7**.

The analogues **CA 1-7** have been tested in radioligand binding assays in order to determine their affinity towards four different classes of nicotinic acetylcholine receptors. It is known that ligands with a quaternary amino function generally show high affinity for nicotinic receptors [388]. However, it is also recognized that incorporating the nitrogen of the quaternary amine group into a rigid ring system [388] can enhance cholinergic potency. This observation prompted us to incorporate the nitrogen of compound **CA1** into diverse azacyclic systems. Two isomeres of the methyl-piperidine derivatives were synthesized, one bearing the phenylcarbamate at position C-2 and the other one at position C-3 of the piperidine moiety (Fig. III/8.7). The prepared compounds **CA 8-20** were evaluated for their ability to compete for (±)-[^{3}H]epibatidine and [^{3}H]MLA binding sites in rat forebrain (α4β2*, α7*), pig adrenals (α3β4*) and *Torpedo californica* electroplax ((α1)$_2$β1γδ) membrane fractions using radioligand binding assays.

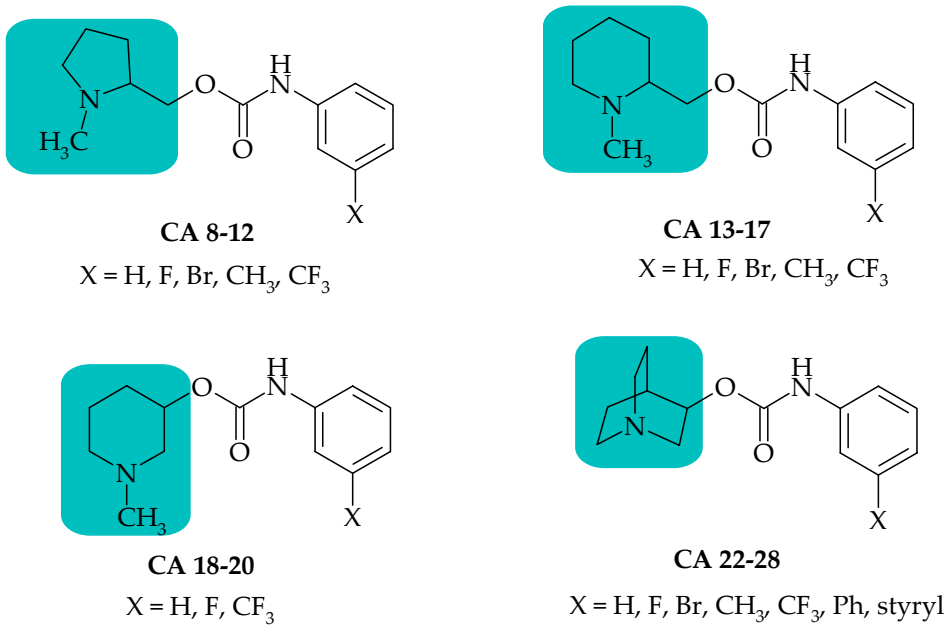

Figure III/8.7: Structures of phenylcarbamate derivatives bearing different azacyclic skeletons.

To discover whether the introduction of the carbamate moiety can improve the selectivity of these quinuclidine analogues in favour of *α7** or other nicotinic AChR subtypes, the ability of the prepared compounds **CA 22-28** (Fig. III/8.7) to compete for four different nAChRs subtypes was evaluated using radioligand binding assays [179 180 374].

III/8.3. Determination of affinities and structure-activity relationships (SAR)

The phenylether of choline **CA 1** showed nanomolar affinities for neuronal nAChR subtypes with a preference for α4β2* (Tab. III/8.1) (K_i = 22.3 nM). The introduction of a carbamate moiety, converting the compound **CA 1** to the corresponding carbamate analogue **CA 3** (K_i = 38.9 nM) leads to an α7* selective compound. Abood and co-workers have reported the ability of **CA 2** and **CA 3** to inhibit the specific binding of neuronal nicotinic and muscarinic receptors but no results were obtained for other nAChR subtypes. The introduction of a fluorine atom at position C-3 of the phenyl moiety leads to a carbamate derivative **CA 5** with slightly reduced affinities for α4β2* and α7* nAChR (K_i = 1,412 and 62 nM, respectively) compared to **CA 3**, but retains the subtype selectivity for α7* nAChR. The selectivity and affinity for the α7* nAChR is increased again by the introduction of a trifluoromethyl group in position C-3 of the phenyl ring (**CA 7,** K_i = 29 nM). In contrast, the analogues **CA 2**, **CA 4** and **CA 6** having a tertiary acyclic amine function show dramatically reduced affinities for nAChRs. Interestingly, the phenylether of choline **CA 1** possesses the highest affinity for the ganglionic (K_i = 135 nM) and the muscle type (K_i = 697 nM). For α3β4* and muscle nAChRs, **CA 1** exhibits 17- and 28-fold higher affinity than the corresponding carbamate analogue **CA 3**.

Table III/8.1: Radioligand binding affinities of the phenyl ether of choline and carbamate analogues of choline for α4β2*, α7*, α3β4*and $(\alpha1)_2\beta1\gamma\delta$ nAChRs.

Phenyl ether of choline and phenylcarbamate analogues					
Structure	**No.**	**α4β2* [³H]EPI rat brain K_i (nM)**	**α7* [³H]MLA rat brain K_i (nM)**	**α3β4* [³H]EPI pig adrenals K_i (nM)**	**$(\alpha1)_2\beta1\gamma\delta$ [³H]EPI Torpedo calif. electroplax K_i (nM)**
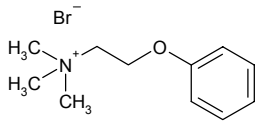	**CA 1**	22.3 ± 4.3	196 ± 9.19	135 $^{n=1}$	697
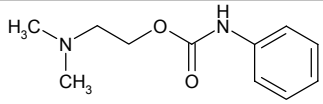	**CA 2**	> 20,000	12,836 ± 2,762	n.d.	n.d.
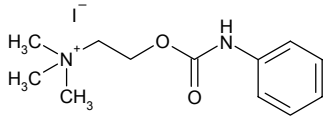	**CA 3**	835 ± 0.7	38.9 ± 2.9	2,200 $^{n=1}$	> 20,000
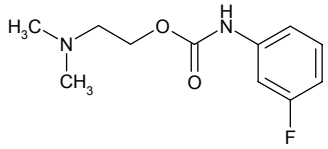	**CA 4**	> 20,000	11,000	23,157 $^{n=1}$	> 20,000
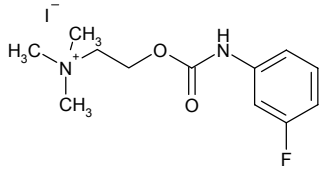	**CA 5**	1,412 ± 17	62	2,500	n.d.
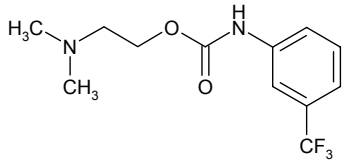	**CA 6**	> 20,000	> 20,000	n.d.	n.d.
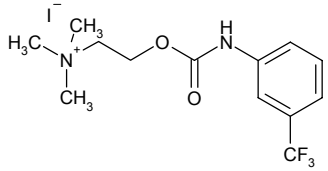	**CA 7**	6,000 ± 23	29 ± 3	3,800	> 20,000

n.d. = not determined
n = number of experiments

The cyclization of the amino function in the pyrrolidine- **(CA 8-12)**, piperidine- (**CA 12-20)** and quinuclidine-rings **(CA 20-28),** produces analogues, which exhibit a surprisingly different binding profile for diverse nAChR subtypes (Tab. 8.2, 8.3, 8.4). Furthermore, they were synthesized with the purpose of penetrating through the blood-brain-barrier.

N-methyl-pyrrolidine analogues

The SAR of N-methyl-pyrrolidine derivative **CA 8-12** does not follow the trend discussed previously for **CA 3, CA 5** and **CA-7**. Compounds **CA 8, CA 9, CA 10, CA 11** and **CA 12** have K_i values for α4β2* nAChRs in the higher nanomolar to the lower micromolar range. Despite the presence of a carbamate moiety that should determine selectivity for the α7* nAChR, they showed only lower affinity (high μM range) for the α7* subtype (Table III/8.2). Thus, analogues **CA 8,CA 9, CA 10, CA 11** and **CA 12** showed an opposing selectivity profile compared to the analogues **CA 3, CA 5** and **CA 7**. The rank order of potency is: α4β2* > α3β4* > α7*. The most potent and selective compound for α4β2* nAChRs was **CA 10** containing a bromine atom at position C-3 of the phenyl ring (K_i = 528 nM). The trifluoromethyl analogue **CA 12** did not significantly influence the affinity for all nAChRs. The analogue **CA 8** showed the highest affinity for the α3β4* nAChRs, in this series (K_i = 2,582 nM). N-methyl-pyrrolidine derivatives **CA 8, CA 9** and **CA 12** showed no effect at $(\alpha1)_2\beta1\gamma\delta$ nAChR (K_i = > 20,000 nM).

Table III/8.2: Radioligand binding affinities of N-methyl-pyrrolidine analogues for α4β2*, α7*, α3β4* and $(\alpha 1)_2\beta 1\gamma\delta$ nAChRs.

N-methyl-pyrrolidine analogues					
Structure	**No.**	**α4β2* [³H]EPI rat brain K_i (nM)**	**α7* [³H]MLA rat brain K_i (nM)**	**α3β4* [³H]EPI pig adrenals K_i (nM)**	**$(\alpha 1)_2\beta 1\gamma\delta$ [³H]EPI Torpedo calif. electroplax K_i (nM)**
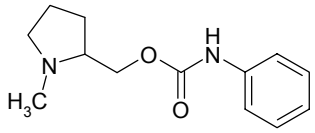 (S)	**CA 8**	1,100 ± 223	5,853 ± 212	2,582 ± 211	> 20,000
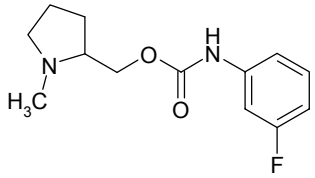 (S)	**CA 9**	1,633 ± 62	15,000 [a]	13,443 [a]	> 20,000
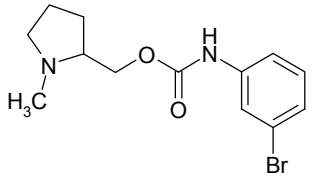 (S)	**CA 10**	526 ± 19	10,810 [a]	6,146 ± 294	n.d.
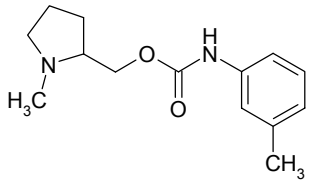 (S)	**CA 11**	1,248 ± 126	14,108 [a]	6,000 [a]	n.d.
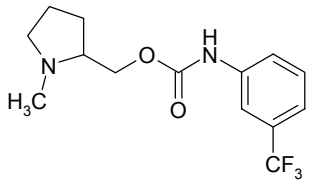 (S)	**CA 12**	1,050 ± 103	13,000 [a]	7,790 [a]	> 20,000
a = values are the mean from n=2 n.d.= not determined.					

N-methyl-piperidine analogues

The N-methyl-piperidine series (**CA 13-20,** Tab. III/8.3) have been evaluated in radioligand binding studies in order to explore whether the position of the carbamate moiety at C-2 or C-3 of the piperidine ring exerts an evident impact on the subtype selectivity of these derivatives. Compounds **CA 18**-**20**, with the phenylcarbamate moiety at position C-3 on the piperidine ring, show a preference for α7* nAChR with K_i values in the low micromolar range (K_i ranging from 2,600 to 4,400 nM) (Tab. III/8.3) and no effect at α4β2* nAChR. **CA 19**, with a K_i value of 2,600 nM for α7* nAChR, is the most selective compound for this subtype over α4β2* nAChR. In contrast **CA 13**-**17**, which have the carbamate function at position C-2 on the piperidine ring, display a complex pattern of subtype selectivity. Analogues **CA 14** and **CA 17** with fluorine and trifluoromethyl substituents demonstrate poor receptor binding affinities for all subtypes under investigation (K_i ranging from 20,000 to 30,000 nM). Interestingly, the unsubstituted compound **CA 13** proves to be the most selective analogue for the α3β4* nAChR. Analogues **CA 15** and **CA 16**, containing a bromine or methyl moiety at the phenyl ring (K_i = 3,700 and 175 nM, respectively), are the most potent ligands in the piperidine series for α4β2* nAChR. They have a subtype profile similar to that of their pyrrolidine analogues **CA 8**-**12,** namely α4β2* > α3β4* > α7*.

Table III/8.3: Radioligand binding affinities of N-methyl-piperidine analogues for α4β2*, α7*, α3β4* and $(\alpha 1)_2\beta 1\gamma\delta$ nAChRs.

N-methyl-piperidine analogues					
Structure	**No.**	**α4β2* [³H]EPI rat brain K_i (nM)**	**α7* [³H]MLA rat brain K_i (nM)**	**α3β4* [³H]EPI pig adrenals K_i (nM)**	**$(\alpha 1)_2\beta 1\gamma\delta$ [³H]EPI Torpedo calif. electroplax K_i (nM)**
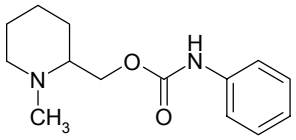	**CA 13**	> 20,000	15,000 [a]	6,100 [a]	> 20,000
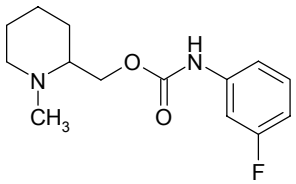	**CA 14**	> 20,000	22,000 [a]	11,392 [a]	> 20,000
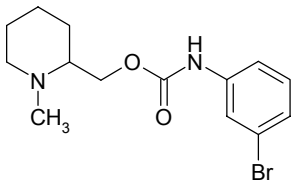	**CA 15**	3,770 ± 79	27,000 [a]	6,357 [a]	n.d.
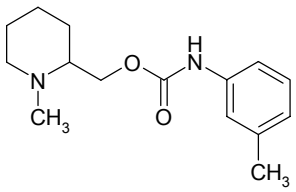	**CA 16**	175 ± 12	31,800 [a]	14,392 [a]	> 20,000
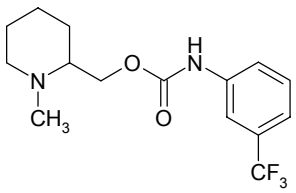	**CA 17**	> 20,000	13,000 [a]	> 20 000	> 20,000
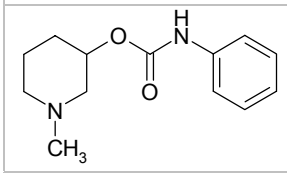	**CA 18**	> 20,000	3,600 [a]	23,712 [a]	> 20,000
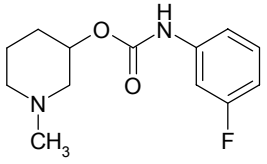	**CA 19**	> 20,000	2,600 [a]	6,963 [a]	> 20,000
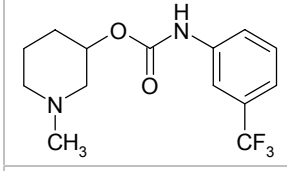	**CA 20**	> 20,000	4,400 [a]	17,303 [a]	> 20,000

a = values are the mean from n=2
n.d.= not determined.

Quinuclidine analogues

The presence of an azabicyclic moiety was investigated in the series **CA 22-27.** The quinuclidine derivatives **CA 22**-**27,** like their corresponding derivatives **CA 3, 5**, **7,** exhibit remarkable selectivity for α7* versus α4β2*. **CA 23** shows the highest selectivity for the α7* nAChRs over the α4β2* (1:113). The affinities of the biphenylderivative **CA 27** and the non-substituted **CA 22** were evaluated by Naito et al. [387] on muscarinic receptors. In 2001, the affinities of these compounds together with **CA 23** and **CA 25** were tested for different nAChR subtypes and proved to be selective α7* nAChRs ligands [389]. The azabicyclic carbamate derivative **CA 22** was used as a lead compound for further substitution at the phenyl moiety, such as a phenyl (**CA 27)** and a styryl moiety (**CA 28)**. Bulkier groups at the phenyl moiety reduce the subtype selectivity for α7* nAChRs and the affinity for α4β2* and α3β4* nAChR (Tab. III/8.4). Analogues in the quinuclidine series **CA 22**-**28** present structural elements that are similar to that of the carbamate derivatives bearing a pyrrolidine or piperidine moiety **CA 8**-**20.** Indeed, they have basic nitrogen, which can be protonated to provide a cationic centre, a carbamate moiety and an π-electron system. Nevertheless, the quinuclidine series **CA 22**-**28** possesses a much higher affinity and selectivity for α7* nAChR compared to analogues **CA 8**-**20**. Moreover, all (*S*)-pyrrolidine derivatives **CA 8**-**12** and the piperidine analogues **CA 15** and **CA 16** exhibit higher affinities for α4β2* nAChR. These results suggested that the carbamate moiety, in combination with a certain spatial distance between the oxygen and the nitrogen of the choline fragment in these derivatives, is crucial for the interaction with the α7* nAChR. The azabicyclic core of the quinuclidine moiety or the acyclic variant can provide a structure with an optimal distance between the choline oxygen and nitrogen. Furthermore, results listed in Table III/8.4 reveal that, compared with the pyrrolidine and piperidine series, the quinuclidine phenylcarbamate derivatives **CA 22**-**27** examined have a higher affinity for α3β4* nAChRs. The K_i values are in the low micromolar range, with the exception of **CA 24** (K_i = 715 nM).

Table III/8.4: Radioligand binding affinities of quinuclidine analogues for α4β2*, α7*, α3β4* and $(\alpha 1)_2\beta 1\gamma\delta$ nAChRs.

Quinuclidine analogues					
Structure	**No.**	**α4β2* [^{3}H]EPI rat brain K_i (nM)**	**α7* [^{3}H]MLA rat brain K_i (nM)**	**α3β4* [^{3}H]EPI pig adrenals K_i (nM)**	**$(\alpha 1)_2\beta 1\gamma\delta$ [^{3}H]EPI Torpedo calif. electroplax K_i (nM)**
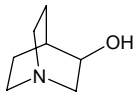	**CA 21**	5,924 ± 624	7,761 [a]	14,604 ± 869	n.d.
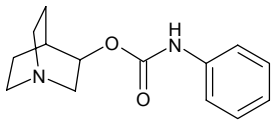	**CA 22**	3,084 [a]	44 ± 23	1,627 ± 123	> 20,000
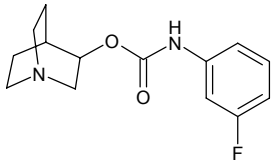	**CA 23**	4,203 [a]	37.3 ± 5	1,581 ± 22	> 20,000
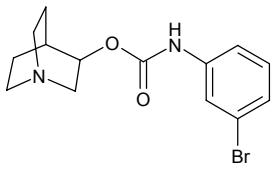	**CA 24**	2,988 ± 66	273 ± 25	715 ± 33	n.d.
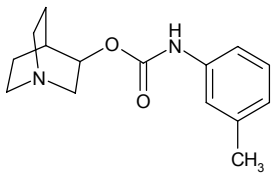	**CA 25**	2,695 [a]	321 ± 3.5	1,478 ± 78	n.d.
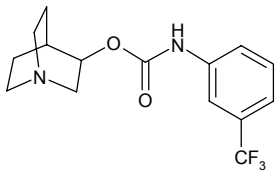	**CA 26**	1,718 [a]	173 ± 23	1,200 ± 66	> 20,000
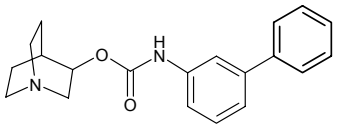	**CA 27**	7,772 [a]	1,135± 431	1,448 ± 66	n.d.
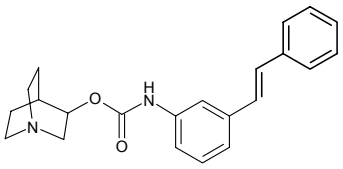	**CA 28**	5,350 [a]	6,100 [a]	5,976 [a]	n.d.

a = values are the mean from n=2
n.d.= not determined.

III/8.4. Discussion

Radioligand binding studies carried out for the phenylether of choline, N-methyl-pyrrolidine, N-methyl-piperidine- and quinuclidine phenylcarbamate derivatives revealed that choline derivatives **CA 1-28** possess different subtype selectivity for nAChRs. Abood and co-workers [385] have reported the ability of **CA 2** (2-dimethylaminoethyl) and **CA 3** (3-trimethylaminoethyl) phenylcarbamate to inhibit the specific binding of (-)-[^{3}H]nicotine and [^{3}H]methylcarbamylcholine in rat brain membranes at milli- (for **CA 2**) and micromolar (for **CA 3**) concentrations, but no results have been obtained for other nAChR subtypes. The phenylcarbamate derivatives **CA 3-5-7** showed the highest affinities and subtype selectivity for α7*. The position of the phenylcarbamate moiety at the piperidine ring within the N-methyl-piperidine series **CA 13-20** influenced the subtype selectivity towards α7* and α3β4* nAChRs. On the contrary, all (*S*)-pyrrolidine derivatives **CA 8-12** and the piperidine analogues **CA 15** and **CA 16** exhibited higher affinities and subtype selectivity for α4β2* nAChR. Furthermore, in order to study the influence of the azacyclic core, a series of phenylcarbamate derivatives was synthesized where the amine function is constrained in a quinuclidine moiety. This azabicyclic system provides quite a rigid structure with a protonable nitrogen. Such compound could cross the blood-brain-barrier (BBB). These properties make the quinuclidine moiety a good basis for the development of ligands for nicotinic receptors in the CNS. The 3-bromophenyl carbamate analogues **CA 10**, **CA 15** and **CA 24** show very remarkable binding profiles. The quinuclidine analogue **CA 24** and the (*S*)-pyrrolidine analogue **CA 10** display a contrary profile for subtype selectivity. The first one **CA 24,** is the most potent compound for α7* with a K_i value of 273 nM, whereas the second one has the highest affinity for α4β2* (K_i = 526 nM). Analogue **CA 24** exhibited the highest affinity for α3β4* nAChR, with a K_i value of 715 nM, whereas **CA 10** and **CA 15** possessed similar but a ca. 9-fold lower affinity for the ganglionic subtype. None of the phenylcarbamate derivatives examined showed activity for the muscle type nAChR. Recently, interest for choline **4** and its derivatives has been renewed due to

the discovery that choline is a full agonist at *α*7* nAChRs. Based on the fact that activation of this subtype produces a variety of biological responses, the biological significance of *α*7* nAChRs is at present a topic of great interest. The most relevant pharmacological effects are *in vitro* neuroprotection and modulation of glutamate and GABA release. Currently, the development of choline derivatives potentially selective for *α*7* nAChRs, is receiving significant attention. AstraZeneca produced a compound (-)-AR-R17779 **20,** containing a spiroquinuclidine moiety as a rotationally restricted analogue of acetylcholine **1**. This compound was the first known ligand to possess in vitro subtype selectivity for α7* over α4β2* nAChRs (K_i value for α7* = 92 nM ([^{125}I]α-Bgt), K_i value for α4β2* = 16,000 nM ((-)-[^{3}H]nicotine)[178]. The 3-quinuclidinole **CA 21** was used for the synthesis of **CA 22-28**. It can be considered a rigid choline derivative. Interestingly, it displays K_i values in the micromolar range for different neuronal nAChRs and no selectivity between α4β2* and α7* nAChRs. Quinuclidine analogues **CA 22-28** not only possess high nanomolar affinities for the neuronal nAChR, but also display the highest affinities and subtype selectivity for α7* nAChRs. The most selective and active compound was the quinuclidine phenylcarbamate **CA 23**, with a selectivity for the α7* nAChRs comparable to that of AR-R17779 **20.**

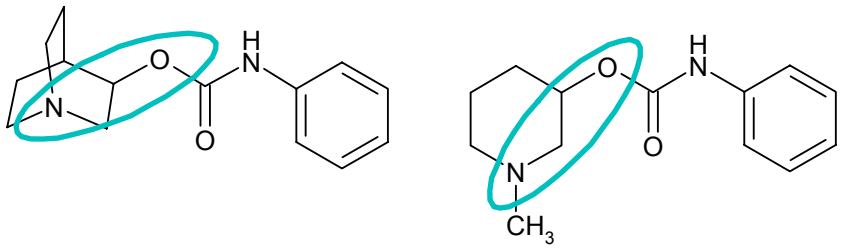

CA 22
K_i = 44 nM (α7* nAChRs)

CA 13
K_i = 15,000 nM (α7* nAChRs)

Figure III/8.9: The structure of choline is highlighted in compound **CA 22** and **CA 13.**

The difference in subtype selectivity among the phenylcarbamate derivatives can be explained on the basis of the choline substructure incorporated (Fig. III/8.9). The **CA 13** derivative, even presenting structural elements similar to that of the quinuclidine derivative **CA 22**, such as a basic nitrogen, which can be protonated to provide a cationic centre, a carbamate moiety and a π-electron system, does not seem to possess

an optimal distance between the nitrogen atom and the oxygen. This parameter seems to be crucial for the interaction with the α7* nAChR.

IV.Summary and Outlook

The *in vitro* characterization and further insight into structure-activity relationships of novel synthetic analogues of the natural toxic alkaloids (-)-cytisine **Cy 1,** (+)-ferruginine **Fe 1**, and (+)-anatoxin-a **An 1** as well as of choline **4** derivatives were the focus of this work. The natural toxins possess high affinity for $\alpha 4\beta 2^*$ nAChR, representing the major population of nACh receptors in mammalian brain, but no appropriate selectivity, i.e. the interaction of these ligands with ganglionic and neuromuscular nAChRs is thought to be responsible for cardiovascular, gastrointestinal and neuromuscular side effects, limiting their utility as therapeutic agents. Therefore, it will be of interest to get more information about the structural requirements of nicotinic ligands for these subtypes. To date, systematically structure-activity relationship studies of (-)-cytisine **Cy 1,** (+)-ferruginine **Fe 1**, and (+)-anatoxin-a **An 1** based ligands have not been reported for different nAChR subtypes.

Beside the templates derived by toxic alkaloids, choline, a selective activator of $\alpha 7$-type nAChRs with neuroprotective activity, is a possible candidate for drug development regarding different diseases of the CNS and PNS.

In general, since the molecular recognition between ligands and nAChRs might be based on cation-π interactions [57] and a hydrogen bond formation between the receptor site and the ligand (HBD-HBA interaction), all high affinity compounds bear the cationic and HBA motifs. Unfortunately, additional characteristics for the ligand receptor interaction, which might be important for subtype selectivity, could not be obtained so far.

Up to now this study is the first one, which evaluated a wide range of mostly novel ligands, based on different templates for four different nAChR subtypes. The findings are:

A successful systematic evaluation of known and novel ligands

Previously described competition assays have been successfully re-evaluated in order to screen different novel analogues of natural toxins and choline derivatives for $\alpha4\beta2^*$, $\alpha7^*$, and $(\alpha1)_2\beta1\gamma\delta$ nAChR subtypes.

A radioligand binding assay for $\alpha3\beta4^*$ nAChRs using native tissue was established

Within the scope of testing novel ligands a new radioligand binding assay using native calf or pig adrenal glands was successfully established. (±)-[^{3}H]Epibatidine has been proved to be a suitable radioligand to characterize $\alpha3\beta4^*$ nAChRs located in native calf or pig adrenal glands. In a concentration range of 2-2400 pM, (±)-[^{3}H]epibatidine binds with a K_D of 54 ± 4.6 pM and shows a B_{max} value of 99 ± 11 fmol/mg protein for whole membrane fractions of pig adrenals and similar values (K_D of 39 ± 5.3 pM and B_{max} of 91 ± 10 fmol/mg protein) for whole membrane fractions of calf adrenals. This novel assay has proved to be a valid procedure for screening novel nicotinic ligands for their affinities to $\alpha3\beta4^*$ nAChRs. In addition, it possesses also economic advantages in comparison to other systems, such as cell cultures or assays performed with rat adrenal glands.

Structure activity relationships studies for toxin analogues

The structure-activity relationships of novel toxins analogues have been evaluated for four different nAChR subtypes. In particular, important information have been obtained concerning the structural requirements that enhance selectivity of toxin analogues for $\alpha4\beta2^*$ nAChR over other nAChRs investigated.

Cytisine analogues

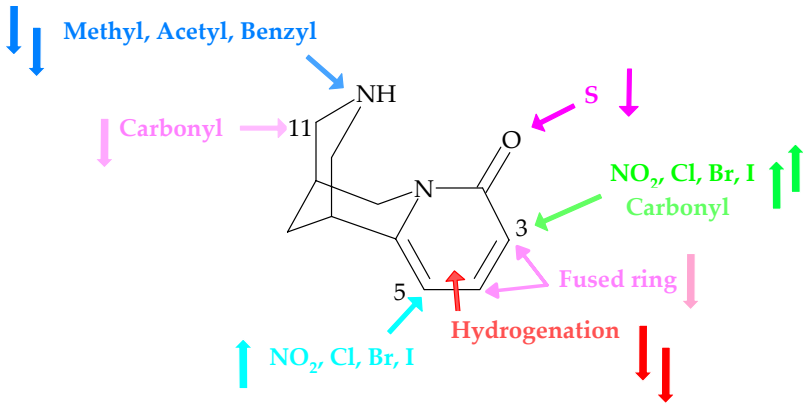

The introduction of a substituent at the secondary nitrogen of the bispidine ring results in a dramatic loss of affinity for all nAChRs investigated. In contrast, a dimethylation, determining the formation of a quaternary amino function, increase the affinity for $\alpha4\beta2^*$ (**Cy 5,** K_i = 0.238 nM). Cytisine **Cy 1** with multiple oxygen functionalities **(Cy 10)** showed a low affinity for the $\alpha4\beta2^*$ subtype and proved to be a weak ligand for $\alpha7^*$, $\alpha3\beta4^*$ and muscle nAChRs (**Cy 10,** K_i = 95,000, 50,000 and 20,000 nM, respectively).

K_i (nM) for $\alpha4\beta2^*$ nAChR		
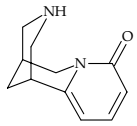	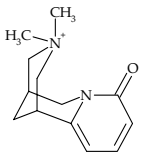	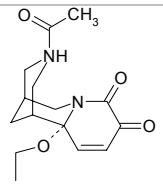
Cytisine Cy 1 K_i (nM) = 0.124	**Cy 5** K_i (nM) = 0.238	**Cy 10** K_i (nM) = 9,400

With the exception of the muscle type, the introduction of a halogen atom in position C-3 of the pyridone ring improves the affinities of cytisine for $\alpha4\beta2^*$ as well as for $\alpha7^*$ and $\alpha3\beta4^*$ nAChRs. Therefore, this structural variation could only greatly improve the selectivity for $\alpha4\beta2^*$ over the muscle nAChR. The introduction of halogen atoms at position C-5 (for example in **Cy 16**) leads to a slightly decrease in

affinity for α4β2* but an increased affinity for the α7* nAChR and α3β4* nAChRs in comparison to **Cy 1**.

	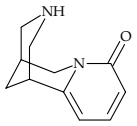	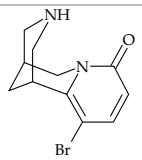	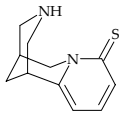
	Cy 1 K_i (nM)	**Cy 16** K_i (nM)	**Cy 29** K_i (nM)
α4β2*	0.124	0.338	0.832
α7*	250	28	4,000
α3β4*	18	5	632

Another observation of particular interest concerns the influence of a bioisosteric replacement of oxygen by sulphur on the pyridone ring. This modification resulted in novel analogue **Cy 29**, which shows a subnanomolar affinity for the α4β2* subtype (K_i = 0.832 nM) and the best affinity-selectivity profile for α4β2* over α7* and α3β4*. Results of radioligand binding assays performed for thiocytisine derivatives showed that none of the additional structural modifications introduced were able to enhance the selectivity for non-α4β2* subtypes under examination. Hydrogenation of the pyridone ring **(Cy 7)** proved to be deleterious for the affinity for all subtypes. The conformationally constrained analogue **Cy 11** showed dramatically reduced affinities for α4β2* and α7* nAChRs in comparison to the lead compound **Cy1**.

	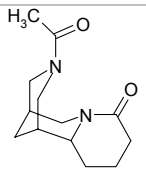	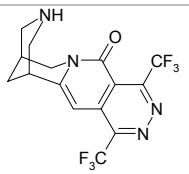
	Cy 7 K_i (nM)	**Cy 11** K_i (nM)
α4β2*	> 20,000	5,333
α7*	> 50,000	> 50,000
α3β4*	> 50,000	n.d.
muscle type	> 50,000	n.d.

Ferruginine analogues

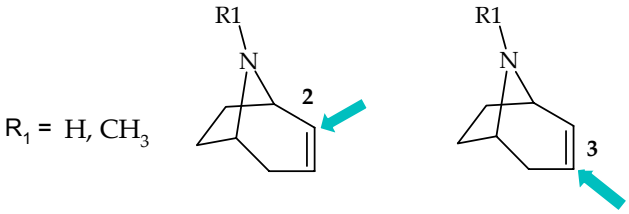

Substituents at C-2 and C-3

Amide moieties at C-2 in the azabicyclic substructure of ferruginine resulted in dramatic decrease of affinity for α4β2* (**Fe 3**, K_i = 3,790 nM; **Fe 6**, K_i = 20,000 nM; **Fe 5**, K_i = 2,027 nM) being not suitable surrogates for the acetyl group of ferruginine **Fe 1** (K_i = 120 nM).

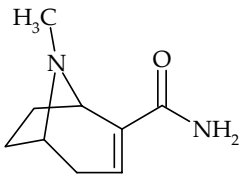

Fe 3

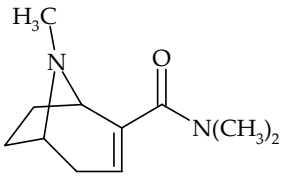

Fe 5

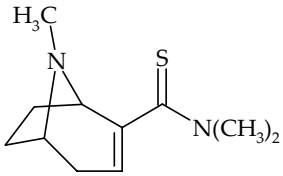

Fe 6

On the contrary, replacement of the acetyl moiety by a heteroaromatic ring increase the binding affinity for α4β2*. The electronic properties of the heterocycles moiety (hydrogen bond acceptor (HBA) capability) influence the potency, therefore the following rank order was observed: pyridine > pyrimidine > pyridazine > pyrazine. Furthermore, the binding affinity proved to be influenced by the position of the pyridine or diazine ring at the 8-azabicyclo[3.2.1]octene skeleton of ferrugine and norferrugine.

K_i (nM) for α4β2* nAChR			
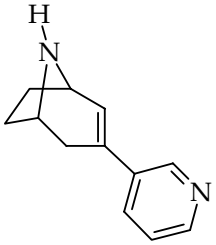	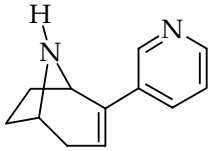	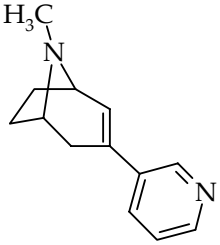	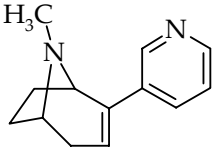
Fe 13 K_i (nM) = 0.25	**Fe 8** K_i (nM) = 1.6	**Fe 14** K_i (nM) = 0.96	**Fe 10** K_i (nM) = 3.4

Compared to analogues with a pyridine moiety at position C-2 (**Fe 8**, **Fe 10**) of the azabicyclic skeleton, analogues bearing a pyridine moiety at position C-3 (**Fe 13**, **Fe 14**) possess a higher affinity for α4β2* nAChR (K_i = 0.25 nM and K_i = 0.96 nM, respectively). A double substitution, such as an additional introduction of an ester moiety in the 8-azabicyclo[3.2.1]octene-skeleton is significantly detrimental to the affinity for all subtypes examined (*ent*-**Fe 16, Fe 14)**.

	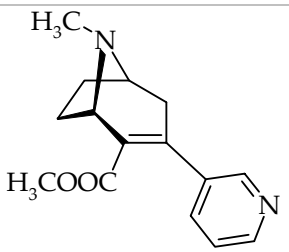	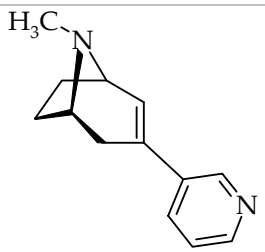
	ent-**Fe 16**	**Fe 14**
α4β2* K_i (nM)	4,931	0.96
α7* K_i (nM)	> 50,000	73.6
α3β4* K_i (nM)	> 30,000	24

A general trend can be observed for the affinities of the ferruginine and norferruginine analogues for the α7* subtypes. N-methylation of the azabicyclic system improves the affinity for this nAChR subtype. The ferruginine **Fe 1** possess 303-fold higher affinity than its desmethylated analogue, norferruginine **Fe 2.** The ferruginine analogue **Fe 10** exhibited the highest affinity for the α7* nAChRs (K_i = 53 nM), which is ca. 7- fold higher than the affinity of its demethylated analogue **(Fe 8).**

K_i (nM) for α7* nAChR	
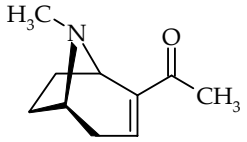	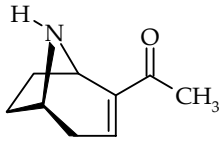
Fe 1 K_i (nM) = 330	**Fe 2** K_i (nM) = 100,000
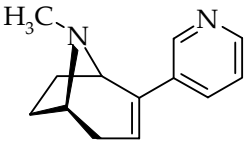	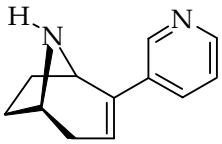
Fe 10 K_i (nM) = 53	**Fe 8** K_i (nM) = 396

The introduction of a pyridyl moiety in position C-3 (**Fe 14)** had a positive influence on the affinity to muscle nAChRs. Compound **Fe 15,** bearing a chloro-pyridyl moiety proved to be the most active ligand at $(\alpha 1)_2\beta 1\gamma\delta$ nAChR subtype (K_i = 80 nM), being 625-fold more potent than the lead compound ferruginine **Fe 1**.

K_i (nM) for $(\alpha 1)_2\beta 1\gamma\delta$ nAChR	
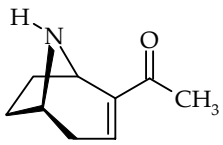	
Fe 1 K_i (nM) = 50,000	
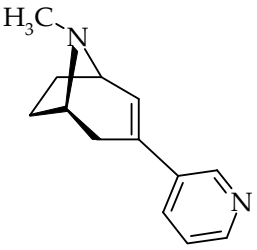	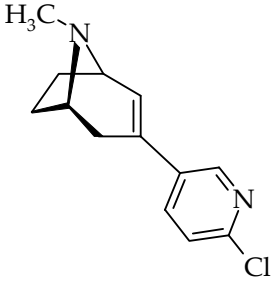
Fe 14 K_i (nM) = 314	**Fe 15** K_i (nM) = 80

Pinnamine analogues

Neither of the two novel pinnamine derivatives retains the affinity of the lead compound (-)-ferruginine **Fe 1** for the α4β2* nAChR subtype. Analogue *cis*-**Pin 1** showed only a weak interaction to the α7* nAChRs subtype (K_i = 22,470 nM), whereas *trans*-**Pin 2** binds in the low micromolar range (K_i = 1,360 nM, α7* nAChR). The loss of the affinity could be due to the unfavourable orientation of the pharmacophoric elements and/or the ethyl moiety cannot be sterically tolerated. Therefore, it will be interesting to investigate whether the presence of a substituent smaller or larger than the ethyl moiety could increase the affinity.

	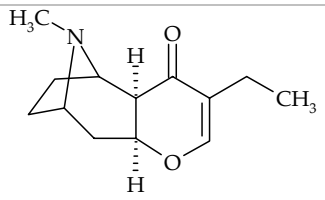	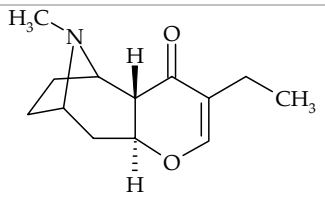
α7* K_i (nM)	*Cis*-**Pin 1** = 22,470	*Trans*-**Pin 2** = 1,360

Anatoxin-a analogues

The binding affinity of the epibatidine-anatoxin-hybrid **UB-165** was re-evaluated for α4β2* and α7* nAChRs and its affinities for the α3β4* and muscle type nAChRs was determined for the first time. The **UB-165** and its novel deschloro analogue, **DUB-165**, showed similar affinities for the α4β2* (K_i = 0.04 nM and 0.051 nM, respectively) and selectivity over the muscle type (K_i values were in the high micromolar range). Interestingly, **DUB-165** showed a 94-fold higher affinity (K_i = 0.95 nM) than **UB-165** for the α7* nAChR. In addition, they displayed K_i values for α3β4* in the lower nanomolar range (K_i = 1.3 nM and 6.2 nM, respectively). On the basis of these data, **UB-165** possess the highest affinity for α4β2* nAChRs (K_i = 0,051 nM), but lower subtype selectivity for α4β2* over α3β4* nAChRs compared with **DUB-165**.

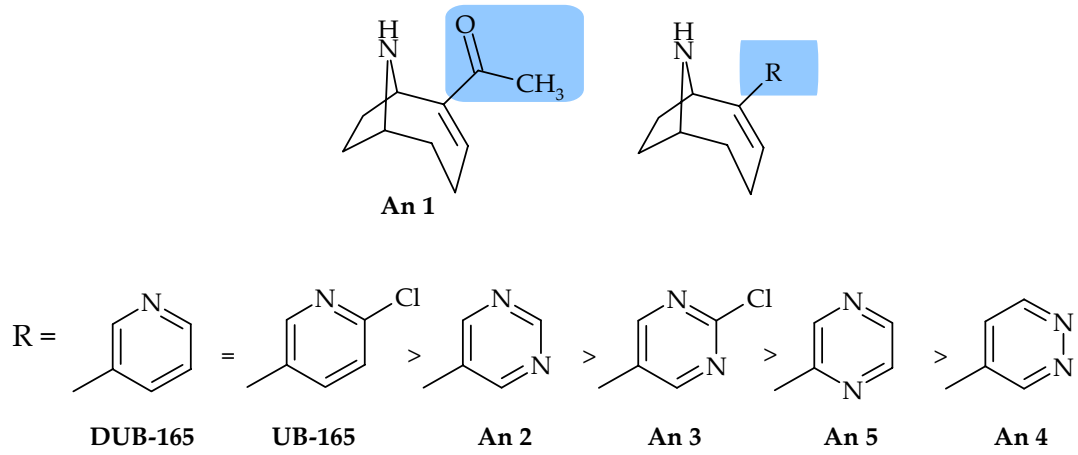

	DUB-165	UB-165	An 2	An 3	An 5	An 4
$\alpha4\beta2^*$ K_i (nM)	0.051	0.04	0.14	0.15	12	19
$\alpha7^*$ K_i (nM)	0.95	12	10.7	n.d.	250	10,000
$\alpha3\beta4^*$ K_i (nM)	6.2	1.3	20	n.d.	259	2,500

Among the diazine biosiosteres (**An 2, An 3, An 4** and **An 5**) the most active compounds described were the pyrimidine and chloro-pyrimidine containing bioisoster **An 2** and **An 3**, with K_i values for $\alpha4\beta2^*$ nAChRs in the picomolar range, 0.14 and 0.15 nM, respectively. **An 2** also showed high affinity for $\alpha7^*$ (K_i = 10.7 nM) and $\alpha3\beta4^*$ nAChRs (K_i = 20 nM) and proved to be more potent, but similarly selective than the natural anatoxin-a **An 1**. The introduction of a pyrazine or pyridazine moiety, resulting in compounds **An 4** and **An 5**, respectively, decreases the binding affinity for all nAChRs.

Diazabicyclo[4.2.1]nonane derivatives

Pyridine and diazine moieties are suitable for high affinity binding at the $\alpha4\beta2^*$ nAChRs (K_i values ranging between 0.62 to 2.09 nM) in the diazabicyclo[4.2.1]nonane series. On the contrary, they possess only moderate affinity for $\alpha7^*$ nAChRs exhibiting a certain degree of preference for the $\alpha4\beta2^*$ compared to the $\alpha7^*$ nAChRs. Analogue **An 13**, bearing a pyrazine moiety, neither interacted with $\alpha7^*$, $\alpha3\beta4^*$ nor with $(\alpha1)_2\beta1\gamma\delta$ nAChRs (K_i > 50,000 nM).

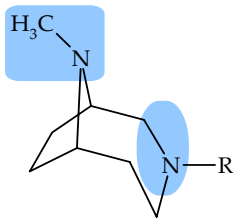

R=	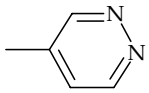	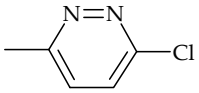	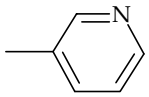	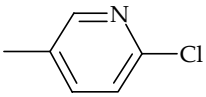	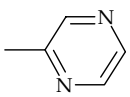
	An 11	**An 10**	**An 8**	**An 7**	**An 13**
α4β2* K_i (nM)	**0.52**	**0.55**	**0.62**	**0,873**	**265**
α7* K_i (nM)	157	190	138	92	**> 50,000**
α3β4* K_i (nM)	9.5	30	23	30,6	**> 50,000**
$(\alpha1)_2\beta1\gamma\delta$ K_i (nM)	2,330	2,540	3,050	2,326	**> 50,000**

In future studies, it would be very interesting to find out whether bulkier substituents at position C-2 or C-3 of the azabicyclooctene or -nonene skeleton of ferruginine or anatoxin-a would be able to improve the selectivity toward a certain type of nACh receptors. First attempts have been very recently shown in a study of Karig et al. using DUB-165 as a template [372]. They introduced a phenyl ring at different positions of the pyridyl moiety and found that a phenyl substituent at position 4′ of the pyridine ring could be favourable for the interaction with α7* nAChR.

Quinuclidine analogues

In the past, the introduction of a pyridine moiety in the quinuclidin-2-ene skeleton proved to be detrimental for the affinity for muscarinic receptors whereas in this actual study, it leads to an analogue with nanomolar affinities for the α4β2* and α7* nAChR (K_i = 7.5 and 83 nM, **Qu 1**). The pyrimidine derivative **Qu 3** showed the highest subtype selectivity for α4β2* over α7* nAChRs.

	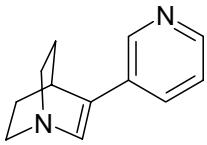	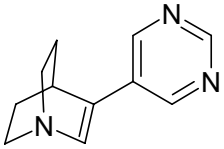
	Qu 1	**Qu 3**
α4β2* K_i (nM)	7.5	12
α7* K_i (nM)	85	751
α3β4* K_i (nM)	103	112
$(\alpha 1)_2\beta 1\gamma\delta$ K_i (nM)	237	100

Structure activity relationship studies for choline analogues

Phenylcarbamate derivatives led to compounds with different subtype selectivity for nAChRs. Compounds **CA 5, CA 7**, together with the quinuclidine analogue **CA 23**, displayed the highest affinities and subtype selectivity for α7*.

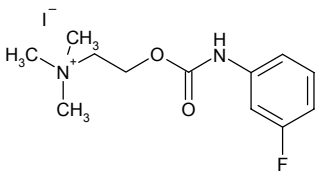	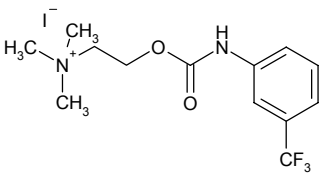	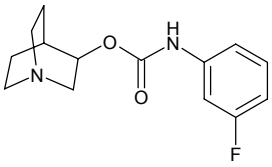
CA 5	CA 7	CA 23
K_i α7* = 62 nM	K_i α7* = 29 nM	K_i α7* = 37 nM
K_i α4β2* = 1,412 nM	K_i α4β2* = 6,000 nM	K_i α4β2* = 4,000 nM

Unexpectedly, the pyrrolidine derivatives (for example, **CA 10** and **CA 11)** and the piperidine analogues **CA 15** and **CA 16** exhibited higher affinities and subtype selectivity for α4β2* nAChR. The difference in subtype selectivity among the phenylcarbamate derivatives could possibly be based on the distance existing between the nitrogen and the oxygen of the choline substructure incorporated.

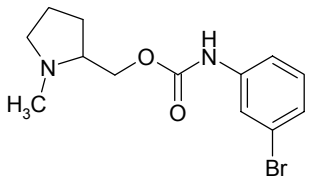	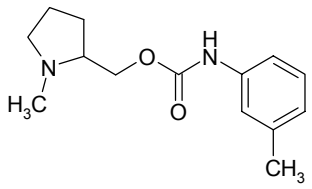	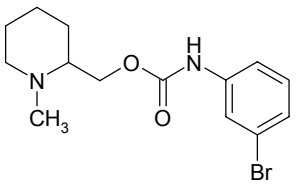	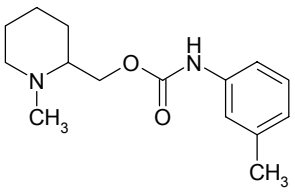
CA 10	**CA 11**	**CA 15**	**CA 16**
K_i α4β2* = 526 nM	K_i α4β2* = 1,248 nM	K_i α4β2* = 3,770 nM	K_i α4β2* = 62 nM
K_i α7* = 10,800 nM	K_i α7* = 14,108 nM	K_i α7* = 27,00 nM	K_i α7* = 31,800 nM

Another important parameter able to influence the subtype selectivity towards α7* and α3β4* nAChRs is the position of the phenylcarbamate moiety at the piperidine ring within the N-methyl-piperidine series (**CA 13** in comparison to **CA 18**).

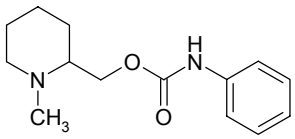	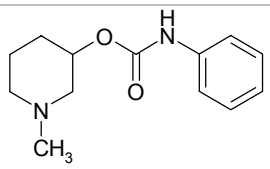
CA 13	**CA 18**
K_i nM α7* = 15,000	K_i α7* = 3,600 nM
K_i nM α3β4* = 6,100	K_i α3β4* =23,712 nM

Carbamates, and specially phenylcarbamates, are known as compounds exhibiting diverse pharmacological profiles. They have analgesic, spasmolytic and local anesthetic properties. Therefore, it will be interesting in future to evaluate these compounds for their affinities to other receptors (muscarinic, 5-HT_3, etc). Further possible structural modification may regard the replacement of the piperidine, pyrrolidine and quinuclidine moiety with other azabicyclic systems and the carbamate moiety by an amide substructure.

In general, it will be of great importance to examine these novel ligands for their functionality using different approaches (FLIPR, patch-clamp, [^{3}H]monoamine release), since affinity values normally reflect the interactions with one or more desensitised states of the nACh receptor.

V. Experimental Section

V/1.1. General Information

V/1.1.1. Instruments

Filter:	Whatman GF/B, Brandell, Gaithersburg, MD, U.S.A.
Harvester:	Brandell M48, M24, Gaithersburg, MD, U.S.A.
Homogenizator:	RW 16 basic, IKA Labortechnik, Germany
LSC-counter:	Tricarb® 2900 TR, Canberra Packard/Perkin Elmer, Dreieich, Germany
pH Meter:	WTW, pH-197, with pH-Electrode SenTix41, IKA Labortechnik, Germany
Photometer:	Beckman DU ®, 530 Life Science, Germany
Pipette:	Eppendorf Research und Eppendorf Multipipette plus
Ultraschallbad:	Sonorex RK52H, Bandelin, Germany
Ultraturrax:	T25 basic, IKA Labortechnik, Germany
Vortex:	MS2, Minischaker, IKA Labortechnik, Germany
Centrifuge:	Beckman Avanti ™, J-20 XP, Beckman Coulter, U.S.A.

V/1.1.2. Materials

Chemical substances

Tris[hydroxymethyl]aminomethane	T 1503 Sigma Aldrich
Tris[hydroxymethyl]aminomethane-hydrochloride	T 3253 Sigma Aldrich
D(+)-Sucrose	84097 Fluka Biochemika
Hepes N-[2-Hydroxyethyl]piperazine-N´[2-ethanesulfonic acid]	H 3375-Sigma Aldrich
Sodium Chloride	S 7653 Sigma Aldrich
Magnesium Chloride Hexahydrate	M 2670 Sigma Aldrich
Calcium Chloride Dihydrate	C 3306 Sigma Aldrich
Potassium Chloride	P 9541 Sigma Aldrich

Ethanol p.a. Merck KG Darmstadt Germany

DMSO (dimethylsulfoxide) Merck KG Darmstadt Germany

Nicotine hydrogen tartrate salt N 5260 Sigma Aldrich

methyllycaconitine citrate (MLA) M 168 Sigma Aldrich

Water ELGA Pure Lab ultra, Vivendi, Water Company

Ultima Gold ™ Perkin Elmer and Analitical Science, M.A, U.S.A.

is a mixture of:

Ethoxylated alkylphenol 10-20 %

Bis(2-ethylhexyl) hydrogen phospate 10-20 %

Docusate sodium ≤ 2.5%

Triethyl phosphate ≤ 2.5%

Diisopropyl naphthalene isomers 60-80 %

2,5-Diphenyloxazole ≤ 2.5%

1,4-bis(4-methyl-alpha-styryl) benzene ≤ 2.5%

Radioligands

(±)-[^{3}H]Epibatidine (S.A.: 33.3 - 66.6 Ci/mmol) obtained from Perkin Elmer Life Science Products (Cologne, Germany).

[^{3}H]Methyllycaconitine ([^{3}H]MLA) (S.A.: 20 - 39.8 Ci/mmol) obtained from TOCRIS Cookson Ltd, Northpoint Fourth Way Avonmouth, Bristol, UK

Tissues

Frozen Torpedo Californica electroplax was purchased from Marinus Inc. (Long Beach, CA, U.S.A.).

Frozen Sprague-Dawley rat brains were purchased from Pel-Freez Biologicals (Rogers, AR, U.S.A.).

Pig adrenals were purchased from Pel-Freez Biologicals (Rogers, AR, U.S.A.).

Calf adrenals were obtained from a local slaughterhouse (Cologne, Germany)

Buffers Solutions

TRIS buffer 25 mM/ pH 7.4 (rinse buffer)

4 mM Tris Base ® (Tris[hydroxymethyl]aminomethane)

21 mM Tris HCl ® (Tris[hydroxymethyl]aminomethane-hydrochloride)

HEPES-salt solution (HSS) pH 7.4 (assays incubation buffer, buffer for membrane preparation)

15 mM HEPES

120 mM NaCl

5.4 mM KCl

0.8 mM $MgCl_2$

1.8 mM $CaCl_2$

adjust pH 7.4

Sucrose Solution (for membrane preparations)

320 mM D(+)-Sucrose

25 mM Tris HCl

adjust pH 7.4

V/1.2. Membrane Preparation

V/1.2.1. General Remarks

Binding assays are carried out using native membrane preparations. Whole membrane preparations have been obtained from pig/calf adrenal glands and Torpedo Californica electroplax, whilst P2 membrane fractions have been prepared from rat forebrain. Both membrane fractions are relatively homogeneous and easy to handle in binding studies. The use of native tissue enriched in synaptosomes (particles containing the organelles of the synapse) avoids the problems that are present with assays on intact cells (e.g. presence of endogenous agonist, and an high non-specific binding). Results obtained from binding assays carried out using P2 membrane fractions are not comparable with results from assays performed using whole membrane fractions. Actually, the P2 membrane fractions represent a first stage of refinement over the crude homogenate and compared to the crude homogenate are 1.5 fold enriched in synaptic receptors. In the next section (V/1.2.2) will be described in major details the procedure used to obtain the P2 membrane

fractions. Sections V/1.2.3, V/1.2.4. and V/1.2.5 report the specific protocols for the preparation of whole membrane fractions. Generally, soft tissue such as brain is homogenized using a Potter homogeniser with a rotating Teflon pestle. The pestle should be motor driven with variable speed and high torque. By the vertical movement in a small diameter tube, small particles are formed and subsequently fractionated. Instead, tough tissue, such as adrenal glands and smooth muscle are best homogenized with a Polytron IKA ultraturrax. This latter instrument relies on a blender principal, with rotating blades contained within a cylindrical cavity through which the homogenate circulates. The particles have different sedimentation constants and may be separated by centrifugation. To avoid or reduce the auto protolysis process, the entire procedure should be conducted on ice.

V/1.2.2. Preparation of rat brains

Frozen rat brains were thawed slowly before the preparation of the P2 rat brain membrane fractions. They were placed on ice for 30 to 60 min and then placed on a plastic plate. A single cut just behind the inferior colliculi was done to exclude the cerebellum and medulla. After the determination of the wet weight, the brains are pressed into a pulp using a syringe and homogenized in sucrose buffers with a glass teflon homogenizator (Potter, 10 seconds). A single rat brain weights on average 1.32 g. The tissue is centrifuged (1,000 x g, 20 min, 4°C) for the production of the supernatant, S1 and the pellet, P1. The supernatant will be aspirated with a Pasteur pipette and stored on ice. The P1 pellet (enriched in cell nuclei, unbroken cells, and brain micro vessels) was re-suspended in sucrose buffer, and the centrifugation was repeated (1,000 x g, 20 min, 4°C) to produce S1′ and P1′. The two supernatant (S1+ S1′) were combined and centrifuged (25 000 x g, 20 min, 4°C) to produce P2 and S2. The P2 fractions obtained represent the so-called crude mitochondria pellet, which contains the majority of the synaptosome. The buffer volume added is calculated on the basis of the wet weight in a ratio of 1:2. The final pellet was re-suspended in assay buffer and stored in aliquots at –80°C. On the day of assay, pellets are thawed, re-suspended in a fresh HSS and used for binding assay.

V/1.2.3. Preparation of pig adrenals

Frozen (-80°C) pig adrenals were thawed on ice for 30 to 60 min before preparation and cut in small pieces. After the determination of the wet weight (every adrenal gland weights ca. 2.8 g) the tissue was homogenized in HSS (pH 7.4, ice-cold) using a motor-driven polytron IKA ultraturrax (setting 6 / rpm = 24,000, 10 sec.). The homogenate was centrifuged (30,000 x g, 10 min, 4°C), the pellets were collected and washed. This procedure was repeated five times. The buffer volume used to re-suspended the pellets is calculated on the basis of the wet weight in a ratio of 1 : 6.5. Afterwards the tissue is stored in aliquots at - 80°C. Before each assay, the tissues were homogenized in HSS. After centrifugation (25,000 x g, 20 min, 4°C), the resultant pellets were re-suspended in fresh HSS and used for binding assay.

V/1.2.4. Preparation of calf adrenals

Frozen (-80°C) calf adrenals were thawed on ice for 30 to 60 min before preparation and cut in small pieces. After the determination of the wet weight (one piece weights in average 4-6 g) the tissue was homogenized in HSS (pH 7.4, ice-cold) using a motor-driven polytron IKA ultraturrax (setting 4 / rpm = 19,000, 5 sec.,2-times). The homogenate was centrifuged (30,000 x g, 10 min., 4°C). The pellets were collected and washed. This procedure was repeated five times. The buffer volume used to re-suspended the pellets was calculated on the basis of the wet weight in a ratio of 1 : 6.5. Afterwards, the tissue is stored in aliquots at - 80°. Before each assay, the tissues were homogenized in HSS. After centrifugation (25,000 x g, 20 min, 4°C), the resultant pellets were re-suspended in fresh HSS and used for binding assay.

V/1.2.5. Preparation of Torpedo californica electroplax

Frozen samples of Torpedo Californica electric organ were thawed for 30 to 60 min before membrane preparation. Total membrane fractions were isolated by homogenisation of the tissue in ice-cold HSS using a Polytron IKA ultraturrax (setting 6 / rpm 24,000,) and followed by centrifugation (30,000 x g, 10 min., 4°C). The pellets were collected, washed four times with HSS through re-homogenisation and

centrifugation at the same settings. The remaining pellets were collected, re-suspended in HSS and stored in aliquots at - 80°C.

For each assay, the samples of membrane fractions were thawed, homogenized, and centrifuged (30,000 x g, 10 min., 4°C). The resultant pellets were re-suspended in HSS and used in binding assays.

V/1.3. Protein Determination

V/1.3.1. Bradford protein determination

The Biorad protein assay **(Nr.500-0002)** is a dye-binding assay based on the observation that the absorbance maximum for an acidic solution of Coomassie Brillant Blue G 250 shifts from λ= 465 nm to λ= 595 nm when binding with protein occurs. To determine the concentration of the protein following the Bradford procedure, a master solution was prepared, made of 0.1 g Coomassie brilliant Blue G diluted in 50 % ethanol (v/v), with 100 ml phosphoric acid (85%) and pure water up to 240 ml. The dye reagent is provided as a 5-fold concentrate. Therefore it must be diluted in a ratio of 1 to 5 with pure water and filtered over paper filters prior to use. The filtration is useful for removing any particulates that may form as a result of the dilution. The dilute reagent should be discarded after 2 weeks due to the formation of precipitates. Bovine's serum albumin was used as a standard protein. The Coomassie protein assay was calibrated within a protein concentration range from 10 to 250 μg (λ = 595 nm). The samples are diluted with pure water so that their concentrations amount to approximately 10-100 μg proteins. A volume of 0.1 ml of these dilutions was mixed with 2.0 ml Bradford reagent. The sample-dye mixtures were assayed within 1 hour of mixing, due to the progressive reduction of the optical density.

V/1.3.2. Lowry protein determination

This procedure (Sigma-Aldrich Protein Assay, No. P5656) is one of the most used for quantification of soluble proteins. Protein concentrations are determined and

reported with reference to standards of a common protein (e.g. bovine serum albumin (BSA)). A series of dilutions of the protein standard is prepared in appropriately labelled test tubes (Tab. V/1.1).

Table V/1.1: Dilutions of the bovine serum albumin (BSA)

Protein standard solution (µl)	deionised water (µl)	protein concentration (µg/ml)
62,5	437,5	50
125	375	100
250	250	200
375	125	300
500	0	400

The Folin-Ciocalteau reagent is prepared by mixing 1 part of 2N phenol reagent of the working solution with 1 part of deionised water (Fig. V/1.1). A volume of 1 ml of Lowry reagent is added to 0.2 ml of protein sample (appropriately diluted) and incubated exactly 10 minutes at room temperature. The last step is to add the Folin-Ciocalteau reagent and incubate it 30 minutes at room temperature (Fig. V/1.1).

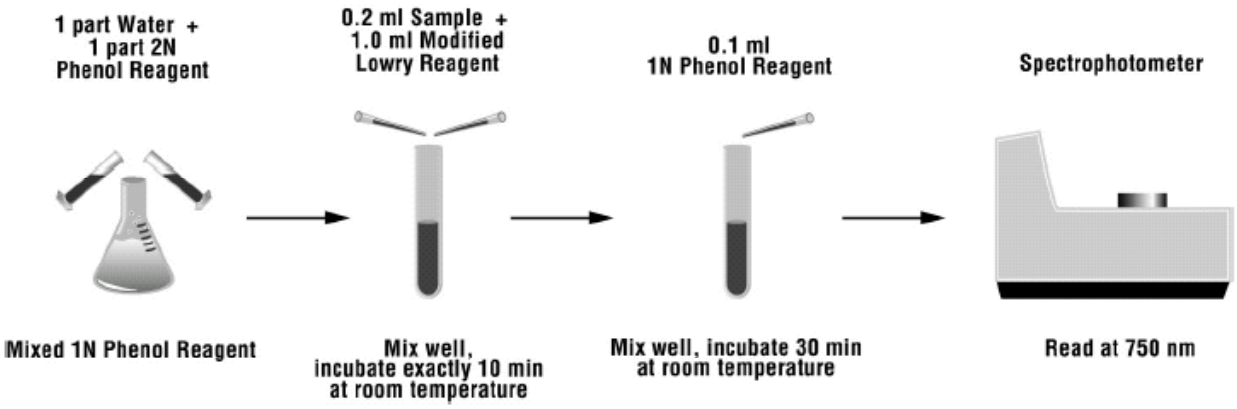

Figure V/1.1: Test tube procedure (Lowry's method) [391]

Absorbance is read at a suitable wavelength of 750 nm. The concentration of each unknown protein sample is determined based on the standard curve.

V/1.4. Radioligand binding studies for α4β2*nAChR

Saturation assays using (±)-[^{3}H]epibatidine and rat brain (P2 fraction)

In saturation studies, membrane preparations (60-90 μg protein) were incubated in the presence of 1-500 pM of (±)-[^{3}H]epibatidine in polypropylene tubes containing HSS. The membranes were incubated at 22 °C for 4 h in a total volume of 4 ml. A dilution series of 11 concentration of the radioligand (±)-[^{3}H]epibatidine was prepared. Non-specific binding was determined in the presence of 300 μM (-)nicotine hydrogen tartrate salt. The experiments were carried out in quadruplicates. Incubations were terminated by vacuum filtration through Whatman GF/B glass fibre filters, pre-soaked in 1 % poly(ethylenimine) using a Brandel 48 - channel cell harvester. The vials were rinsed three times with 4 ml aliquots of ice-cold Tris buffer (25 mM, pH 7.4). Thus, the bound and the free radioligands were separated. The filters are punched out, transferred in 4 ml scintillations vials and filled with 2.5 ml Ultima Gold Cocktail. The samples are left to incubate with scintillation fluid, long enough (> than 9 hours) for the tritium to diffuse out of the filter and interact with the scintillator. The radioactivity was measured, 1 minute per sample, using a liquid scintillation counter (LSC) (Tri-Carb 2100 TR, Packard, Dreieich, Germany).

Competition assay using (±)-[^{3}H]epibatidine and rat brain (P2 fraction)

Assays were carried out in HSS at 22°C. Each assay was performed in duplicates. The test substances were dissolved in ethanol (EtOH), dimethylsulfoxide (DMSO) or acetonitrile (ACN) depending on the stability of the substances. A dilution row of 7-9 concentrations of the test compound was prepared. Non-specific binding was determined in the presence of 300 μM (-)nicotine hydrogen tartrate salt. Each assay sample, with a total volume of 0.5 ml contained: 100 μl of membrane protein (60 μg), 100 μl of (±)-[^{3}H]epibatidine (0.5 nM), 100 μl of HSS and 200 μl of a test compound (Tab. V/1.2). The tissue was added last of all and all the components were mixed very well with the help of a vortex. The samples were incubated for 90 min, and the incubation was terminated by vacuum filtration through Whatman GF/B glass fibre

filters, pre-soaked in 1 % poly(ethylenimine) using a Brandel 48 - channel cell harvester. The vials were rinsed three times with 4 ml aliquots of ice-cold Tris buffer (25 mM, pH 7.4). Thus, the bound and the free radioligands were separated. The filters were punched out, transferred in 4 ml scintillations vials and filled with 2.5 ml Ultima Gold Cocktail. The samples were left to incubate with scintillation fluid long enough (> than 9 hours) for the tritium to diffuse out of the filter and interact with the scintillator. The radioactivity was measured, 1 minute per sample, using a liquid scintillation counter (LSC) (Tri-Carb 2100 TR, Packard, Dreieich, Germany).

Table V/1.2: Competition assay with (±)-[^{3}H]epibatidine and rat brain (P2 fraction)

	Parameter	Concentration	Volume
1	Buffer (HSS)		100 µl
2	Radioligand: (±)-[^{3}H]epibatidine	0.5 nM	100 µl
3	Protein: rat brain (P2 fraction)	60 µg/vial	100 µl
4a	Test-compound	Defined concentrations	200 µl
4b	Total binding	Buffer (HSS)	200 µl
4c	Nonspecific binding	(-)nicotine hydrogen tartrate salt (300 µM)	50 µl + 150 µl buffer(HSS)
	Final Volume		500 µl

V/1.5. Radioligand binding studies for α7* nAChR

Saturation assay with [^{3}H]MLA and rat brain (P2 fraction)

Saturation experiments for the α7* subtype were carried out in quadruplicates by incubating rat brain membranes (120 µg protein) at 22 °C for 2.5 h in HSS with concentrations of [^{3}H]MLA ranging between 0.1 and 40 nM (Tab. V/1.3). A dilution series of 11 concentrations was prepared. Nonspecific binding was determined in the presence of MLA (50 µM). Incubations were terminated by rapid filtrations under vacuum through Whatman GF/B filters pre-soaked in 1% poly(ethylenimine). The filters were punched out, transferred in 4 ml Scintillations vials and filled with 2.5 ml

Ultima Gold Cocktail. The samples were allowed to incubate with scintillation fluid long enough (> than 9 hours) for the tritium to diffuse out of the filter and interact with the scintillator. The radioactivity was measured, 1 minute per sample, using a liquid scintillation counter (LSC) (Tri-Carb 2100 TR, Packard, Dreieich, Germany).

Table V/1.3: Saturation assay with [^{3}H]MLA and native rat brain P2 fraction (α7* nAChR)

	Parameter	Concentration	Volume
1	Radioligand: [^{3}H]MLA (S.A. = 20 Ci/mmol)	0.1 nM to 40 nM	100 µl
2	Protein: rat brain, P2 fraction	100-120 µg/vial	100 µl
3a	Total binding	Buffer (HSS)	50 µl
3b	Nonspecific binding	MLA (50 µM)	50 µl
	Final Volume		250 µl

Competition assay with [^{3}H]MLA and rat brain (P2 fraction)

Assays for the α7* subtype were carried out in HSS at 22°C and were performed in quadruplicates following published procedures [349] [355]. Nonspecific binding was determined in the presence of 1 µM MLA (methyllycaconitine). Each assay sample contained 50 µl of the test compound, 100 µl [^{3}H]MLA to achieve a final concentration of 1 nM, and 100 µl re-suspended membranes (Tab. V/1.4). The samples were incubated for 2 hours at 22°C. Incubations were terminated by rapid filtrations under vacuum through Whatman GF/B filters pre-soaked in 1% poly(ethylenimine). The filters were punched out, transferred in 4 ml scintillations vials and filled with 2.5 ml Ultima Gold Cocktail. The samples were left to incubate with scintillation fluid long enough (> than 9 hours) for the tritium to diffuse out of the filter and interact with the scintillator. The radioactivity was measured, 1 minute per sample, using a liquid scintillation counter (LSC) (Tri-Carb 2100 TR, Packard, Dreieich, Germany).

Table V/1.4: Competition assay with [^{3}H]MLA and native rat brain P2 fraction (α7* nAChR)

	Parameter	Concentration	Volume
1	Radioligand: [^{3}H]MLA	1 nM	100 µl
2	Protein: rat brain P2 fraction	100-120 µg/vial	100 µl
3a	Test-Compound	Defined concentrations	50 µl
3b	Total binding	Buffer (HSS)	50 µl
3c	Nonspecific binding	MLA (1 µM)	50 µl
	Final Volume		250 µl

V/1.6. Radioligand binding studies for α3β4*nAChR

Saturation assay with (±)-[^{3}H]epibatidine and native pig and calf adrenal membrane (α3β4* nAChR)

In saturation studies, whole membrane fractions of pig adrenals (60-90 µg protein) were incubated in the presence of 2-2400 pM of (±)-[^{3}H]epibatidine in polypropylene tubes containing HSS. The membranes were incubated at 22 °C for 4 h in a total volume of 4 ml. A dilution series of 11 concentration of the radioligand (±)-[^{3}H]epibatidine was prepared. Nonspecific binding was determined in the presence of 600 µM (-)nicotine hydrogen tartrate salt. The experiments were carried out in quadruplicates (Tab. V/1.5). Incubations were terminated by vacuum filtration through Whatman GF/B glass fibre filters, pre-soaked in 1% poly(ethylenimine) using a Brandel 48 - channel cell harvester. The vials were rinsed three times with 4 ml ice-cold tris buffer, in order to separate the bound and the free radio ligands. The filters were punched out, transferred in 4 ml scintillations vials and filled with 2.5 ml Ultima Gold Cocktail. The samples were left to incubate with scintillation fluid long enough (> than 9 hours) for the tritium to diffuse out of the filter and interact with the scintillator. The radioactivity was measured, 1 minute per sample, using a liquid scintillation counter (LSC) (Tri-Carb 2100 TR, Packard, Dreieich, Germany).

Table V/1.5: Saturation assay with (±)-[^{3}H]epibatidine and native pig and calf adrenal membrane (α3β4*nAChR)

	Parameter	Concentration	Volume
1	Radioligand:(±)-[^{3}H]epibatidine	2 -2400 pM	100 µl
2	Protein: pig and calf adrenals	60 µg/vial	100 µl
3a	Total binding	Buffer (HSS)	2000 µl
3b	Nonspecific binding	(-)nicotine hydrogen tartrate salt (600 µM)	50 µl + 1950 µl (HSS)
	Final Volume		2200 µl

Competition assay with (±)-[^{3}H] epibatidine and native pig and calf adrenal membrane (α3β4*nAChR)

The binding assay was performed following a new procedure. Pig and calf adrenal membranes were prepared following a procedure described in sections V/1.2.3 and V/1.2.4., respectively. On the day of the assay, in order to reduce the presence of the fat, the whole membrane fractions of pig and calf adrenals were washed and then centrifuged (25,000 x g, 10 min., 4°C). Dilution series of tested compounds (200 µl) were put in the tubes. (±)-[^{3}H]Epibatidine (100 µl) and the tissue (100 µl) were added (Tab. V/1.6). The nonspecific binding was determined in the presence of 600 µM (-)-nicotine hydrogen tartrate salt. Each assay was performed in duplicates. After incubation (90 min), the samples were filtrated through Whatman GF/B glass fibre filters; pre-soaked for 20 minutes in 1 % poly(ethylenimine). The filters were punched out, transferred in 4 ml scintillations vials and filled with 2.5 ml Ultima Gold Cocktail. The samples were left to incubate with scintillation fluid long enough (> than 9 hours) for the tritium to diffuse out of the filter and interact with the scintillator. The radioactivity was measured, 1 minute per sample, using a liquid scintillation counter (LSC) (Tri-Carb 2100 TR, Packard, Dreieich, Germany).

Table V/1.6: Competition assay with (±)-[^{3}H]epibatidine and native pig and calf adrenal membranes (α3β4*nAChR)

	Parameter	Concentration	Volume
1	Radioligand (±)-[^{3}H]epibatidine	0.5 nM	100 µl
2	Protein: whole membrane fractions of pig or calf adrenals	60 µg/vial	100 µl
3	Buffer	(HSS)	100 µl
4a	Test-Compound	Defined concentrations	200 µl
4b	Total binding	Buffer (HSS)	200µl
4c	Nonspecific binding	(-)nicotine hydrogen tartrate salt (600 µM)	50 µl + 150 µl (HSS)
	Final Volume		500 µl

V/1.7. Radioligand binding studies for $(\alpha 1)_2\beta 1\gamma\delta$ nAChR

Competition assay with (±)-[^{3}H]epibatidine and Torpedo Californica electroplax

Assays were carried out in HSS at 22°C. Each assay was performed in duplicates. Nonspecific binding was determined in the presence of 300 µM (-)-nicotine hydrogen tartrate salt. Membranes were incubated for 90 min in 0.5 ml HSS containing 2 nM (±)-[^{3}H]epibatidine and different concentrations of test compounds (Tab. V/1.76). The reaction was terminated by vacuum filtration through Whatman GF/B glass fibre filters, pre-soaked in 1% poly(ethylenimine) using a Brandel 48 - channel cell harvester. The filters were punched out, transferred in 4 ml scintillations vials and filled with 2.5 ml Ultima Gold Cocktail. The samples were left to incubate with scintillation fluid long enough (> than 9 hours) for the tritium to diffuse out of the filter and interact with the scintillator. The radioactivity was measured, 1 minute per sample, using a liquid scintillation counter (LSC) (Tri-Carb 2100 TR; Packard, Dreieich, Germany).

Table V/1.7: Competition assay with (±)-[^{3}H]epibatidine and Torpedo Californica Electroplax

	Parameter	Concentration	Volume
1	Buffer (HSS)		100 µl
2	Radioligand: (±)-[^{3}H]epibatidine	2 nM	100 µl
3	Protein: Torpedo Californica	60 µg/vial	100 µl
4a	Test Compound	Defined concentrations	200 µl
4b	Total binding	Buffer (HSS)	200 µl
4c	Nonspecific binding	(-)nicotine hydrogen tartrate salt (300 µM)	50 µl + 150 µl buffer (HSS)
	Final Volume		500 µl

V/1.8. Analysis of data

V/1.8.1. Competition experiments

The competition binding data was analysed using non-linear regression analysis. The K_i values were derived from measured IC_{50} and K_D values by the Cheng-Prusoff equation ($K_i = IC_{50}/(1 + F/K_D)$[276] where F is the concentration of unbound radioligand. The K_D value is 0.01 nM for binding of (±)-[^{3}H]epibatidine to α4β2*, the K_D value is 0.05 nM for binding of (±)-[^{3}H]epibatidine to α3β4*. The K_D value is 2 nM for binding of (±)-[^{3}H]epibatidine to muscle type nAChR and the K_D value is 1 nM for [^{3}H]MLA.

V/1.8.2. Saturation experiments

Data of the binding saturation experiments was analysed using Scatchard-Rosenthal plot (linear regression analysis). The K_D values were obtained from experiments performed in quadruplicate on the membrane preparations that were used for the competition assays.

VI. Abbreviations

α	Intrinsic activity
ABT-089	2-methyl-3-((S)-1-pyrrolidin-2-ylmethoxy)-pyridine
ABT-418	3-methyl-5-((S)-1-methyl-pyrrolidin-2-yl)-isoxazole
ABT-594	5-((R)-1-azetidin-2-ylmethoxy)-2-chloro-pyridine
α-Bgt	α-bungarotoxin
AC	Adenilyl cyclase
ACh	Acetylcholine
AChE	Acetylcholinesterase
AChPB	Acetylcholine binding protein
AD	Alzheimer's Disease
ADHD	Attention deficit hyperactivity disorders
A-85380	3-((R)-1-azetidin-2-ylmethoxy)-pyridine
An 1	Anatoxin-a
ANS	Autonomic nervous system
APLs	Allosterically potentiating ligands
AR-R17779	Spiro[1-azabicyclo[2.2.2]octane-3,5´-oxazolidin-2´-one]
B_{max}	Receptor density
Bq	Bequerel
cAMP	cyclic Adenosine-3´-5´monophosphate
CCh	Carbamoylcholine
CD	Crohn´s disease
Ch	Choline
ChCA	Ccholinergic channel activator
Ci	Curies
Ci/mmol	Curies per mili moles
CNS	Central Nervous System
Cy 1	Cytisine

cpm	Counts/min
DA	Dopamine
DHβE	Dihydro-beta-erythroidine
DMAE	(2-dimethylaminoethyl) phenylcarbamate
DMCC	N,N dimethycarbamoylcholine
DMSO	Dimethylsulfoxide
dpm	Disintegrations per minute
dps	Disintegration per second
DUB-165	(5-pyridyl)-9-azabicyclo[4.2.1.]non-2-ene
E	Efficacy
EC	Electron capture
EPI	(exo-2-(6-chloro-3-pyridyl)-7-azabicyclo-[2.2.1] heptane)
Fe 1	Ferruginine
FLIPR	Fluorescence image plate reader
$GABA_AR$	γ-aminobutyric acid receptor type Areceptors
$GABA_CR$	γ-aminobutyric acid receptor type C receptors
GPCRs	Protein coupled receptor family
GTS-21 (DMXBA)	(3-(2,4)-dimethoxybenzylidine)anabaseine
GluRCl	Chloride permeable glutamate receptors
GlyR	Glycine receptors
H_3	Histamine
HADNFLE	Human autosomal dominant nocturnal frontal lobe epilepsy
HBA	Hydrogen bond acceptor
HBD	Hydrogen bond donator
HEK	Human embryonic kidney
HEPES	N-[2-Hydroxyethyl]piperazine-N´[2-ethanesulfonic acid]
HSS	HEPES-salt solution
5-HT	5-hydroxytryptamine, serotonin

ΔE	Energy emitted
H_3	Histamine
K_D	Dissociation constant
eV	Electron voltage
K_i	Inhibition constant
k_{on}	Rate constant for association
k_{off}	Rate constant of dissociation
KO	Knock Out
K_D	Dissociation constant
IC_{50}	Concentration of the inhibitor required to inhibit the binding by 50%
IBD	Inflammatory bowel disease
L	Ligand
LD_{50}	Lethal Dosis
LGIC	Ligand-gated ion channel
LR	Ligand-receptor complex
LSC	Liquid scintillation counting
mAChR	Muscarinic acetylcholine receptor
MAO-B	Monoamine oxidase B
MCC	Methylcarbamoylcholine
MHb	Media habenula
min	Minutes
MLA	Methyllycaconitine
n	Neutron
nAChR	Nicotinic acetylcholine receptor
NaI	Sodium iodide
NCA	Non competitive antagonist
NCB	Non competitive blockers
n.d.	Not determined

NE	Norepinephrine
nm	Nanometer
nM	Nanomolar
NMDA	N-methyl-D-aspartic acid
NMR	Nuclear magnetic resonance
NMS	N-methyl-scopolamine
NS	Nonspecific
NSAIDs	Non-steroidal anti-inflammatory drugs
p	Proton
PD	Parkinson's Disease
PEI	polyethylenimine
PET	Positron Emission Tomography
PHT	Pyrido[3.4b]homotropane
Pin	Pinnamine
pM	Picomolar
PM	Photomultiplier
PNS	Peripheral nervous system
P2	Second pellet
PX2R	Purinoreceptor
R	Receptor
Rpm	Rounds pro minutes
RT	Room temperature
S	Specific
SDS	Sodium dodecylsulfate
Sec	Seconds
SIB-1508Y	3-Ethynyl-5-((S)-1-methyl-pyrrolidin-2-yl)-pyridine
SIB-1663	7-methoxy-2,3,3a,4,5,9b-hexahydro-1-H-pyrrolo[3,2-h]isoquinoline
SIB-1553A	4-[2-((S)1-methyl-pyrrolidin-2-yl)ethylsulfanyl]phenol
SPECT	Single photon emission computer tomography

Tab.	Table
TB	Total binding
TC-2599	[(E)-4-(5-ethoxy-pyridin-3-yl]-but-3-enyl]methyl-amine
TMAE	3-trimethylaminoethyl phenylcarbamate
TNF	Tumor necrosis factor
$T_{1/2}$	Half life
TRIS	Tris[hydroxymethyl]aminomethane
TRIS-HCl	Tris[hydroxymethyl]aminomethane-hydrochloride
TS	Gilles de la Tourette´s syndrome
UB-165	(2-chloro-5-pyridyl)-9-azabicyclo[4.2.1.]non-2-ene
UC	Ulcerative colitis
UV	Ultraviolet
VIP	Vasoactive intestinal polypeptide
VTA	Ventral tegmental area

VII. References

1. Langley, J. N. . N. Langley. On the reaction of cells and of nerve-endings to certain poisons, chiefly as regards the reaction of striated muscle to nicotine and to curare. *J.Physiol.* **33**, 347-413 (1905).
2. Schild. H.O. Dale and the development of pharmacology**.** *Br. J. Pharmacol.* 56, 3 (1976).
3. Langley, J. N. On nerve endings and on special excitable substances in cells. *Proc. R. Soc. London Ser. B* **78**, 170-184 (1906).
4. Dale. The action of certain esters and ethers of choline, and their relation to muscarine. *J.Pharmacol.Exp.Ther.* **6,** 147-190,(1914).
5. Mc Murry, C. (1995) Fundamentals of General, Organic, and Biological Chemistry, Third Edition.
6. Itier, V. & Bertrand, D. Neuronal nicotinic receptors: from protein structure to function. *FEBS Lett* **504**, 118-25 (2001).
7. Watling, K. J. *The RBI Handbook of Receptor Classification and Signal Transduction* (ed. RBI) (1998).
8. Foye, W. O., T.L. Lemke and D.A. Williams. *Principles of Medicinal Chemistry.* (Williams & Wilkins, 1995).
9. Eglen, R. M., Choppin, A. & Watson, N. Therapeutic opportunities from muscarinic receptor research. *Trends Pharmacol Sci* **22**, 409-14 (2001).
10. www.neurosci.pharm.utoledo.edu/mbc3320/muscarinic.htm.
11. Changeux, J. P. & Edelstein, S. J. Allosteric receptors after 30 years. *Neuron* **21**, 959-80 (1998).
12. Galzi, J. L. & Changeux, J. P. Neuronal nicotinic receptors: molecular organization and regulations. *Neuropharmacology* **34**, 563-82 (1995).
13. Holladay, M. W., Dart, M. J. & Lynch, J. K. Neuronal nicotinic acetylcholine receptors as targets for drug discovery. *J Med Chem* **40**, 4169-94 (1997).
14. Clementi, F., Fornasari, D. & Gotti, C. Neuronal nicotinic receptors, important new players in brain function. *Eur J Pharmacol* **393**, 3-10 (2000).
15. Karlin, A. Emerging structure of the nicotinic acetylcholine receptors. *Nat Rev Neurosci* **3**, 102-14 (2002).
16. Laube B, K. J., Betz H. Evidence for a tetrameric structure of recombinant NMDA receptors. *J Neurosci* **18**, 2954-2961 (1998).
17. Hucho F, W. C. Ligand-gated ion channels. *Angew Chem Int Ed 2001* **40**, 3100-3116 (2001).
18. Utkin Yu, N., Tsetlin, V. I. & Hucho, F. Structural organization of nicotinic acetylcholine receptors. *Membr Cell Biol* **13**, 143-64 (2000).
19. Wilson, G. & Karlin, A. Acetylcholine receptor channel structure in the resting, open, and desensitized states probed with the substituted-cysteine-accessibility method. *Proc Natl Acad Sci U S A* **98**, 1241-8 (2001).
20. Gotti, C., Fornasari, D. & Clementi, F. Human neuronal nicotinic receptors. *Prog Neurobiol* **53**, 199-237 (1997).

21. http://caltest.vet.upenn.edu/poison/plants/pptobac.htm.
22. Haustein, K.-O. in *Deutscher Ärzte-Verlag 2001* (2001).
23. Changeaux, B. D. a. J. Nicotinic receptor: an allosteric protein specialized for intercellular communication. *The Neuroscience* **7**, 75-90 (1995).
24. Arias, H. R. Localization of agonist and competitive antagonist binding sites on nicotinic acetylcholine receptors. *Neurochem Int* **36**, 595-645 (2000).
25. Paterson, D. & Nordberg, A. Neuronal nicotinic receptors in the human brain. *Prog Neurobiol* **61**, 75-111 (2000).
26. Corringer, P. J., Le Novere, N. & Changeux, J. P. Nicotinic receptors at the amino acid level. *Annu Rev Pharmacol Toxicol* **40**, 431-58 (2000).
27. Ortells, M. O. & Lunt, G. G. Evolutionary history of the ligand-gated ion-channel superfamily of receptors. *Trends Neurosci* **18**, 121-7 (1995).
28. Valor, L. M. et al. Role of the large cytoplasmic loop of the alpha 7 neuronal nicotinic acetylcholine receptor subunit in receptor expression and function. *Biochemistry* **41**, 7931-8 (2002).
29. Karlin, A. & Akabas, M. H. Toward a structural basis for the function of nicotinic acetylcholine receptors and their cousins. *Neuron* **15**, 1231-44 (1995).
30. Wonnacott, S. C. G. V. a. Neuronal nicotinic receptors. *Tocris reviews* **19** (2001).
31. Sakmann, B. Nobel Lecture. Elementary steps in synaptic transmission revealed by currents through single ion channels. *Neuron* **8**, 613-29 (1992).
32. Arias, H. R. Topology of ligand binding sites on the nicotinic acetylcholine receptor. *Brain Res Brain Res Rev* **25**, 133-91 (1997).
33. Le Novere, N. & Changeux, J. P. Molecular evolution of the nicotinic acetylcholine receptor: an example of multigene family in excitable cells. *J Mol Evol* **40**, 155-72 (1995).
34. Palma, E., Bertrand, S., Binzoni, T. & Bertrand, D. Neuronal nicotinic alpha 7 receptor expressed in Xenopus oocytes presents five putative binding sites for methyllycaconitine. *J Physiol* **491 (Pt 1)**, 151-61 (1996).
35. Chen, S. J., Spathis, R. & Schmidt, J. Binding sites for [3H]-acetylcholine and 125I-alpha-bungarotoxin in the optic ganglion of Loligo pealii. *Comp Biochem Physiol C* **90**, 317-23 (1988).
36. Raftery, M. A., Vandlen, R. L., Reed, K. L. & Lee, T. Characterization of Torpedo californica acetylcholine receptor: its subunit composition and ligand-binding properties. *Cold Spring Harb Symp Quant Biol* **40**, 193-202 (1976).
37. Salpeter, M. M. & Loring, R. H. Nicotinic acetylcholine receptors in vertebrate muscle: properties, distribution and neural control. *Prog Neurobiol* **25**, 297-325 (1985).
38. Sargent, P. B. The diversity of neuronal nicotinic acetylcholine receptors. *Annu Rev Neurosci* **16**, 403-43 (1993).
39. Hogg, R. C., Raggenbass, M. & Bertrand, D. Nicotinic acetylcholine receptors: from structure to brain function. *Rev Physiol Biochem Pharmacol* **147**, 1-46 (2003).

40. Lukas, R. J. et al. International Union of Pharmacology. XX. Current status of the nomenclature for nicotinic acetylcholine receptors and their subunits. *Pharmacol Rev* **51**, 397-401 (1999).
41. Elgoyhen, A. B. et al. alpha10: a determinant of nicotinic cholinergic receptor function in mammalian vestibular and cochlear mechanosensory hair cells. *Proc Natl Acad Sci U S A* **98**, 3501-6 (2001).
42. McGehee, D. S. & Role, L. W. Physiological diversity of nicotinic acetylcholine receptors expressed by vertebrate neurons. *Annu Rev Physiol* **57**, 521-46 (1995).
43. Parker, M. J., Beck, A. & Luetje, C. W. Neuronal nicotinic receptor beta2 and beta4 subunits confer large differences in agonist binding affinity. *Mol Pharmacol* **54**, 1132-9 (1998).
44. Ramirez-Latorre, J. et al. Functional contributions of alpha5 subunit to neuronal acetylcholine receptor channels. *Nature* **380**, 347-51 (1996).
45. Boorman, J. P., Groot-Kormelink, P. J. & Sivilotti, L. G. Stoichiometry of human recombinant neuronal nicotinic receptors containing the b3 subunit expressed in Xenopus oocytes. *J Physiol* **529 Pt 3**, 565-77 (2000).
46. Wada, E. et al. Distribution of alpha 2, alpha 3, alpha 4, and beta 2 neuronal nicotinic receptor subunit mRNAs in the central nervous system: a hybridization histochemical study in the rat. *J Comp Neurol* **284**, 314-35 (1989).
47. Deneris, E. S., Boulter, J., Swanson, L. W., Patrick, J. & Heinemann, S. Beta 3: a new member of nicotinic acetylcholine receptor gene family is expressed in brain. *J Biol Chem* **264**, 6268-72 (1989).
48. Anand, R., Conroy, W. G., Schoepfer, R., Whiting, P. & Lindstrom, J. Neuronal nicotinic acetylcholine receptors expressed in Xenopus oocytes have a pentameric quaternary structure. *J Biol Chem* **266**, 11192-8 (1991).
49. Elgoyhen, A. B., Johnson, D. S., Boulter, J., Vetter, D. E. & Heinemann, S. Alpha 9: an acetylcholine receptor with novel pharmacological properties expressed in rat cochlear hair cells. *Cell* **79**, 705-15 (1994).
50. Gotti, C. et al. Pharmacology and biophysical properties of alpha 7 and alpha 7-alpha 8 alpha-bungarotoxin receptor subtypes immunopurified from the chick optic lobe. *Eur J Neurosci* **6**, 1281-91 (1994).
51. Gerzanich, V., Anand, R. & Lindstrom, J. Homomers of alpha 8 and alpha 7 subunits of nicotinic receptors exhibit similar channel but contrasting binding site properties. *Mol Pharmacol* **45**, 212-20 (1994).
52. Unwin, N. Acetylcholine receptor channel imaged in the open state. *Nature* **373**, 37-43 (1995).
53. Corringer, P. J. et al. Identification of a new component of the agonist binding site of the nicotinic alpha 7 homooligomeric receptor. *J Biol Chem* **270**, 11749-52 (1995).
54. Grutter, T. & Changeux, J. P. Nicotinic receptors in wonderland. *Trends Biochem Sci* **26**, 459-63 (2001).
55. Dennis A. Dougherty, H. A. L. "Snails, synapses and smokers". *Nature* **411**, 252-254 (17 May 2001).

56. Smit, A. B. et al. A glia-derived acetylcholine-binding protein that modulates synaptic transmission. *Nature* **411**, 261-8 (2001).
57. Brejc, K. et al. Crystal structure of an ACh-binding protein reveals the ligand-binding domain of nicotinic receptors. *Nature* **411**, 269-76 (2001).
58. Pereira, E. F., Reinhardt-Maelicke, S., Schrattenholz, A., Maelicke, A. & Albuquerque, E. X. Identification and functional characterization of a new agonist site on nicotinic acetylcholine receptors of cultured hippocampal neurons. *J Pharmacol Exp Ther* **265**, 1474-91 (1993).
59. Pereira, E. F. et al. Unconventional ligands and modulators of nicotinic receptors. *J Neurobiol* **53**, 479-500 (2002).
60. Samochocki, M. et al. Galantamine is an allosterically potentiating ligand of the human alpha4/beta2 nAChR. *Acta Neurol Scand Suppl* **176**, 68-73 (2000).
61. Maelicke, A. & Albuquerque, E. X. Allosteric modulation of nicotinic acetylcholine receptors as a treatment strategy for Alzheimer's disease. *Eur J Pharmacol* **393**, 165-70 (2000).
62. Maelicke, A., Schrattenholz, A., Samochocki, M., Radina, M. & Albuquerque, E. X. Allosterically potentiating ligands of nicotinic receptors as a treatment strategy for Alzheimer's disease. *Behav Brain Res* **113**, 199-206 (2000).
63. Krause, R. M. et al. Ivermectin: a positive allosteric effector of the alpha7 neuronal nicotinic acetylcholine receptor. *Mol Pharmacol* **53**, 283-94 (1998).
64. Valenzuela, C. F., Dowding, A. J., Arias, H. R. & Johnson, D. A. Antibody-induced conformational changes in the Torpedo nicotinic acetylcholine receptor: a fluorescence study. *Biochemistry* **33**, 6586-94 (1994).
65. Lopez, M. G. et al. The nicotinic acetylcholine receptor of the bovine chromaffin cell, a new target for dihydropyridines. *Eur J Pharmacol* **247**, 199-207 (1993).
66. Valera, S., Ballivet, M. & Bertrand, D. Progesterone modulates a neuronal nicotinic acetylcholine receptor. *Proc Natl Acad Sci U S A* **89**, 9949-53 (1992).
67. Katz, B. & Thesleff, S. A study of the desensitization produced by acetylcholine at the motor end-plate. *J Physiol* **138**, 63-80 (1957).
68. Monod, J., Wyman, J. & Changeux, J. P. On the Nature of Allosteric Transitions: A Plausible Model. *J Mol Biol* **12**, 88-118 (1965).
69. Creese, I. & Sibley, D. R. Receptor adaptations to centrally acting drugs. *Annu Rev Pharmacol Toxicol* **21**, 357-91 (1981).
70. Buisson, B. & Bertrand, D. Nicotine addiction: the possible role of functional upregulation. *Trends Pharmacol Sci* **23**, 130-6 (2002).
71. Wang, F. et al. Chronic nicotine treatment up-regulates human alpha3 beta2 but not alpha3 beta4 acetylcholine receptors stably transfected in human embryonic kidney cells. *J Biol Chem* **273**, 28721-32 (1998).
72. Bohler, S. et al. Desensitization of neuronal nicotinic acetylcholine receptors conferred by N-terminal segments of the beta 2 subunit. *Biochemistry* **40**, 2066-74 (2001).
73. Nguyen, H. N., Rasmussen, B. A. & Perry, D. C. Subtype-selective up-regulation by chronic nicotine of high-affinity nicotinic receptors in rat brain

demonstrated by receptor autoradiography. *J Pharmacol Exp Ther* **307**, 1090-7 (2003).

74. Zoli, M., Lena, C., Picciotto, M. R. & Changeux, J. P. Identification of four classes of brain nicotinic receptors using beta2 mutant mice. *J Neurosci* **18**, 4461-72 (1998).
75. Marks, M. J., Stitzel, J. A., Romm, E., Wehner, J. M. & Collins, A. C. Nicotinic binding sites in rat and mouse brain: comparison of acetylcholine, nicotine, and alpha-bungarotoxin. *Mol Pharmacol* **30**, 427-36 (1986).
76. Clarke, P. B., Hamill, G. S., Nadi, N. S., Jacobowitz, D. M. & Pert, A. 3H-nicotine- and 125I-alpha-bungarotoxin-labeled nicotinic receptors in the interpeduncular nucleus of rats. II. Effects of habenular deafferentation. *J Comp Neurol* **251**, 407-13 (1986).
77. Clarke, P. B., Schwartz, R. D., Paul, S. M., Pert, C. B. & Pert, A. Nicotinic binding in rat brain: autoradiographic comparison of [3H]acetylcholine, [3H]nicotine, and [125I]-alpha-bungarotoxin. *J Neurosci* **5**, 1307-15 (1985).
78. Wang, D. X. & Abood, L. G. Expression and characterization of the rat alpha 4 beta 2 neuronal nicotinic cholinergic receptor in baculovirus-infected insect cells. *J Neurosci Res* **44**, 350-4 (1996).
79. Conroy, W. G. & Berg, D. K. Neurons can maintain multiple classes of nicotinic acetylcholine receptors distinguished by different subunit compositions. *J Biol Chem* **270**, 4424-31 (1995).
80. Perry, E. et al. Nicotinic receptor subtypes in human brain ageing, Alzheimer and Lewy body diseases. *Eur J Pharmacol* **393**, 215-22 (2000).
81. Le Novere, N., Zoli, M. & Changeux, J. P. Neuronal nicotinic receptor alpha 6 subunit mRNA is selectively concentrated in catecholaminergic nuclei of the rat brain. *Eur J Neurosci* **8**, 2428-39 (1996).
82. Champtiaux, N. et al. Subunit composition of functional nicotinic receptors in dopaminergic neurons investigated with knock-out mice. *J Neurosci* **23**, 7820-9 (2003).
83. Flores, C. M., DeCamp, R. M., Kilo, S., Rogers, S. W. & Hargreaves, K. M. Neuronal nicotinic receptor expression in sensory neurons of the rat trigeminal ganglion: demonstration of alpha3beta4, a novel subtype in the mammalian nervous system. *J Neurosci* **16**, 7892-901 (1996).
84. Gerzanich, V., Wang, F., Kuryatov, A. & Lindstrom, J. alpha 5 Subunit alters desensitization, pharmacology, Ca^{++} permeability and Ca^{++} modulation of human neuronal alpha 3 nicotinic receptors. *J Pharmacol Exp Ther* **286**, 311-20 (1998).
85. Wang, N. et al. Autonomic function in mice lacking alpha5 neuronal nicotinic acetylcholine receptor subunit. *J Physiol* **542**, 347-54 (2002).
86. Seguela, P., Wadiche, J., Dineley-Miller, K., Dani, J. A. & Patrick, J. W. Molecular cloning, functional properties, and distribution of rat brain alpha 7: a nicotinic cation channel highly permeable to calcium. *J Neurosci* **13**, 596-604 (1993).

87. Poth, K. et al. Heterogeneity of nicotinic receptor class and subunit mRNA expression among individual parasympathetic neurons from rat intracardiac ganglia. *J Neurosci* **17**, 586-96 (1997).
88. Xu, W. et al. Megacystis, mydriasis, and ion channel defect in mice lacking the alpha3 neuronal nicotinic acetylcholine receptor. *Proc Natl Acad Sci U S A* **96**, 5746-51 (1999).
89. Xu, W. et al. Multiorgan autonomic dysfunction in mice lacking the beta2 and the beta4 subunits of neuronal nicotinic acetylcholine receptors. *J Neurosci* **19**, 9298-305 (1999).
90. De Biasi, M., Nigro, F. & Xu, W. Nicotinic acetylcholine receptors in the autonomic control of bladder function. *Eur J Pharmacol* **393**, 137-40 (2000).
91. Ji, S. et al. Differential rate responses to nicotine in rat heart: evidence for two classes of nicotinic receptors. *J Pharmacol Exp Ther* **301**, 893-9 (2002).
92. De Biasi, M. Nicotinic mechanisms in the autonomic control of organ systems. *J Neurobiol* **53**, 568-79 (2002).
93. Richardson, C. E. et al. Megacystis-microcolon-intestinal hypoperistalsis syndrome and the absence of the alpha3 nicotinic acetylcholine receptor subunit. *Gastroenterology* **121**, 350-7 (2001).
94. Grando, S. A. Biological functions of keratinocyte cholinergic receptors. *J Investig Dermatol Symp Proc* **2**, 41-8 (1997).
95. Maus, A. D. et al. Human and rodent bronchial epithelial cells express functional nicotinic acetylcholine receptors. *Mol Pharmacol* **54**, 779-88 (1998).
96. Nguyen, V. T. et al. Choline acetyltransferase, acetylcholinesterase, and nicotinic acetylcholine receptors of human gingival and esophageal epithelia. *J Dent Res* **79**, 939-49 (2000).
97. Skok, M. V. et al. Functional nicotinic acetylcholine receptors are expressed in B lymphocyte-derived cell lines. *Mol Pharmacol* **64**, 885-9 (2003).
98. Baker, E. R., Zwart, R., Sher, E. & Millar, N. S. Pharmacological properties of alpha9alpha10 nicotinic acetylcholine receptors revealed by heterologous expression of subunit chimeras. *Mol Pharmacol* **65**, 453-60 (2004).
99. Macklin, K. D., Maus, A. D., Pereira, E. F., Albuquerque, E. X. & Conti-Fine, B. M. Human vascular endothelial cells express functional nicotinic acetylcholine receptors. *J Pharmacol Exp Ther* **287**, 435-9 (1998).
100. Labarca, C. et al. Point mutant mice with hypersensitive alpha 4 nicotinic receptors show dopaminergic deficits and increased anxiety. *Proc Natl Acad Sci U S A* **98**, 2786-91 (2001).
101. Picciotto, M. R. et al. Abnormal avoidance learning in mice lacking functional high-affinity nicotine receptor in the brain. *Nature* **374**, 65-7 (1995).
102. Marubio, L. M. et al. Reduced antinociception in mice lacking neuronal nicotinic receptor subunits. *Nature* **398**, 805-10 (1999).
103. Ross, S. A. et al. Phenotypic characterization of an alpha 4 neuronal nicotinic acetylcholine receptor subunit knock-out mouse. *J Neurosci* **20**, 6431-41 (2000).

104. Champtiaux, N. et al. Distribution and pharmacology of alpha 6-containing nicotinic acetylcholine receptors analyzed with mutant mice. *J Neurosci* **22**, 1208-17 (2002).
105. Franceschini, D. et al. Absence of alpha7-containing neuronal nicotinic acetylcholine receptors does not prevent nicotine-induced seizures. *Brain Res Mol Brain Res* **98**, 29-40 (2002).
106. Vetter, D. E. et al. Role of alpha9 nicotinic ACh receptor subunits in the development and function of cochlear efferent innervation. *Neuron* **23**, 93-103 (1999).
107. Zoli, M., Picciotto, M. R., Ferrari, R., Cocchi, D. & Changeux, J. P. Increased neurodegeneration during ageing in mice lacking high-affinity nicotine receptors. *Embo J* **18**, 1235-44 (1999).
108. Picciotto, M. R. et al. Acetylcholine receptors containing the beta2 subunit are involved in the reinforcing properties of nicotine. *Nature* **391**, 173-7 (1998).
109. Salas, R. et al. The nicotinic acetylcholine receptor subunit alpha 5 mediates short-term effects of nicotine in vivo. *Mol Pharmacol* **63**, 1059-66 (2003).
110. Boorman, J. P., Beato, M., Groot-Kormelink, P. J., Broadbent, S. D. & Sivilotti, L. G. The effects of beta3 subunit incorporation on the pharmacology and single channel properties of oocyte-expressed human alpha3beta4 neuronal nicotinic receptors. *J Biol Chem* **278**, 44033-40 (2003).
111. Whiteaker, P. et al. Involvement of the alpha3 subunit in central nicotinic binding populations. *J Neurosci* **22**, 2522-9 (2002).
112. Lena, C. & Changeux, J. P. Pathological mutations of nicotinic receptors and nicotine-based therapies for brain disorders. *Curr Opin Neurobiol* **7**, 674-82 (1997).
113. Jones, S., Sudweeks, S. & Yakel, J. L. Nicotinic receptors in the brain: correlating physiology with function. *Trends Neurosci* **22**, 555-61 (1999).
114. Whitehouse, P. J. et al. Reductions in [3H]nicotinic acetylcholine binding in Alzheimer's disease and Parkinson's disease: an autoradiographic study. *Neurology* **38**, 720-3 (1988).
115. Coyle, J. T., McKinney, M., Johnston, M. V. & Hedreen, J. C. Synaptic neurochemistry of the basal forebrain cholinergic projection. *Psychopharmacol Bull* **19**, 441-7 (1983).
116. Steinlein, O. K. et al. An insertion mutation of the CHRNA4 gene in a family with autosomal dominant nocturnal frontal lobe epilepsy. *Hum Mol Genet* **6**, 943-7 (1997).
117. Freedman, R., Hall, M., Adler, L. E. & Leonard, S. Evidence in postmortem brain tissue for decreased numbers of hippocampal nicotinic receptors in schizophrenia. *Biol Psychiatry* **38**, 22-33 (1995).
118. Decker, M. W. et al. The role of neuronal nicotinic acetylcholine receptors in antinociception: effects of ABT-594. *J Physiol Paris* **92**, 221-4 (1998).
119. Lloyd, G. K. & Williams, M. Neuronal nicotinic acetylcholine receptors as novel drug targets. *J Pharmacol Exp Ther* **292**, 461-7 (2000).
120. Peto, R. et al. Mortality from smoking worldwide. *Br Med Bull* **52**, 12-21 (1996).

121. Dani, J. A., Ji, D. & Zhou, F. M. Synaptic plasticity and nicotine addiction. *Neuron* **31**, 349-52 (2001).
122. Henningfield, J. E., Miyasato, K. & Jasinski, D. R. Abuse liability and pharmacodynamic characteristics of intravenous and inhaled nicotine. *J Pharmacol Exp Ther* **234**, 1-12 (1985).
123. Gentry, C. L. & Lukas, R. J. Regulation of nicotinic acetylcholine receptor numbers and function by chronic nicotine exposure. *Curr Drug Target CNS Neurol Disord* **1**, 359-85 (2002).
124. Rose, J. E. & Corrigall, W. A. Nicotine self-administration in animals and humans: similarities and differences. *Psychopharmacology (Berl)* **130**, 28-40 (1997).
125. Laviolette, S. R. & Van Der Kooy, D. The neurobiology of nicotine addiction: bridging the gap from molecules to behaviour. *Nat Rev Neurosci* **5**, 55-65 (2004).
126. Selkoe, D. J. Normal and abnormal biology of the beta-amyloid precursor protein. *Annu Rev Neurosci* **17**, 489-517 (1994).
127. Selkoe, D. J. Alzheimer's disease: genes, proteins, and therapy. *Physiol Rev* **81**, 741-66 (2001).
128. Neve, R. L., McPhie, D. L. & Chen, Y. Alzheimer's disease: a dysfunction of the amyloid precursor protein(1). *Brain Res* **886**, 54-66 (2000).
129. Terry, A. V., Jr. & Buccafusco, J. J. The cholinergic hypothesis of age and Alzheimer's disease-related cognitive deficits: recent challenges and their implications for novel drug development. *J Pharmacol Exp Ther* **306**, 821-7 (2003).
130. Schroder, H., Giacobini, E., Struble, R. G., Zilles, K. & Maelicke, A. Nicotinic cholinoceptive neurons of the frontal cortex are reduced in Alzheimer's disease. *Neurobiol Aging* **12**, 259-62 (1991).
131. Mustazza, C. et al. Synthesis and cholinesterase activity of phenylcarbamates related to Rivastigmine, a therapeutic agent for Alzheimer's disease. *Eur J Med Chem* **37**, 91-109 (2002).
132. Potter, A. et al. Acute effects of the selective cholinergic channel activator (nicotinic agonist) ABT-418 in Alzheimer's disease. *Psychopharmacology (Berl)* **142**, 334-42 (1999).
133. Newhouse, P. A. & Kelton, M. Nicotinic systems in central nervous systems disease: degenerative disorders and beyond. *Pharm Acta Helv* **74**, 91-101 (2000).
134. Quik, M. & Jeyarasasingam, G. Nicotinic receptors and Parkinson's disease. *Eur J Pharmacol* **393**, 223-30 (2000).
135. Morens, D. M., Grandinetti, A., Reed, D., White, L. R. & Ross, G. W. Cigarette smoking and protection from Parkinson's disease: false association or etiologic clue? *Neurology* **45**, 1041-51 (1995).
136. Fowler Joanna S., J. L., Gene-Jack Wang, Nora D. Volkow, Frank Telang, Wei Zhu, Dinko Franceschi, Naomi Pappas, Richard Ferrieri, Colleen Shea, Victor Garza, Youwen Xu, David Schlyer, S. John Gatley, Yu-Shin Ding, David Alexoff, Donald Warner, Noelwah Netusil, Pauline Carter, Millard Jayne,

Payton King, and Paul Vaska. Low monoamine oxidase B in peripheral organs in smokers. *PNSA* **20**, 11600-11605 (2003).

137. Arroyo-Jim nez, M. M. et al. Ultrastructural localization of the alpha4-subunit of the neuronal acetylcholine nicotinic receptor in the rat substantia nigra. *J Neurosci* **19**, 6475-87 (1999).
138. Schneider, J. S., Tinker, J. P., Van Velson, M., Menzaghi, F. & Lloyd, G. K. Nicotinic acetylcholine receptor agonist SIB-1508Y improves cognitive functioning in chronic low-dose MPTP-treated monkeys. *J Pharmacol Exp Ther* **290**, 731-9 (1999).
139. Jonnala, R. R. & Buccafusco, J. J. Relationship between the increased cell surface alpha7 nicotinic receptor expression and neuroprotection induced by several nicotinic receptor agonists. *J Neurosci Res* **66**, 565-72 (2001).
140. Court, J. et al. Neuronal nicotinic receptors in dementia with Lewy bodies and schizophrenia: alpha-bungarotoxin and nicotine binding in the thalamus. *J Neurochem* **73**, 1590-7 (1999).
141. Silver, A. A. et al. Transdermal nicotine and haloperidol in Tourette's disorder: a double-blind placebo-controlled study. *J Clin Psychiatry* **62**, 707-14 (2001).
142. Sanberg, P. R. et al. Nicotine gum and haloperidol in Tourette's syndrome. *Lancet* **1**, 592 (1988).
143. Sanberg, P. R., Shytle, R. D. & Silver, A. A. Treatment of Tourette's syndrome with mecamylamine. *Lancet* **352**, 705-6 (1998).
144. Sanberg, P. R. et al. Nicotine for the treatment of Tourette's syndrome. *Pharmacol Ther* **74**, 21-5 (1997).
145. Olale, F., Gerzanich, V., Kuryatov, A., Wang, F. & Lindstrom, J. Chronic nicotine exposure differentially affects the function of human alpha3, alpha4, and alpha7 neuronal nicotinic receptor subtypes. *J Pharmacol Exp Ther* **283**, 675-83 (1997).
146. Leonard, S. et al. Smoking and schizophrenia: abnormal nicotinic receptor expression. *Eur J Pharmacol* **393**, 237-42 (2000).
147. Lohr, J. B. & Flynn, K. Smoking and schizophrenia. *Schizophr Res* **8**, 93-102 (1992).
148. Dalack, G. W. & Meador-Woodruff, J. H. Smoking, smoking withdrawal and schizophrenia: case reports and a review of the literature. *Schizophr Res* **22**, 133-41 (1996).
149. Freedman, R. et al. Linkage of a neurophysiological deficit in schizophrenia to a chromosome 15 locus. *Proc Natl Acad Sci U S A* **94**, 587-92 (1997).
150. Marubio, L. M. & Changeux, J. Nicotinic acetylcholine receptor knockout mice as animal models for studying receptor function. *Eur J Pharmacol* **393**, 113-21 (2000).
151. Steinlein, O. K. et al. Neuronal nicotinic acetylcholine receptor alpha 4 subunit (CHRNA4) and panic disorder: an association study. *Am J Med Genet* **74**, 199-201 (1997).
152. Steinlein, O. K. Neuronal nicotinic receptors in human epilepsy. *Eur J Pharmacol* **393**, 243-7 (2000).

153. Barrantes, F. J., Aztiria, E., Rauschemberger, M. B. & Vasconsuelo, A. The neuronal nicotinic acetylcholine receptor in some hereditary epilepsies. *Neurochem Res* **25**, 583-90 (2000).
154. Scheffer, I. E. et al. Autosomal dominant frontal epilepsy misdiagnosed as sleep disorder. *Lancet* **343**, 515-7 (1994).
155. Covey, L. S., Glassman, A. H. & Stetner, F. Cigarette smoking and major depression. *J Addict Dis* **17**, 35-46 (1998).
156. Hughes JR, S. L., Lancaster T. antidepressant for smoking cessation. *Cochrane Database Syst. Rev.* **1** (2003).
157. Badio, B. & Daly, J. W. Epibatidine, a potent analgetic and nicotinic agonist. *Mol Pharmacol* **45**, 563-9 (1994).
158. Holladay, M. W. et al. Structure-activity studies related to ABT-594, a potent nonopioid analgesic agent: effect of pyridine and azetidine ring substitutions on nicotinic acetylcholine receptor binding affinity and analgesic activity in mice. *Bioorg Med Chem Lett* **8**, 2797-802 (1998).
159. Bannon, A. W. et al. ABT-594 [(R)-5-(2-azetidinylmethoxy)-2-chloropyridine]: a novel, orally effective antinociceptive agent acting via neuronal nicotinic acetylcholine receptors: II. In vivo characterization. *J Pharmacol Exp Ther* **285**, 787-94 (1998).
160. Tracey, K. J. The inflammatory reflex. *Nature* **420**, 853-9 (2002).
161. Thomas, G. A., Rhodes, J., Green, J. T. & Richardson, C. Role of smoking in inflammatory bowel disease: implications for therapy. *Postgrad Med J* **76**, 273-9 (2000).
162. Bernik, T. R. et al. Pharmacological stimulation of the cholinergic antiinflammatory pathway. *J Exp Med* **195**, 781-8 (2002).
163. Wang, H. et al. Nicotinic acetylcholine receptor alpha7 subunit is an essential regulator of inflammation. *Nature* **421**, 384-8 (2003).
164. Jick, H. & Walker, A. M. Cigarette smoking and ulcerative colitis. *N Engl J Med* **308**, 261-3 (1983).
165. Guslandi, M. Nicotine treatment for ulcerative colitis. *Br J Clin Pharmacol* **48**, 481-4 (1999).
166. Thomas, G. A., Rhodes, J. & Green, J. Nicotine and gastrointestinal disease. *Qjm* **89**, 485-8 (1996).
167. Galeazzi, F., Blennerhassett, P. A., Qiu, B., O'Byrne, P. M. & Collins, S. M. Cigarette smoke aggravates experimental colitis in rats. *Gastroenterology* **117**, 877-83 (1999).
168. Brioni, J. D., Decker, M. W., Sullivan, J. P. & Arneric, S. P. The pharmacology of (-)-nicotine and novel cholinergic channel modulators. *Adv Pharmacol* **37**, 153-214 (1997).
169. Champe, R. A. H. a. P. C. (ed.) *Lipincott's Illustrated Reviews: Pharmacology.* (Lipencott Williams & Williams, 2000., 2000).
170. Goodmann, A., Gilman A. *The Pharmacological Basis of Therapeutics* (ed. edition, I.) (NewbYork: McGrow-Hill, 1996).

171. Papke, R. L., Bencherif, M. & Lippiello, P. An evaluation of neuronal nicotinic acetylcholine receptor activation by quaternary nitrogen compounds indicates that choline is selective for the alpha 7 subtype. *Neurosci Lett* **213**, 201-4 (1996).
172. Albuquerque, E. X. et al. Properties of neuronal nicotinic acetylcholine receptors: pharmacological characterization and modulation of synaptic function. *J Pharmacol Exp Ther* **280**, 1117-36 (1997).
173. Whiteaker, P., Sharples, C. G. & Wonnacott, S. Agonist-induced up-regulation of alpha4beta2 nicotinic acetylcholine receptors in M10 cells: pharmacological and spatial definition. *Mol Pharmacol* **53**, 950-62 (1998).
174. De Fiebre, C. M. et al. Characterization of a series of anabaseine-derived compounds reveals that the 3-(4)-dimethylaminocinnamylidine derivative is a selective agonist at neuronal nicotinic alpha 7/125I-alpha-bungarotoxin receptor subtypes. *Mol Pharmacol* **47**, 164-71 (1995).
175. Dunn, S. M. & Raftery, M. A. Agonist binding to the Torpedo acetylcholine receptor. 2. Complexities revealed by association kinetics. *Biochemistry* **36**, 3854-63 (1997).
176. Holton P., H. R. I. *Br J Pharmacol* **4**, 190 (1949).
177. Jensen, A. A. et al. Carbamoylcholine homologs: novel and potent agonists at neuronal nicotinic acetylcholine receptors. *Mol Pharmacol* **64**, 865-75 (2003).
178. Mullen, G. et al. (-)-Spiro[1-azabicyclo[2.2.2]octane-3,5'-oxazolidin-2'-one], a conformationally restricted analogue of acetylcholine, is a highly selective full agonist at the alpha 7 nicotinic acetylcholine receptor. *J Med Chem* **43**, 4045-50 (2000).
179. Gündisch, D., London, E. D., Terry, P., Hill, G. R. & Mukhin, A. G. High affinity binding of [3H]epibatidine to rat brain membranes. *Neuroreport* **10**, 1631-6 (1999).
180. Mukhin, A. G. et al. 5-Iodo-A-85380, an alpha4beta2 subtype-selective ligand for nicotinic acetylcholine receptors. *Mol Pharmacol* **57**, 642-9 (2000).
181. London, E. D., Ball, M. J. & Waller, S. B. Nicotinic binding sites in cerebral cortex and hippocampus in Alzheimer's dementia. *Neurochem Res* **14**, 745-50 (1989).
182. Nordberg, A. et al. Uptake and regional distribution of (+)-(R)- and (-)-(S)-N-[methyl-11C]-nicotine in the brains of rhesus monkey. An attempt to study nicotinic receptors in vivo. *J Neural Transm Park Dis Dement Sect* **1**, 195-205 (1989).
183. Anderson, D. J. & Arneric, S. P. Nicotinic receptor binding of [3H]cytisine, [3H]nicotine and [3H]methylcarbamylcholine in rat brain. *Eur J Pharmacol* **253**, 261-7 (1994).
184. Damaj, M. I., Glassco W.; M.Dukat. Pharmacology of Novel Nicotinic Analogs. *Drug Development Research* **38**, 177-187 (1996).
185. Tonder, J. E. & Olesen, P. H. Agonists at the alpha4beta2 nicotinic acetylcholine receptors: structure-activity relationships and molecular modelling. *Curr Med Chem* **8**, 651-74 (2001).

186. Dukat, M. et al. Functional diversity among 5-substituted nicotine analogs; in vitro and in vivo investigations. *Eur J Pharmacol* **435**, 171-80 (2002).
187. Dukat M., D. M., Damaj M. I., Martin B., El-Zahabi M. A., Glennon R. A.,. Synthesis, receptor binding and QSAR studies on 6-substituted nicotine derivatives as cholinergic ligands. *Eur. J. Med. Chem.* **34**, 31-40 (1999).
188. Schmitt, J. D. Exploring the nature of molecular recognition in nicotinic acetylcholine receptors. *Curr Med Chem* **7**, 749-800 (2000).
189. Ferretti, G. et al. Binding of nicotine and homoazanicotine analogues at neuronal nicotinic acetylcholinergic (nACh) receptors. *Bioorg Med Chem Lett* **13**, 733-5 (2003).
190. Ferretti, G. et al. Homoazanicotine: a structure-affinity study for nicotinic acetylcholine (nACh) receptor binding. *J Med Chem* **45**, 4724-31 (2002).
191. Kim, K. H., Lin, N. H. & Anderson, D. J. Quantitative structure-activity relationships of nicotine analogues as neuronal nicotinic acetylcholine receptor ligands. *Bioorg Med Chem* **4**, 2211-7 (1996).
192. Cosford, N. D. et al. Recombinant human receptors and functional assays in the discovery of altinicline (SIB-1508Y), a novel acetylcholine-gated ion channel (nAChR) agonist. *Pharm Acta Helv* **74**, 125-30 (2000).
193. Sacaan, A. I. et al. Pharmacological characterization of SIB-1765F: a novel cholinergic ion channel agonist. *J Pharmacol Exp Ther* **280**, 373-83 (1997).
194. Menzaghi, F., Whelan, K. T., Risbrough, V. B., Rao, T. S. & Lloyd, G. K. Effects of a novel cholinergic ion channel agonist SIB-1765F on locomotor activity in rats. *J Pharmacol Exp Ther* **280**, 384-92 (1997).
195. Vernier J. M., H. H., Cosford N. D., Whitten J. P., Menzaghi F., Reid R., Rao T. S., Sacaan A. I., Lloyd G. K., Suto C. M., Chavez-Noriega L. E., Washburn M. S., Urrutia A., McDonald I. A., . Conformationally restricted analogues of nicotine and anabasine. *Bioorg. Med. Chem. Lett.* **8**, 2173-2178 (1998).
196. Rao, T. S. et al. In vivo pharmacological characterization of (+/-)-4-[2-(1-methyl-2-pyrrolidinyl)ethyl]thiophenol hydrochloride (SIB-1553A), a novel cholinergic ligand: microdialysis studies. *Brain Res* **986**, 71-81 (2003).
197. Bencherif, M., Bane, A. J., Miller, C. H., Dull, G. M. & Gatto, G. J. TC-2559: a novel orally active ligand selective at neuronal acetylcholine receptors. *Eur J Pharmacol* **409**, 45-55 (2000).
198. Gorham PJ, M. J., Hameer UT, Kim WK. Isolation and toxic strains of Anabaena flos.aquae (Lyngb.). *Breb Vehr Internat Verein Limnol* **15**, 796-804 (1964).
199. Donnelly-Roberts, D. L., Xue, I. C., Arneric, S. P. & Sullivan, J. P. In vitro neuroprotective properties of the novel cholinergic channel activator (ChCA), ABT-418. *Brain Res* **719**, 36-44 (1996).
200. Arneric, S. P. et al. (S)-3-methyl-5-(1-methyl-2-pyrrolidinyl) isoxazole (ABT 418): a novel cholinergic ligand with cognition-enhancing and anxiolytic activities: I. In vitro characterization. *J Pharmacol Exp Ther* **270**, 310-8 (1994).

201. Papke, R. L., Thinschmidt, J. S., Moulton, B. A., Meyer, E. M. & Poirier, A. Activation and inhibition of rat neuronal nicotinic receptors by ABT-418. *Br J Pharmacol* **120**, 429-38 (1997).
202. Abreo, M. A. et al. Novel 3-Pyridyl ethers with subnanomolar affinity for central neuronal nicotinic acetylcholine receptors. *J Med Chem* **39**, 817-25 (1996).
203. Lin, N. H. et al. Structure-activity studies on 2-methyl-3-(2(S)-pyrrolidinylmethoxy) pyridine (ABT-089): an orally bioavailable 3-pyridyl ether nicotinic acetylcholine receptor ligand with cognition-enhancing properties. *J Med Chem* **40**, 385-90 (1997).
204. Decker M. W., B. A. W., Curzon P., Gunther K. L., Brioni J. D., Holladay M. W., Lin N.-H., Li Y., Daanen J. F., Buccafusco J. J., Prendergast M. A., Jackson W. J., Arneric S. P.,. ABT-089 [2-methyl-3-(2-(S)-pyrrolidinylmethoxy)pyridine dihydro-chloride]: II. A novel cholinergic channel modulator with effects on cognitive performance in rats and monkeys. *J. Pharmacol. Exp. Ther.* **283**, 247-258 (1997).
205. Sullivan, J. P. et al. A-85380 [3-(2(S)-azetidinylmethoxy) pyridine]: in vitro pharmacological properties of a novel, high affinity alpha 4 beta 2 nicotinic acetylcholine receptor ligand. *Neuropharmacology* **35**, 725-34 (1996).
206. Boyce, S. et al. Analgesic and toxic effects of ABT-594 resemble epibatidine and nicotine in rats. *Pain* **85**, 443-50 (2000).
207. Kem, W. R. A study of the occurrence of anabaseine in Paranemertes and other nemertines. *Toxicon* **9**, 23-32 (1971).
208. Seeman, J. I. Recent studies in nicotine chemistry.Conformational analysis, chemical reactivity studies, and theoretical modeling. *Heterocycles* **22**, 165-193 (1984).
209. Kem, W. R., Mahnir, V. M., Papke, R. L. & Lingle, C. J. Anabaseine is a potent agonist on muscle and neuronal alpha-bungarotoxin-sensitive nicotinic receptors. *J Pharmacol Exp Ther* **283**, 979-92 (1997).
210. Meyer, E. M., Kuryatov, A., Gerzanich, V., Lindstrom, J. & Papke, R. L. Analysis of 3-(4-hydroxy, 2-Methoxybenzylidene)anabaseine selectivity and activity at human and rat alpha-7 nicotinic receptors. *J Pharmacol Exp Ther* **287**, 918-25 (1998).
211. Papke, R. L., Meyer, E., Nutter, T. & Uteshev, V. V. alpha7 receptor-selective agonists and modes of alpha7 receptor activation. *Eur J Pharmacol* **393**, 179-95 (2000).
212. William R. Kem, V. M. M., 1 Laszlo Prokai, Roger L. Papke, Xuefang Cao,Susan LeFrancois, Kristin Wildeboer, Katalin Prokai-Tatrai, Julia PorterPapke, andFerenc Soti. Hydroxy Metabolites of the Alzheimer's Drug Candidate 3-[(2,4-Dimethoxy)Benzylidene]Anabaseine Dihydrochloride(GTS-21): Their Molecular Properties, Interactions with Brain Nicotinic Receptors, and Brain Penetration. *Molelular Pharmacology* **65**, 56-67 (2004).

213. Flammia, D., Dukat, M., Damaj, M. I., Martin, B. & Glennon, R. A. Lobeline: structure-affinity investigation of nicotinic acetylcholinergic receptor binding. *J Med Chem* **42**, 3726-31 (1999).
214. Damaj, M. I., Patrick, G. S., Creasy, K. R. & Martin, B. R. Pharmacology of lobeline, a nicotinic receptor ligand. *J Pharmacol Exp Ther* **282**, 410-9 (1997).
215. Miller, D. K., Crooks, P. A. & Dwoskin, L. P. Lobeline inhibits nicotine-evoked [(3)H]dopamine overflow from rat striatal slices and nicotine-evoked (86)Rb(+) efflux from thalamic synaptosomes. *Neuropharmacology* **39**, 2654-62 (2000).
216. Glennon, R. A. & Dukat, M. Central nicotinic receptor ligands and pharmacophores. *Pharm Acta Helv* **74**, 103-14 (2000).
217. Dukat, M. & Glennon, R. A. Epibatidine: impact on nicotinic receptor research. *Cell Mol Neurobiol* **23**, 365-78 (2003).
218. Rupniak, N. M. et al. Antinociceptive and toxic effects of (+)-epibatidine oxalate attributable to nicotinic agonist activity. *Br J Pharmacol* **113**, 1487-93 (1994).
219. Whiteaker, P. et al. Pharmacological and null mutation approaches reveal nicotinic receptor diversity. *Eur J Pharmacol* **393**, 123-35 (2000).
220. Davila-Garcia, M. I. et al. [125I]IPH, an epibatidine analog, binds with high affinity to neuronal nicotinic cholinergic receptors. *J Pharmacol Exp Ther* **282**, 445-51 (1997).
221. Whiteaker, P., Jimenez, M., McIntosh, J. M., Collins, A. C. & Marks, M. J. Identification of a novel nicotinic binding site in mouse brain using [(125)I]-epibatidine. *Br J Pharmacol* **131**, 729-39 (2000).
222. Badio, B., Garraffo, H. M., Plummer, C. V., Padgett, W. L. & Daly, J. W. Synthesis and nicotinic activity of epiboxidine: an isoxazole analogue of epibatidine. *Eur J Pharmacol* **321**, 189-94 (1997).
223. Bai, D., Xu, R., Chu, G. & Zhu, X. Synthesis of (+/-)-Epibatidine and Its Analogues. *J Org Chem* **61**, 4600-4606 (1996).
224. Barlocco, D. et al. Mono- and disubstituted-3,8-diazabicyclo[3.2.1]octane derivatives as analgesics structurally related to epibatidine: synthesis, activity, and modeling. *J Med Chem* **41**, 674-81 (1998).
225. Ghelardini, C. G., N.; Barlocco, D.; Bartolini, A. Antinociceptive Profile of the New Nicotinic Agonist DBO-83. *Drug. Dev. Res* **40**, 251-258 (1997).
226. Malpass JR, H., Wallis AL, Fletcher SR, Patel S. . Synthesis and nicotine acetylcholine-binding properties of epibatidine homologues: Homoepibatidine and dihomoepibatidine. *J Chem Soc*, 1044-1050. (2001).
227. Spivak, C. E., Waters, J., Witkop, B. & Albuquerque, E. X. Potencies and channel properties induced by semirigid agonists at frog nicotinic acetylcholine receptors. *Mol Pharmacol* **23**, 337-43 (1983).
228. Gündisch, D. et al. Synthesis and evaluation of diazine containing bioisosteres of (-) -ferruginine as ligands for nicotinic acetylcholine receptors. *Bioorg Med Chem* **9**, 2683-91 (2001).

229. Wright, E. G. T., Sharples C.G.V. Wonnacott S. Synthesis of UB 165: A novel nicotinic Ligand and Anatoxin-a /Epibatidine Hybrid. *Bioorg Med Chem Lett* **7**, 2867-2870 (1997).
230. Imming, P., Klaperski, P., Stubbs, M. T., Seitz, G. & Gündisch, D. Syntheses and evaluation of halogenated cytisine derivatives and of bioisosteric thiocytisine as potent and selective nAChR ligands. *Eur J Med Chem* **36**, 375-88 (2001).
231. Papke, R. L. & Heinemann, S. F. Partial agonist properties of cytisine on neuronal nicotinic receptors containing the beta 2 subunit. *Mol Pharmacol* **45**, 142-9 (1994).
232. Pabreza, L. A., Dhawan, S. & Kellar, K. J. [3H]cytisine binding to nicotinic cholinergic receptors in brain. *Mol Pharmacol* **39**, 9-12 (1991).
233. www.laytonbio.com.
234. www.inversine.com.
235. Bergmeier, S. C., Lapinsky, D. J., Free, R. B. & McKay, D. B. Ring E analogs of methyllycaconitine (MLA) as novel nicotinic antagonists. *Bioorg Med Chem Lett* **9**, 2263-6 (1999).
236. Yum, L., Wolf, K. M. & Chiappinelli, V. A. Nicotinic acetylcholine receptors in separate brain regions exhibit different affinities for methyllycaconitine. *Neuroscience* **72**, 545-55 (1996).
237. Cartier, G. E. et al. A new alpha-conotoxin which targets alpha3beta2 nicotinic acetylcholine receptors. *J Biol Chem* **271**, 7522-8 (1996).
238. Mogg, A. J. et al. Methyllycaconitine is a potent antagonist of alpha-conotoxin-MII-sensitive presynaptic nicotinic acetylcholine receptors in rat striatum. *J Pharmacol Exp Ther* **302**, 197-204 (2002).
239. Davies, A. R. et al. Characterisation of the binding of [3H]methyllycaconitine: a new radioligand for labelling alpha 7-type neuronal nicotinic acetylcholine receptors. *Neuropharmacology* **38**, 679-90 (1999).
240. Chavez-Noriega, L. E. et al. Pharmacological characterization of recombinant human neuronal nicotinic acetylcholine receptors h alpha 2 beta 2, h alpha 2 beta 4, h alpha 3 beta 2, h alpha 3 beta 4, h alpha 4 beta 2, h alpha 4 beta 4 and h alpha 7 expressed in Xenopus oocytes. *J Pharmacol Exp Ther* **280**, 346-56 (1997).
241. Decker, M. W., Brioni, J. D., Bannon, A. W. & Arneric, S. P. Diversity of neuronal nicotinic acetylcholine receptors: lessons from behavior and implications for CNS therapeutics. *Life Sci* **56**, 545-70 (1995).
242. Scarselli, M. et al. NMR structure of alpha-bungarotoxin free and bound to a mimotope of the nicotinic acetylcholine receptor. *Biochemistry* **41**, 1457-63 (2002).
243. Gotti, C. et al. Purification and characterization of an alpha-bungarotoxin receptor that forms a functional nicotinic channel. *Proc Natl Acad Sci U S A* **88**, 3258-62 (1991).

244. Navarro, H. A., Xu, H., Zhong, D., Abraham, P. & Carroll, F. I. In vitro and in vivo characterization of [125I]iodomethyllycaconitine in the rat. *Synapse* **44**, 117-23 (2002).
245. Johnson, D. S., Martinez, J., Elgoyhen, A. B., Heinemann, S. F. & McIntosh, J. M. alpha-Conotoxin ImI exhibits subtype-specific nicotinic acetylcholine receptor blockade: preferential inhibition of homomeric alpha 7 and alpha 9 receptors. *Mol Pharmacol* **48**, 194-9 (1995).
246. Dutton, J. L. et al. A new level of conotoxin diversity, a non-native disulfide bond connectivity in alpha-conotoxin AuIB reduces structural definition but increases biological activity. *J Biol Chem* **277**, 48849-57 (2002).
247. Luo, S. et al. alpha-conotoxin AuIB selectively blocks alpha3 beta4 nicotinic acetylcholine receptors and nicotine-evoked norepinephrine release. *J Neurosci* **18**, 8571-9 (1998).
248. Dwoskin, L. P. & Crooks, P. A. Competitive neuronal nicotinic receptor antagonists: a new direction for drug discovery. *J Pharmacol Exp Ther* **298**, 395-402 (2001).
249. Nicolotti, O., Altomare, C., Pellegrini-Calace, M. & Carotti, A. Neuronal nicotinic acetylcholine receptor agonists: pharmacophores, evolutionary QSAR and 3D-QSAR models. *Curr Top Med Chem* **4**, 335-60 (2004).
250. Barlow, R. B. & Johnson, O. Relations between structure and nicotine-like activity: X-ray crystal structure analysis of (-)-cytisine and (-)-lobeline hydrochloride and a comparison with (-)-nicotine and other nicotine-like compounds. *Br J Pharmacol* **98**, 799-808 (1989).
251. Nicolotti, O., Canu Boido, C., Sparatore, F. & Carotti, A. Cytisine derivatives as high affinity nAChR ligands: synthesis and comparative molecular field analysis. *Farmaco* **57**, 469-78 (2002).
252. Nicolotti, O., Gillet, V. J., Fleming, P. J. & Green, D. V. Multiobjective optimization in quantitative structure-activity relationships: deriving accurate and interpretable QSARs. *J Med Chem* **45**, 5069-80 (2002).
253. Nicolotti, O. et al. Ligands of neuronal nicotinic acetylcholine receptor (nAChR): inferences from the Hansch and 3-D quantitative structure-activity relationship (QSAR) Models. *Curr Med Chem* **9**, 1-29 (2002).
254. Nicolotti, O. et al. Neuronal nicotinic receptor agonists: a multi-approach development of the pharmacophore. *J Comput Aided Mol Des* **15**, 859-72 (2001).
255. Glennon, R. A. & Dukat, M. alpha4beta2 nACh Receptor pharmacophore models. *Bioorg Med Chem Lett* **14**, 1841-1844 (2004).
256. Tonder, J. E., Olesen, P. H., Hansen, J. B., Begtrup, M. & Pettersson, I. An improved nicotinic pharmacophore and a stereoselective CoMFA-model for nicotinic agonists acting at the central nicotinic acetylcholine receptors labelled by. *J Comput Aided Mol Des* **15**, 247-58 (2001).
257. Tonder, J. E. et al. Improving the nicotinic pharmacophore with a series of (Isoxazole)methylene-1-azacyclic compounds: synthesis, structure-activity relationship, and molecular modeling. *J Med Chem* **42**, 4970-80 (1999).

258. Beers, W. H. & Reich, E. Structure and activity of acetylcholine. *Nature* **228**, 917-22 (1970).
259. Sheridan, R. P., Nilakantan, R., Dixon, J. S. & Venkataraghavan, R. The ensemble approach to distance geometry: application to the nicotinic pharmacophore. *J Med Chem* **29**, 899-906 (1986).
260. Glennon, R. A. H., J. L.; Dukat. Epibatidine aided studies towatrds definition of a nicotine receptor pharmacophore. *Med. Chem. Res.*, 461-473 (1994).
261. Koren, A. O. et al. 2-, 5-, and 6-Halo-3-(2(S)-azetidinylmethoxy)pyridines: synthesis, affinity for nicotinic acetylcholine receptors, and molecular modeling. *J Med Chem* **41**, 3690-8 (1998).
262. Dukat, M. et al. (-)6-n-Propylnicotine antagonizes the antinociceptive effects of (-) nicotine. *Bioorg Med Chem Lett* **12**, 3005-7 (2002).
263. Horti, A. G. et al. 6-[18F]fluoro-A-85380, a novel radioligand for in vivo imaging of central nicotinic acetylcholine receptors. *Life Sci* **67**, 463-9 (2000).
264. Wonnacott, S., Jackman, S., Swanson, K. L., Rapoport, H. & Albuquerque, E. X. Nicotinic pharmacology of anatoxin analogs. II. Side chain structure-activity relationships at neuronal nicotinic ligand binding sites. *J Pharmacol Exp Ther* **259**, 387-91 (1991).
265. Yamamura, H. I. Y., R. L. , Hulme. Receptor-Ligand Interactions : A Practical Approach. *ISBN: 0199630917,* **Oxford University Press: New York** (1992).
266. Bylund, D. B. Graphic Presentation and Analysis of Inhibition Data from Ligand-Binding Experiments. *Anal. Biochem.*, 50-57 (1986).
267. Bylund, J. D. D. a. D. B. Basic principles and techniques for Receptor Binding. 1-8 (2002).
268. Bylund, D. B. A Practical Guide for Receptor Binding. *Du Pont Biotech Update*, 19-21 (1983).
269. Hulme E.C., B. N. J. M. 63-174 (Oxford University Press, New York, 1992).
270. J.Wang, Y. H. R. W. in *Receptor ligand interactions a pratical approach* (ed. Hulme) 213-233 (oxford city press, london, 1992).
271. Bylund, D. B. a. T. Radioligand binding methods:practical guide and tips. *Am. J. Physiol.* **265**, 421 (1993).
272. Borea PA, D. A., Varani K, Gilli P, Gilli G. Can Thermodynamic measurements of receptor binding yield information on drug affinity and efficacy? *Biochem Pharmacol* **60**, 1549-1556 (2000).
273. Bylund, D. B. Short Course on Receptor Binding Techniques. *Society for Neuroscience, Cincinnati, Ohio* (1980).
274. Bruns, R. F. L.-W., K.; Pugsley, T. A Rapid Filtration Assay for Soluble Receptors Using Polyethylenimine-treated Filters. *Anal. Biochem* **132** (1983).
275. Rosenthal, H. E. Graphic Method for the Determination and Presentation of Binding Parameters in a Complex System. *Anal. Biochem.* **20**, 525-532 (1967).
276. Cheng, Y. & Prusoff, W. H. Relationship between the inhibition constant (K1) and the concentration of inhibitor which causes 50 per cent inhibition (I50) of an enzymatic reaction. *Biochem Pharmacol* **22**, 3099-108 (1973).
277. Clark, A. *General Pharmacology* (1937).

278. Ariens, E. Affinity and intrinsic activity in the theory of competitive inhibition. *Arch Int Pharmacodyn Ther* **99** (1954).
279. Bradford, M. Rapid and Sensitive Method for Quantisation of Microgram Quantities of Protein Utilizing Principle of Dye-binding. *Anal. Biochem.*, 248-254. (1976).
280. Lowry, O. H. R., N. J.; Farr, A. L.; Randall, R. J. . Protein Measurement with the Folin Phenol Reagent. *J. Biol. Chem*, 265-275 (1951).
281. Xiao, Y. et al. Rat alpha3/beta4 subtype of neuronal nicotinic acetylcholine receptor stably expressed in a transfected cell line: pharmacology of ligand binding and function. *Mol Pharmacol* **54**, 322-33 (1998).
282. Johansson, G. et al. Antimuscarinic 3-(2-furanyl)quinuclidin-2-ene derivatives: synthesis and structure-activity relationships. *J Med Chem* **40**, 3804-19 (1997).
283. Limbeck, M. G., D. Rigidified Choline Analogues as Ligands for Nicotinic Acetylcholine Receptors. *J. Heterocyclic Chem.* **40**, 895 (2003).
284. Alkondon, M., Pereira, E. F., Cortes, W. S., Maelicke, A. & Albuquerque, E. X. Choline is a selective agonist of alpha7 nicotinic acetylcholine receptors in the rat brain neurons. *Eur J Neurosci* **9**, 2734-42 (1997).
285. Houghtling, R. A., Davila-Garcia, M. I. & Kellar, K. J. Characterization of (±)(-)-[3H]epibatidine binding to nicotinic cholinergic receptors in rat and human brain. *Mol Pharmacol* **48**, 280-7 (1995).
286. Houghtling, R. A., Davila-Garcia, M. I., Hurt, S. & Kellar, K. J. [3H]epibatidine binding to nicotinic cholinergic receptors in brain. *Med. Chem. Res.* **4**, 538-546 (1994).
287. Marks, M. J., Smith, K. W. & Collins, A. C. Differential agonist inhibition identifies multiple epibatidine binding sites in mouse brain. *J Pharmacol Exp Ther* **285**, 377-86 (1998).
288. Xu, R., Dwoskin, L. P., Grinevich, V. P., Deaciuc, G. & Crooks, P. A. Neuronal nicotinic acetylcholine receptor binding affinities of boron-containing nicotine analogues. *Bioorg Med Chem Lett* **11**, 1245-8 (2001).
289. Tilotta, M. C. E., G.; Gündisch, D.; Seitz, G. in *XVIIth Int Symp on Med Chem* 273 (Drugs Fut 2002, 27 (Suppl. A), Barcelona, Spain., 2002).
290. Tilotta, M. C. Gündisch., D; Stehl, A.; Seifert, S.; Seitz, G.. In vitro evaluation of novel ferruginine and quinuclidin-2-ene derivatives as ligands for different subtypes of neuronal nicotinic acetylcholine receptors (nAChRs). *Polish-Austrian-German-Hungarian-Italian Joint Meeting on Medicinal Chemistry, Oct 15-18, 2003, Krakow, Poland* (2003).
291. Gündisch, D. A., M.; Munoz, L.; Tilotta, M. C. Synthesis and evaluation of phenylcarbamate derivatives as nicotinic acetylcholine receptor (nAChRs) ligands. *Bioorg & Med Chem* **12**,4953-4962 (2004).
292. Gündisch, D. S., G.; Tilotta, M. C.; Schwarz, S.; Wegge, T.; Klaperski, P.; Seifert, S.; Stehl, A.; Eichler, G.; Munoz, L.; Andrä, M.; Limbeck, M. in *1st UK Nicotinic Receptor Club Meeting* (Lilly Research Centre, Erl Wood Manor, Windlesham, UK, 2003).

293. Zlotos D.P., Gündisch. D., Ferraro S., Tilotta C.M., Stiefl N. and Baumann K. Bisquaternary Caracurine V and iso-Caracurine V Analogues as well as Bisquaternary Dimers of Strychnine as Ligands of the Muscle Type of Nicotinic Acetylcholine Receptors: SAR and QSAR Studies. *Bioorg & Med Chem* (2003).
294. Seifert, S. S., A.; Tilotta, M. C.; Gündisch, D.; Seitz, G. . Novel enantiopure ferrugininoids active as nicotinic agents: Synthesis and radioligand binding studies. *Pharmazie* **59**, 427-434 (2004).
295. Markwell, M. A. K. H., S. M.; Bieber, L. L.; Tolbert, N. E. A Modification of the Lowry Procedure to Simplify Protein Determination in Membrane and Lipoprotein Samples. *Anal. Biochem.* **87**, 206-210 (1978).
296. Criado, M., Alamo, L. & Navarro, A. Primary structure of an agonist binding subunit of the nicotinic acetylcholine receptor from bovine adrenal chromaffin cells. *Neurochem Res* **17**, 281-7 (1992).
297. Garcia-Guzman, M. et al. alpha-Bungarotoxin-sensitive nicotinic receptors on bovine chromaffin cells: molecular cloning, functional expression and alternative splicing of the alpha 7 subunit. *Eur J Neurosci* **7**, 647-55 (1995).
298. Campos-Caro, A. et al. Neuronal nicotinic acetylcholine receptors on bovine chromaffin cells: cloning, expression, and genomic organization of receptor subunits. *J Neurochem* **68**, 488-97 (1997).
299. Wenger, B. W., Bryant, D. L., Boyd, R. T. & McKay, D. B. Evidence for spare nicotinic acetylcholine receptors and a beta 4 subunit in bovine adrenal chromaffin cells: studies using bromoacetylcholine, epibatidine, cytisine and mAb35. *J Pharmacol Exp Ther* **281**, 905-13 (1997).
300. Quick, M. W., Ceballos, R. M., Kasten, M., McIntosh, J. M. & Lester, R. A. Alpha3beta4 subunit-containing nicotinic receptors dominate function in rat medial habenula neurons. *Neuropharmacology* **38**, 769-83 (1999).
301. Cordero-Erausquin, M., Marubio, L. M., Klink, R. & Changeux, J. P. Nicotinic receptor function: new perspectives from knockout mice. *Trends Pharmacol Sci* **21**, 211-7 (2000).
302. Zoli, M., Le Novere, N., Hill, J. A., Jr. & Changeux, J. P. Developmental regulation of nicotinic ACh receptor subunit mRNAs in the rat central and peripheral nervous systems. *J Neurosci* **15**, 1912-39 (1995).
303. Sershen, H., Balla, A., Lajtha, A. & Vizi, E. S. Characterization of nicotinic receptors involved in the release of noradrenaline from the hippocampus. *Neuroscience* **77**, 121-30 (1997).
304. Bryant, D. L. et al. Structure-activity studies with ring E analogues of methyllycaconitine on bovine adrenal alpha3beta4* nicotinic receptors. *Neurosci Res* **42**, 57-63 (2002).
305. Marutle, A., Warpman, U., Bogdanovic, N. & Nordberg, A. Regional distribution of subtypes of nicotinic receptors in human brain and effect of aging studied by (+/-)-[3H]epibatidine. *Brain Res* **801**, 143-9 (1998).
306. Davila-Garcia, M. I., Musachio, J. L. & Kellar, K. J. Chronic nicotine administration does not increase nicotinic receptors labeled by

[125I]epibatidine in adrenal gland, superior cervical ganglia, pineal or retina. *J Neurochem* **85**, 1237-46 (2003).

307. Meyer, E. L., Xiao, Y. & Kellar, K. J. Agonist regulation of rat alpha 3 beta 4 nicotinic acetylcholine receptors stably expressed in human embryonic kidney 293 cells. *Mol Pharmacol* **60**, 568-76 (2001).
308. Stauderman, K. A. et al. Characterization of human recombinant neuronal nicotinic acetylcholine receptor subunit combinations alpha2beta4, alpha3beta4 and alpha4beta4 stably expressed in HEK293 cells. *J Pharmacol Exp Ther* **284**, 777-89 (1998).
309. Free, R. B., Bryant, D. L., McKay, S. B., Kaser, D. J. & McKay, D. B. [3H]Epibatidine binding to bovine adrenal medulla: evidence for alpha3beta4* nicotinic receptors. *Neurosci Lett* **318**, 98-102 (2002).
310. Free, R. B., von Fischer, N. D., Boyd, R. T. & McKay, D. B. Pharmacological characterization of recombinant bovine alpha3beta4 neuronal nicotinic receptors stably expressed in HEK 293 cells. *Neurosci Lett* **343**, 180-4 (2003).
311. Higgins, L. S. & Berg, D. K. A desensitized form of neuronal acetylcholine receptor detected by 3H-nicotine binding on bovine adrenal chromaffin cells. *J Neurosci* **8**, 1436-46 (1988).
312. Hernandez S.C., V. S. a. K. K. J. The functional characteristic of neuronal nicotinic acetylcholine receptors in the rat pineal gland. *Soc.Neurosci. Abstr.* **26**, 105 (2004).
313. Wilson, S. P. N. K. the acetylcholine receptor of the adrenal medulla. *J. Neurochem.* **28**, 687-695 (1977).
314. Schwartz, R. D. & Kellar, K. J. In vivo regulation of [3H]acetylcholine recognition sites in brain by nicotinic cholinergic drugs. *J Neurochem* **45**, 427-33 (1985).
315. Hall, M., Zerbe, L., Leonard, S. & Freedman, R. Characterization of [3H]cytisine binding to human brain membrane preparations. *Brain Res* **600**, 127-33 (1993).
316. Okuda, S. T. K. *Chem.Ind.* **1751** (1961).
317. Goina, T., Radu, A., Petcu, P. & Tamas, M. [Extraction of cytisine]. *Planta Med* **20**, 114-7 (1971).
318. Bojadschiewa, M., Issaev, I., Totev, I. & Dimov, C. [New method for extraction of cytisin from seeds of Cytisus laburnum]. *Pharmazie* **26**, 643 (1971).
319. Sopharma, U. C. (1999).
320. Izaddoost, M., Harris, B. G. & Gracy, R. W. Structure and toxicity of alkaloids and amino acids of Sophora secundiflora. *J Pharm Sci* **65**, 352-4 (1976).
321. Moll, F. K. A. M. M. in *Deutsche Apotheker Zeitung 2001* (2001).
322. http://209.17.131.1/poison.htm.
323. Khan, I. M., Yaksh, T. L. & Taylor, P. Ligand specificity of nicotinic acetylcholine receptors in rat spinal cord: studies with nicotine and cytisine. *J Pharmacol Exp Ther* **270**, 159-66 (1994).

324. Peng, X., Gerzanich, V., Anand, R., Whiting, P. J. & Lindstrom, J. Nicotine-induced increase in neuronal nicotinic receptors results from a decrease in the rate of receptor turnover. *Mol Pharmacol* **46**, 523-30 (1994).
325. Houlihan, L. M. et al. Activity of cytisine and its brominated isosteres on recombinant human alpha7, alpha4beta2 and alpha4beta4 nicotinic acetylcholine receptors. *J Neurochem* **78**, 1029-43 (2001).
326. Luetje, C. W. & Patrick, J. Both alpha- and beta-subunits contribute to the agonist sensitivity of neuronal nicotinic acetylcholine receptors. *J Neurosci* **11**, 837-45 (1991).
327. Canu Boido, C. & Sparatore, F. Synthesis and preliminary pharmacological evaluation of some cytisine derivatives. *Farmaco* **54**, 438-51 (1999).
328. M.G.Dallemagne, C. H. H. Respiratory stimulants. *The Alkaloids* **5**, 109-139 (1955).
329. Murakoshi, I. F., Yuichi; Takeda, Shigefumi; Arai, Ichiro. in *7 pp. CODEN: JKXXAF 04295480 A2 19921020 Heisei. CAN 118:45733 AN 1993:45733 CAPLUS* (JP, 1992).
330. Murakoshi, I. F., Yuichi; Kawamura, Hideki; Maruyama, Hirobumi. in *Jpn. Kokai Tokkyo Koho* (JP, 1992).
331. Lippiello, P. M. C., William S. U.S. (1993), in *5 pp.CODEN: USXXAM US 5242916 A 19930907 CAN 119:217429 AN 1993:617429 CAPLUS* (USA, 1993).
332. O'Neill, B. T. in *PCT Int. Appl. 75 pp. CODEN: PIXXD2 WO 9818798 A1 19980507 CAN 129:4774 AN 1998:293506 CAPLUS* (1998).
333. O'Neill, B. T. in *Pfizer US* (USA, 1999).
334. Maulenovich, G. A. & Evich, V. A. Z. in *international Russian* (RU199990102541, Russia, 2000).
335. Museo, E. & Wise, R. A. Cytisine-induced behavioral activation: delineation of neuroanatomical locus of action. *Brain Res* **670**, 257-63 (1995).
336. Rao, T. S., Correa, L. D., Reid, R. T. & Lloyd, G. K. Evaluation of anti-nociceptive effects of neuronal nicotinic acetylcholine receptor (NAChR) ligands in the rat tail-flick assay. *Neuropharmacology* **35**, 393-405 (1996).
337. Luputiu, G. & Gilau, L. [N-aryl-thiocarbamyl-cytisine-derivatives. 1. Cytisine]. *Arch Pharm Ber Dtsch Pharm Ges* **302**, 943-6 (1969).
338. Patel, I. H. R. R. P. Synthesis of local anesthetics from cytisine. *J.Chem.Soc.*, 1774-1775 (1936).
339. Boido, C. C., Tasso, B., Boido, V. & Sparatore, F. Cytisine derivatives as ligands for neuronal nicotine receptors and with various pharmacological activities. *Farmaco* **58**, 265-77 (2003).
340. Carbonnelle, E. et al. Nitrogen substitution modifies the activity of cytisine on neuronal nicotinic receptor subtypes. *Eur J Pharmacol* **471**, 85-96 (2003).
341. Slater, Y. E. et al. Halogenated cytisine derivatives as agonists at human neuronal nicotinic acetylcholine receptor subtypes. *Neuropharmacology* **44**, 503-15 (2003).
342. Ferraro, S. 1-58 Novel Nicotinic Acetylcholine Receptors Ligands: In Vitro evaluation for $(\alpha 1)_2\beta 1\gamma\delta$ and $\alpha 7$* Subtypes. (Padova, 2003).

343. Endres, J. in *Pharmazeutische Chemie* 76 (Rheinische Friedrich-Wilhelms Universität, Bonn, 2002).
344. Bick, I. R. C. G., J. W.; Leow, H. M. *Aust J. Chem..* **32**, 2523-36 and 2537-43. (1979).
345. Griffin, W. J. & Lin, G. D. Chemotaxonomy and geographical distribution of tropane alkaloids. *Phytochemistry* **53**, 623-37 (2000).
346. http://rainforest-australia.com/silky_oak.htm.
347. Wegge, T., Schwarz, S. & Seitz, G. An alternative improved synthesis of (-)-norferruginine, a potent nAChR agonist. *Pharmazie* **55**, 779-80 (2000).
348. Swanson, K. L. A., E. X. Selective Neurotoxicity. *Handbook of Expt.Pharmacology,* **Vol. 102**, 620-621 (1992).
349. Gündisch, D. et al. Syntheses and evaluation of pyridazine and pyrimidine containing bioisosteres of (+/-)-pyrido[3.4-b]homotropane and pyrido-[3.4-b]tropane as novel nAChR ligands. *Bioorg Med Chem* **10**, 1-9 (2002).
350. Spande, T. F. G., H. M.; Edwards, M. W.; Yeh, H. J. C.; Pannell, L.; Daly, J. W. J. *J. Am. Chem. Soc.* **114**, 3475 (1992).
351. Seerden, J. P., Tulp, M. T., Scheeren, H. W. & Kruse, C. G. Synthesis and structure-activity data of some new epibatidine analogues. *Bioorg Med Chem* **6**, 2103-10 (1998).
352. Che, D. et al. exo-2-(Pyridazin-4-yl)-7-azabicyclo[2.2.1]heptanes: syntheses and nicotinic acetylcholine receptor agonist activity of potent pyridazine analogues of (+/-)-epibatidine. *J Med Chem* **44**, 47-57 (2001).
353. Manallack, D. T. G., T.; Livingstone, D. J. In Deviller. Neural networks in QSAR and drug design. *J. (Ed.)* (1996).
354. Glennon, R. A. D. M. Nicotine Receptors Ligands. *Med. Chem. Res.*, 465-486 (1996).
355. Gohlke, H. et al. Synthesis and nicotinic binding studies on enantiopure diazine analogues of the novel (2-chloro-5-pyridyl)-9-azabicyclo[4.2.1]non-2-ene UB-165. *J Med Chem* **45**, 1064-72 (2002).
356. Dart, M. J. et al. Structural aspects of high affinity ligands for the alpha 4 beta 2 neuronal nicotinic receptor. *Pharm Acta Helv* **74**, 115-23 (2000).
357. Sharples, C. G. et al. Synthesis and pharmacological characterization of novel analogues of the nicotinic acetylcholine receptor agonist (+/-)-UB-165. *J Med Chem* **45**, 3235-45 (2002).
358. Gohlke, H. et al. 3D QSAR analyses-guided rational design of novel ligands for the (alpha4)2(beta2)3 nicotinic acetylcholine receptor. *J Med Chem* **46**, 2031-48 (2003).
359. Macallan, D. R. et al. Methyllycaconitine and (+)-anatoxin-a differentiate between nicotinic receptors in vertebrate and invertebrate nervous systems. *FEBS Lett* **226**, 357-63 (1988).
360. Takada, N. I., M; Suenaga K.; Uemara D.; *Tetrahedron Letter* **41**, 6425 (2000).
361. Kigoshi, N. H. D. U. H. *Tetrahedron Lett.* **42**, 7496 (2001).

362. Devlin, J. P., Edwards, E. O., Gorham, P. R., Hunter, N. R.;Pike, R. K. & Stavric, B. Anatoxin-a, a toxical alkaloid from Anabaena flos-aquae. *Can. J. Chem.*, 1367-1371 (1977).
363. http://www.biol.uni.lodz.pl/~kes/wersja_ang/phytoplankton.htm.
364. Aronstam, R., S. and Bernhard Witkpot. Anatoxin-a interactions with cholinergic synaptic molecules. *Neurobiology* **78**, 4639-4643 (1981).
365. Swanson, K. L., Allen, C. N., Aronstam, R. S., Rapoport, H. & Albuquerque, E. X. Molecular mechanisms of the potent and stereospecific nicotinic receptor agonist (+)-anatoxin-a. *Mol Pharmacol* **29**, 250-7 (1986).
366. Stredab, J. P. L. in *The ASA Newsletter* 1-11 (2002).
367. Swanson, K. L., Aronstam, R. S., Wonnacott, S., Rapoport, H. & Albuquerque, E. X. Nicotinic pharmacology of anatoxin analogs. I. Side chain structure-activity relationships at peripheral agonist and noncompetitive antagonist sites. *J Pharmacol Exp Ther* **259**, 377-86 (1991).
368. Kofuji, P. et al. Activation and blockade of the acetylcholine receptor-ion channel by the agonists (+)-anatoxin-a, the N-methyl derivative and the enantiomer. *J Pharmacol Exp Ther* **252**, 517-25 (1990).
369. Kanne, D. B. & Abood, L. G. Synthesis and biological characterization of pyridohomotropanes. Structure-activity relationships of conformationally restricted nicotinoids. *J Med Chem* **31**, 506-9 (1988).
370. Schmitt, J. D., Sharples, C. G. & Caldwell, W. S. Molecular recognition in nicotinic acetylcholine receptors: the importance of pi-cation interactions. *J Med Chem* **42**, 3066-74 (1999).
371. Sharples, C. G. et al. UB-165: a novel nicotinic agonist with subtype selectivity implicates the alpha4beta2* subtype in the modulation of dopamine release from rat striatal synaptosomes. *J Neurosci* **20**, 2783-91 (2000).
372. Karig, G. et al. Synthesis and nicotinic binding of novel phenyl derivatives of UB-165. Identifying factors associated with alpha7 selectivity. *Bioorg Med Chem Lett* **13**, 2825-8 (2003).
373. Nilsson, B. M. et al. 3-Heteroaryl-substituted quinuclidin-3-ol and quinuclidin-2-ene derivatives as muscarinic antagonists. Synthesis and structure-activity relationships. *J Med Chem* **38**, 473-87 (1995).
374. Andrä M., T. C. M. G. D. Phenylcarbamates and cholinethers: synthesis and in vitro evaluation as ligands for nicotinic acetylcholine receptors (nAChRs). *Drugs Fut.* **27**, p113 (2003).
375. Allen, D. D. & Smith, Q. R. Characterization of the blood-brain barrier choline transporter using the in situ rat brain perfusion technique. *J Neurochem* **76**, 1032-41 (2001).
376. Food and Drug Administration, U. S. nutrient content claims notification for choline containing food. *http://vm.cfsan.fda.gov/~dms(fcholin.html.* august 30 (2001).
377. Buchman, A. L. et al. Verbal and visual memory improve after choline supplementation in long-term total parenteral nutrition: a pilot study. *JPEN J Parenter Enteral Nutr* **25**, 30-5 (2001).

378. D.D. Allen, P. R. L. The blood-brain barrier choline transporter as a brain drug delivery vector. *Life Sciences* **73**, 1609-1615 (2003).
379. Meyer, E. M. et al. Neuroprotective and memory-related actions of novel alpha-7 nicotinic agents with different mixed agonist/antagonist properties. *J Pharmacol Exp Ther* **284**, 1026-32 (1998).
380. Jonnala, R. R. et al. Relative levels of cytoprotection produced by analogs of choline and the role of alpha7-nicotinic acetylcholine receptors. *Synapse* **47**, 262-9 (2003).
381. R., H. R. a. R. R. *J Pharmacol.* **37** (1929).
382. Brown, B. G. & Hey, P. Choline phenyl ethers as inhibitors of amine oxidase. *Br J Pharmacol* **11**, 58-65 (1956).
383. Hey, P. On relationships between structure and nicotine-like stimulant activity in choline esters and ethers. *Br J Pharmacol* **7**, 117-129 (1952).
384. Simsek, R. et al. Quaternary ammonium 3-(aminoethoxy)pyridines as antinociceptive agents. *Bioorg Med Chem Lett* **13**, 2917-20 (2003).
385. Abood, L. G., Shahid Salles, K. & Maiti, A. Structure-activity studies of carbamate and other esters: agonists and antagonists to nicotine. *Pharmacol Biochem Behav* **30**, 403-8 (1988).
386. Terry, in *US2003050316* (USA, 2003).
387. Naito, R. et al. Selective muscarinic antagonists. II. Synthesis and antimuscarinic properties of biphenylylcarbamate derivatives. *Chem Pharm Bull (Tokyo)* **46**, 1286-94 (1998).
388. Sokilde, B. et al. Analogues of carbacholine: synthesis and relationship between structure and affinity for muscarinic and nicotinic acetylcholine receptors. *Arch Pharm (Weinheim)* **329**, 95-104 (1996).
389. Macor, J. W. E. in *WO 97/30998* 1804 (35, PCT Int Appl., 2001).
390. Dougherty, D. A. Cation-pi interactions in chemistry and biology: a new view of benzene, Phe, Tyr, and Trp. *Science* **271**, 163-8 (1996)
391. www.piercenet.com

VIII. Publications

- Gündisch, D.; Limbeck, M.; Tilotta, M.C.
  Rigidified Choline Analogues as Ligands for Nicotinic Acetylcholine Receptors.
  2004, submitted.

- Zlotos, D. P.; Gündisch, D.; Ferraro, S.; Tilotta, M.C.; Stiefl, N.; Baumann, K.
  Bisquaternary Caracurine V and iso-Caracurine V Analogues as well as Bisquaternary Dimers of Strychnine as Ligands of the Muscle Type of Nicotinic Acetylcholine Receptors: SAR and QSAR Studies.
  Bioorganic & Medicinal Chemistry, 2004, 12, (23), 6277-6285.

- Peters, L.; Wright, A. D.; Kehraus, S.; Gündisch, D.; Tilotta, M.C.; König, G. M.
  Prenylated Indole Alkaloids from Flustra foliacea with Subtype Specific Binding on nAChRs.
  Planta medica, 2004, 70, 883-886.

- Gündisch, D.; Andrä, M.; Munoz, L.; Tilotta, M. C.
  Synthesis and evaluation of phenylcarbamate derivatives as nicotinic acetylcholine receptor (nAChRs) ligands.
  Bioorganic & Medicinal Chemistry , 2004, 12, 4953–4962

- Seifert, S.; Stehl, A.; Tilotta, M.C.; Gündisch, D.; Seitz, G.
  Novel enantiopure ferrugininoids active as nicotinic agents: Synthesis and radioligand binding studies
  Pharmazie, 2004, 59, 427-434

- Seifert, S.; Gündisch, D.; Tilotta, M.C.; Seitz, G.
  An improved synthesis and in vitro evaluation of quinuclidin-2-ene based ligands for the nicotinic acetylcholine receptor.
  Pharmazie, 2003, 58, 353-354

- Schwarz, S.; Kämpchen, T.; Tilotta, M.C.; Gündisch, D.; Seitz, G.
  Synthesis and nicotinic binding studies on enantiopure pinnamine variants with an 8-azabicyclo[3.2.1]octane moiety.
  Pharmazie, 2003, 58, 295-299

- Gohlke H.; Schwarz, S.; Gündisch, D.; Tilotta, M.C.; Wegge, T.; Seitz, G.
  3D-QSAR Analyses-guided Rational Design of Novel Ligands for the $(\alpha 4)_2(\beta 2)_3$ Nicotinic Acetylcholine Receptor.
  J Med Chem, 2003, 46, 2031-2148

- Gohlke H.; Gündisch, D.; Schwarz, S.; Tilotta, M.C.; Seitz, G.; Wegge, T.
  Synthesis and receptor binding studies of novel enantiopure diazine bioisosteres of UB-165.
  J Med Chem, 2002, 45, 1064-1072

Meetings and Conferences
Presenting author

- **Tilotta, M.C.;**
  In vitro evaluation of novel nicotinic acetylcholine receptor ligands: bioisosteres of the highly toxic alkaloids cytisine, ferruginine and anatoxin-a
  ESMEC-European School of Medicinal Chemistry-XXIV Advanced Course of Medicinal Chemistry and "E. Duranti" Seminar for PhD students; July 4-8,2004, Urbino, Italy

- Munoz, L.; Andrä, M.; Tilotta, M.C.; Gündisch, D.
  Synthesis and evaluation of phenylcarbamates and choline phenyl ether derivatives for nicotinic acetylcholine receptors (nAChRs).
  Soc Neurosci Abstr 2003, Nov 8-12, 2003, New Orleans, U.S.A.

- Andrä, M.; Tilotta, M.C.; Gündisch, D.
  Phenylcarbamates and choline phenyl ethers as subtype-selective ligands for nicotinic acetylcholine receptors (nAChRs).
  AIMECS 2003, 5th AFMC International Medicinal Chemistry Symposium, Oct 14-17, 2003, Kyoto, Japan.

- **Tilotta, M.C.;** Gündisch, D; Stehl, A.; Seifert, S.; Seitz, G.
  In vitro evaluation of novel ferruginine and quinuclidin-2-ene derivatives as ligands for different subtypes of neuronal nicotinic acetylcholine receptors (nAChRs).
  Polish-Austrian-German-Hungarian-Italian Joint Meeting on Medicinal Chemistry, Oct 15-18, 2003, Krakow, Poland.

- Gündisch, D.; Seitz, G.; Tilotta, M.C.; Schwarz, S.; Wegge, T.; Klaperski, P.; Seifert, S.; Stehl, A.; Eichler, G.; Munoz, L.; Andrä, M.; Limbeck, M.
  Synthesis and in vitro evaluation of structural variants of choline, cytisine, ferruginine, anatoxin-a, diazabicyclononane- and quinuclidin-2-ene based ligands for nicotinic acetylcholine receptors.
  14th Camerino-Noordwijkerhout Symposium, Sept 7-11, 2003, Camerino, Italy.

- Ferraro, S.; Tilotta, M.C.; Gündisch, D.; Zlotos, D.P.
  Analogues of Caracurine V, iso-Caracurine V and dimeric Strychnine as ligands for the muscle type of the nicotinic acetylcholine receptor (nAChR)

1st UK Nicotinic Receptor Club Meeting, July 1st, 2003, Lilly Research Centre, Erl Wood Manor, Windlesham, UK.

- Gündisch, D.; Seitz, G.; Tilotta, M.C.; Schwarz, S.; Wegge, T.; Klaperski, P.; Seifert, S.; Stehl, A.; Eichler, G.; Munoz, L.; Andrä, M.; Limbeck, M.
  Synthesis and In Vitro Evaluation of Novel Ligands for Nicotinic Acetylcholine Receptors (nAChRs): Structural Variants of Choline; Alkaloidal Toxins; 3,9-Diazabicyclo[4.2.1]nonane and Quinuclidin-2-ene based Derivatives.
  1st UK Nicotinic Receptor Club Meeting, July 1st, 2003, Lilly Research Centre, Erl Wood Manor, Windlesham, UK

- Limbeck, M.; Tilotta, M.C.; Gündisch, D.
  Choline derivatives as ligands for nicotinic acetylcholine receptors (nAChRs): Synthesis and radioligand binding studies.
  Soc Neurosci Abstr 2002, Nov 2-7, 2002, Orlando, U.S.A.

- Andrä, M.; Tilotta, M.C.; Gündisch, D.
  Phenylcarbamates and cholinethers: synthesis and in vitro evaluation as ligands fornicotinic acetylcholine receptors (nAChRs).
  Drugs Fut 2002, 27 (Suppl. A), P113: XVIIth Int Symp on Med Chem, Sept 1-5, 2002, Barcelona, Spain

- **Tilotta, M.C.;** Eichler, G.; Gündisch, D.; Seitz, G.
  Synthesis, evaluation and structure affinity relationship of novel diazabicyclo[4.2.1]nonane derivatives as ligands for nicotinic acetylcholine receptors (nAChRs)
  Drugs Fut 2002, 27 (Suppl. A), P273: XVIIth Int Symp on Med Chem, Sept 1-5, 2002, Barcelona, Spain

- Limbeck, M.; Tilotta, M. C.; Gündisch, D.
  Synthesis and evaluation of novel choline derivatives as ligands for nicotinic acetylcholine receptors (nAChRs)
  Drugs Fut 2002, 27 (Suppl. A), P274: XVIIth Int Symp on Med Chem, Sept 1-5, 2002, Barcelona, Spain

- **Tilotta, M.C.;** Klaperski, P.; Schwarz, S.; Wegge, T.; Seitz, G.; Gündisch, D.
  Novel analogs of thiocytisine and tetrahydrocytisine – in vitro evaluation for different nicotinic acetylcholine receptors (nAChRs)
  Soc Neurosci Abstr 2001, Oct 10-15, 2001, San Diego, U.S.A.

Acknowledgments

At the end of this difficult and important work, I would like to thank all the people that helped me to achieve it.

First of all, I would like to thank my supervisor Prof. Dr. Daniela Gündisch. She gave me the opportunity to work on such an interesting subject and gain very formative and valuable experience. I wish to thank her not only for the scientific support and being open to any kind of discussion, but also for her patience, trust and friendship.

I wish to thank Prof. Dr. C. Müller for supervising this thesis.

I wish to express my gratitude to all the people in Endenich and Poppelsdorf who since the beginning of my PhD studies in Bonn, helped me to overcome all the everyday problems, such as providing me with a bicycle, furniture, help me with bureaucracy, etc. I would especially like to thank to Martina Dieckmann for her help in the first months of my life in Germany.

Many thanks also to all my colleagues in the Pharmaceutical Institute in Poppelsdorf. I would like to thank Jeannette Endres and Silvia Ferraro, with whom I worked for some months in the same project in the isotope laboratory. Obviously, I would like to thank all the other people working in the isotope laboratory. I spent four years in a very friendly working atmosphere. In particular, my gratitude goes to Sonja Hinz, Dieter Baumert, Meryem Köse, Markus Genau and Birgit Preiss.

I wish to thank Lenka Münoz not only for her helpful advice and encouragement in these years but especially for her friendship, her dancing lessons and her wonderful and delicious cakes and dinners.

Furthermore, I would like to thank Frauke Van Hoorn for her patience for listening to my countless resumés of my daily work, my problems in the laboratory everyday, my difficulty in learning German, for her constant presence and continuous help, and (not less important) her friendship. She instilled me a little bit of East Frisia temperament. She taught me what "gemütlich" means.

A special thanks goes to all my Italian friends. First of all, I wish to remember the people that come from Sicily: Violetta, Giuseppe, Giorgio, Giansalvo and Claudia. I will never forget our "Sicilian style" dinner. I also have to thank other Italian friends, in particular Elena and Lucia, for their friendship whenever I needed it. I would like to thank Riccardo for his patience in answering my strange questions about nuclear medicine.

The person that made the writing of the doctoral thesis possible is my boyfriend, Antonio. He was always close to me, although so far away in Pisa, with his love and support.

In particular, I want to share my pride with my family. They encouraged me to start this project, even it means going abroad. They did more for me than I could ever expect. Even though they live so far away they have always given me so much love, and I feel them close to me.